

Lipid Biomarkers in Lacustrine Sedimentary Archives – An Inventory and Evaluation as Proxies for Environmental and Climatic Change

vorgelegt von
Dipl.-Chem. (Umweltchemie)
Thomas Fischer
aus Leipzig

Von der Fakultät VI - Bauingenieurwesen und Angewandte Geowissenschaften
der Technischen Universität Berlin
zur Erlangung des akademischen Grades

Doktor der Naturwissenschaften
- Dr. rer. nat. -

genehmigte Dissertation

Promotionsausschuss:

Vorsitzender: Prof. Dr. G. Franz
Berichter: Prof. Dr. B. Horsfield
Berichter: Prof. Dr. J. F. W. Negendank

Tag der mündlichen Prüfung: 26. November 2003

Berlin 2004
D 83

Acknowledgement

First of all I wish to extend my thanks to my supervisors Prof. Brian Horsfield and Dr. Heinz Wilkes at the Forschungszentrum Jülich and later at the GeoForschungsZentrum Potsdam. In defiance of the spatial distance, I always met them ready for discussion of scientific ideas and problems, conducting my to bring the research project to fruition.

I also wish to thank Prof. Negendank from the GeoForschungsZentrum Potsdam for support of this work and for taking over the co-report of this thesis.

Many thanks for pleasant co-operation are extended to all persons involved in this study. Dr. Achim Brauer and Prof. Bernd Zolitschka (GeoForschungsZentrum Potsdam; Geomorphologie und Polarforschung (GEOPOL), University Bremen) provided sample material of Lake Meerfelder Maar and Lake Holzmaar. Dr. Ilka Schönfelder (Institut für Gewässerökologie und Binnenfischerei, Berlin) provided the sample set of Lake Großer Treppensee. I want to extend special thanks to all of them for many fruitful discussions about the archives under investigation, especially about geological and limnological background.

A lot of the ICG-4 staff contributed to the successful finish of this work. The support from Dr. Matthias Radke, Anne Richter, Werner Laumer, Ulrich Disko, Franz Leistner, Helmut Willsch and many others from the Organic Geochemistry Workgroup is gratefully acknowledged. Also the assistance and discussions with people from affiliated workgroups, especially Dr. Andreas Lücke, are acknowledged in the same way.

Beside the paleoclimatic conditions this thesis deals with, the „working-climate“ was substantially improved by the exchange with all of my colleagues from the FZ Jülich, not limited to the scientific issues. I wish to thank especially Dr. Andreas Fuhrmann, who worked together with me on the bulk organic geochemical characterisation of the investigated archives. I also wish to thank Dipl.-Chem. Antje Armstroff and Thomas Oldenburg as well as Dipl.-Geol. Marina Kloppisch, Jochen Naeth, Oliver Kranendonck and Ullrich Herten.

This Ph.D. thesis is part of the DFG priority programme „Wandel der Geobiosphäre in den letzten 15,000 Jahren – Kontinentale Sedimente als Ausdruck sich verändernder Umweltbedingungen“ (Grant Wi 1359/1-2). I wish to thank for financial support as well as the opportunity for fruitful discussions with many other scientists of various fields at the DFG-meetings.

Abstract

With the growing understanding of human influence on the Earth system, an increasing number of scientific investigations focuses on vegetation responses to changing environmental and/or climatic conditions. A detailed prediction, how e.g. increasing atmospheric temperatures affect the composition of terrestrial and aquatic vegetation composition, however, remains difficult without a detailed knowledge of comparable changes during the past.

A number of archives recording changes in environmental and/or climatic conditions under varying temporal integration and resolution have been evaluated up to now. Changing conditions are, however, not recorded directly. Measured proxy-parameters need to be interpreted and correlated to environmental and climatic parameters.

Lacustrine sedimentary archives are generally regarded as excellent archives in terms of paleolimnology. Sediments of two maar lakes, a special form of crater lakes, have been selected as sedimentary records for the study presented here. The lipid composition of Lake Holzmaar and Lake Meerfelder Maar sediments has been evaluated with respect to varying proportions of autochthonous and allochthonous organic matter contribution. In a second step, detected changes in organic matter contributing sources were correlated to environmental and climatic changes. In order to overcome the regional scale of this investigation, sediments from Lake Großer Treppensee, eastern Brandenburg, were added to this study and investigated under the same programme. A selected section of Lake Meerfelder Maar sedimentary profile including the Younger Dryas cold period and the transition to the early Ho-

locene was finally analysed under highest achievable temporal resolution to detect vegetation response to climatic change in high detail.

Bulk organic geochemical parameters (TOC, TIC, TS, TN, HI, OI) were measured as fundamental data. Lipids were extracted using a flow blending method and further separated into compound specific fractions using a semi-preparative liquid-chromatographic separation procedure. The fractions of aliphatic hydrocarbons, carboxylic acids and alcohols plus sterols were inventoried by means of gas chromatography (GC) and gas chromatography-mass spectrometry (GC-MS). GC-MS was performed in order to identify individual compounds by interpretation of mass spectra and comparison with authentic standards and/or literature data; GC was performed for quantification of these compounds.

A compelling prerequisite for the connection between lipid distributions and environmental and/or climatic conditions is a good preservation of the investigated sedimentary matter. Using three different parameters, TOC/TS, Pristane/Phytane and UR_{FA} ratios, it could be confirmed that the investigated sedimentary records are well preserved. A partial loss of organic matter could not be excluded, however, the organic matter composition was found to be not overprinted by diagenetic effects by far. It was therefore concluded, that changes in the lipid composition are related to changes in the organic matter contributing community in and around the investigated lakes as a result of changing environmental and/or climatic conditions.

At next, detected lipids were assigned to their respective source- and/or source organism groups. In the case of normal chain lipids, the generally accepted assignment to aquatic sources and land plants could be confirmed by cluster analysis. Based on this analysis, the recently suggested marker molecules of aquatic macrophytes in the middle chain length range, however, had to be modified due to a slightly different assignment of the respective homologues.

The application of these findings to the investigated sedimentary profiles identified a prominent contribution of higher land plants to the sedimentary organic matter fraction of all three profiles, that developed after the last Glacial. Important differences in aquatic macrophyte growth were further found between the two Eifel Maar Lakes. The investigation of selected long chain homologues further allowed

a specification of changes in the contribution of herbs and shrubs *vs.* trees during times.

After the primary production seemed to be underestimated as an organic matter source from the detected normal chain lipids, a more reliable reconstruction was allowed by the composition of several sterol homologues in the sedimentary records. In addition to the more general approach based on carbon numbers of detected individual sterols, known compound specific parameters were applied and modified in the present study.

The changing composition of the organic matter contributors in and around the investigated lakes was finally used as a framework to assess the development of environmental and/or climatic conditions in the respective catchment areas. Beside the reconstruction of the climate amelioration at the late Glacial/early Holocene transition and further towards the Holocene climate optimum, that was shown to effect both autochthonous and allochthonous productivity, a regional phenomenon of Lake Meerfelder Maar became obvious from various biomarker parameters. Accordingly, a slightly increased lake level during the Holocene climate optimum seems to have caused an extensive shallow water zone. The consequently changed composition of the ecosystem was shown to be reflected in the biomarker composition.

The investigation of the temporally high resolved core section of Lake Meerfelder Maar finally substantially supported the recent discussion on climatic change during the Younger Dryas period of cooler temperatures, which was former seen to be homogeneous. The data of the investigated profile section yielded a significant and sharp shift in the composition of the sedimentary organic matter during the Younger Dryas. A supposed change of the Meerbach stream into Lake Meerfelder Maar during the late Younger Dryas might explain the abrupt shifts. The more continuous shifts of other proxy compounds, however, also support a climatically driven change of the vegetation in the catchment area of Lake Meerfelder Maar. A comparison with sediments from other maar lake sediments thus may be useful to separate local phenomena from climatic change and to support the ongoing discussion on the Younger Dryas climate.

Kurzfassung

Mit dem wachsenden Verständnis des menschlichen Einflusses auf das System Erde zielt eine zunehmende Anzahl von wissenschaftlichen Untersuchungen auf die Auswirkungen sich verändernder Umwelt- und Klimabedingungen. Eine detaillierte Voraussage, wie sich beispielsweise zunehmende atmosphärische Temperaturen auf die Zusammensetzung von terrestrischer und aquatischer Vegetation auswirken, bleibt allerdings ohne ein detailliertes Wissen vergleichbarer klimatischer Änderungen während der Vergangenheit schwierig.

Mehrere Archive, die Veränderungen von Umwelt- und Klimabedingungen auf variierenden Zeitskalen und in unterschiedlicher zeitlicher Auflösung konservieren, wurden bisher evaluiert. Dabei werden Veränderungen allerdings nicht direkt messbar aufgezeichnet. Vielmehr müssen die gemessenen Proxy-Daten interpretiert und mit Umwelt- und Klima-Parametern korreliert werden.

Lakustrine Sedimente werden im Sinne der Paläolimnologie im allgemeinen als ausgezeichnete Archive betrachtet. Sedimente von zwei Maar-Seen, eine Sonderform von Kraterseen vulkanischen Ursprungs, wurden für die vorliegende Untersuchung als Archive ausgewählt. Die Lipid-Zusammensetzung von Sedimenten des Holzmaars und des Meerfelder Maars wurde hinsichtlich unterschiedlicher Anteile an autochthonem und allochthonem organischen Material untersucht. In einem zweiten Schritt wurden detektierte Änderungen der Quellen des löslichen organischen Materials mit umweltspezifischen und klimatischen Änderungen korreliert. Um den regionalen Charakter dieser Untersuchung zu überwinden, wurden Sedimente des Großen Treppelsee im Osten Brandenburgs unter der gleichen Zielsetzung un-

tersucht. Ein ausgewählter Profilschnitt des Meerfelder Maars, der die Jüngere Dryas und den Übergang zum frühen Holozän enthält, wurde schließlich unter der höchsten erreichbaren zeitlichen Auflösung untersucht, um die Reaktion der Vegetation auf die klimatischen Veränderungen möglichst detailliert zu untersuchen.

Geochemische Summenparameter (TOC, TIC, TS, TN, HI, OI) wurden als Basis-Daten gemessen. Die Lipide wurden mit Hilfe eines Flow-Blending Verfahrens extrahiert und anschließend unter Benutzung eines semipräparativen flüssigkeitschromatographischen Verfahrens in Substanzklassen getrennt. Die Fraktionen der aliphatischen Kohlenwasserstoffe, der Karbonsäuren sowie der Alkohole und Sterole wurden mittels Gaschromatographie (GC) und Gaschromatographie-Massenspektrometrie (GC-MS) inventarisiert. Die GC-MS Analysen dienten der Identifizierung von einzelnen Verbindungen anhand ihrer Massenspektren und durch Vergleich dieser mit authentischen Standards bzw. Literaturdaten. GC Analysen dienten der Quantifizierung von Einzelverbindungen.

Eine zwingende Voraussetzung für die Korrelation von Lipidverteilungen mit Umwelt- und Klimabedingungen ist ein guter Erhaltungszustand des untersuchten sedimentären Materials. Durch die Verwendung verschiedener Parameter (TOC/TS-, Pristan/Phytan- und UR_{FA} -Verhältnisse) konnte ein guter Erhaltungszustand der untersuchten sedimentären Archive bestätigt werden. Ein teilweiser Verlust von organischem Material konnte zwar nicht ausgeschlossen werden, aber die Zusammensetzung des organischen Materials erwies sich als gering durch diagenetische Effekte überprägt. Es konnte daher geschlußfolgert werden, daß Veränderungen der Lipid-Zusammensetzung in Verbindung mit Variationen der Quell-Populationen in den Seen und ihren Einzugsgebieten als Ergebnis sich ändernder Umwelt- bzw. Klimabedingungen stehen.

Anschließend wurden die detektierten Lipide ihren Quell-Organismen bzw. Organismengruppen zugeordnet. Im Falle der gesättigten, unverzweigten Lipide konnte die allgemein akzeptierte Zuordnung zu aquatischen Organismen bzw. Landpflanzen durch Clusteranalyse bestätigt werden. Aufgrund der Ergebnisse mussten jedoch die in jüngster Zeit vorgeschlagenen Proxy-Verbindungen für aquatische Macrophyten im mittleren Kettenlängenbereich modifiziert werden.

Die Anwendung der Ergebnisse auf die untersuchten Sedimentprofile ergab einen bedeutenden Beitrag terrestrischer Vegetation, die sich nach der letzten Eiszeit in

den Einzugsgebieten entwickelte, zum sedimentären organischen Material. Wesentliche Unterschiede im Wachstum aquatischer Macrophyten fanden sich darüber hinaus zwischen den beiden Maarseen. Die Untersuchung ausgewählter langkettiger Homologe erlaubte außerdem eine Spezifizierung variierender Anteile von Busch- und Strauch- gegenüber Baum-Vegetation.

Nachdem die Primärproduktion als Quelle organischen Materials durch die Verwendung geradkettiger Lipide unterrepräsentiert erschien, erlaubte die Detektion verschiedener Sterol-Homologe eine verlässlichere Rekonstruktion. Zusätzlich zu einem generellen Ansatz, der auf der Anzahl von Kohlenstoff-Atomen basiert, wurden komponenten-spezifische Parameter angewandt und modifiziert.

Die Variationen der verschiedenen Quellen organischen Materials in den untersuchten Seen und deren Einzugsgebieten bildeten schließlich den Rahmen zur Rekonstruktion der Entwicklung von Umwelt- bzw. Klimabedingungen. Neben der Rekonstruktion der generellen Klimaverbesserung am Übergang von der letzten Eiszeit zum Holozän und weiter zum Holozänen Optimum, die sowohl die autochthone als auch die allochthone Produktivität beeinflusst hat, konnte auch ein lokales Phänomen des Meerfelder Maars anhand verschiedener Biomarker-Parameter nachgewiesen werden. Ein gegenüber heute leicht erhöhter Wasserspiegel während des Holozänen Optimums hat offensichtlich zur Ausbildung einer ausgedehnten Flachwasserzone geführt. Die hierdurch veränderte Zusammensetzung des Ökosystems spiegelt sich in der Zusammensetzung zahlreicher Biomarker-Parameter wider.

Die Untersuchung eines zeitlich hochaufgelösten Profilabschnitts aus dem Meerfelder Maar trägt schließlich entscheidend zur derzeitigen Diskussion über Klimaveränderungen während der Jüngeren Dryas bei. Die Daten des untersuchten Profilabschnitts zeigen eine deutliche und zeitlich scharf abgegrenzte Veränderung der Zusammensetzung des sedimentären organischen Materials. Eine vermutete Änderung des Laufes des Meerbaches in das Meerfelder Maar hinein während der späteren Jüngeren Dryas kann die abrupte Änderung der Zusammensetzung des organischen Material erklären. Die kontinuierlicheren Variationen anderer Parameter sind jedoch eher auf klimatisch bedingte Veränderungen der Vegetation im Einzugsgebiet des Meerfelder Maars zurückzuführen. Ein Vergleich mit anderen Maarseen der Eifelregion erscheint daher sinnvoll, um die lokalen Phänomene von

Klimavariabilitäten besser zu unterscheiden und die bestehende Diskussion um das Klima zur Jüngeren Dryas zu unterstützen.

Contents

Acknowledgement	III
Abstract	V
Kurzfassung	IX
Contents	XIII
List of Figures	XVII
List of Tables	XXI
List of Abbreviations	XXIII
1 Introduction	1
1.1 The Climate over the past 15,000 years	3
1.2 Archives for Paleoenvironmental Studies	7
1.2.1 Lake Sediments as Geological Archives	9
1.2.2 Maar Lakes	11
1.3 Organic Matter as Paleolimnological Indicator	14
2 Objectives	29
3 Study Areas and Samples	31
3.1 Eifel Maar Lakes	32
3.1.1 Lake Holzmaar	37

3.1.2	Lake Meerfelder Maar	38
3.2	Lake Großer Treppensee	43
4	Preparative & Analytical Methods	47
4.1	Sample Preparation, Elemental Composition	48
4.2	Extraction and Liquid Chromatographic Fractionation	52
4.3	Derivatisation and Standard Addition	55
4.4	Gas Chromatography (GC)	57
4.5	Gas Chromatography-Mass Spectrometry (GC-MS)	57
4.6	Gas Chromatography-Isotope Ratio Mass Spectrometry (GC-IRMS)	57
4.7	Statistical Analysis	59
5	Results	61
5.1	General Geochemical Characterisation	61
5.1.1	Elemental Analysis	61
5.1.2	Rock-Eval Pyrolysis	72
5.2	Distribution of Lipid Biomarkers	79
5.2.1	Aliphatic Hydrocarbons	82
5.2.1.1	<i>n</i> -Alkanes	82
5.2.1.2	Steroidal and Triterpenoidal Hydrocarbons	95
5.2.1.3	Pristane and Phytane	100
5.2.1.4	Isotopic Composition of Aliphatic Hydrocarbons	104
5.2.2	Carboxylic Acids	108
5.2.2.1	Fatty Acids	108
5.2.2.2	Hopanoic Acids	119
5.2.3	Alcohols and Sterols	122
5.2.3.1	<i>n</i> -Fatty Alcohols	125
5.2.3.2	Sterols	129
6	Discussion	137
6.1	Preservation of Organic Matter	137
6.1.1	TOC/ TS as Indicators of Preservation	138
6.1.2	Unsaturated Fatty Acids as Indicators of Preservation	139
6.1.3	Pristane/ Phytane as Indicators of Preservation	141
6.2	Origin of Organic Matter in the investigated Lake Sediments	147
6.2.1	Normal Chain Compounds as Source Indicators	147

6.2.2	Steroids and Triterpenoids as Source Indicators	185
6.2.2.1	Sterols as Source Indicators	185
6.2.2.2	Cholestane- and Hopane Derivatives as Source Indicators	203
6.3	Paleoenvironmental Implications	208
6.3.1	Eifel Maar Lakes	208
6.3.1.1	The Lateglacial to Holocene Transition	217
6.3.2	Lake Großer Treppensee	222
7	Summary and Conclusions	225
	References	229

A	List of Equations	A1
A.1	Carbon Preference Indexes	A1
B	Structures of Identified Compounds	A3
C	Sample Inventory	A7
D	Data Compilation	A13

List of Figures

1.1	Paleotemperatures after Dansgaard <i>et al.</i> (1971)	3
1.2	Simulated air temperatures after Ganopolski <i>et al.</i> (1998)	4
1.3	Formation of maar lake basins	11
1.4	Sampled half-core section	12
1.5	One year varve	13
1.6	<i>n</i> -Alkane distribution of macrophytes and land plants	20
1.7	C ₂₇ <i>n</i> -alkane concentration relative to the C ₃₁ homologue of Lake Baikal sediments	21
1.8	Ternary plot of <i>n</i> -alkane percentages	22
1.9	<i>n</i> -Alcohol distributions of macrophytes and land plants	24
1.10	Biosynthetic pathway of sterol synthesis	25
1.11	Carbon number based source assignment of sterols	27
3.1	Location of investigated lakes	31
3.2	Bathymetrical maps of the investigated maar lakes	34
3.3	Photographs of Lake Holzmaar	35
3.4	Stratigraphy of Lake Holzmaar	36
3.5	Photographs of Lake Meerfelder Maar	39
3.6	Stratigraphy of Lake Meerfelder Maar	40
3.7	Stratigraphy of Lake Meerfelder Maars high resolved core section	41
3.8	Location of Lake Großer Treppensee	43
3.9	Stratigraphy of Lake Großer Treppensee	45
4.1	Preparative and analytical procedure	47
4.2	van Krevelen Plot	51

4.3	Semipreparative chromatographic separation	53
4.4	Exemplary dendrogram	60
5.1	Bulk parameters: Lake Holzmaar	62
5.2	Bulk parameters: Lake Meerfelder Maar	63
5.3	Bulk parameters: Lake Meerfelder Maar (high resolution)	64
5.4	Bulk parameters: Lake Großer Treppelsee	65
5.5	TOC <i>vs.</i> TS for investigated lakes	69
5.6	van-Krevelen-Diagram: Lake Holzmaar	73
5.7	van-Krevelen-Diagram: Lake Meerfelder Maar	74
5.8	van-Krevelen-Diagram: Lake Großer Treppelsee	75
5.9	Exemplary chromatograms of aliphatic fractions	83
5.10	Absolute and relative abundances of alkanes	84
5.11	Summed and selected individual downcore concentrations of <i>n</i> - alkanes of Lake Holzmaar	85
5.12	Summed and selected individual downcore concentrations of <i>n</i> - alkanes of Lake Meerfelder Maar	87
5.13	Summed and selected individual downcore concentrations of <i>n</i> - alkanes of Lake Meerfelder Maar (high resolution sequence)	89
5.14	Summed and selected individual downcore concentrations of <i>n</i> - alkanes of Lake Großer Treppelsee	93
5.15	Summed cholestane + cholestene and hopane + hopene concentrations	97
5.16	Pristane and phytane downcore concentrations	101
5.17	Downcore $\delta^{13}\text{C}$ -values for odd <i>n</i> -alkanes	105
5.18	Exemplary chromatograms of acid fractions	109
5.19	Absolute and relative abundances of acids	110
5.20	Summed and selected individual downcore concentrations of <i>n</i> -fatty acids of Lake Holzmaar	111
5.21	Summed downcore concentrations of C _{16:1} and C _{18:1} fatty acids . .	112
5.22	Summed and selected individual downcore concentrations of <i>n</i> -fatty acids of Lake Meerfelder Maar	115
5.23	Summed and selected individual downcore concentrations of <i>n</i> -fatty acids of Lake Meerfelder Maars high resolution sequence	118
5.24	Downcore concentrations of 22 <i>R</i> -17 β (H),21 β (H)- dihomohopanecarboxylic acid	120
5.25	Exemplary chromatograms of alcohol fractions	123

5.26	Absolute and relative abundances of sterols	124
5.27	Summed and selected individual downcore concentrations of <i>n</i> -alcohols of Lake Holzmaar	126
5.28	Summed and selected individual downcore concentrations of <i>n</i> -alcohols of Lake Meerfelder Maar	128
5.29	Summed and selected individual downcore concentrations of <i>n</i> -alcohols of Lake Meerfelder Maars high resolution sequence	130
5.30	Summed downcore concentrations of sterols	131
6.1	Downcore UR _{FA} ratio	140
6.2	Phytol sedimentary diagenesis	142
6.3	Downcore pristane/phytane ratios	144
6.4	Cluster diagram for normal chain homologues	151
6.5	Percentages of algally derived <i>n</i> -alkyl lipids	155
6.6	Percentages of aquatic macrophyte derived <i>n</i> -alkyl lipids	160
6.7	Percentages of land plant derived <i>n</i> -alkyl lipids	164
6.8	HFR _{HC} and HFR _{FA} downcore plot of Lake Holzmaar	169
6.9	Ternary diagrams of long chain alkanes and fatty acids for Lake Holzmaar	170
6.10	HFR _{HC} and HFR _{FA} downcore plot of Lake Meerfelder Maar	172
6.11	Ternary diagrams of long chain alkanes and fatty acids for Lake Meerfelder Maar	173
6.12	HFR _{HC} and HFR _{FA} downcore plot of Lake Meerfelder Maar (high resolution sequence)	175
6.13	Ternary diagrams of long chain alkanes and fatty acids for Lake Meerfelder Maar (high resolution sequence)	176
6.14	HFR _{HC} downcore plot and ternary diagram of long chain <i>n</i> -alkanes for Lake Großer Treppensee	177
6.15	Type I relation between CH ₄ and CO ₂ stable carbon isotopic composition	181
6.16	Type II relation between CH ₄ and CO ₂ stable carbon isotopic composition	183
6.17	Ternary plots of sterols: Lake Holzmaar	188
6.18	Ternary plots of sterols: Lake Meerfelder Maar	189
6.19	Ternary plots of sterols: Lake Meerfelder Maar (high resolution sequence)	191

6.20	Cluster diagram for individual sterols	192
6.21	Downcore dinosterol concentrations	194
6.22	Downcore brassicasterol concentrations	198
6.23	Downcore variation of the DBR ratio	201
6.24	Downcore variation of the BTR_{FA} ratio	204
6.25	Downcore variation of the BTR_{HC} ratio	205
6.26	Changing organic matter composition during middle Holocene . .	213
6.27	Downcore C_{27} - C_{31} <i>n</i> -alkane concentration for Lake Meerfelder Maar	220
B.1	Structures of normal chain lipids	A3
B.2	Structures of hydrocarbons	A4
B.3	Structures of sterols	A5

List of Tables

1.1	Common archives and covered time range	7
3.1	Morphometry and hydrology of Lakes Holzmaar and Meerfelder Maar	42
4.1	Chromatographic setup	58
4.2	Mass spectrometric setup	59
5.1	Numbers of investigated compound fractions	79
5.2	Constituents of hydrocarbon fractions	95
5.3	Constituents of acid fractions	119
5.4	Constituents of alcohol fractions	122
6.1	CPI for <i>n</i> -alkane distributions	148
6.2	CPI for <i>n</i> -fatty acid distributions	148
6.3	CPI for <i>n</i> -fatty alcohol distributions	149
6.4	Chain length ranges, representing organic matter sources	154
6.5	Homologues used for ternary plots of C ₂₇ - to C ₃₀ sterols	186
6.6	Parameters, partitioning the Younger Dryas period	218

List of Abbreviations

ATR _{ST} :	Aquatic/ terrigenous ratio for sterols
BTR _{HC} :	Bacterial/ terrigenous ratio for hydrocarbons
BTR _{FA} :	Bacterial/ terrigenous ratio for fatty acids
CPI:	Carbon Preference Index
DBR:	Dinosterol <i>vs.</i> brassicasterol ratio
EOP:	Even-Over-Odd Predominance
FID:	Flame Ionisation Detector
GC-MS:	Gas Chromatography - Mass Spectrometry
HC:	Hydrocarbons
HI:	Hydrogen Index
HMPLC:	Heterocompound Medium Pressure Liquid Chromatography
MPLC:	Medium Pressure Liquid Chromatography
MS:	Mass Spectrometry
MSL:	Mean Sea Level
OEP:	Odd-Over-Even Predominance
OI:	Oxygen Index
OM:	Organic Matter
TC:	Total Carbon

TIC: Total Inorganic Carbon
TN: Total Nitrogen
TOC: Total Organic Carbon
TCD: Thermal Conductivity Detector
UR_{FA}: Unsaturation ratio for fatty acids
YD: Younger Dryas
vyears BP: Varve Years Before Present

1 Introduction

As part of the growing understanding of how human activities influence the Earth system, investigations dealing with the future climate evolution and its consequences for human as well as animal- and plant life are more and more in the center of scientific interest.

Reliable forecastings, however, cannot be made solely from the present day state. Naturally induced shifts of climatic conditions and their effects on the Earth's biosphere need to be distinguished from those induced by human activities. Thus, a detailed look into the past is prerequisite.

The time period between the Last Glacial and today is of special interest: starting at a weakening ice age, atmospheric temperatures increased, flora and fauna developed and humans began to influence the landscape irrevocably. Interesting aspects are the rate and frequency of changing environmental conditions, e. g. temperature and precipitation, as well as possible responses of flora and fauna to the changed conditions. On this basis, forecasts for future climate shifts become conceivable and, moreover, allow consequences of human influences to the Earth system to be predicted. Proportions of atmospheric warming attributed to human influence are on an increasing trend during the last decades ([Kerr, 1997](#)) whereas consequences of increasing greenhouse gas concentrations on Earth temperatures are still discussed. Another prominent example is the reduced stratospheric ozone concentration over the south polar region leading to increased solar radiation, which is also supposed to be caused by anthropogenic pollution. On the other hand, also naturally driven variations of stratospheric ozone concentrations with essential consequences for the radiation at the Earths surface became obvious recently ([Rozema *et al.*, 2002](#)).

With respect to the methodology, the present climate related research can be subdivided into two general divisions as follows. Computer models of the Earth system are used for simulation experiments. In that kind of research, a model is influenced by various possible driving forces and the effects to the Earth system, for example temperature, precipitation or vegetation cover, are studied. This method is regarded as a useful tool to estimate the future climate development due to the human influence. The models in use are subdivided by their state of complexity into conceptional, more inductive models on the one hand and highly sophisticated, three-dimensional comprehensive models (GCMs), which work on the highest spatial and temporal resolution, on the other hand. A third group of the so-called Earth system models of intermediate complexity (EMICs) becomes more and more popular during recent times due to the rising availability of computing power. A prominent example is the CLIMBER-2 model (Claussen *et al.*, 1999a; Petoukhov *et al.*, 2000) which was developed at the Potsdam Institute for Climate Impact Research. A comprehensive overview of other EMICs is available from http://www.pik-potsdam.de/data/emic/table_of_emics.pdf.

A necessary prerequisite for the modelling of future climate, however, is the simulation of the present-day and/or known past climatic conditions as precise as possible. The past environmental and climatic parameters can be reconstructed by evaluation and interpretation of proxy-data. A proxy in this context is any measurable data in any archive that can be traced back to changing conditions. Thus, at least to basic prerequisites are needed for a reconstruction of paleoclimatic conditions:

- An appropriate archive, being sensitive to changing environmental and/or climatic conditions in a sufficient time range and under high temporal resolution
- Appropriate proxy-data that can be measured in the respective archive and traced back to defined environmental and/or climatic characteristics

The resulting framework of proxy-data interpretation finally allows the reconstruction of past dynamics of the climate and the biosphere as well as the forecast of future changes resulting from natural and/or human influences to the Earth system. The present-day state of both evaluation of appropriate archives and suitable

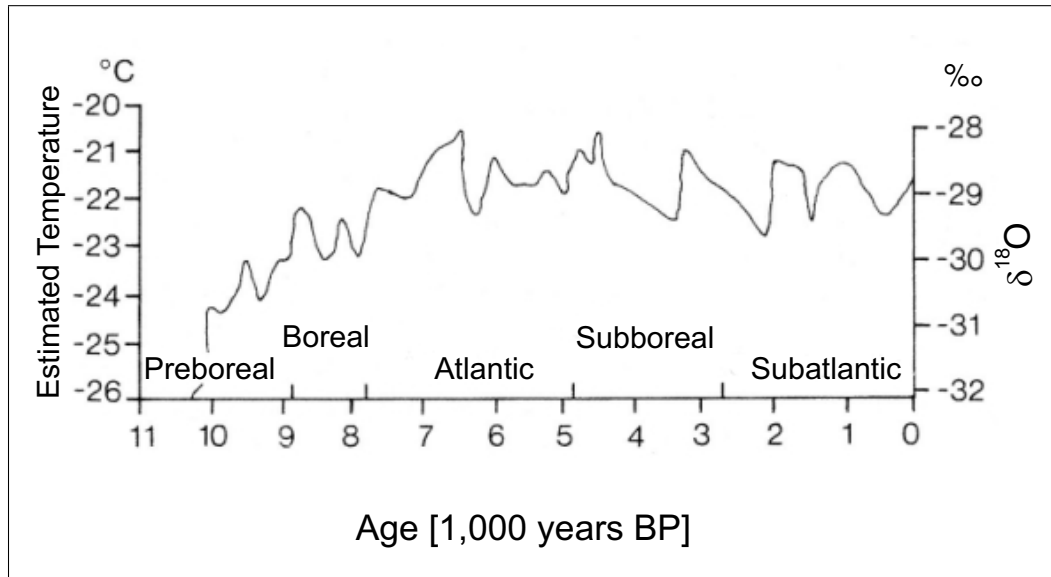


Figure 1.1: Paleotemperatures reconstructed from oxygen isotope ratios of an ice core after Dansgaard *et al.* (1971)

proxy parameters will be introduced in the following sections after a brief introduction of climatic changes during the past 15,000 years as known today.

1.1 The Climate over the past 15,000 years

The present study is a part of the priority programme „*Changes of the Geo- Biosphere during the last 15,000 years*“, which is sponsored by the German Research Council (DFG). Thus, changing environmental and climatic conditions in this range of time are in the center of interest. A summary of climate evolution will be given in this section.

Various investigations showed rapid climatic changes to have occurred after the Weichselian glacial maximum (22,000 – 18,000 years BP), *Fig. 1.1* for example illustrates paleotemperatures reconstructed from $\delta^{18}\text{O}$ values of the Camp Century ice core (Dansgaard *et al.*, 1971).

The warming period after the deglaciation is initiated with the Allerød and Bølling ages, where temperatures increased rapidly. This increase, however, occurred not continuously to the Holocene climate optimum. Rather, an intermediate cooling, the so called Younger Dryas characterised by significantly cooler tem-

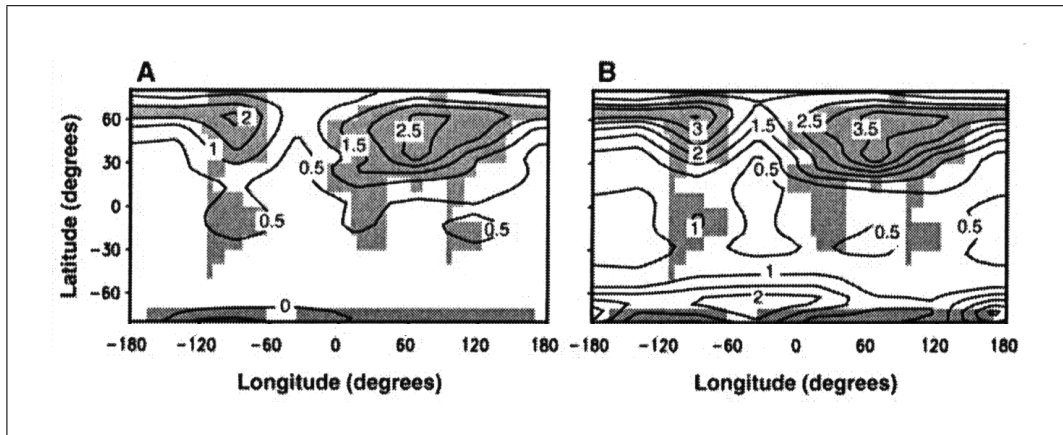


Figure 1.2: Simulated differences in near-surface air temperatures between the middle Holocene and a control simulation of the present-day climate in degree Celsius using the atmosphere model only (A) and a combined atmosphere-ocean-vegetation model (B) after [Ganopolski *et al.* \(1998\)](#)

peratures and dryer conditions, interrupted the post-glacial amelioration of the climatic conditions. The duration of this cooling period was determined between 12,680 – 12,665 vyears BP and 11,640 – 11,590 vyears BP ([Brauer *et al.*, 1999a](#)). Beside this clear temporal localisation, the reasons for the cooling are still discussed controversially; changing oceanic circulations as well as varying solar activity are most favored ([Goslar *et al.*, 1999, 2000](#)). More recently, a few investigations give evidence for changing climatic conditions and vegetation response even within the Younger Dryas period ([von Grafenstein *et al.*, 1999](#); [Schwark *et al.*, 2002](#)).

The subsequent Holocene age is characterised by substantially ameliorated climatic conditions, a rapid warming occurred especially during the Preboreal and Atlantic as visible from *Fig. 1.1*. These conditions led to increased bioproductivity in both aquatic and terrestrial ecosystems. The Atlantic is generally regarded as the period with most optimal climatic conditions and temperatures higher than during preceding and following periods ([Kalis *et al.*, 2003](#)). As observed from various climate modelling experiments, the orbital constellation, especially the inclination of the Earth axis, during that time is believed to have caused this substantial change in the climatic conditions due to a changed solar insolation. [Ganopolski *et al.* \(1998\)](#) for example report on a modelling experiment of the mid-Holocene climate using an Earth System Model of intermediate complexity. They set the orbital parameters as well as the atmospheric carbon dioxide concentration to the respective values and then calculated the development of climatic

conditions. Considering only the atmosphere, the authors obtained increasing summer temperatures and precipitation on the Northern Hemisphere in contrast to *vice versa* conditions during winter. Including the vegetation cover to the simulation, a remarkable expansion of forests was inferred from the warmer summer temperatures and longer growing seasons. A final calculation, additionally including the oceans as a compartment of the Earth system as well as the feedbacks between the modules included in this experiment resulted in summer temperatures up to 4 °C and winter temperatures up to 3 °C higher than today's climate in the northern parts of Europe, Asia and North America (*cf. Fig. 1.2*). These substantially ameliorated climatic conditions are believed to have allowed a forest expansion to the north as well as a shrinking of desert areas. The tree line was calculated to be about 250 km northward compared to its present latitude. This result was found to be consistent with pollen estimations by [Kutzbach *et al.* \(1996\)](#) and by [Prentice *et al.* \(1996\)](#) which indicate a northward forest expansion during the middle Holocene by 50 – 300 km.

Climatic conditions during times younger than 5,600 years BP are characterised by generally decreased temperatures. [Claussen *et al.* \(1999b\)](#) were able to explain this cooling and drying after the Holocene climate optimum conditions with the changed Earth's orbit again. This result was valid for the northern regions, whereas the desertification of the North Africa area was assumed to be caused in terms of internal and regional vegetation- atmosphere feedbacks since orbital changes occurred rather smoothly than the desertification. Another interpretation was published by [Bond *et al.* \(1997\)](#) who found this cooling to be triggered by cold water masses penetrating the North Atlantic as inferred from ice rafted debris on the sea bottom. In consistence, several stages of deteriorated climatic conditions have been reported by [O'Brien *et al.* \(1995\)](#) who inferred periods of cooler temperatures between 5,300–4,400 as well as 2,900–2,400 years BP from a Greenland ice core.

A strongly increasing trend of human influence to the Earth climate must be finally expected for the most recent times, especially after the industrialisation, and further for the future. Representatively for the actual influences, the development of the atmospheric carbon dioxide concentration will be mentioned here. Resulting from the increasing combustion of fossil fuels, the concentration of this green house gas strongly increases and is believed to be able to cause an increase in

air temperatures and enhanced plant growth. [Brovkin *et al.* \(2003\)](#) accordingly calculated a doubling of the vegetation growth rate from 1 % to 2 % per decade under growing CO₂ content after a disequilibrium between the atmosphere and the vegetation. In consistency with that scenario of present-day climate development, [Zolitschka *et al.* \(2003\)](#) interpreted the melting of the 5,300 years old ice man „Ötzi“ ([Bonani *et al.*, 1992](#)) in 1991 out of glacier ice masses with temperatures up to that time being lower than during the Holocene period of optimum conditions.

1.2 Archives for Paleoenvironmental Studies

Table 1.1: Common archives and covered time range

Archive	Covered Time Range
Tree Year Rings	<10.000 years
Ice Cores	<500.000 years
Lacustrine Sediments	<5.000.000 years
Marine Sediments	>5.000.000 years

A number of archives recording environmental and climatic changes based on various proxy-data in different time scales and temporal resolutions were established in the past. Prominent representatives are listed in *Tab. 1.1*.

On the uppermost level, archives have to be separated into terrestrial and marine ones. Marine sediments have been most widely investigated, especially during the Ocean Drilling Project (ODP) and the Deep Sea Drilling Project (DSDP). Due to the major sedimentation of autochthonous organic matter contribution e.g. from planktonic algae and, as the secondary part of the food-chain, zooplankton as well as its wide distribution, marine sediments are characterised by relatively low sedimentation rates and organic carbon contents (Stein *et al.*, 1989; Stein, 1990). Higher primary production merely occurs in coastal regions, benefitting from terrestrial influx. Therefore, coastal sediments are the most important sinks of oceanic organic carbon (Berner, 1989). As a result of the continuous sedimentation, marine sediments serve as archives for global changes and, moreover, integrate the highest overall time range (cf. *Table 1.1*). Beside the information retrieved from organic carbon content, biomarkers serve as an important group of proxy-data. These chemical fossils only make up a trace quantity of the sedimentary organic matter (Tissot and Welte, 1984) but their original structures are either preserved or can be traced back to an unambiguous precursor compound. They can therefore be assigned to source organisms and/or source organism groups (e.g. Brassell, 1993). The known contribution of organisms to the sum of sedimentary organic matter and variations therein can be finally used to infer changes of environmental and/or climatic conditions.

Switching focus from the oceans to terrestrial systems, ice cores, e.g. from Greenland (GISP, GRIP), integrate atmospheric changes on a relatively large time scale

under high temporal resolution. Dansgaard *et al.* (1993) and Johnsen *et al.* (1997) used oxygen isotope data ($\delta^{18}\text{O}$) as proxy parameters for temperature reconstructions. A limiting aspect is the compaction of deeper ice layers by the pressure from overlying ice masses; the achievable temporal resolution as well as the absolute dating of investigated layers decrease and/or become more complicated with increasing core depth.

Tree year rings are another kind of terrestrial archives, reflecting environmental and climatic conditions under which the plant lived. The temporal integration is comparably low, usually in the range of a couple of hundred years. The temporal resolution on the other hand is very high due to the formation of a new ring every year. Proxy data can therefore be combined with single calendar years whereas an absolute dating becomes easiest on living trees. Typical proxy-data are the ring widths (Schweingruber, 1996) and various stable isotope data (Leavitt and Long, 1983).

The temporal integration of lake sediments is lower compared to marine sediments (cf. Table 1.1), but included terrestrial organic matter leads to increased sedimentation rates and organic carbon content. Thus, the achievable temporal resolution is in general higher than for marine sediments. Furthermore, exposure of sedimentary matter to oxidation is lower in lacustrine archives due to the less diverse benthos and lower depth of bioturbation (Meyers, 1997). Complicating facts in contrast to marine archives are the more influential disturbances, e.g. chemical composition of the lake water, water depth, being connected to turbulent sediment mixing, relative contribution of terrestrial clastics to the sedimentary matter, trophic state and oxygen consumption. All these parameters may vary by higher degree as observed for the more stable marine conditions. A great advantage of lacustrine archives in comparison with marine ones is finally the restriction of included proxy-parameters to changing environmental and/or climatic changes on a local to regional scale since the respective catchment areas limit sedimentary matter influx.

On this background, lacustrine sediments are regarded as excellent archives, recording several environmental or climatic conditions. A more detailed introduction of that group of sedimentary archives will follow in this section.

In addition to the bulk organic data, biomarkers serve as an important proxy data group. Summarising reviews of biomarker usage were published for example by Meyers and Ishiwatari (1993a), Meyers (1997), Meyers and Lallier-Vergès (1998) and Meyers (2003); a more detailed introduction of their use in paleolimnology will follow in *Section 1.3*.

1.2.1 Lake Sediments as Geological Archives

In general, two types of lakes have to be distinguished: hydrologically open and hydrologically closed lake systems. Important water sources are in both cases precipitation and inflow from the catchment area, the area that is drained by a river and all of its influxes both, on and below the surface into the lake. These sources are balanced by evaporation and outflow. The important feature of closed lake systems is that they do not have a permanent outflow and thus store organic matter more efficiently than those having that outflow. The water body is usually separated into three distinct layers which are characterised by different water temperatures and temperature gradients. The uppermost layer, called *epilimnion*, is strongly influenced by atmospheric temperatures. It is well mixed and thus oxygenated. The lowermost layer, called *hypolimnion*, is not affected by atmospheric influences and therefore cooler and less oxygenated to anoxic. Its water temperature is generally lower than that of the epilimnion. Between them, a third layer, called *metalimnion*, marks the border between the two major water layers. It is characterised by a high temperature gradient.

The stratification as described above can be disturbed due to water cooling and/or wind during autumn (*autumn circulation*). Depending on the degree of the seasonal temperature change, this circulation may affect the whole water body (*holomixis*) which leads to oxygenated bottom waters. A second circulation may occur during the spring warming; these lakes are called *dimictic*.

After formation, e. g. after the last Pleistocene glaciation by melting ice masses or by volcanic eruptions, lakes accumulate sedimentary matter. Most dominant sources are clastics and organic input with the water influx from the catchment area (*allochthonous* sedimentary matter), direct input of organic matter from surrounding vegetation and bioproductivity in the water body itself (*autochthonous* sedimentary matter, e. g. from macrophyte plants, algae, bacteria). An impressive

example is Lake Baikal in Siberia where approximately 7,500 m of sediment have been accumulated (Hutchinson *et al.*, 1992). The initial sediment bodies are well stratified resulting from the typical seasonal cycle and if the oxygen supply to the sediment is limited. This feature, however, is missed in more equatorial regions with less dominant divergences between the seasons.

During sinking through the water column and further after the sedimentation, organic matter undergoes biochemical transformation (*diagenesis*). Typical biochemical processes are sulfate- and nitrate reduction or methanogenesis. The initial chemical composition is changed hereby, but known pathways also allow to trace back diagenetic products to distinct precursor compounds. They may therefore equally serve as proxy-compounds.

Another form of sedimentary matter change is due to microbial mixing (*bioturbation*) and/or reworking that analogously depends on oxygen supply to the water/sediment surface. It not necessarily changes the chemical composition, but at least the layered structure will be lost leading to increased difficulties in terms of dating and reduced temporal resolution. Thus, lacustrine sedimentary archives best preserve the initial composition and morphological structure under oxygen poor to anoxic conditions. Maar lake basins, a special morphological appearance of volcanic activity, ideally fit this prerequisite and will be introduced in more detail in *Section 1.2.2*.

1.2.2 Maar Lakes

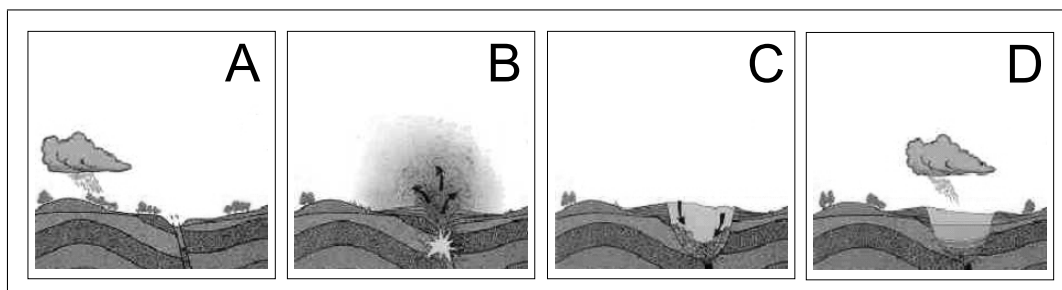


Figure 1.3: Formation of maar lake basins

Crater and maar lakes are the two possible morphological appearances of volcanic activity. In most cases, molten lava reaches the earth surface, and piles are heaped up to form a crater. If this crater becomes closed during the actual or a later eruption as well as by assailing parts of the rock face, a crater lake may arise depending on the local precipitation stage. On account of their origin, crater lakes are hydrologically closed and lake levels are compulsorily higher than the surrounding ground level.

Maar lakes are formed by a different mechanism, and that is when upstreaming lava meets ground water layers before reaching the Earth surface (*cf.* Fig. 1.3 A). Subterranean eruptions occur due to the huge thermal difference between both media resulting in a high pressure that is built up from evaporated water. Cavities are formed under the Earth surface (*cf.* Fig. 1.3 B). If the material situated above the formed cavities becomes unstable during the actual or a following eruption, these cavities may tumble down resulting in a crater whose base is lower than the former ground level (*cf.* Fig. 1.3 C). Lakes may arise within the so formed basins by contact to ground water layers as well as filling up with precipitation water from the catchment area (*cf.* Fig. 1.3 D). Consequently, the position of the lake bottom in relation to the surrounding ground level is the most important criterion for distinguishing between crater lakes and maar lakes.

It is not necessarily required that maar lakes are formed in their final shape during one single eruption. Instead, they may be built up by a series of eruptions with a high temporal distance. Lorenz (1984) for example assumed a series of eruptions approximately 1,000 – 1,500 m below the Earth surface during several months



Figure 1.4: Sampled half-core section

having formed the Meerfelder Maar. The collapse of the subterranean cavity accordingly occurred during this series of eruptions.

Especially maar lakes are well suited for the planned investigations on account of the relationship between surface and water depth: As a result of the small ratio of diameter *vs.* depth, oxygen supply to bottom waters is often limited leading to reduced biodegradation and bioturbation. Therefore, maar lakes may be regarded as ideal archives for paleolimnological studies using organic-geochemical methods. Additionally, the catchment area is relatively small and sharply separated compared to other lakes due to the setting of the former surface line during maar lake formation. Thus, only molecular fossils from a small area are preserved in the sedimentary record. Influxes and effluxes are small or are completely absent. Lake Holzmaar in the Eifel Volcanic field as an example was found to serve as an highly effective sediment trap with an only 2 – 7 % sedimentary matter loss rate by efflux in relation to influxes (Negendank and Zolitschka, 1993a). Therefore, a nearly undisturbed sedimentation is developed and the resulting sediments are laminated up to distinguishable seasonal layers. These varves can be used for dating, on the other hand, they allow a time scale resolution not achieved up to now by means of paleolimnological investigations. An exemplary half-core section from Lake Meerfelder Maar is given in *Fig. 1.4*.

Zolitschka (1989) has published a detailed description of the formation of these individual varve layers, an illustration is given in *Fig. 1.5*. Accordingly, an early spring time layer consists of Chrysophyceae cysts, followed by diatoms accompanied by blossom layers, e. g. hazel, blooming between February and April. Pine pollen are identifiable too, blooming time is between May and June. The midsummer layers are characterised by calcite which is felled authigenically since there are no carbonate outcrops in the catchment area. Therefore it is not to

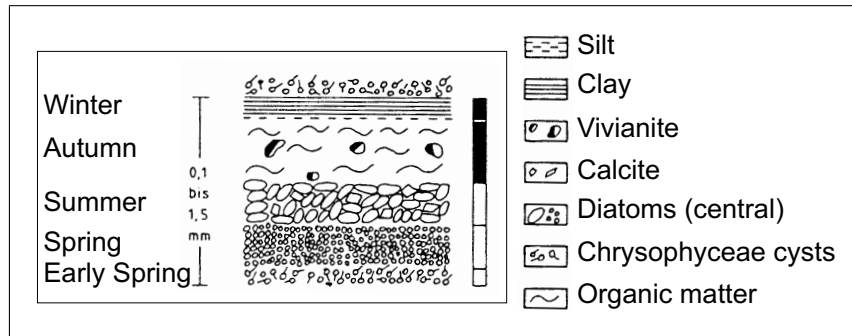


Figure 1.5: One year varve after Zolitschka (1989)

be gone out by detrital calcareous spars. The organic substance examined here mainly sediments in the autumn and, finally, a one year varve is completed with clastic components (silt, clay). Based on these findings, the varve structure of laminated sediments allows a precise sample dating and, moreover, a comparably high temporal resolution of geochemical investigation.

A further argument for choosing maar lake sediments out of the terrestrial archives is the large number of available scientific investigations, especially dealing with the Eifel Maar Lakes, that can be used for correlation of the planned lipid inventarisation. Based on the oxygen-poor to anoxic conditions at the water/sediment interface, that lead to annually separated sediment layers during wide parts of maar lake profiles (Zolitschka *et al.*, 2000; Brauer *et al.*, 1999b), a detailed varve chronology is available for Lake Holzmaar and Lake Meerfelder Maar. Thus, temporal resolutions up to calendar year scales in correlation to absolute ages are possible. Moreover, extensive pollen analysis for both maar lakes providing insight into the terrestrial vegetation development in very detail are available (Litt and Stebich, 1999; Litt, 2000; Litt *et al.*, 2001).

1.3 Organic Matter as Paleolimnological Indicator

Typical proxy-data used in paleolimnology are varve chronologies, bulk organic geochemical parameters (e. g. TOC, TIC, TN), inorganic elemental compositions, Rock-Eval hydrogen- and oxygen parameters, bulk- and compound specific isotopic compositions, pollen compositions, pigment compositions, compositions of lignin derived derivatives and lipid distributions.

Varve Chronologies can be recorded from annually laminated archives and for example give information on the sediment accumulation during times by the thickness of individual layers. They additionally provide an important framework for further interpretation of proxy data since the data can be assigned to exact calendar dates by counting techniques.

Bulk Organic Geochemical Parameters are usually fundamental proxies with a limited source specification. Total organic carbon (TOC) for example reflects the amount of organic matter supply to the sedimentary record whereas total inorganic carbon (TIC) basically represents the degree of mineral deposition. Since these data are not source specific, an interpretation in terms of paleolimnology, however, remains difficult. Nevertheless, [Tenzer *et al.* \(1997\)](#) distinguished between autochthonous and allochthonous organic matter contribution to the sediment of Pyramid Lake, Nevada based on water depth and organic carbon content. The dependency between organic carbon content and the distance from the shore due to varying organic matter sources were figured out by [Talbot and Laerdal \(2000\)](#) upon sedimentary matter of Lake Victoria, East Africa.

Total nitrogen concentrations are commonly interpreted in relation to TOC; a general difference in this ratio exists between algal and land plant derived organic matter. The first named organic matter type is enriched in proteins determining C/N ratios between four to ten whereas land plants typically contain high proportions of carbon-rich cellulose leading to ratios of 20 and higher.

Rock-Eval Pyrolysis was introduced by [Espitalié *et al.* \(1977\)](#) for the estimation of oil and gas generation potential during exploration. In context with paleolimnological studies the Hydrogen Index (HI) is of special interest. It reflects the amount of volatile organic hydrocarbons that can be generated from bulk sedimentary matter by pyrolysis. High HI values are typical for algally derived organic matter or cuticular leaf waxes whereas land plant derived organic matter is characterised

by higher oxygen content resulting in lower HI and higher OI values (Oxygen Index, the second Rock-Eval parameter reflecting the amount of carbon dioxide generated during pyrolysis). The usability of Rock-Eval parameters as paleolimnological indicators was discussed in detail for example by [Talbot and Livingstone \(1989\)](#), [Ariztegui *et al.* \(1996\)](#), [Wilkes *et al.* \(1999\)](#) and [Ariztegui *et al.* \(2001\)](#).

Pollen Assemblages of sedimentary records bear highly specific information, especially about the terrestrial plant diversity and abundance in the respective catchment. Even if the determination of pollen diagrams is often very work-extensive, they are very useful to reconstruct changes in the plant community that can be traced back to climatic changes. A large number of pollen diagrams exists for various terrestrial archives, also for the lake sediments investigated during this study ([Litt and Stebich, 1999](#); [Litt, 2000](#); [Litt *et al.*, 2001](#); [Giesecke, 1999](#)). As shown by [Schwark *et al.* \(2002\)](#), pollen compositions can be useful combined with lipid distributions to determine climatic shifts.

Pigment compositions originate from algae, microbes and higher plants. The most prominent representative by far is chlorophyll *a*, but a variety of carotenoids is synthesised especially by aquatic plants to carry out photosynthesis under the lack of red wavelength light. The usage of pigment distributions for the reconstruction of paleovegetational assemblages may be limited due to the probable postdepositional modification since all of these compounds contain multiple unsaturations which are usually easy to attack.

Nevertheless, a number of studies using pigment compositions exists, [Griffiths \(1978\)](#) for example reconstructed the changing trophic state of Eastwaite Water using carotenoids of blue-green algae. More recently, [Schouten *et al.* \(2001\)](#) detected changing carotenoid compositions in sediments of Ace Lake, Antarctica and concluded a change in the bacterial community of this lake based on climatic shift.

Lignin Derivatives are phenolic polymers synthesised by all living vascular plants. Most of them are of terrestrial nature, an exception are emergent macrophytes. General differences in the structure of synthesised lignins exist between angiosperms and gymnosperms ([Hedges and Mann, 1979](#)), but macromolecules of both sources are relatively resistant against diagenetic attack. They therefore preserve the development of the terrestrial vegetation that can be reconstructed

using phenolic monomer ratios after cracking the macromolecules by cupric oxide oxidation. Common parameters are the C/V (cinnamyl/vanillyl) and S/V (syringyl/vanillyl) ratios with cinnamyl being the sum of *p*-coumaric and ferrulic acid, vanillyl the sum of all three vanillyl phenols and syringyl the sum of all three syringyl phenols. Non-woody land plants are characterised by high C/V ratios whereas gymnosperm sources of sedimentary matter are distinguished from angiosperm ones by low S/V values. Based on this framework, [Hedges *et al.* \(1982\)](#) reconstructed the change from dominant grass vegetation via angiosperm woody vegetation towards a dominant conifer coverage in the catchment of Lake Washington after the Lateglacial.

Lipids are one of the major pools of organic carbon in all living organisms. They are mainly used as constituents of biological membranes (e.g. phospholipids), for energy storage (e.g. triglycerides) and as structural components in the cuticular waxes of all higher plants. Compared to other abundant fractions of biogenic organic matter (for example polysaccharides and proteins), they are often more resistant against biotic and abiotic degradation processes. They therefore may be well preserved in sediments as a source of information about the organisms which contributed to the sedimentary organic matter. Additionally, many lipids are specific indicators of their respective source organisms adopting their lipid composition to changing environmental and climatic conditions. Thus, lipid biomarkers as chemical fossils can provide information about the organisms which are not preserved in the sedimentary record themselves and the conditions under which these organisms lived. After their death, all types of organisms, living in any environment under different environmental and climatic conditions, contribute to the sedimentary matter as a minor constituent beside the bulk fraction consisting of minerals. Since this lipid composition varies between the different kinds of living organisms and, furthermore, reflects environmental impacts, these molecules can be used as proxy data to reconstruct population developments and environmental conditions.

The sum of established marker molecules can be divided into several groups, regarding the depositional environment (marine *vs.* lacustrine), the type of source organisms (e.g. terrestrial *vs.* aquatic; bacteria *vs.* algae), the chemical classification (e.g. aliphatic *vs.* aromatic hydrocarbons, alcohols, carboxylic acids) and the depositional origin (biosynthetic *vs.* diagenetic). The analysis of sedimen-

tary organic matter therefore allows a detailed multi-parameter reconstruction of paleo-ecosystems, including their compositions from individual organism types and compositional variations. Because all species are adopted to a defined range of environmental conditions, the knowledge about the composition of an ecosystem from various types of organisms allows inferences to environment and climate during the organisms life time. Sedimentation rates and primary productivity of lakes are generally higher compared to the oceans. Thus, the quantity of sedimentary matter provided in lacustrine sedimentary archives is higher and also short term variations of climatic and/or environmental conditions become detectable using distributions of lipid biomarkers as proxy data.

A wide range of lipid marker molecules is known today. An outstanding example for marine biomarkers is the distribution of long chain alkenones, mainly originating from the alga *Emiliania huxleyi* (Volkman *et al.*, 1980a,b). This species controls its cell membrane flexibility depending on the water temperature by varying the number of unsaturated carbon-carbon bonds (Prahl and Wakeham, 1987). Thus, the ratio between those alkenones having two, three or four sites of unsaturation (U_{37}^k ; $U_{37}^{k'}$) can be used for the reconstruction of marine sea surface temperatures (Brassell *et al.*, 1986; Brassell, 1993). Based on culture experiments, linear equations were determined for calculation of sea surface temperatures (Prahl and Wakeham, 1987; Prahl *et al.*, 1988; Volkman *et al.*, 1995).

A limiting aspect of alkenone based paleo-thermometry is the restriction of the habitat of *Emiliania huxleyi* to marine systems. Even if these compounds were recently detected in lacustrine archives, for example in sediments of Lake Steisslingen, Germany (Zink, 2000), and used for the reconstruction of paleotemperatures, the origin of these compounds is still discussed.

Lake sediments have been investigated extensively with respect to the development of terrestrial ecosystems. Meyers and Lallier-Vergès (1998) for example reviewed bulk organic matter compositions of quaternary lacustrine sediments as proxy parameters for changing climate. Attention was also focussed on early diagenetic alteration of sedimentary organic matter (Meyers and Ishiwatari, 1993a).

Proxy parameter evaluations using distributions of lipid biomarkers have often focussed on certain compound classes as they will be introduced here.

n-**Alkanes** are widespread lipid biomarkers in marine and terrestrial archives. In addition to direct input to the sedimentary record, degradation of precursor compounds is a second source (Tissot and Welte, 1984). Due to the relatively simple structure of the members of this compound class, *n*-alkane distributions have been widely investigated in various types of possible source organisms as well as in sedimentary settings. A pronounced content of short chain length *n*-alkanes showing a typical odd-over-even predominance is often limited to autochthonous organic matter contributors (algae, bacteria) (Nishimoto, 1974; Weete, 1976).

The typical carbon number range of *n*-alkanes between C₁₅-C₂₁ was detected in algae (Clark and Blumer, 1967; Blumer *et al.*, 1971). Out of this chain length range, the C₁₇ homologue was found to be the dominant *n*-alkane in green algae beside single and twice unsaturated homologues (Youngblood and Blumer, 1973; Gelpi *et al.*, 1970). Brown algal derived *n*-alkane fractions contrastingly maximise at the C₁₅ homologue and show more dominant proportions of unsaturated C₂₁ alkenes (Youngblood and Blumer, 1973). In the case of blue-green algae of marine nature, the detectable *n*-alkane chain length range is limited to C₁₅-C₁₉ (Gelpi *et al.*, 1970).

Despite these general findings, some deviations for individual species are known. Gelpi *et al.* (1968) for example report on high molecular weight (C₂₇-C₃₁) *n*-alkenes in *Botryococcus braunii*. Nichols *et al.* (1988) detected aquatic derived *n*-alkanes in Antarctic diatoms which did not show the pronounced odd over even predominance.

Long chain homologues are dominant constituents of higher land plant leaf waxes where they protect from water loss (Eglinton and Hamilton, 1967; Kolattukudy *et al.*, 1976). Terrestrial derived *n*-alkane distributions are characterised by a marked odd-over-even predominance (Eglinton and Hamilton, 1967; Collister *et al.*, 1994). The chain length range for terrestrial derived *n*-alkanes can be further subdivided with respect to their sources. High amounts of the C₃₁ homologue point to grasses as dominant organic matter sources whereas the shorter chain length derivatives C₂₇ and C₂₉ were found to mainly originate from tree-leaves (Cranwell, 1973a). Conifers were additionally identified as a prominent source of the C₃₁ *n*-alkane (Herbin and Robins, 1968).

Despite the widespread sources of *n*-alkanes making a source assignment relatively complicated, a number of studies exists. Especially during the last decade, *n*-

alkane distributions were frequently used as a tool to distinguish between aquatic and terrestrial organic matter input to sedimentary archives and, moreover, to specify terrestrial sources as well as climatically driven changes between them in more detail. Note at this place, that these studies not primary focus on individual source organisms of individual *n*-alkanes; the potential of complex *n*-alkane fractions is rather evaluated to reconstruct climatically and/or environmentally driven changes in the community of organic matter contributors to sedimentary archives. An overview of these approaches is given in the following.

A well investigated lacustrine setting is the Green River Formation, Wyoming, USA, an important petroleum reservoir. [Horsfield *et al.* \(1994\)](#) for example reported on bulk organic geochemical data as well as hydrocarbon compositions of the Laney Shale and the Luman Tongue, two members of this formation which clearly differ in relation to different climatic and limnologic conditions and separate the hydrologically closed, alkaline lake system from the freshwater lake. Low hopane/sterane ratios and predominant tricyclic terpenoids in comparison to pentacyclic homologues were traced back to the high alkalinity and salinity of the Laney Shale, which was deposited under arid conditions while opposite trends became obvious for the Luman Tongue, which was deposited under a humid climate.

[Ficken *et al.* \(1998a, 2000, 2002\)](#) extensively use abundances and isotopic compositions of normal chain lipids (*n*-alkanes, *n*-fatty acids, *n*-alcohols) for organic matter source assignment in lacustrine archives. An important result is the P_{aq} parameter ([Ficken *et al.*, 2000](#)) which quantifies aquatic macrophyte contribution to the sedimentary organic matter in relation to land plants. The parameter was defined after analysis of *n*-alkane distributions of submerged and emergent macrophytes as well as terrestrial vegetation around Lake Mt. Kenya, Africa. Relatively high proportions of mid-chain homologues in the chain length range from C₂₃ to C₂₅ were detected for the submerged macrophytes (*cf.* [Fig. 1.6](#)). Emergent species and land plants contrastingly yielded elevated percentages of longer chain *n*-alkanes >C₂₉. Known changes especially of aquatic and land plant vegetation composition further allow a correlation to changing environmental and/or climatic conditions.

In a similar way, [Nott *et al.* \(2000\)](#) use medium chain length *n*-alkane ratios from a peat profile from Bolton Fell Moss, UK to quantify the contribution of macro-

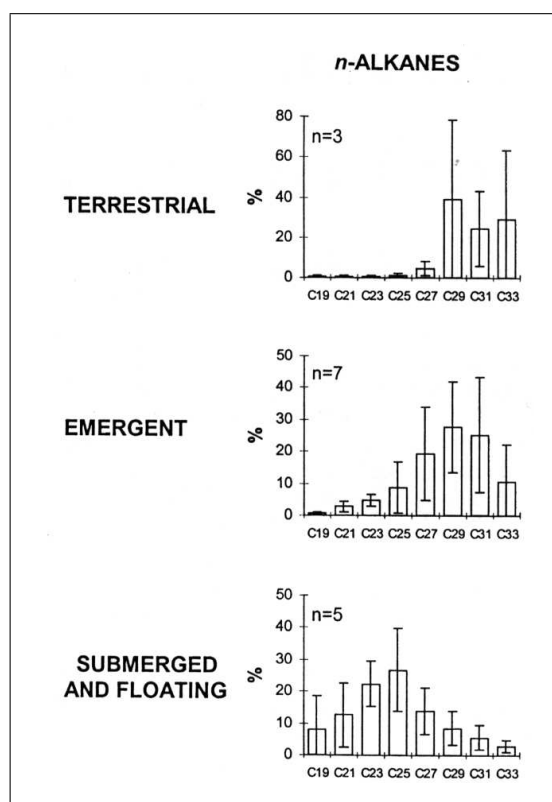


Figure 1.6: *n*-Alkane distribution of macrophytes and land plants as published by Ficken *et al.* (2000)

phyte derived sedimentary organic matter that can be traced back to changing climatic conditions in turn.

More specialised, Brincat *et al.* (2000) reconstructed the climatically induced tree vegetation establishment surrounding Lake Baikal at the Last Glacial/Holocene transition based on relative proportions of two long chain *n*-alkanes (*cf.* Fig. 1.7). The obvious shift of the C₂₇ *vs.* C₃₁ *n*-alkane ratio, indicating the establishment of a forest dominated vegetation type during the Holocene in the catchment of Lake Baikal was found to coincide with changes (i) the total organic carbon content (Ishiwatari *et al.*, 1992), (ii) the ¹³C isotopic composition of total organic carbon (Ishiwatari *et al.*, 1992), (iii) the pollen assemblage as described by Fuji (1992) and (iv) the lithology as described by Takemura *et al.* (1992).

Schwark *et al.* (2002) measured different proportions of C₂₇, C₂₉ and C₃₁ *n*-alkanes in sediments of Lake Steisslingen, Germany. According to the assignment of the

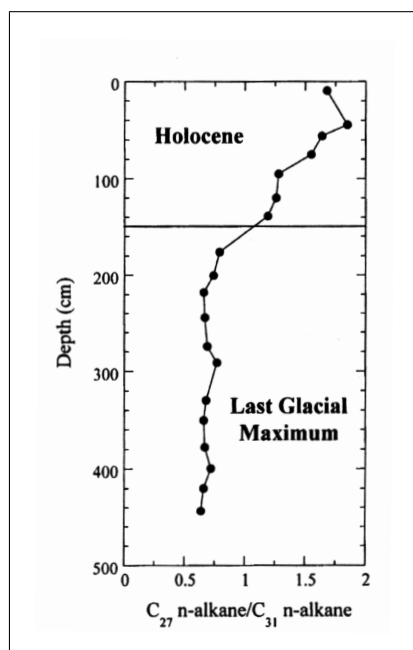


Figure 1.7: C_{27} *n*-alkane concentration relative to the C_{31} homologue of Lake Baikal sediments as published by Brincat *et al.* (2000)

individual homologues to the respective source plants, the illustration of the the *n*-alkane percentages in a ternary plot (*cf.* Fig. 1.8) allowed a reconstruction of the land vegetation development in the catchment area of Lake Steisslingen. This evolution could be further correlated to variations yielded from pollen analysis of the same archive. As an interesting feature, the study yielded evidence for a warming interval during the Younger Dryas period, expressed by elevated C_{27} *n*-alkane concentrations and betula pollen.

Fatty Acids are constituents of the widespread triglycerides as these compounds are synthesised from all living organisms for energy storage. Even numbered short chain homologues from *n*- C_{16} to *n*- C_{18} are ubiquitous biotic compounds (Meyers, 2003) and therefore do not bear source related information. Nevertheless, occurrence of fatty acids in planktonic algae is limited to the short chain length range between C_{14} - C_{18} (Schneider *et al.*, 1970) with a typical even over odd predominance (Holton *et al.*, 1964, 1968). Thus, a lack in longer chain fatty acids may point to an important autochthonous contribution to the sedimentary organic matter.

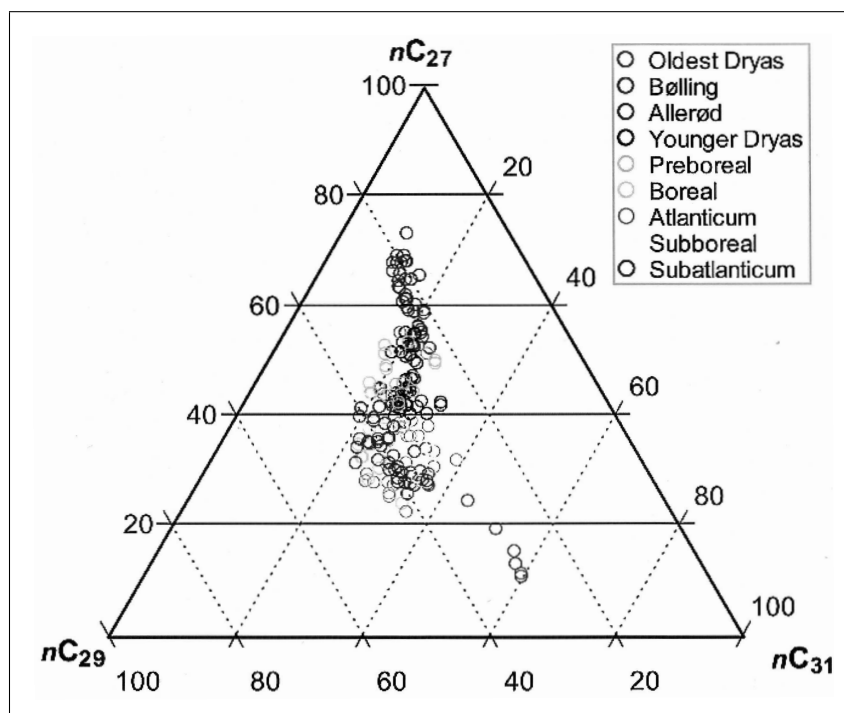


Figure 1.8: Ternary plot of n -alkane percentages as published by Schwark *et al.* (2002)

Higher land plants preferentially contain longer chain length fatty acids (C_{24} to C_{30}) with dominant even numbered homologues as cuticular waxy esters (Eglinton and Hamilton, 1967; Cranwell, 1974). These compounds therefore represent the land plant derived organic matter supply to the sedimentary matter.

Unsaturated n - C_{16} - C_{18} homologues are frequently found in freshwater algae, but they are rapidly reworked during sedimentation and even after incorporation to the sedimentary body (Cranwell, 1976) resulting in a modified acid composition (Cranwell *et al.*, 1987). The n - C_{15} and *anteiso* C_{15} acids are synthesised by microbes from primary organic matter (Cranwell, 1973a). Their abundances thus reflect the degree of microbial organic matter reworking. The higher susceptibility of fatty acids to degradation in comparison with other lipid classes is of general character (Meyers and Ishiwatari, 1993a); Matsuda and Koyama (1977a,b) compared the downcore concentrations of fatty acids in relation to total organic carbon in a sediment core of Lake Suwa, Japan. Concentrations of long chain homologues between n - C_{24} - n - C_{28} were found to decrease only little in relation to TOC. Contrastingly, a more marked reduction was detected for the short chain homologues n - C_{15} , n - C_{16} and n - C_{18} in relation to TOC with increasing profile

depth. Reworking of the initial fatty acid content was figured out to be a reason for this reduction beside changing sources of sedimentary fatty acids. Analogously Haddad *et al.* (1992) report these short chain fatty acids to be degraded six to seven times faster in comparison to long chain homologues based on fatty acid distributions of a coastal marine sediment of the Cape Lookout Bight. Meyers and Eadie (1993) calculated the remineralisation rates of fatty acids being ten times higher as for *n*-alkanes and Kawamura *et al.* (1980) detected a loss of unsaturated fatty acids in comparison to their saturated homologues by factor 10 in the uppermost 8 cm sediment layer of a Japanese lake.

Because of these facts and the broad occurrence in all living organisms, the relevance of fatty acids as indicators for organic matter reworking seems to be more important than that as indicators for the initial organic matter contributors. Consequently, Wilkes *et al.* (1999) used an UR_{FA} ratio of unsaturated *vs.* saturated C_{18} fatty acids to demonstrate the good preservation state of sedimentary organic matter from Lake Lago di Mezzano, Italy.

Sedimentary **Alcoholic Compounds** are usually subdivided into two general subgroups: *n*-alcohols and sterols. The first named are wide spread in sedimentary archives and in case of the longer chain homologues (C_{22} to C_{30}) with a prominent even-over-odd predominance originate from the waxy esters of higher land plant leaves (Eglinton and Hamilton, 1967; Rieley *et al.*, 1991). These are hydrolytically cracked after sedimentation making the free *n*-alcohols detectable in the sedimentary record.

Aquatic algae and bacteria contribute shorter chain length homologues to the sedimentary organic matter. Typical chain length ranges are between *n*- C_{14} to *n*- C_{22} (Robinson *et al.*, 1984a; Volkman *et al.*, 1999), Schulte (1997) interpreted increased C_{14} to C_{18} *n*-alcohol abundances as indicators for marine algal derived organic matter contribution. To less dominant extend, however, also long chain *n*-alkanols were detected in bacteria and phytoplankton e.g. by Volkman *et al.* (1999) in the chain length range between C_{22} to C_{28} .

Recent studies using *n*-alkanol distributions as indicators for organic matter sources were published for example by Ficken *et al.* (1998b, 2000), where these compounds beside other abundant *n*-alkyl lipids evidence varying contributions of algae, macrophytes and land plants to the sediment of Lake Nkunga, Africa (*cf.* Fig. 1.9) based on their carbon number distribution. Especially prominent abun-

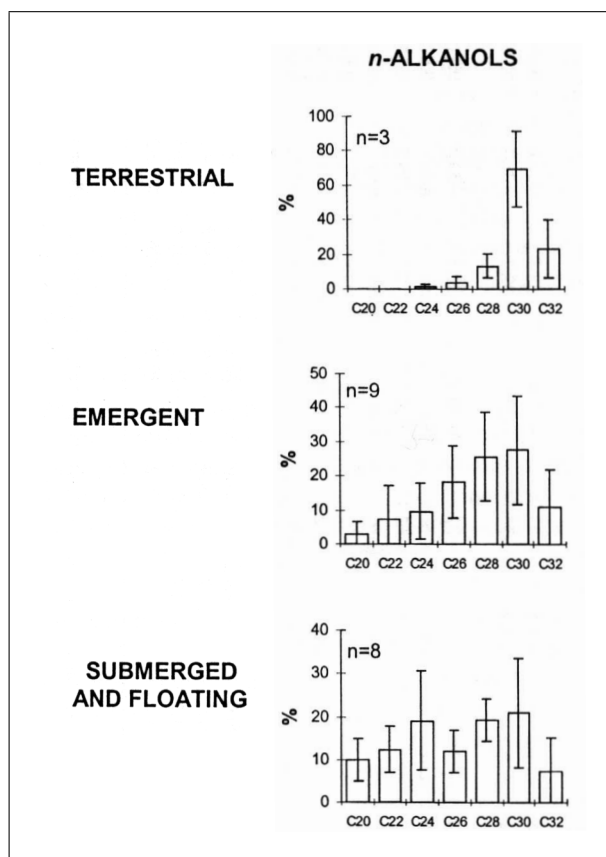


Figure 1.9: *n*-Alcohol distributions of macrophytes and land plants as published by Ficken *et al.* (2000)

dances of the C₂₄ homologue were interpreted with enhanced macrophyte and/or cyanobacteria growth. Filley *et al.* (2001) used high concentrations of the same compound in younger sediments of Mud Lake, Florida as evidence for enhanced activity of cyanobacteria after relatively dry conditions during the early Holocene.

Sterols build up a highly complex group of biomarkers. They are in general synthesised from squalene epoxide by cyclisation in all eucaryotic organisms, but biosynthetic pathways differ between land plants and algae on the one hand and animals and fungi on the other hand (*cf.* Fig. 1.10). Structural differences consist of the number of carbon atoms, saturation state, methyl groups in the base carbon skeleton as well as the side-chain and stereochemistry (Volkman, 1986).

Assignment of single derivatives to distinct sources is difficult, but in general C₂₇ and C₂₉ sterols have been evaluated as indicators for algae and land plants,

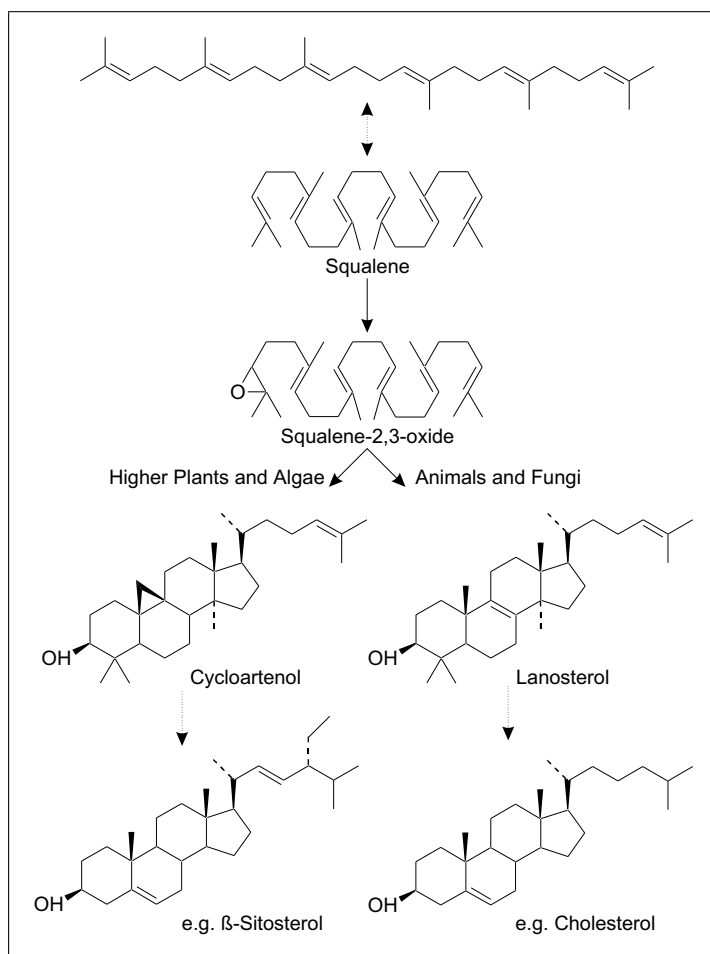


Figure 1.10: Biosynthetic pathway of sterol synthesis, modified after [Killops and Killops \(1993\)](#)

respectively, in case of marine sediments ([Huang and Meinschein, 1976, 1979](#)). This general criterion can also be applied for terrestrial settings as published by [Nishimura and Koyama \(1977\)](#). Based on this assignment, [Huang and Meinschein \(1979\)](#) used a ternary plot illustrating relative contributions of C₂₇-, C₂₈- and C₂₉ sterols (*cf. Fig. 1.11 A*). Even if this relatively easy approach fits in most cases, some deviations exist. Marine phytoplankton and lacustrine algae were found to synthesise also C₂₉ sterols (ethylsterols) as published by [Volkman \(1986\)](#). [Matsumoto *et al.* \(1982\)](#) for example detected 24-ethylcholesterol, a C₂₉ sterol, to be a major constituent in lake sediments of Victoria Land, Antarctica despite the lack of higher land plants in the catchment area. Thus, blue-green algae were identified as appropriate sterol sources. More recently, [Matsumoto *et al.* \(2001\)](#) investigated the $\delta^{13}\text{C}$ isotopic composition of this compound in Japan Sea

sediments over the last 30,000 years. The results yield a shift in the isotopic composition in correlation to climatic change in that region. Accordingly, the data suggest a marine source of 24-ethylcholesterol after the Last Glacial period whereas a terrestrial origin was taken into account for glacial sediments.

Robinson *et al.* (1984b) identified dinosterol, a C₃₀ sterol, to be derived from lacustrine dinoflagellate algae, but marine prymnesiophyte algae and the marine diatom *Navicula* species are also known as appropriate source organisms (Volkman *et al.*, 1990, 1993). Ariztegui *et al.* (1996) used varying dinosterol content in sediments of the alpine Lake St. Moritz, Switzerland, for the reconstruction of the primary productivity during Holocene and Wilkes *et al.* (1999) used abundances of two C₃₀ sterols in relation to β -sitosterol and stigmastanol, which were believed to be land plant derived C₂₉ homologues, to distinguish between aquatic and terrestrial derived organic matter supply to the sediment of Lake Lago di Mezzano, central Italy. In opposition, Barrett *et al.* (1995) detected considerable amounts of β -sitosterol in the diatom *Haslea ostrearia*. Volkman (1986) thus summarises, that high amounts of C₂₉ sterols not necessarily indicate a dominant terrestrial organic matter contribution to the sedimentary body.

Considering that kind of complication during the initial carbon number based source assignment of sterols to source groups, Schulte (1997) suggested that the ternary plot of C₂₇ to C₂₉ sterols needs to be interpreted carefully since important C₃₀ homologues are neglected and thus argued for a modification of the sterol ternary plot used by Huang and Meinschein (1979) by adding the C₃₀ sterols to the C₂₈ sterol group. This approach allows a distinction of dominant marine *vs.* terrestrial organic matter sources as illustrated in Fig. 1.11 B.

The Cholesterol out of the C₂₇ sterols is a typical marker molecule for zooplankton derived organic matter supply (*cf. sterol synthesis as illustrated in Fig. 1.10*). Even if this compound can not be synthesised by all types of zooplankton themselves (Goad, 1981), its concentration becomes enriched after passing the organisms in relation to the algal diet (Harvey *et al.*, 1987).

Despite the initially assumed lower source specificity of C₂₈ sterols, brassicasterol was recently found in several diatom species (Volkman, 1986; Barrett *et al.*, 1995) and thus used as a specific biomarker for diatom derived organic matter.

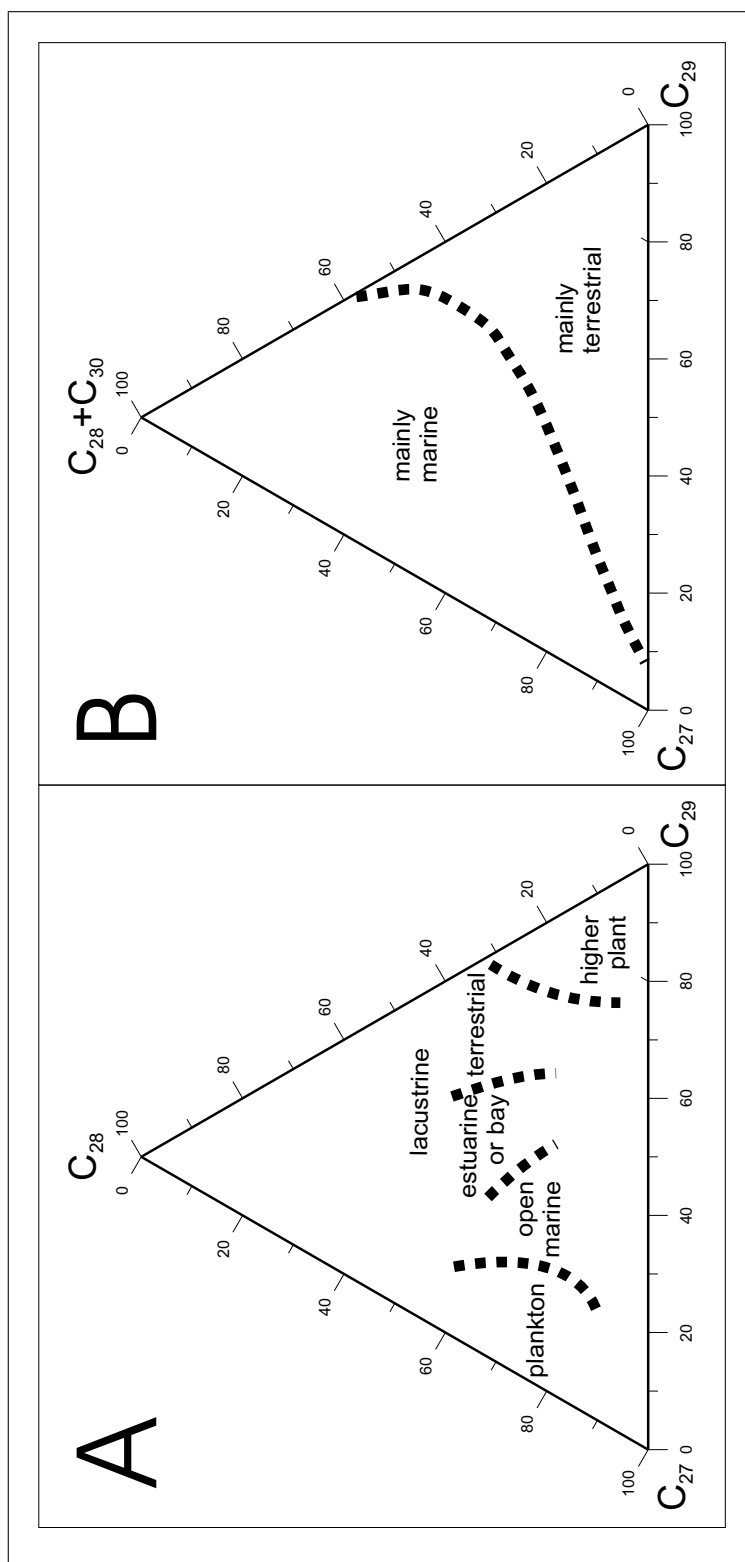


Figure 1.11: Carbon number based source assignment of sterols after [Huang and Meinschein \(1979\)](#) (A) and [Schulte \(1997\)](#) (B)

2 Objectives

Anoxic and annually laminated sediments of crater lakes are regarded as ideal archives for the investigation of biomarkers as indicators of paleoclimatic and paleoenvironmental conditions. At least three aspects are of major importance in this context:

- Lacustrine sediments are often organic rich in comparison to marine sediments and thus contain a variety of paleolimnological and paleoecological information
- The relatively high sedimentation rates as well as the relatively high organic carbon content allow a temporal resolution that can not be easily reached using other, e. g. marine, archives
- Anoxic conditions lead to enhanced organic matter preservation. Thus, the original paleolimnological and paleoecological signal is not overprinted by diagenetic transformation to a high extend

Beside the comprehensive knowledge of Eifel Maar Lake sediments, western Germany, e.g. in terms of sedimentology, varve counting, and dating, a detailed organic-geochemical characterisation of these sediments is not available up to now. The study presented in this thesis therefore has three major objectives:

- Determination of usual bulk organic geochemical and Rock-Eval parameters as a base for the subsequent lipid-geochemical investigation

- Complete inventarisation of lipid biomarkers in anoxic laminated sediments of Eifel Maar Lakes and their evaluation as environmental and/or climatic proxies
- Application of biomarkers and/or biomarker-parameters for the reconstruction of paleolimnological and paleoecological conditions under temporal resolution as high as possible on a selected time slice

Since no comparable lipid data of Eifel Maar lakes exist up to now, the first step of this work consists of an as complete as possible inventarisation of detectable lipids to reach an extensive qualitative and quantitative characterisation on a limited sample set. To consider local to regional variations, two Eifel Maar Lakes, Lake Holzmaar and Lake Meerfelder Maar in the western German Eifel Volcanic Field as well as Lake Großer Treppensee, eastern Brandenburg, were included into this study.

The findings of this step should further be applied to a higher resolved sample set, which had to be selected based on the results of the first stage, also considering periods of important climatic and/or environmental change in the respective catchment area. Therefore, an approximately 2,500 calendar year section of Lake Meerfelder Maars sedimentary was selected, including the Younger Dryas period, an intermediate cooling between the last European glaciation and Holocene age as well as the transition to this period of ameliorated climatic conditions.

3 Study Areas and Samples



Figure 3.1: Location of investigated lakes

Under investigation were two volcanic maar lakes in the Westeifel Volcanic Field, Lake Holzmaar and Lake Meerfelder Maar, as well as Lake Großer Treppensee, which was formed at the outgoing Lateglacial in south east Brandenburg, Germany. Geographical positions of investigated lakes are given in *Fig. 3.1*.

Both maar lakes lie in close proximity to one another but were formed at different times and have different catchment areas. This gives the opportunity to examine

the influence of local peculiarities on the composition of the sedimentary organic matter.

In order to consider a broader spectrum of natural environmental and climate variability in this study, a third profile section from Lake Großer Treppensee was included as well. This lake represents a different type of archive, age and origin history. Additionally, the catchment area of this lake is more extensive by far compared to the Eifel Maar Lakes under investigation. Thus, the sedimentary record is believed to preserve information about the allochthonous productivity from a much wider area and to provide insight to the development of terrestrial vegetation forms on a more regional scale.

3.1 Eifel Maar Lakes

About 60 maar craters are known in the Westeifel Volcanic Field, and nine of them are water filled today. The others are dry maars.

Scientific publications dealing with the Eifel Maar Lakes can be traced back to 1821 ([Steininger, 1821](#)), the first limnological investigations were published by [Halbfass \(1896, 1897\)](#). Based on observations of different water colors, water temperatures and temperature stratification, oxygen content as well as diatom and plankton counting studies, [Thienemann \(1913, 1914, 1917\)](#) further subdivided the water filled Eifel Maar Lakes into two groups. Accordingly, the investigated Lakes Holzmaar and Meerfelder Maar as well as Lake Schalkenmehrener Maar are characterised by higher water temperatures, yellow to green colored water that points to an increased amount of dissolved humic substances, and higher plankton productivity. The opposite group includes the Lakes Pulvermaar, Weinfelder Maar and Gemündener Maar, which are known to be oligotrophic lakes today whereas the members of the first named group are known to be mesotrophic to eutrophic. These substantial differences in the extend of nutrient content in the water body substantially influence the growth of planktonic organisms. Thus, recent sedimentological investigations are often focussed on the eutrophic, plankton rich maar lakes, whereas only little information about autochthonous productivity is preserved in the oligotrophic, plankton poor maar lakes.

Peculiarities which are valid for both investigated maar lakes will be figured out

in the following prior to a detailed introduction of the archives under investigation in *Sections 3.1.1, 3.1.2*. An overview of morphologic and hydrologic data after [Scharf and Menn \(1992\)](#) is given in *Table 3.1*.

In all of the water-filled maars existing today two significant terraces below the water level could be proved at in each case the same depth of water. Both of them can be traced back to climatic induced lake level fluctuations ([Negendank et al., 1990](#)).

The first terrace (approximately 2 – 3 m below the present lake level) can be assigned to humid conditions during Atlanticum, whereas the second (approximately 10 – 12 m below the present lake level) is associated with arid conditions during the Weichselian-Glacial. Additionally, a third terrace was found in Lake Meerfelder Maar 2,5 – 3 m above the contemporary lake level. It represents the water level before 1840 which was artificially lowered at this time for land reclamation. Another lowering of the lake level occurred between 1877 and 1880, but it was removed by restoration in the following years. Therefore, the resulting terrace can be found 3 m below the lake level. The knowledge of these climate driven lake level varieties over time is of special interest for this study since they may also be preserved in the composition of sedimentary organic matter as a result of the probably changing inputs of autochthonous and allochthonous organic matter.

All sampled cores were drilled by the GFZ Potsdam in each case in the deepest part of the lake to reach a profile with horizontal varves and without interferences from inclination slips that occur from the inclined crater walls towards the deeper parts of the maar lakes. The length of single samples varies depending on available material because at least 5 g were needed for organic geochemical analysis of each sample. Therefore, every sample covers a different time range with a maximum of 250 years. In contrast, the samples of the higher resolved sample set of Lake Meerfelder Maar, including the Younger Dryas period and the early Holocene, were taken with a constant sample thickness of 1 cm. The integrated time range therefore only depends on sedimentation rate and is approximately 10 varve years per sample.

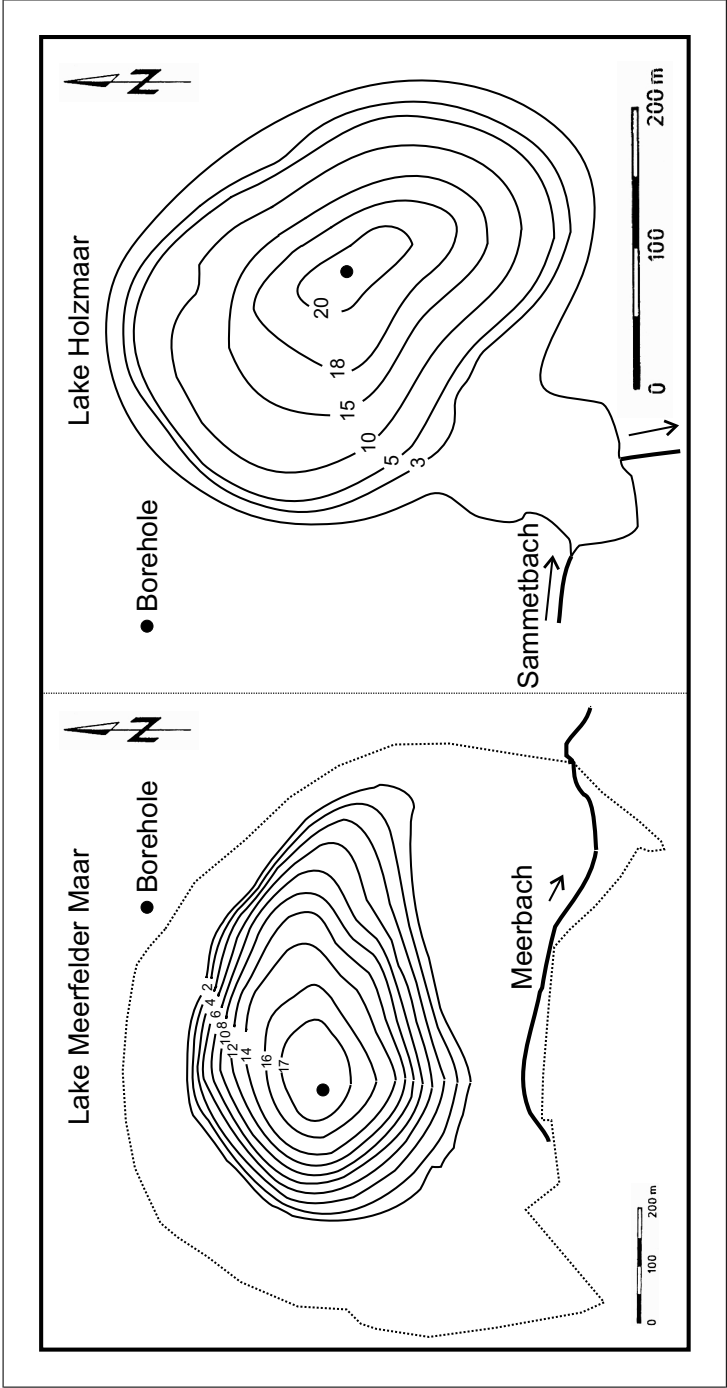


Figure 3.2: Bathymetrical maps of the investigated maar lakes



Figure 3.3: Photographs of Lake Holzmaar

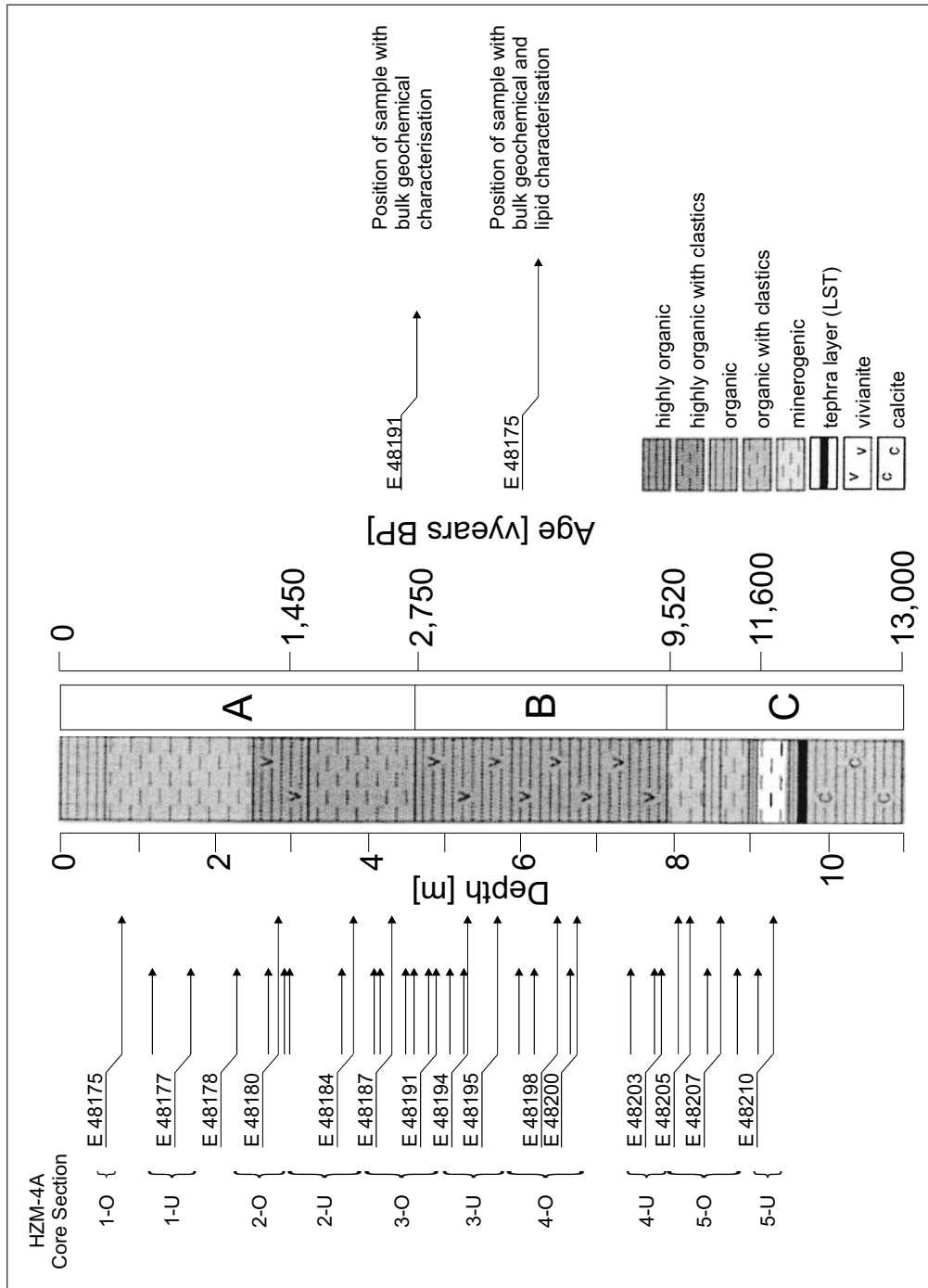


Figure 3.4: Stratigraphy of Lake Holzmaar after [Zolitschka and Negendank \(1998\)](#); LST: Lake Lacher See Tephra; positions of individual samples in relation to profile depth and affiliation to core sections are indicated by arrows (short arrows: sample with bulk geochemical characterisation, long arrows: samples with bulk geochemical and lipid characterisation)

3.1.1 Lake Holzmaar

Lake Holzmaar (see *Fig. 3.3* for illustration) is situated at 50 °07 'N, 6 °53 ' E and 425 m above the MSL. The initial crater has a diameter of 400 m, the contemporary lake of 325 m. The maximum depth is about 19 m. The catchment area is very small at 2 km² and only drained by the small brook Sammetbach. The lake is dimictic and mesotrophic to eutrophic. Lake Holzmaar is the smallest one out of the nine water filled maar lakes in the Westeifel Volcanic Field. Its age is about 40 – 70 ky.

The stratigraphy of Lake Holzmaar was described by [Zolitschka and Negendank \(1998\)](#) and is illustrated in *Fig. 3.4*, which also contains positions of individual samples in relation to depth as well as affiliation to the respective core sections used for sampling. Accordingly, the profile can be subdivided into three lithological zones:

Section A (top to 460 cm depth and/or today to 2,750 vyears BP) is characterised by highly organic rich deposits with clastic intercalations and was deposited during the Subatlantic. **section B** (460 – 780 cm depth and/or 2,750 – 9,520 vyears BP) shows a dominant deposition of autochthonous organic matter with a well marked lamination reflecting stable climatic conditions during the middle Holocene. **section C** (>780 cm depth and/or > 9,520 vyears BP) includes the Lateglacial and the beginning of the Holocene. It is characterised by organic rich deposits changing with minerogenic sedimentation that are related to glacial to interglacial conditions. Section C includes the Younger Dryas cold period between 913 – 943 cm depth and/or 11,600 – 12,300 vyears BP ([Zolitschka, 1998](#)). The core dating was established by [Rein \(1996\)](#), who combined three sedimentary cores to a composite profile using characteristic reference layers and additionally defined 148 micro-lithozones, groups of similar one-year varves. Differing contributions of autochthonous and allochthonous organic matter could be proofed between these micro-lithozones.

The investigated 10 m profile section of core HZM-4A represents the last 12,5000 years, the position of the drilling leg is illustrated in *Fig. 3.2*. 33 sediment samples were taken at the GFZ Potsdam; detailed sample characteristics are listed in *Appendix C*.

3.1.2 Lake Meerfelder Maar

Lake Meerfelder Maar (see *Fig. 3.5* for illustration) is situated at 50 °06 ' N, 6 °45 ' E and is located in the biggest of the nine maar basins in the Eifel volcanic area. The maximum depth is 17 m, but this maar lake has a comparably flat crater wall, resulting in an extensive bank zone with much lower water depths. The contemporary lake fills a third of the initial crater, the rest is filled with glacial deposits of the Lateglacial. The villages Meerfeld and Bettenfeld (partially) are located in the alluvial zone, and until 1950 the brook Meerbach, which drained the catchment area, carried waste water from these villages into the lake, which was polytrophic. Therefore, the brooks course was redirected to the lake outlet in 1950 which resulted in a drastical reduction of the catchment area (see *Table 3.1*), however, the trophic state became not improved by this measure. Therefore, a protected area surrounding the lake was arranged and a system draining the hypolimnion built up in 1981. This led to an eutrophic to mesotrophic state in the following time (*Scharf and Oehms, 1992*). The age of Lake Meerfelder Maar is considered to be 35 ky at minimum.

The stratigraphy of Lake Meerfelder Maar is described in detail by *Brauer et al. (1999b)* and illustrated in *Figs. 3.6 and 3.7*, which also contain positions of individual samples in relation to depth as well as affiliation to the respective core sections used for sampling.

The uppermost part of the profile (top to 175 cm depth and/ or 1, 210 vyears BP) consists of organic rich deposits with clastic intercalations that are partly laminated. The underlying section between 175 – 960 cm depth and/ or 14, 500 vyears BP is annually varved (12,000 single year layers). The deepest parts of Lake Meerfelder Maar mainly consist of non-laminated clastic sediments.

Within the first sampling campaign, 41 samples from core sections MFM X1–Y5 (for position of drilling legs see *Fig. 3.2*) were taken at the GFZ Potsdam. The Lake Meerfelder Maar profile consists of a number of single cores which were drilled in 1992 and 1996. Depending on availability, samples were taken from different cores which were time-correlated to each other by varve counting (*Brauer et al., 1999a*). Detailed sample characteristics are listed in *Appendix C*.



Figure 3.5: Photographs of Lake Meerfelder Maar

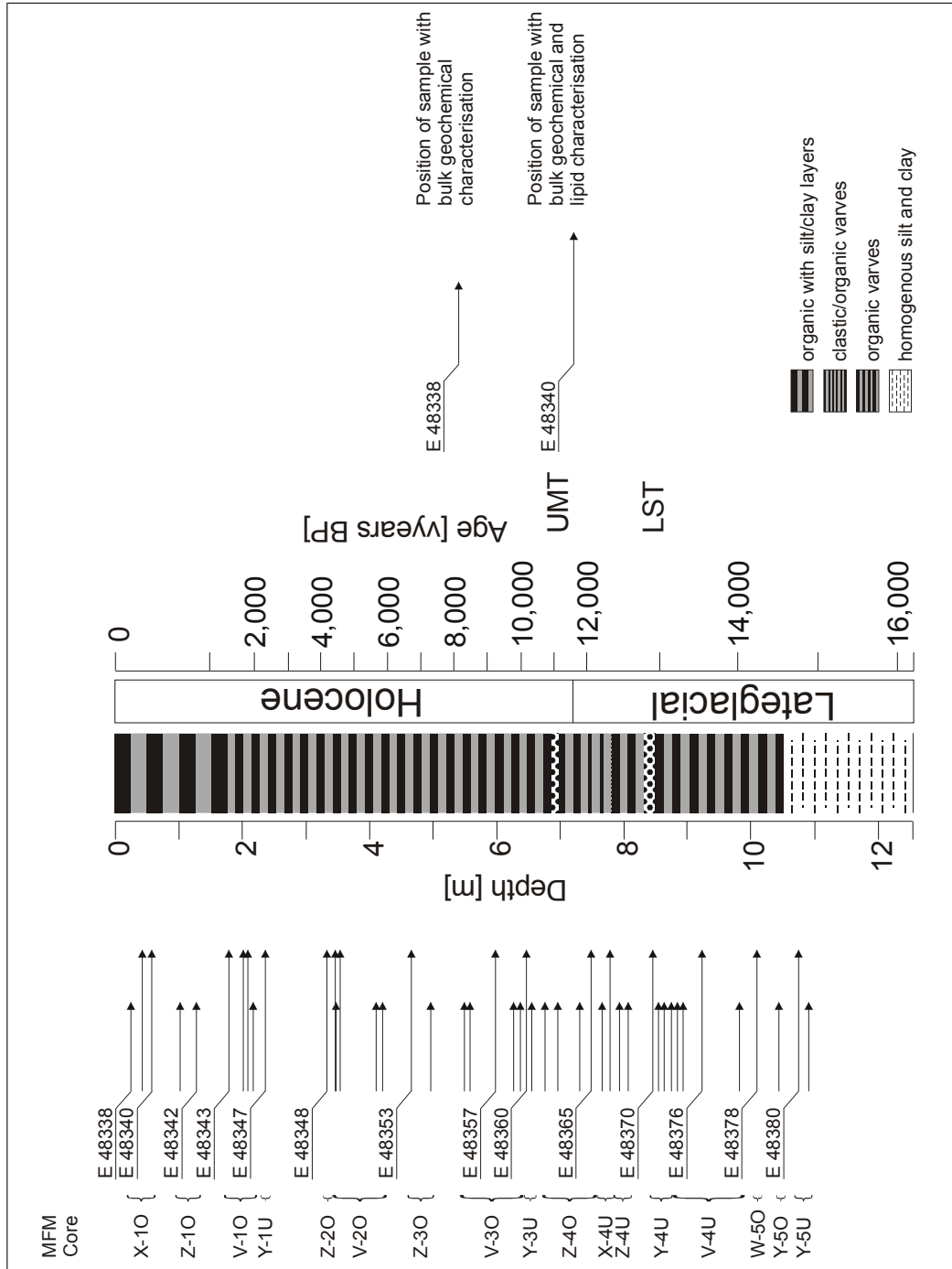


Figure 3.6: Stratigraphy of Lake Meerfelder Maar after Brauer (unpublished); UMT: Lake Ulmener Maar Tephra; LST: Lake Lacher See Tephra; positions of individual samples in relation to profile depth and affiliation to core sections are indicated by arrows (short arrows: sample with bulk geochemical characterisation, long arrows: samples with bulk geochemical and lipid characterisation)

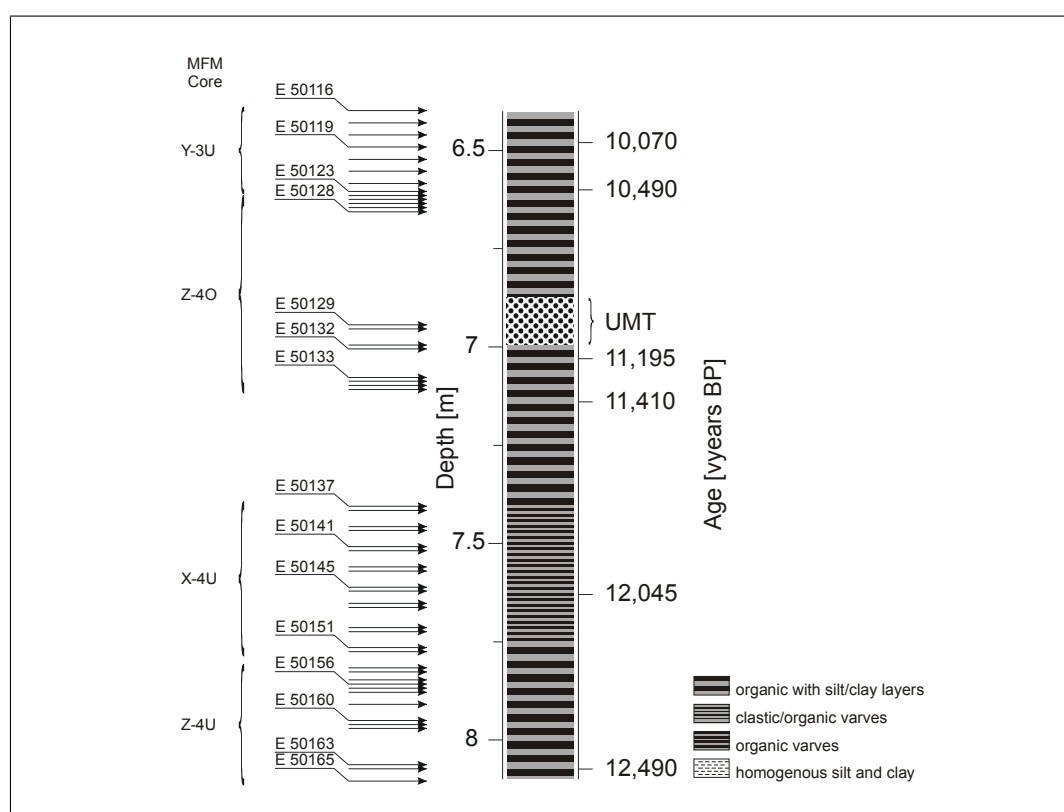


Figure 3.7: Stratigraphy of Lake Meerfelder Maars high resolved core section after Brauer (unpublished); UMT: Lake Ulmener Maar Tephra; LST: Lake Lacher See Tephra; positions of individual samples in relation to profile depth and affiliation to core sections are indicated by arrows (bulk geochemical and lipid characterisation are available for all samples)

3 Study Areas and Samples

Table 3.1: Morphometry and hydrology of Lakes Holzmaar and Meerfelder Maar

Parameter	Lake Holzmaar	Lake Meerfelder Maar
Geographical Position	50,07°N ; 6,53°E	50,06°N ; 6,45°E
Age (in kyears)	40-70	min. 35
Height via MSL (in m)	425,1	336,5
Length (in m)	275	750
Width (in m)	250	450
Shore-line (in m)	1100	1975
Average Depth (in m)	8,8	2,31
Maximum Depth (in m)	20	17
Surface Area (in 10 ³ m ²)	58	256
Volume (in 10 ⁶ m ³)	0,51	2,31
Catchment Area (in km ²)	2,058	5,766 (since 1950: 1,526)
Trophic State (today)	mesotrophic to eutrophic	eutrophic

In a second sampling campaign, 50 additional samples of Lake Meerfelder Maar sediments were taken from cores MFM Y3-Z4 with a higher time scale resolution; sample positions are illustrated in *Fig. 3.7* and listed in *Appendix C*. These samples lie between 6.45 m and 8.10 m depth and thus include the Younger Dryas and the transition to Preboreal/Boreal (Negendank and Zolitschka, 1993b) with a constant sample thickness of 1 cm, yielding a maximum temporal integration width of approximately 10 varve years per sample. This sample set was taken for a detailed study of a selected time period beginning at the Younger Dryas and including the overlying transition to the early Holocene with the highest possible time scale resolution. However, results from both sampling campaigns are not combined in any of the following sections due to the strongly differing temporal integration width of individual samples within the two sample sets; the better resolved sample set is rather used to additionally discuss the Lateglacial/ Holocene transition in more detail.

3.2 Lake Großer Treppensee

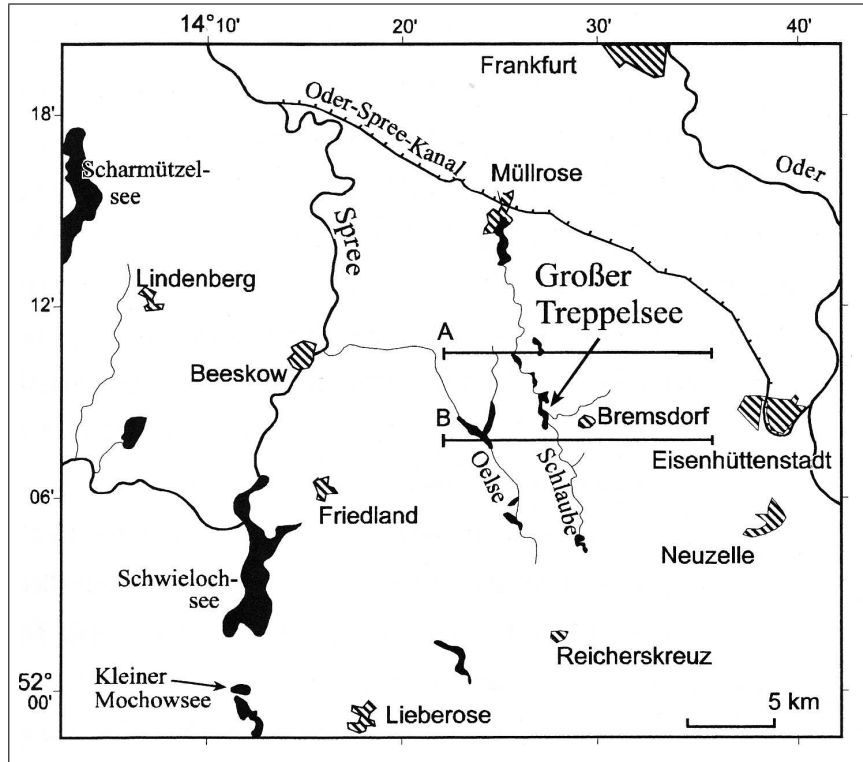


Figure 3.8: Location of Lake Großer Treppensee

Lake Großer Treppensee ($52^{\circ}8'60''$ N/ $14^{\circ}27'10''$ E) is situated in the valley Schlaubetal within the Brandenburger Jungmoränenlandschaft southeast Berlin, Germany; the location is illustrated in *Fig. 3.8*. It was formed from defrosted ice masses at the end of the last European glaciation and is therefore about 11 kyears old (Schönfelder and Steinberg, 1999). The lake is flowed through by the brook Schlaube originating in Lake Wirschensee and flowing through Lake Großer Treppensee, Lake Hammersee, Lake Kleiner Schinkensee, Lake Langer See and Lake Müllroser See on its further course. The delta lies in straight proximity of the last one into the Oder-Spree-channel. The overground catchment area of Lake Großer Treppensee is about $58,3 \text{ km}^2$ (Giesecke, 1999).

According to pollen analytical investigations and AMS-dating, the sampled 26 m profile section contains sediments from the Younger Dryas cold period (11,000 vyears BP) until today. Older sediments can be excluded due to the missing of the *Lake Laacher See* tephra layer, a European-wide detectable ash-layer

from an eruption of this lake during the late Allerød (Giesecke, 1999). The author further supports this finding with pollen analytical data that give evidence for a woody tundra-like vegetation for the oldest sediments, being typical for opening forests due to deteriorated climatic conditions during Younger Dryas. Additionally, less abundant *Betula*- and missed *Hippophae*-pollen indicate a classification to the Younger Dryas instead of the earlier Allerød. A further continuous core-dating as used for the Eifel Maar Lakes is not available for Lake Großer Treppensee. Specific core section were, however, assigned to geological epochs by Giesecke (1999) as illustrated in *Fig. 3.9*.

A representative set of 27 samples with a medium sample distance of approximately 1 m and 1 cm thickness of each sample was made available from the Institut für Gewässerökologie und Binnenfischerei (Berlin, Germany). The two cores were drilled in 1998, a first frozen core from the sediment surface to 2,7 m depth and a second core using the Usinger-Method between 1,8 – 27,8 m depth in 2 m sections (Giesecke, 1999). The positions in relation to the profile depth of the investigated samples are illustrated in *Fig. 3.9*; a detailed listing of the sample characteristics is additionally available from *Appendix C*.

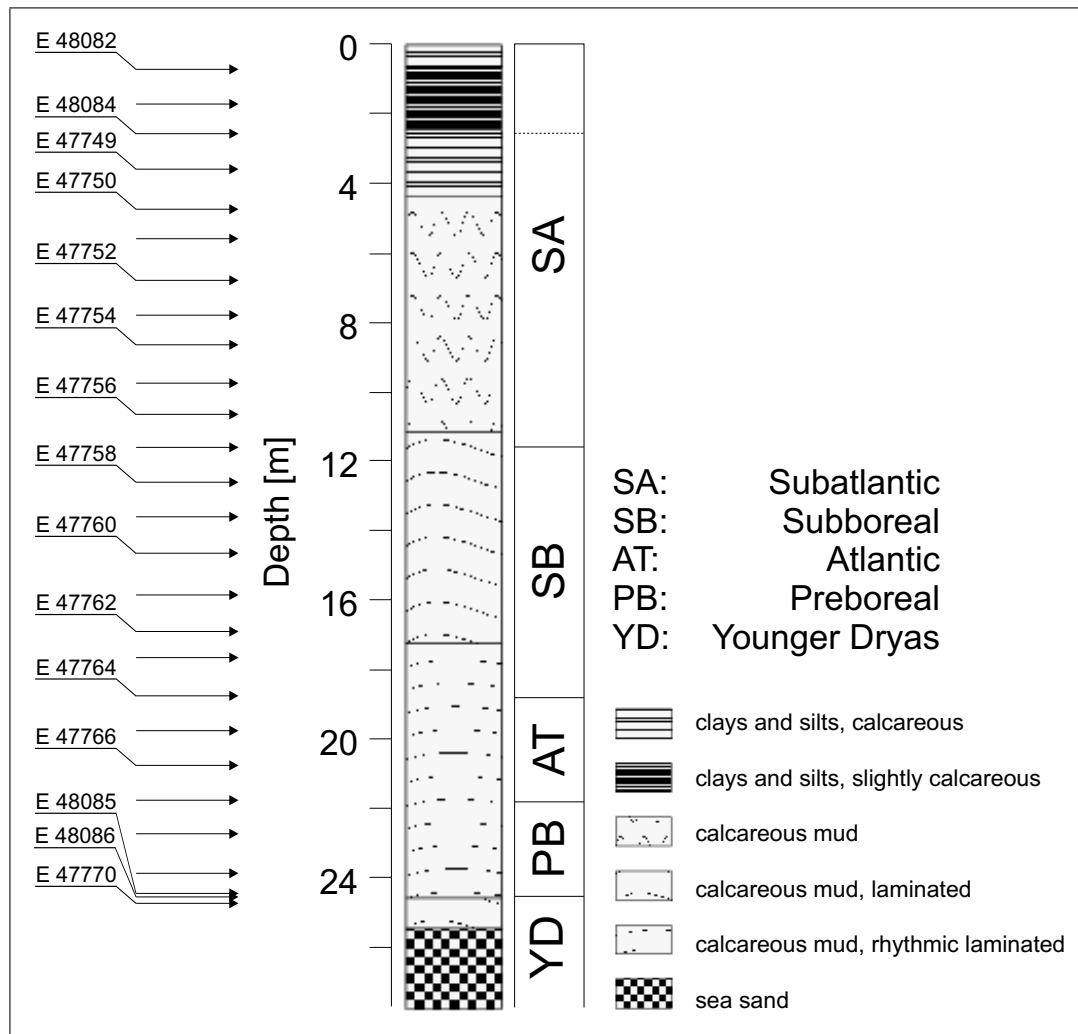


Figure 3.9: Stratigraphy of Lake Großer Treppensee; simplified after [Giesecke \(1999\)](#); positions of individual samples in relation to profile depth are indicated by arrows (bulk geochemical and lipid characterisation are available for all samples)

4 Preparative & Analytical Methods

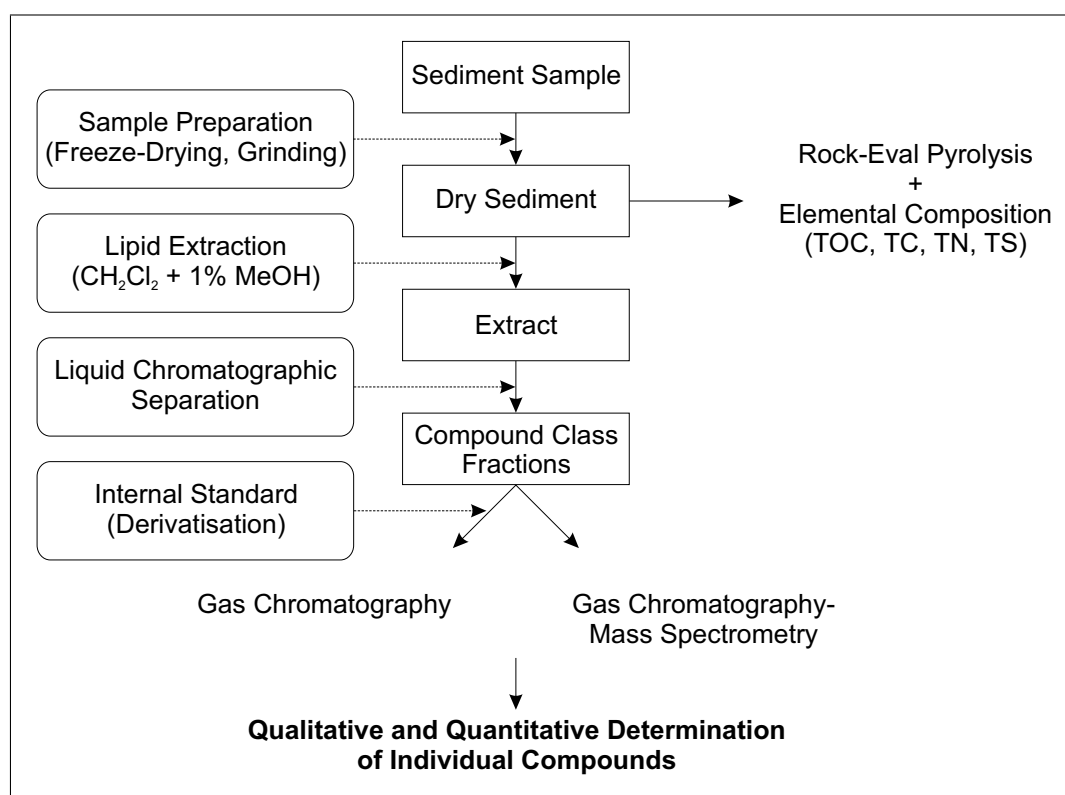


Figure 4.1: Preparative and analytical procedure

A flow-chart of preparative and analytical methods is given in *Fig. 4.1*. Sample preparation includes freeze-drying and grinding of each sample. Next, different subsamples were prepared for the determination of the elemental composition and the extraction of lipids. The obtained whole extracts were separated into eight compound class fractions by means of two affinity and polarity specific liquid

chromatographic separation methods. These fractions were subjected to GC and GC-MS measurements directly or after derivatisation in case of the alcohols and carboxylic acids.

4.1 Sample Preparation and Determination of Elemental Composition

All samples were stored at -20°C until further processing. They were firstly freeze-dried for 48 hours (LYOVAC GT 2TM, AMSCO/FINN-AQUATM). Grinding was performed manually by means of a mortar and pestle in the connection. Samples were then divided into subsamples for extraction (0.4 – 14 g, depending on availability) and determination of the elemental composition (approximately 500 mg) and then stored at -20°C again.

Determined elemental parameters include TC, TOC, TS, TH and TN as well as the Rock-Eval values S_1 , S_2 , S_3 and T_{\max} . The S_2 and S_3 values were used for the calculation of the Hydrogen Index (HI) and Oxygen Index (OI) parameters.

Measurement of TC, TOC, TS was carried out using a CS-225 IR 112 (LECO, USA). The samples were completely combusted in duplicate under oxygen flux and the combustion gases SO_2 as well as CO_2 were detected by IR-Cells. Data were automatically calculated from the intensity-time signals of the IR-Cells, sample weight and calibration data. Certified sulfur- and carbon standards (LECO, USA) were used for calibration. Original subsamples were used for measurements of TC and TS. For TOC determination inorganic carbon was removed prior to the sample combustion by treatment with hydrochloric acid and washing with deionised water followed by drying at 90°C . TIC values were calculated as the difference between TC and TOC. Assuming all inorganic carbon being bound as calcite, percentage of CaCO_3 was calculated from equations (4.1) and (4.2) with M_{CaCO_3} and M_C being the molecular weights of calcite and carbon, respectively. It should be noted in this context, that the calcite content may be overestimated by this measure if other carbonates such as siderite are present in higher amounts.

$$CaCO_3 (\%) = TIC * \frac{M_{CaCO_3}}{M_C} \quad (4.1)$$

$$CaCO_3 (\%) = TIC * \frac{100}{12} \quad (4.2)$$

All data presented in this thesis are mean values from the duplicate measurements; a third analysis was performed in the case of variations between duplicates being higher than 3 %. Between 30 mg and 100 mg dry sediment were used for each analysis.

Measurement of TN and TH was carried out with a CHNS-Analyser against sulfanilic acid as standard substance at the Central Department of Analytical Chemistry (ZCH, FZ Jülich). Hydrogen was determined by oxidation and infrared detection of the resulting H₂O. Known amounts of sulphanilamide were used to calibrate the instrument and to calculate the quantities of nitrogen released from the samples.

Rock-Eval-Pyrolysis is a screening method originally described for estimation of oil- and gas generation potential of sedimentary rocks in petroleum exploration studies (Espitalié *et al.*, 1977, 1985).

Analysis was carried out using a Rock-Eval II (DELSI, USA). The samples were heated up to 550 °C time controlled in gas permeable crucibles. The resulting gaseous products were measured quantitatively (organic compounds⇒FID; CO₂⇒TCD). A certified standard (IFP 15.000, DELSI, USA) was used for calibrating the system and measured at the beginning of a series as well as after every 20th sample. Multichrom was used for online-recording of peak data.

Within the first step, samples were heated at 300 °C over a 3 min isothermal period. Thermovaporised volatile organic compounds were swept by a helium gas stream (50 ml/min) to the FID and monitored as the **S₁**-peak. Next, the furnace was heated up to 550 °C at 25 °C/min. Organic compounds originating from cracked macromolecules were registered at the FID as the **S₂**-peak. Additionally, the CO₂ generated between 300 °C and 390 °C was trapped in a molecular sieve and desorbed to give the **S₃**-peak after the entire heating programme had been

completed. T_{max} denotes the temperature at which the highest rate of pyrogenic volatile compounds is observed (temperature at **S₂**-maximum). S_1 , S_2 and S_3 yields were calculated from peak area, sample weight and calibration data. Equations (4.3) and (4.4) were used to calculate the Hydrogen Index (HI) and Oxygen Index (OI).

$$HI = \frac{S_2 * 100}{TOC} \quad [HI] = \frac{mg \text{ HC}}{g \text{ TOC}} \quad (4.3)$$

$$OI = \frac{S_3 * 100}{TOC} \quad [OI] = \frac{mg \text{ CO}_2}{g \text{ TOC}} \quad (4.4)$$

These two parameters provide general information on the composition of organic matter for thermally immature lacustrine sediments. High *OI* values often refer to high portions of allochthonous land plant derived terrestrial material while high *HI* values are typical for algal derived autochthonous organic matter or leaf waxes of higher plants (allochthonous). Displayed in a *van Krevelen-plot*, organic matter can be subdivided into three different groups (see *Figure 4.2*, areas between the dashed lines):

- TYPE I is rich in hydrogen and originates from microbial biomass (autochthonous organic matter) or from cuticular waxes of leaves (allochthonous organic matter)
- TYPE II is poorer in hydrogen and dominated by the primary inputs of algae or plant exines
- TYPE III organic matter originates from ligneous parts of higher land plants and is therefore marked by higher OI-values

However, the initial state may be changed due to oxidation processes as indicated in *Fig. 4.2* during sinking through the water column and after incorporation into the sediment body as it especially occurs in oxic lakes. As a result, the assignment shifts to higher numbered organic matter types.

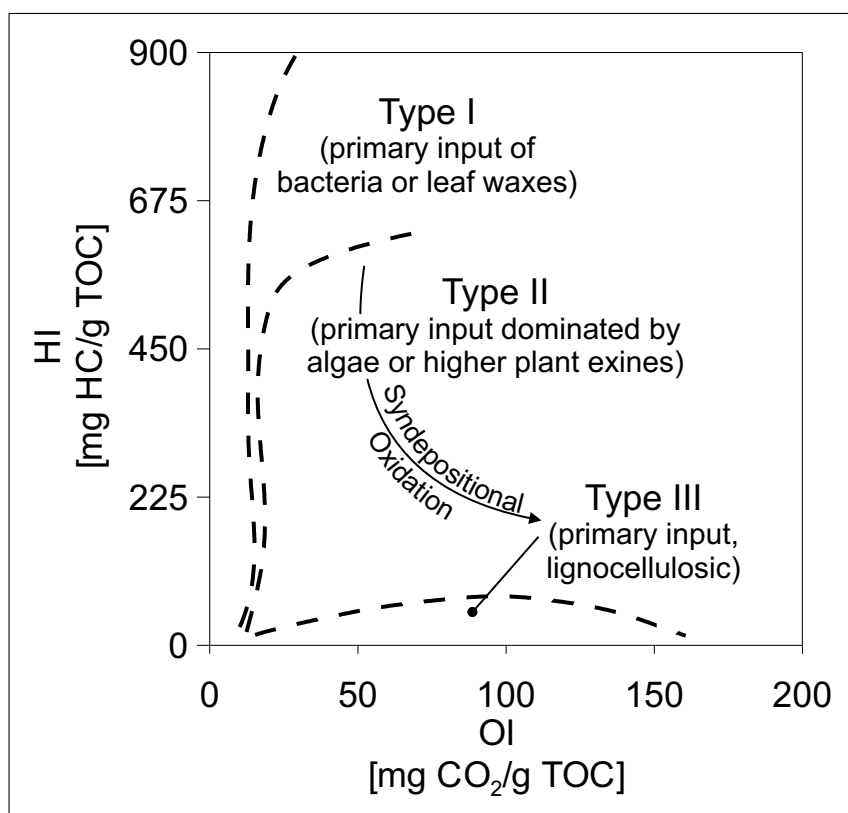


Figure 4.2: van Krevelen Plot; dashed lines separate organic matter types I to III

4.2 Extraction and Liquid Chromatographic Fractionation

A modified flow-blending method after Radke *et al.* (1978) was used for the extraction. The material that had to be extracted and an appropriate solvent were stirred at a rotation speed of 16.000 min^{-1} for 5 min at room temperature. This method ensures a very sensitive extraction compared to other well-known methods (e.g. Soxhlet extraction) due to the short processing time and a low thermal load. Between 0.4 – 14 g sediment were used per sample. A mixture of dichloromethane/methanol (99:1 *vol.*) was used as solvent. All equipment (stirrer, extraction vessel) was cleaned with the same solvent and under the same conditions prior to the extraction.

All extracts were concentrated after extraction using a Turbovap (Zymark; Hopkinton, USA) at 39 °C and transferred to pre-weighed sample vials after which the remaining solvent was removed in a slow nitrogen stream. After the determination of the extraction yield by weight difference, the extracts were redissolved in solvent and stored at –20 °C until further processing.

Due to their complexity, whole extracts are not convenient for direct GC or GC-MS analysis. They therefore were separated into several compound class fractions. Two semi-preparative chromatographic separation procedures based on polarity and affinity interactions as described by Willsch *et al.* (1997) and Radke *et al.* (1980) were used for fractionation, a schematic is presented in *Fig. 4.3*. The Heterocompound Medium Pressure Liquid Chromatographic (HMPLC) apparatus consisted of four consecutive columns filled with selective stationary phases. The solvent extracts, dissolved in dichloromethane/methanol (99:1 *vol.*), were pumped through these columns. High polarity compounds were trapped on untreated silica gel (SiO_2), bases were trapped as their corresponding hydrochlorides on silica gel treated with hydrochloric acid (HCl) and acids were trapped on silica gel treated with potassium hydroxide (KOH). The low- and medium-polarity fractions were obtained from the fourth column according to their retention time.

Trapped high-polarity compounds were eluted from the first column with methanol as mobile phase. Hydrochlorides of bases were eluted from the second to a fifth column filled with KOH-treated silica gel using methanol as solvent in order to

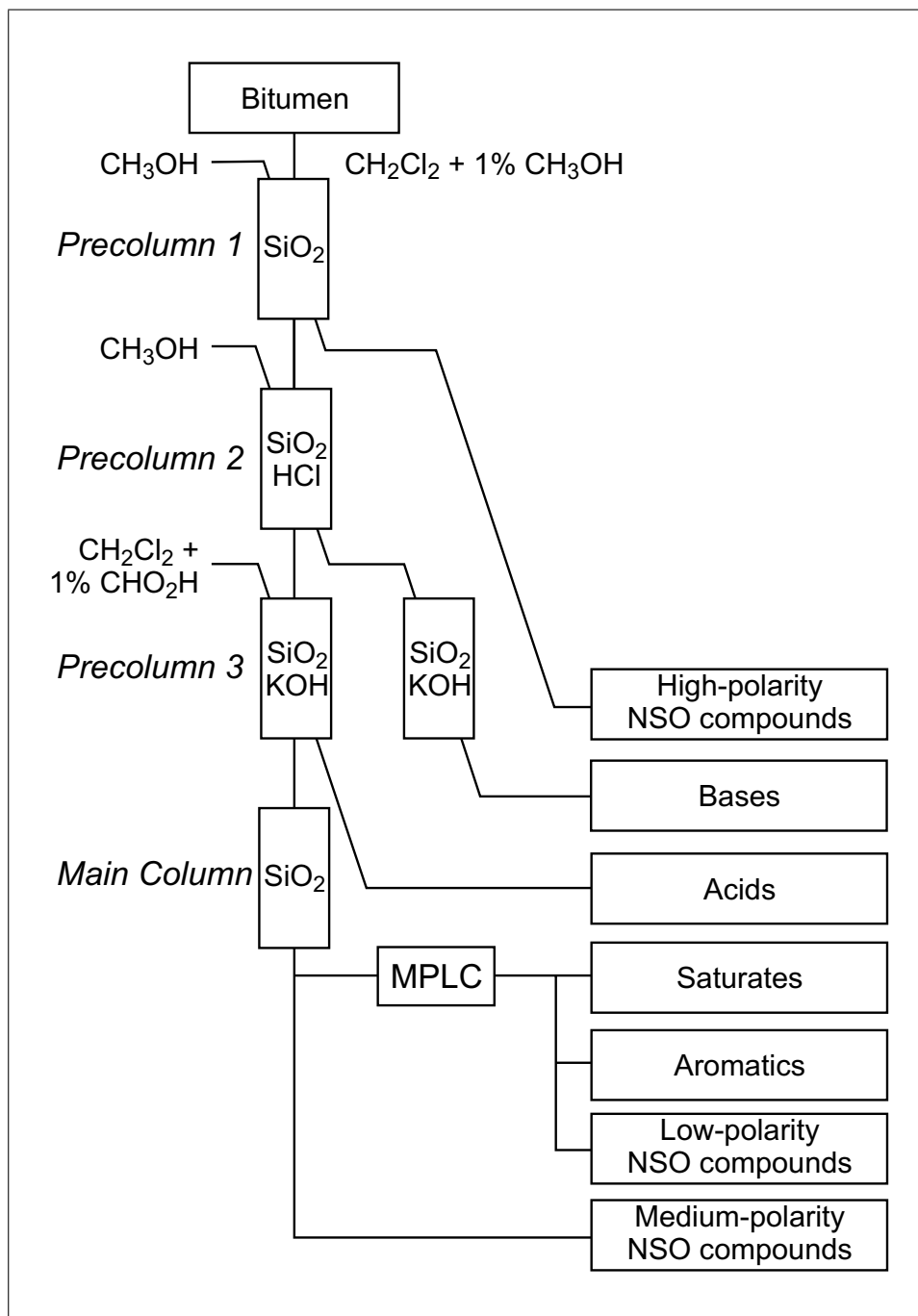


Figure 4.3: Semipreparative chromatographic separation (schematic)

recover the free bases. Acid compounds were eluted from their respective column with dichloromethane/formic acid (99:1 *vol.*). Due to an irreparable failure in the liquid chromatographic separation procedure, carboxylic acid data are not available for the whole sample sequence from Lake Großer Treppensee.

The medium polar fractions contain mainly alcohols and sterols. The low-polarity fractions contain saturated and single unsaturated hydrocarbons, aromatic hydrocarbons as well as heterocompounds (containing at least one Nitrogen, Sulfur or Oxygen atom instead of carbon, NSO compounds). These three subfractions were separated by Medium Pressure Liquid Chromatography (MPLC), a semi automatic separation procedure. The device was equipped with an injection system with 16 sample loops and 16 pre-columns, one main column and an automated fraction collector. The low-polarity fractions were dissolved in *n*-hexane and then pumped through an untreated silica gel pre-column. Heterocompounds were retained whereas aliphatic and aromatic hydrocarbons eluted onto the main column. The flow direction was reversed after the elution of aliphatic hydrocarbons from the main column to obtain the stronger retarding aromatic hydrocarbons. Finally, NSO compounds were eluted from the pre-column with dichloromethane/methanol (95:5 *vol.*). All fractions were concentrated, weighed and stored as described above for whole extracts.

4.3 Derivatisation and Standard Addition

Fatty acids, sterols and alcohols are compounds with polar functional groups making a direct gas chromatographic analysis complicated. The chromatographic behavior of these compounds, however, can be substantially improved by derivatisation into less polar derivatives. An additional argument for derivatisation is the rising number of chromatographic and mass spectrometric data available from present literature that can be used for comparison and identification of individual compounds.

Fatty Acids were converted to their corresponding methyl esters using diazomethane. This reagent was freshly synthesised from Diazald under addition of ethanolic potassium hydroxide and dissolved in chilled (dry ice/acetone) diethylether. Samples were stored in closed vials for 2 h before the excessive ether was evaporated at room temperature.

Alcohols and Sterols were converted to their corresponding trimethylsilyl ethers using bis(trimethylsilyl)trifluoroacetamide/trimethylchlorosilane (99:1 *vol.*), (*Silyl 911*, Macherey&Nagel, Düren, Germany). Samples with added reagent were heated at 60 °C for 30 min and then injected into the GC column as soon as possible to prevent hydrolysis of trimethylsilyl-groups during storage.

In order to quantify GC- and GC-MS data, internal standards have to be added in a defined concentration to every sample prior to measurement. Standard substances have to be selected very carefully because they must not be contained in the original sample and not coelute with compounds contained in the original sample. Unknown concentrations can then be calculated from peak areas as well as peak area and concentration of internal standard since the ratio of concentration and peak area is known to be linear in a relatively wide range of concentration in the case of FID detection ([Schomburg, 1987](#)). This is not fully valid for mass spectrometric detection since detected signals additionally depend on the ionisation yields of individual compounds. All given concentrations, however, were calculated from GC-FID measurements.

5 α -Androstane (5 μ g/ml) was used for aliphatic fractions and methylated perdeu-

terated icosanoic acid (1 $\mu\text{g}/\text{ml}$) for the fatty acid and alcohol plus sterol fractions. A mixture of six aromatic compounds (phenylhexane, phenylheptane, 1,6-dimethylnaphthalene, 1-phenylnaphthalene, ethylpyrene and butylpyrene) was added to the fraction of aromatic hydrocarbons.

4.4 Gas Chromatography (GC)

All gas chromatograms were recorded on 5890 Series II chromatographs (Hewlett Packard, USA). Injections were carried out by autosamplers (Hewlett Packard, USA and CTC, Germany) into a temperature controlled cold injection system (Gerstel, USA). Only aliphatic and aromatic fractions were injected directly *on column* for GC-FID measurements. The carrier gas was helium with a pressure controlled flow rate of 1 ml/min. Detection occurred by means of FID. GC-FID measurements were performed for quantification of peak areas because of the higher sampling rate compared to mass spectrometric detection and the independency of peak areas from ionisation potentials of different compounds. A detailed description of the chromatographic setup is given in *Table 4.1*.

4.5 Gas Chromatography-Mass Spectrometry (GC-MS)

GC-MS measurements were performed for identification of individual compounds by means of their gas chromatographic retention times and mass spectrometric behavior as well as comparison of mass spectra with published data and those of authentic standards.

The chromatographic setup was identical to that used for GC-FID measurements. The gas chromatograph was coupled to a Finnigan MAT 95 SQ mass spectrometer (ThermoQuest Finnigan; Bremen, Germany). A detailed setup is given in *Tab. 4.2*.

4.6 Gas Chromatography-Isotope Ratio Mass Spectrometry (GC-IRMS)

The isotopic composition of selected hydrocarbon fractions was measured under subcontract by Applied Petroleum Technology AS (apt), Kjeller, Norway.

From representative samples, compound specific $\delta^{13}\text{C}$ -values of detectable *n*-

Table 4.1: Chromatographic setup

Chromatograph:	HP 5890 Series II
Injector:	Gerstel KAS III Gerstel On Column Injector (Aliphatic and Aromatic Hydrocarbons)
Injection Volume:	1 – 3 μ l
Temperature Programme: (Injector)	–50 °C (2 min) 50 °C/min \Rightarrow 320 °C
Carrier Gas:	Helium
Flow Rate:	1 ml/min (Pressure Controlled)
Split Ratio:	1:10
Column: (Aliphatic Hydrocarbons)	HP Ultra 1 (length: 50 m inner diameter: 0.22 mm; film thickness: 0.33 μ m)
Column: (Other Fractions)	SGE BPX 5 (length: 50 m; inner diameter: 0.22 mm; film thickness: 0.33 μ m)
Oven Programme: (Aliphatic Hydrocarbons)	90 °C (2 min) 4 °C/min \Rightarrow 310 °C 310 °C (63 min)
Oven Programme: (Aromatic Hydrocarbons)	90 °C (4 min) 50 °C/min \Rightarrow 120 °C 120 °C (1 min) 4 °C/min \Rightarrow 310 °C 310 °C (53 min)
Oven Programme: (Other Fractions)	1200 °C (2 min) 3 °C/min \Rightarrow 310 °C 310 °C (55 min)
Detector:	FID (300 °C) synthetic air (200 ml/min) hydrogen (40 ml/min)
Data Acquisition/-Evaluation	Multichrom on-line

Table 4.2: Mass spectrometric setup

Mass Spectrometer	Finnigan MAT 95 SQ
Ionisation Mode	EI
Ion Source Temperature	260 °C
Energy	70 eV
Scan Range	50 – 600 amu
Scan Cycle Time	1 s
Data Acquisition/-Evaluation	ICIS (Finnigan MAT)

alkanes were recorded, apart from a few exceptions, in the chain length range from n -C₂₁ to n -C₃₃.

A Thermo-Finnigan GC equipped with a GC combustion III unit was connected to a Delta Plus XP mass spectrometer. A 60 m CP-SIL-5 fused silica capillary column with an inner diameter of 0.25 mm and a film thickness of 0.25 µm was used as chromatographic column. The oven program was started with an isothermal period of 2 min at 80 °C, followed by a heating rate of 4 °C/min up to 340 °C. The final isothermal period was 8 min (P. E. Johansen, pers. comm.). Carbon isotopic data of n -alkanes were transmitted in tabular form.

4.7 Statistical Analysis

Data sets obtained by analytical methods as described up to this point yielded a huge data base. Thus, cluster analysis was used as a clinometrical method to yield a maximum of information by reducing the huge data set.

The general principle is a combination of variables with a high relative similarity, expressed by low distances in a multidimensional coordinate system, into several groups. Variables in the context of this study were individual compounds, which have been assigned to compound groups if their concentration change was similar in relation to age and/or depth. Such kind of similarity in changing concentrations points to an equal source of the compounds within each group.

As a prerequisite for the following analysis, data needed to be standardised in order to prevent different ranges of concentration from affecting the group assignment. Then the data matrix was transformed into a symmetric distance matrix

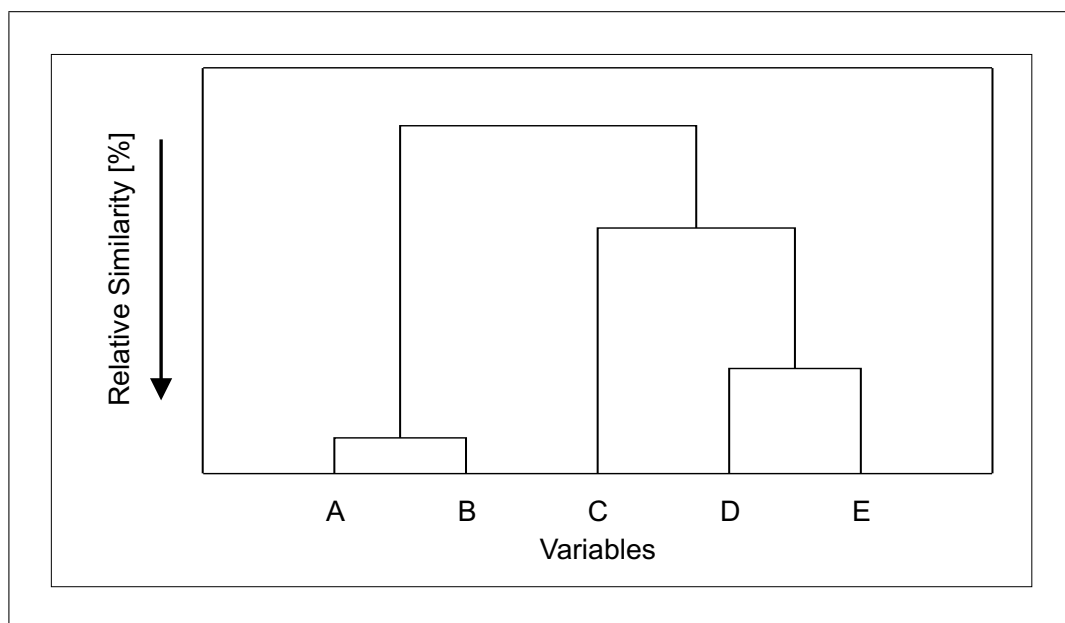


Figure 4.4: Exemplary dendrogram

by calculating squared Euclidian distances (Doerffel *et al.*, 1990). In the following, group formation was carried out using the Ward method, The objects are grouped here with variances decreasing as low as possible within each group. Presentation of the results is finally carried out using dendrograms in which the order of combination is a measure for the similarity.

Following the exemplary illustration in Fig. 4.4, A and B (two individual compounds in the context of this study) are very similar within a given number of cases (samples in the context of this study). Similarity between E and D is less significant and C is combined to them with further decreased similarity. Lowest relative similarity can be finally retrieved between A and B on the one hand and C, D and E on the other hand.

5 Results

All following data of Lake Holzmaar and Lake Meerfelder Maar is presented on a varve year time scale and age related due to the laminated structure of both maar lake profiles. Since comparable continuous dating throughout the Lake Großer Treppensee profile is not available, these data is presented in relation to core depths and stratigraphic zonation.

The presentation of results is divided into general geochemical characterisation, including elemental analysis as well as Rock-Eval pyrolysis and a separate chapter for the distribution of lipid biomarkers.

Bulk organic geochemical data as well as Rock-Eval parameters of the Eifel Maar Lakes (with the exception of the high resolved core section of Lake Meerfelder Maar) were determined in co-operation with Andreas Fuhrmann. They were analogously used as a data framework in his own thesis ([Fuhrmann, 2003](#)).

5.1 General Geochemical Characterisation

5.1.1 Elemental Analysis

Downcore profiles of the bulk parameters TOC, TIC, TS as well as of the Rock-Eval parameters S_2 plus HI and S_3 plus OI are illustrated in *Figures 5.1 to 5.4*. T_{max} values are less specific in the present study since this parameter increases with increasing thermal maturity. The detected temperatures between 409 °C and 420 °C are typical for immature organic matter ([Tissot and Welte, 1984](#)) as

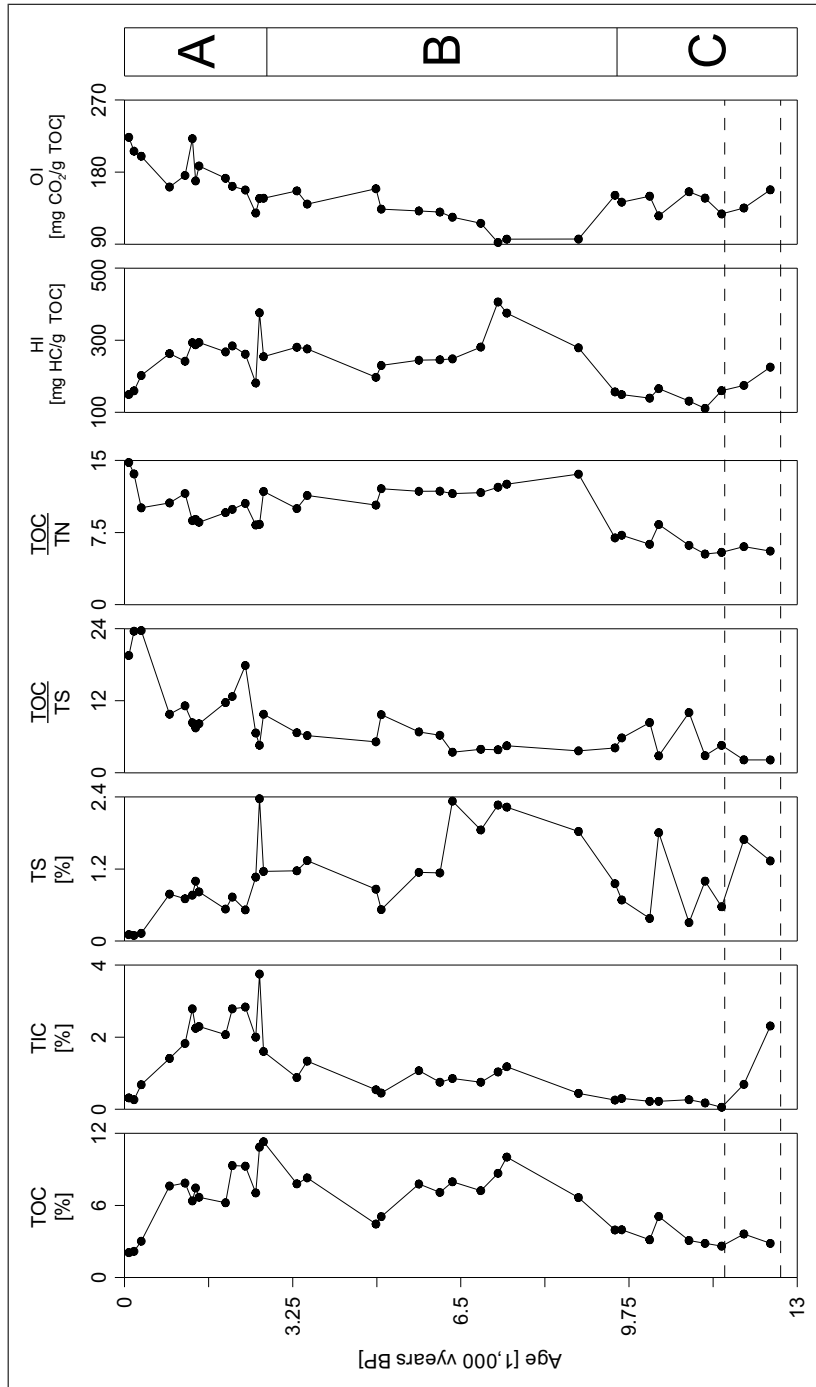


Figure 5.1: Bulk parameters related to age for Lake Holzmaar; dashed lines indicate the Younger Dryas cold period; profile sections A to C refer to the lithological zones after [Zolitschka and Negendank \(1998\)](#)

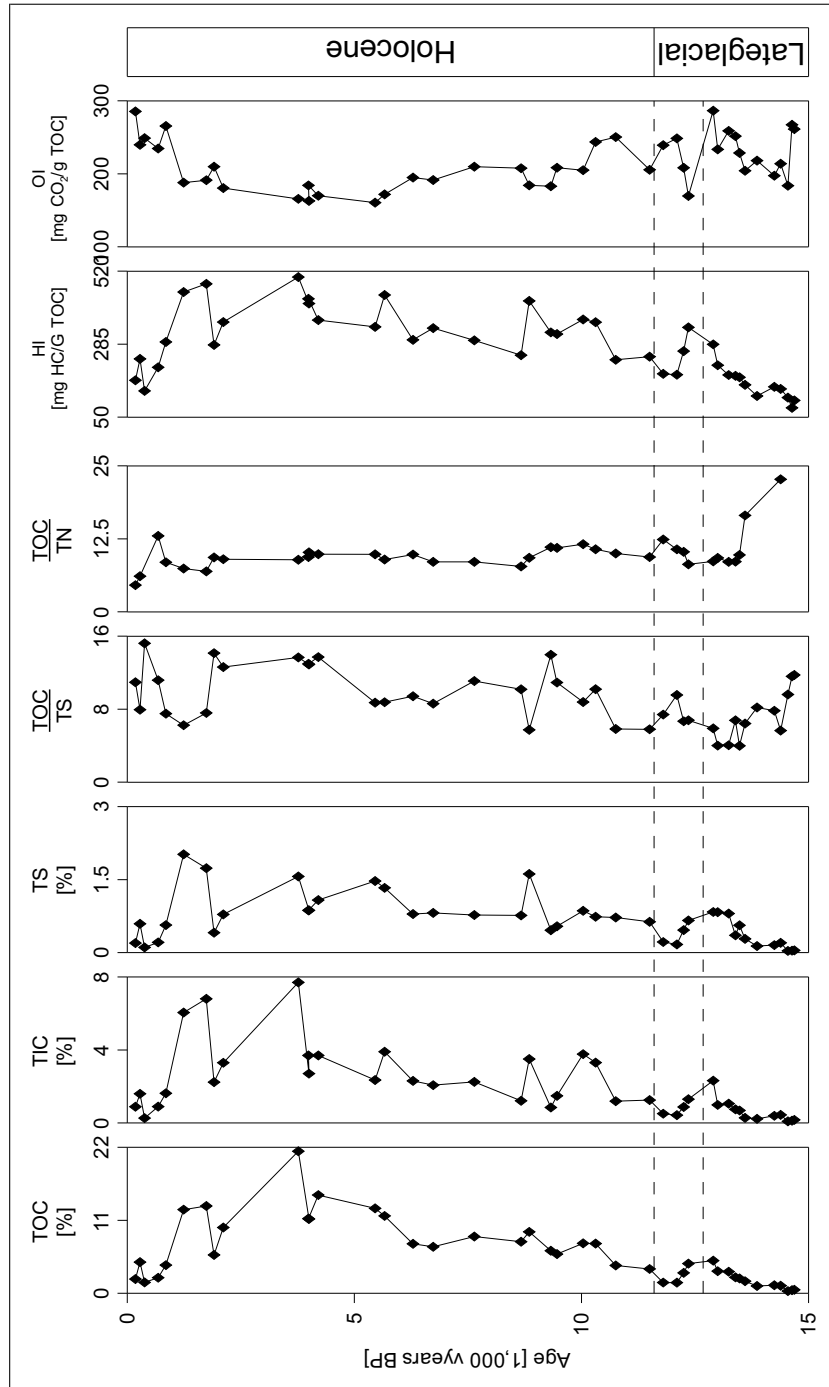


Figure 5.2: Bulk parameters related to age for Lake Meerfelder Maar (full-range sample set with low temporal resolution); dashed lines indicate the Younger Dryas cold period

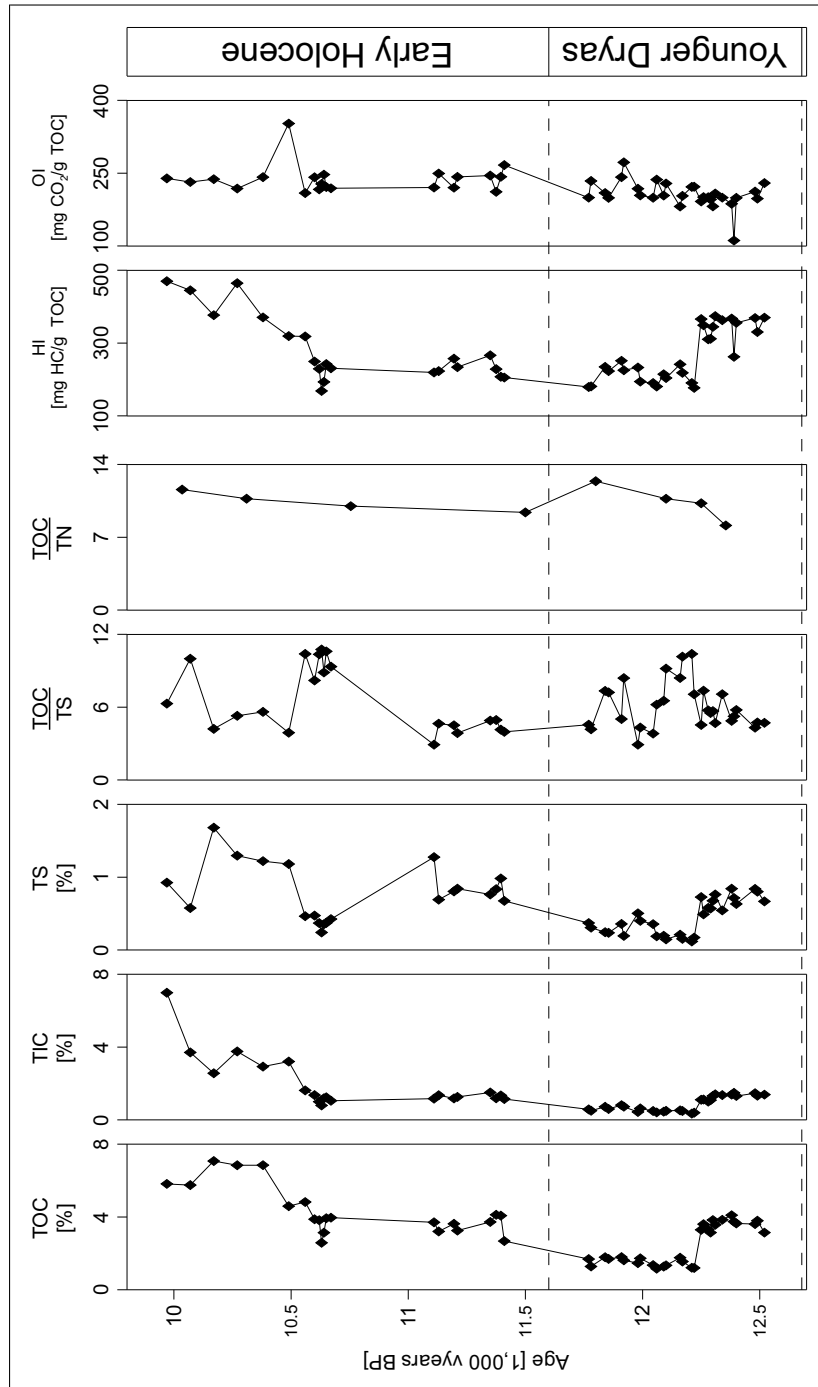


Figure 5.3: Bulk parameters related to age for Lake Meerfelder Maars sample set with higher temporal resolution for the Younger Dryas period and Holocene transition; dashed lines indicate the Younger Dryas cold period

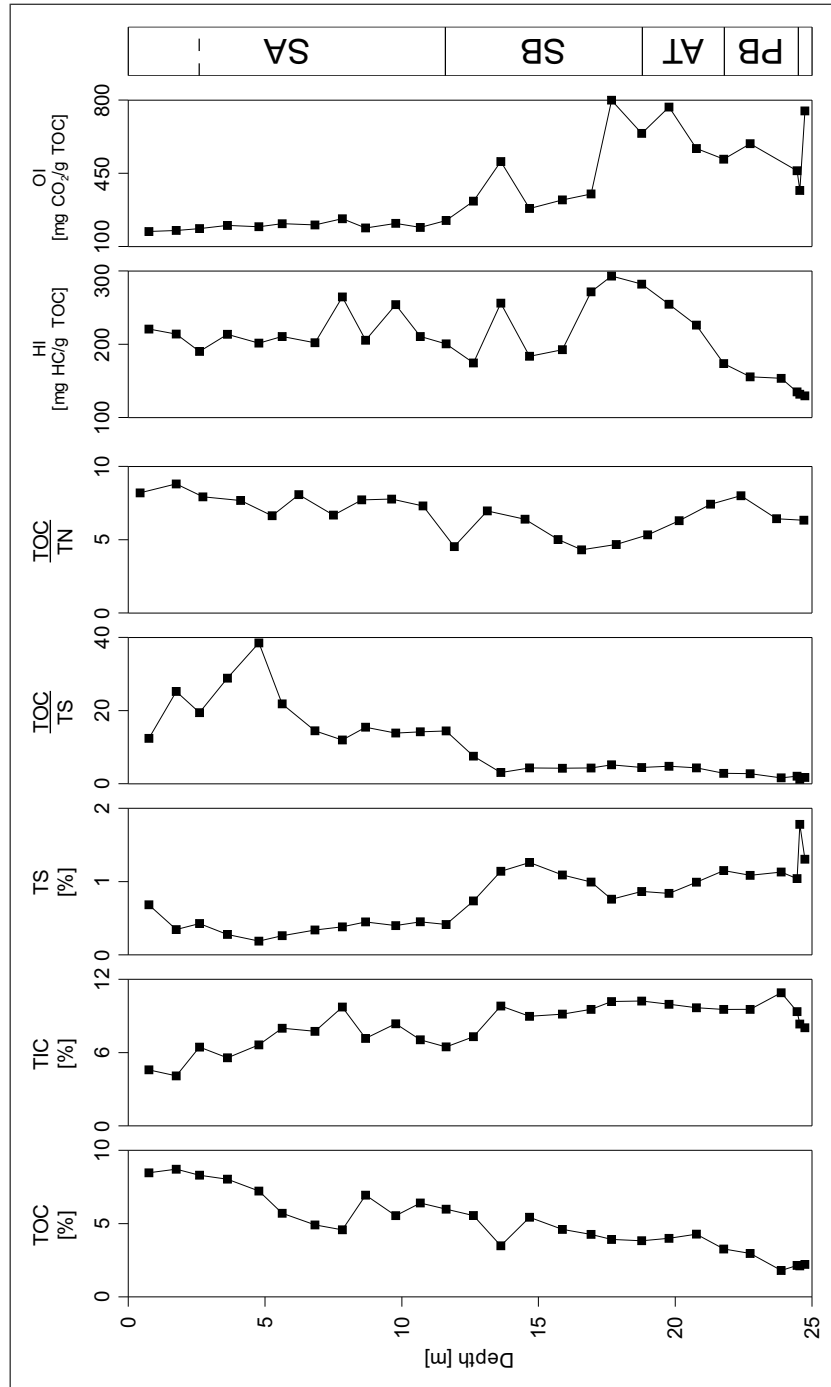


Figure 5.4: Bulk parameters related to depth for Lake Großer Treppensee; lithology after Giesecke (1999); SA: Subatlantic; SB: Subboreal; AT: Atlantic; PB: Preboreal

expected for the the examined sample sets. These data were thus excluded from the presentation of the results and the discussion.

TOC values vary between 2.0 % and 11.3 % within the Lake Holzmaar profile, clearly falling into trends which conform to the three lithological zones as previously published by [Zolitschka and Negendank \(1998\)](#). Zone A shows increasing amounts of TOC with increasing age. Smallest amounts of 2.1 % on average were measured for the two uppermost samples, whereas a significant maximum of 11.3 % was detected at 2,686 vyears BP, the base of zone A. Section B is characterised by slightly higher amounts of 7.1 % TOC on average, reaching a maximum value of 10.0 % at 7,390 vyears BP in good temporal correlation to the Holocene optimum. Finally, TOC content is generally low in the Lateglacial/Holocene zone C, showing a maximum value of 5.1 % at 10,325 vyears BP and a minimum value of 2.6 % at 11,540 vyears BP.

TOC values of the Lake Meerfelder Maar are generally higher compared to those of Lake Holzmaar. Increasing amounts from 2.1 % up to 21.4 % between the uppermost sample and 3,765 vyears BP and then decreasing values down to 3.7 % were measured within the upper Holocene section. Starting at 4.9 %, continuously decreasing amounts of TOC content with increasing age were measured for the lower Lateglacial section of Lake Meerfelder Maar profile to reach a minimum value of 0.5 % in the oldest sample. An intermediate shift to increased TOC contents is obvious during the middle of the Younger Dryas period.

Including the higher resolved sample set of Lake Meerfelder Maar, the general trend of decreasing TOC content with increasing age during early Holocene is confirmed. TOC data during the Younger Dryas cold period yield a significant bipartitioning. The values are relative uniform (1.5 % on average) between 11,840–12,220 vyears BP. A significant shift to higher and further relatively constant values of 3.6 % on average is obvious below this date. The determined values are closely comparable to those published by [Negendank *et al.* \(1990\)](#).

TOC content in the Lake Großer Treppensee profile shows the smallest fluctuation compared to the two maar lakes in spite of a variation between 1.8 – 8.7 %. From the uppermost samples with highest TOC content, values nearly continuously

decrease with increasing depth. A partial maximum of 6.9 % as well as a partial minimum of 3.5 % were measured at 8.7 m and 13.6 m depth, respectively.

TIC values are low in both maar lake profiles and generally lowest in Lake Holzmaar, but variations similar to TOC were measured. lithozone A of Lake Holzmaar profile shows strongly increasing amounts between 0.3 – 3.8 % with increasing age. The maximum value is reached at the lithozone A to B transition. Within lithozone B, values decrease with increasing age, showing a slight plateau of higher amounts between 5,690 – 7,390 vyears BP. Continuously low TIC content was measured for the upper section C samples, whereas strongly increasing amounts up to 2.3 % were found for the last two samples within the Younger Dryas cold period.

Variation of TIC content in Lake Meerfelder Maar is comparable to the corresponding TOC profile too: Values increase in the upper Holocene section from 0.3 % to the maximum value of 7.7 % at 3,765 vyears BP, which is correlated to the TOC maximum, and furthermore decrease within this section. Slightly higher values were measured between 8,850 – 10,310 vyears BP. The lower Lateglacial section is characterised by relatively low TIC values (0.7 % on average) with a maximum content of 2.3 % at 12,900 vyears BP.

The results obtained from the higher resolved sample set confirm the reduction of TIC with increasing age during early Holocene. Even if it is less marked compared to the TOC values, the bi-partitioning of the Younger Dryas period below 12,220 vyears BP is also obvious for TIC content. The average value shifts from 0.5 % to 1.3 % between the respective samples.

Compared to both maar lakes, TIC values for Lake Großer Treppensee are drastically higher. This is because of the higher carbonate content in the catchment area of Lake Großer Treppensee (Giesecke, 1999). Within the upper 18.8 m, values increase from 4.1 % to 10.2 %, relatively lower TIC contents were measured between 10.7 – 12.6 m depth. The maximum value corresponds to a carbonate content of 91 % and coincides with the TOC minimum. The deeper part of the profile shows nearly constant TIC of 9.6 % on average; merely at 23.9 m depth, a partial maximum was detected, whereas the minimum TIC content of 4.1 % still corresponds to a carbonate content of 34 %.

TS values vary between 0.1 – 2.4 % in Lake Holzmaar. They are only weakly correlated to organic carbon content (cf. *Fig. 5.5 A*). As shown in *Fig. 5.1*, section A of Lake Holzmaar profile shows slightly increasing amounts from 0.1 % in the two uppermost samples to reach a sharp maximum of 2.4 % in the oldest part of this section. Section B starts with decreasing sulfur content until 4,960 vyears BP to reach a stage of high TS content (1.8 % on average) between 5,690 – 8,775 vyears BP. Older parts of this section are characterised by continuously decreasing TS values. Largest fluctuations of TS values were measured for section C of Lake Holzmaar profile: A sharp maximum of 1.8 % is followed by relatively low sulfur content between 10,910 – 11,540 vyears BP. Towards the Younger Dryas cold period, increasing amounts were detected, whereas another decrease was observed during this period of relatively cold and dry climate.

After relatively low TS values (0.3 % on average) within the uppermost five samples of Lake Meerfelder Maar, the overall maximum of 1.7 – 2.0 % TS was measured between 1,240 – 1,740 vyearsBP followed by slightly decreasing sulfur content with increasing age in the Holocene profile section. This trend is interrupted by significant maxima at the same ages where TOC maxima were observed (cf. *Fig. 5.5 B*). The Lateglacial section is characterised by low sulfur content during the upper Younger Dryas cold period and further increasing values with increasing age. Before 13,600 vyears BP very low sulfur concentrations of 0.1 % on average were measured.

As figured out for all elemental parameters up to now, the higher resolved sample set indicates a partitioning of the Younger Dryas by significantly increased sulfur contents below 12,220 vyears BP.

In contrast to both maar lakes, TS is negatively correlated to TOC in Lake Großer Treppensee sediments (cf. *Fig. 5.5 C*). Fluctuation of the total sulfur content profile is as low as observed for organic and inorganic carbon before. After a slight decrease from the first to second sample, relatively uniform concentrations of 0.4 % on average were measured until 11.63 m depth. Afterwards, a rapid increase up to 1.1 % (15.88 m depth) was observed, that is followed by another decrease at the next 1.8 m of the sedimentary record. Within the lowest profile section, TS values slightly increase with a sharp maximum at 24.56 m depth.

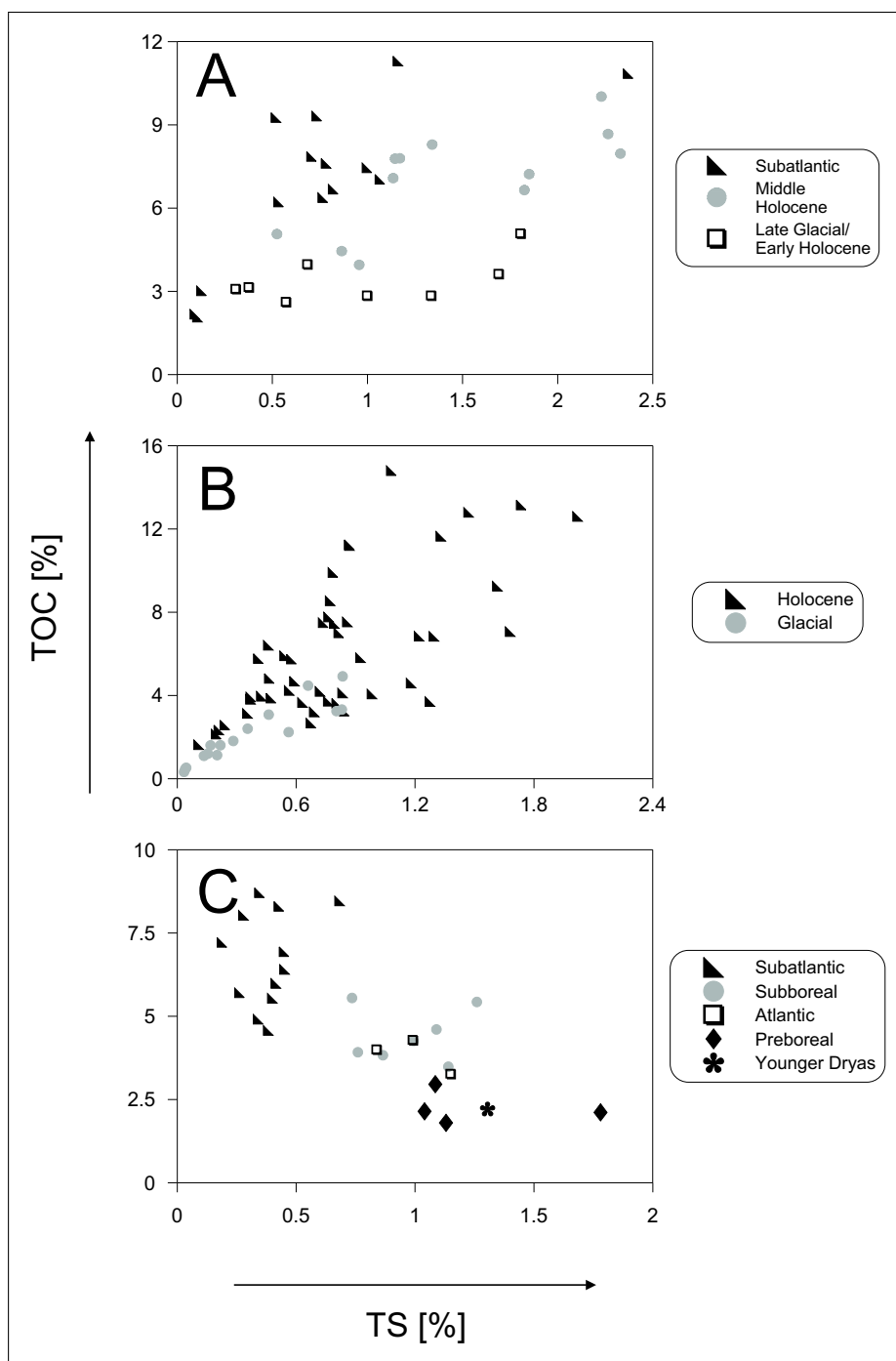


Figure 5.5: TOC *vs.* TS for Lake Holzmaar (A), Lake Meerfelder Maar (both sample sets, B) and Lake Großer Treppensee (C)

The TOC/TS and TOC/TN Ratios were calculated from the bulk organic geochemical parameters described above and are illustrated in *Figs. 5.1–5.4* too.

After the highest overall TOC/TS ratios in the uppermost three samples of the sedimentary sequence of Lake Holzmaar, values decrease before reaching a maximum at 2,334 vyears BP. Section B is characterised by slightly decreasing ratios before the sections maximum of 9.7 is reached at 4,960 vyears BP. Further in this section, ratios decrease to reach nearly constant values of 3.9 on average between 6,340 – 9,480 vyears BP. Section C shows strong variations before constant and low ratios were determined for the Younger Dryas cold period. TOC/TN ratios are highest at the top section too. The partial maximum at 2,334 vyears BP is weaker than that for the TOC/TS ratio, and values remain relatively constant between 4,960 – 8775 vyears BP in section B before a strong shift to lower values was determined for the section B to C transition. Within the oldest section, ratios are uniform with a slight maximum of 8.3 at 10,325 vyears BP.

Also TOC/TS ratios of Lake Meerfelder Maar profile show highest overall values in the uppermost samples, but absolute values are lower compared to Lake Holzmaar. At 1,000 vyears BP, a strong shift to lower ratios was observed, before the TOC/TS ratio increases to 14.1 within 670 years and remains on a high level until 3,990 vyears BP. The older parts of the Holocene sections are characterised by higher variations until the Younger Dryas. Within the Lateglacial profile section, TOC/TS ratios of 5.2 on average were calculated until 13,865 vyears BP, before values significantly increase in the oldest part of the profile. However, TOC/TN ratios are less variable. They reach a partial maximum of 13.0 at 680 vyears BP and then remain on a low level of 9.4 on average throughout the whole Holocene section. Between 13,480 – 14,385 vyears BP a strong increase up to 22.7 was calculated.

Deviating from the clear partitioning of the Younger Dryas cold period as introduced for elemental parameters up to now, the TOC/TS ratios of the higher resolved sample set show a stage of increased values between 12,060 – 12,220 vyears BP.

TOC/TN ratios of five samples could not be calculated since nitrogen content was below the detection limit of 0.05 %.

TOC/TS ratios of Lake Großer Treppensee are higher compared to Eifel Maar Lakes in the upper 11.2 m section. Values increase from the uppermost sample to

the overall maximum of 38.5 at 4.78 m depth and further decrease within the next 2.2 m. Between 6.83 – 11.63 m ratios remain at 14.1 on average before another decrease was observed. In the lower 11.1 m, TOC/TS ratios are very uniform at 3.3 on average with a slightly decreasing trend. In contrast, TOC/TN ratios are less variable in the upper part of the sedimentary sequence: values scatter closely around the average of 7.7 up to 12.6 m, before a partial minimum of 4.5 was determined at 13.63 m. This is followed by a significant minimum of 4.3 at 17.68 m depth and further continuously increasing values. The TOC/TN ratios are lower again for the two deepest samples and same as calculated for the upper section.

According to [Rudd *et al.* \(1986\)](#), high TOC/TS ratios like those measured for Lake Holzmaar profile sections between 1,952 – 2,334 vyears BP and at 10,910 vyears BP as well as Lake Meerfelder Maar sections between 1,910 – 4,205 vyears BP and 9,325 – 1030 vyears BP and finally the upper 11.63 m of Lake Großer Treppensee indicate periods of enhanced allochthonous organic matter influx since land plants show higher C/S ratios compared to aquatic organisms. In case of Lake Holzmaar, these findings are in agreement with [Zolitschka and Negendank \(1998\)](#) who found periods of increased allochthonous production around 2,750 vyears BP and between 9,500 – 12,300 vyears BP which were interrupted by periods of enhanced autochthonous production.

Similarly, TOC/TN ratios are also used to distinguish between different sources of organic matter contribution as reviewed by [Meyers and Ishiwatari \(1993a\)](#) and [Meyers and Lallier-Vergès \(1999\)](#). Accordingly, land plant derived organic matter input is characterised by ratios commonly higher than 20, sometimes up to 200 ([Hedges *et al.*, 1986](#); [Meyers, 1990, 1994](#)). In contrast, values between 4 to 10 were reported for autochthonous organic matter, with diatoms having values between 5.5 and 7.5 and zooplankton and bacteria between 4.0 and 6.0 ([Bordowskiy, 1965a,b](#)). These significantly lower values are due to the higher relative amounts of nitrogen rich proteins in these organisms. Thus, the periods of enhanced allochthonous organic matter influx to the investigated archives as identified by TOC/TS ratios are confirmed by the TOC/TN ratios.

5.1.2 Rock-Eval Pyrolysis

Age and/or depth related plots of the Rock-Eval parameters HI and OI are part of *Figs. 5.1 to 5.4*. Additionally, van Krevelen plots for each lake are given in *Figs. 5.6 to 5.8*. The initially measured values of S_1 to S_3 will not be introduced separately since S_2 and S_3 are part of HI and OI (*cf. Equations 4.3 and 4.4*).

Hydrogen Index values between 111 – 406 mg HC/g TOC were measured within the Lake Holzmaar sedimentary sequence. Analogous to organic carbon contents, relatively low HI values were measured for the uppermost samples. The underlying zone of section A, that has more clastic intercalations compared to the upper zone, shows slight variations around the average content of 274 mg HC/g TOC. A characteristic minimum, immediately followed by the section A maximum of 376 mg HC/g TOC, was detected directly before the section A to B boundary. At the beginning of section B, a reduction of HI was observed before relatively constant values around the average of 241 mg HC/g TOC were measured. The overall maximum content of HI was detected as 406 mg HC/g TOC at 7,220 vyears BP. Towards section C, values continuously decrease. Within the oldest section, average HI values of 143 mg HC/g TOC were found prior to an increase during the Younger Dryas cold period.

The average HI value of 273 mg HC/g TOC in the Lake Meerfelder Maar sediment is comparable to that of Lake Holzmaar, but the variability between 80 – 501 mg HC/g TOC is slightly higher. As described for bulk organic geochemical parameters above, increasing values from the profile top towards two characteristic maxima at 1,740 vyears BP and 3,765 vyears BP were measured before the HI decreases towards the Younger Dryas cold period. After a sharp increase during this period of colder temperatures, that is also confirmed by the results of the higher resolved sample set at the same age as found for the elemental composition, HI values continuously decrease in the Lateglacial section.

Hydrogen index values of Lake Großer Treppensee show strong variations in the upper 16 m core section without a significant trend. At 17.7 m depth, the overall maximum of 293 mg HC/g TOC was detected. Deeper samples show continuously decreasing values.

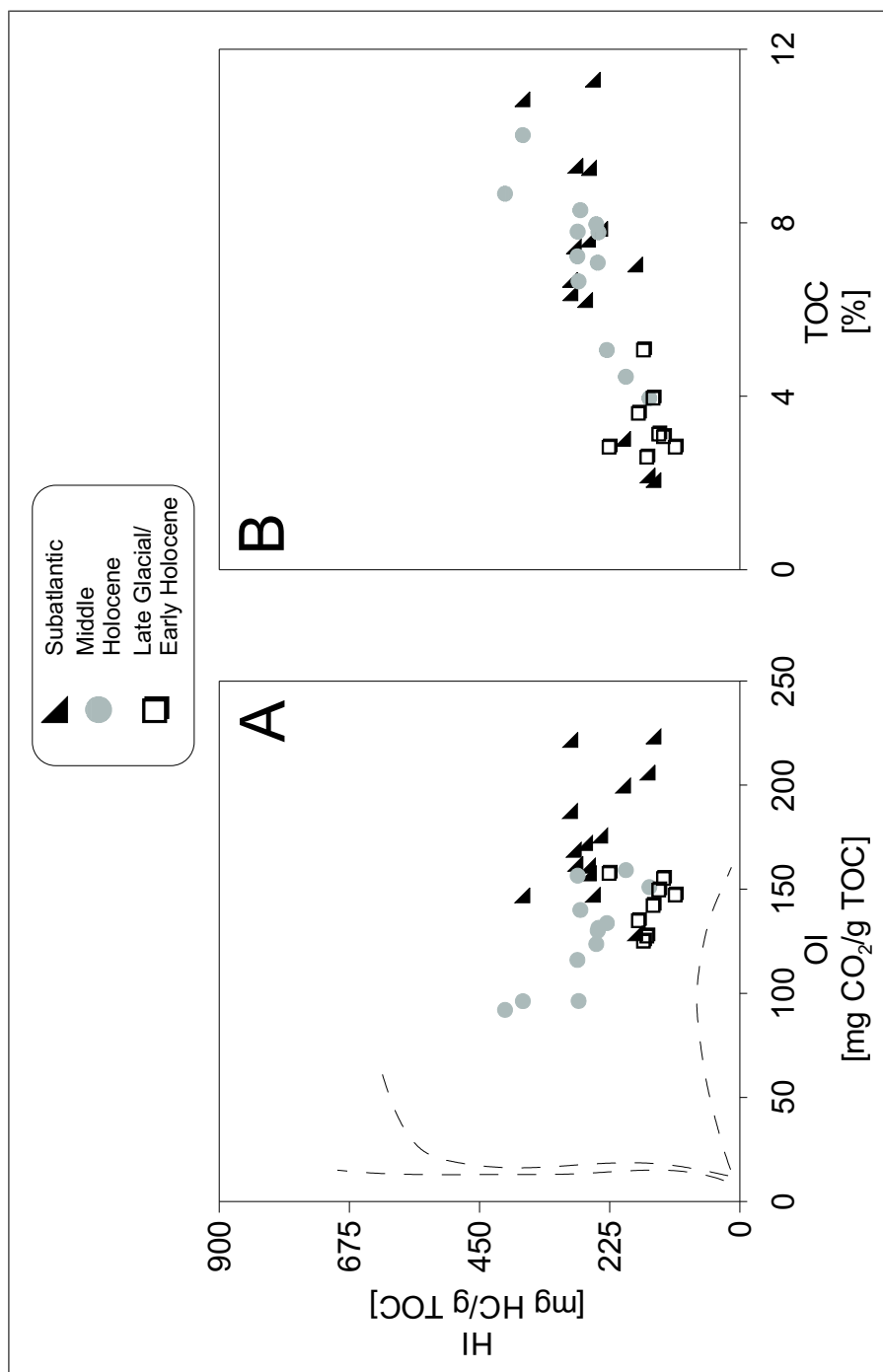


Figure 5.6: van-Krevelen-Diagram (A) and HI *vs.* TOC plot (B) for Lake Holzmaar samples

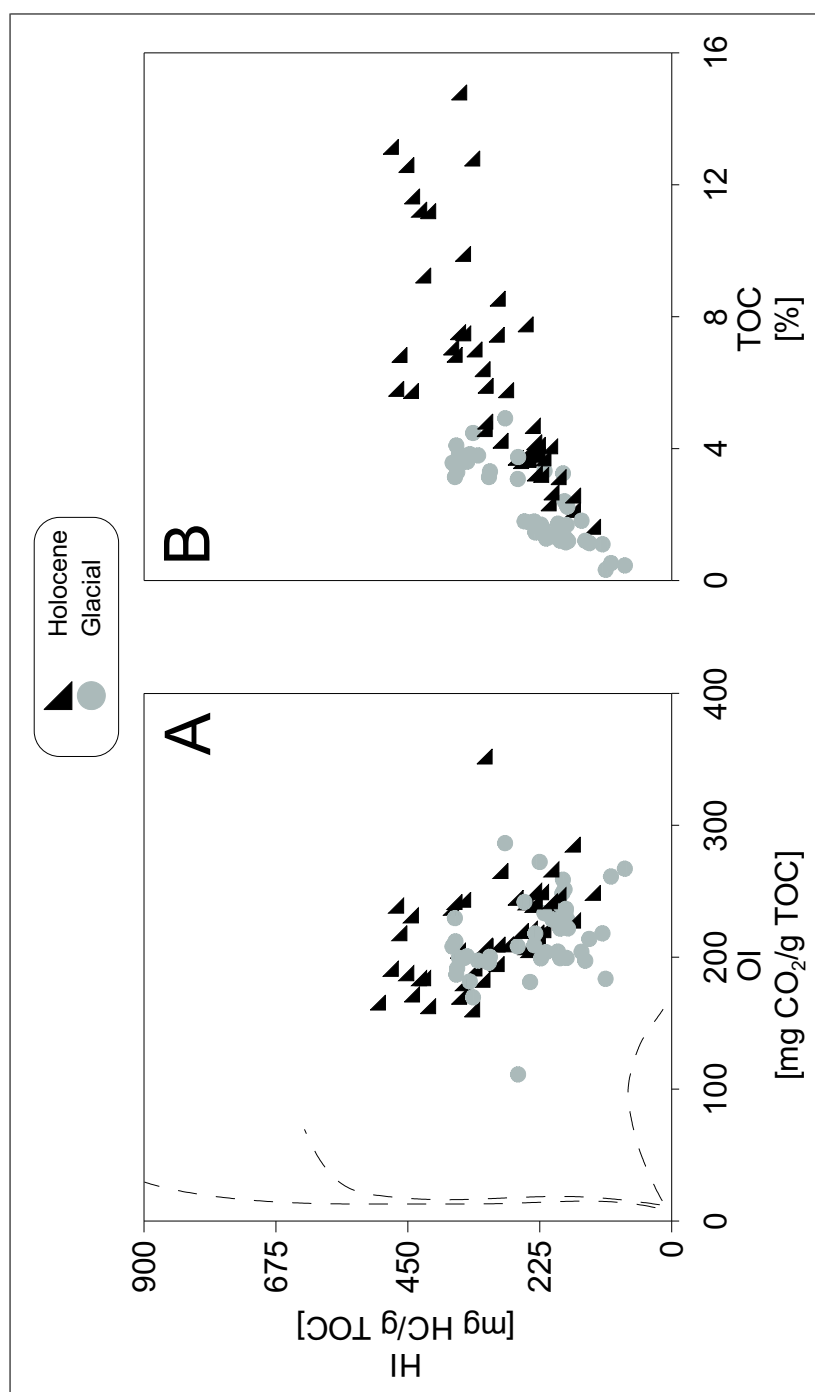


Figure 5.7: van-Krevelen-Diagram (A) and HI *vs.* TOC plot (B) for Lake Meerfelder Maar samples

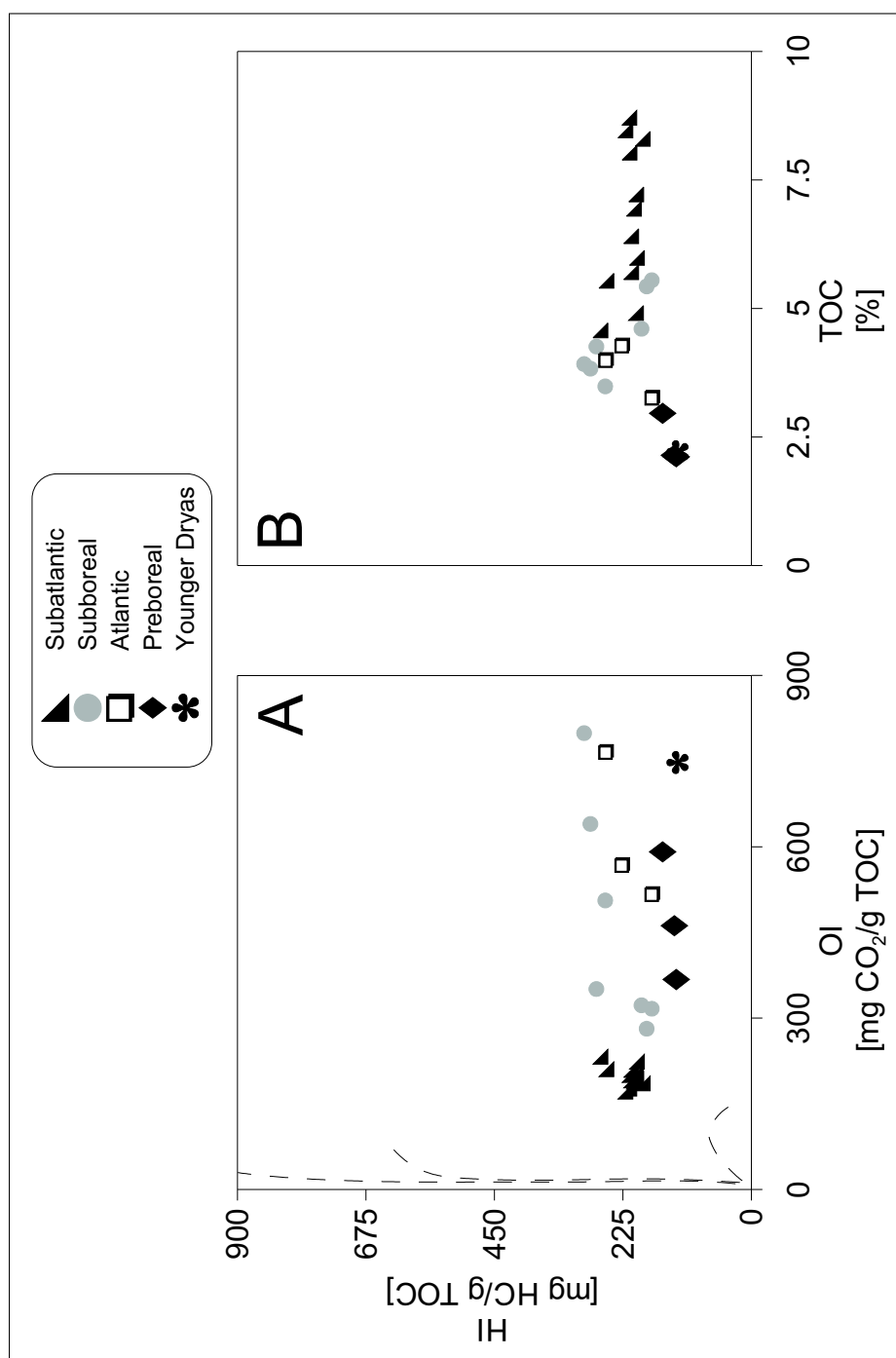


Figure 5.8: van-Krevelen-Diagram (A) and HI *vs.* TOC plot (B) for Lake Großer Treppensee samples

OI values of Lake Holzmaar nearly continuously decrease from 223 mg CO₂/g TOC in the uppermost sample to 116 mg CO₂/g TOC at 6,888 vyears BP. Constantly low values around 95 mg CO₂/g TOC between 7,220 – 8,775 vyears BP were measured prior to higher values of 144 mg CO₂/g TOC on average in the deepest part of the sedimentary sequence.

The OI downcore profiles from Lake Meerfelder Maar show little fluctuations between 111 – 352 mg CO₂/g TOC. Slightly higher values were measured for the uppermost 1,000 vyears BP, whereas the lower part of the Holocene section is characterised by small variations. A local maximum was detected at the outgoing Younger Dryas cold period in contrast to very low OI values at the beginning of this period. These well marked variations in the OI content during the Younger Dryas period could, however, not be confirmed from the higher resolved sample set with the exception of a sharply separated minimum at 12,390 vyears BP. Within the Glacial section, OI decreases continuously with exception of the two oldest samples.

Considerably higher OI values were determined for the Lake Großer Treppensee profile. Values slightly increase in the upper 11 m and then increase drastically up to 799 mg CO₂/g TOC in correlation to increasing TIC content in the same depth. On account of the equal detection of CO₂ yielded from both, organic and labile inorganic precursors like previously described as mineral matrix effect by [Katz \(1983\)](#), these data should be interpreted with caution since inorganic carbon content is very high Lake Großer Treppensee sediments compared to the investigated maar lakes (*cf. Fig. 5.4*) and thus may strongly distort the OI data.

The van Krevelen plots for investigated lakes show similar results for both maar lakes: organic matter is assigned to types II to III. Additionally, the lithological zones of both profiles can be confirmed by these plots since samples from different zones plot in distinct areas. Section A of Lake Holzmaar is characterised by mid range HI and high OI values, whereas samples from section B show higher HI and lower OI values. Section C finally shows the lowest yields of volatile organic compounds. Similar relations between lithological sections and Rock-Eval parameters were observed for Lake Meerfelder Maar: Younger samples from the Holocene sequence are slightly separated from Glacial samples by higher HI and lower OI

values. This points to different organic matter sources and varying compositions of the sedimentary organic matter during geological times. Supporting this hypothesis, HI and TOC are well correlated in both maar lakes and the two zones of Lake Meerfelder Maar profile show different slopes of the regression curves in the HI *vs.* TOC plot. Therefore, a change of organic matter composition with changing quantity of organic matter sedimentation must be considered.

Nevertheless, HI and OI may be influenced by oxidation processes during sedimentation through the water column and after incorporation to the sedimentary body (Talbot and Livingstone, 1989): HI values decrease whereas OI increases during respiration processes (cf. oxidation line in *Fig. 4.2*). Since that kind of diagenetic organic matter composition change might overprint the initial source signal from contributing organisms in the respective catchment areas, the interpretation of lipid biomarker distributions (*Chapter 6*) will be introduced with a separate section dealing with the organic matter preservation state as a necessary prerequisite for source assignment of individual biomarker compounds.

The van Krevelen plot for Lake Großer Treppelsee samples might indicate a strong organic matter oxidation during sinking through the water column and/or incorporation to the sedimentary body because of the high OI values and relatively low HI values. This would be in agreement with Talbot and Livingstone (1989), who found sedimentary organic matter with HI values lower than 200 mg HC/g TOC to be oxidised at sedimentation. On the other hand, OI data of Lake Großer Treppelsee need to be used with caution due to the relatively high inorganic carbon content, that leads to mineral-matrix effects as figured out above. Thus, the preservation state of Lake Großer Treppelsee sedimentary organic matter will be further investigated using suitable biomarkers (pristane/phytane ratios, unsaturated fatty acids) in the same way as for the Eifel Maar Lakes in *Section 6.1*.

5.2 Distribution of Lipid Biomarkers

Table 5.1: Numbers of investigated compound fractions

Lake	Hydrocarbons	Fatty Acids	Alcohols & Sterols
Holzmaar	11	12	12
Meerfelder Maar	15	16	17
Meerfelder Maar (High Resolution Sequence)	46	49	49
Großer Treppensee	22	—	—

Out of the lipid fractions isolated by means of liquid chromatography, aliphatic hydrocarbon, carboxylic acid and alcohol fractions were analysed using gas chromatographic methods as described in *Chapter 4*.

This chapter will introduce the identified compounds and their respective abundances in the investigated profiles prior to a detailed description of every compound class and interpretation of paleoclimatic and -environmental implications in the following chapters. Deviating from the previously presented bulk geochemical characterisation, specific samples out of the whole sample sets were selected based on these data for lipid investigation. Selection criteria were significant changes in the elemental composition or Rock-Eval parameters as well as transitions between the lithological zones. A listing of numbers of samples selected for the lipid inventarisation is available from *Table 5.1*; the positions of selected samples are indicated in *Figs. 3.4, 3.6, 3.7 and 3.9*.

Due to the complex composition of the selected lipid fractions and the high number of investigated samples, quantification was limited to the dominant constituents in order to obtain complete profiles of these compounds.

All three fractions are dominated by ubiquitous compounds. Within the aliphatic hydrocarbons, 56 individual compounds were identified. Homologous *n*-alkanes in the chain length range from *n*-C₁₄ to *n*-C₃₃ are the dominant constituents. Within the short chain length range, unsaturated and/or branched alkanes were additionally found. Beside the *n*-alkanes, various steroidal and triterpenoidal hydrocarbons were detected and quantified. No evidence was found for the presence of botryococcenes in both, aromatic and aliphatic hydrocarbon fractions. These compounds are highly specific markers for the resting stage of the alga *Botryococcus braunii* (Metzger *et al.*, 1985, 1988) whereas mono- and diunsaturated alkenes

in the chain length range from C₂₇-C₃₁ were formerly found to be present in higher amounts in this species during their active green state (Gelpi *et al.*, 1968, 1970). *Botryococcus braunii* occurs in various strains which produce characteristic lipids depending on climatic conditions (Huang *et al.*, 1999). The absence of botryococenes in the Eifel Maar lakes and Lake Großer Treppelsee sediments is in agreement with organic-petrological investigations of the same sample set, where no evidence for the presence of *Botryococcus braunii* was found too (Fuhrmann, 2003). Methodical failures in the detection of botryococenes can be clearly excluded since Fuhrmann (2003) detected these compounds in sediment extracts of Lake Huguang Maar, China. Hence, the absence of this compound class in the sediments of the Eifel Maar lakes as well as Lake Großer Treppelsee appears reasonable, in particular since *Botryococcus braunii* prefers higher temperatures than those typical for the area under investigation.

In the acid fractions, 40 individual compounds were identified. These fractions are dominated by normal chain fatty acid homologues in the chain length range between *n*-C₁₂ and *n*-C₃₄. Some hopanoic acids were identified in addition to the fatty acids.

Finally, 40 individual compounds were identified in the alcohol fractions. These are dominated by normal fatty alcohols, the detected chain length ranges from *n*-C₁₅ to *n*-C₃₃. Beside these normal chain compounds, 18 steroids and/or triterpenoids were identified.

Beside the detailed investigation of these compound specific lipid fractions, a fourth fraction of low polar NSO-compounds, mainly containing esters, ketones and aldehydes, was screened for the presence of unsaturated long-chain alkenones. The C_{37:2} and C_{37:3} homologues were initially discovered in marine sediments and the ratios of alkenones (U_{37}^k ; $U_{37}^{k'}$) are widely used for the reconstruction of paleo-sea-surface-temperatures (Brassell *et al.*, 1986; Brassell, 1993). The occurrence of these compounds has been reported for lake sediments as well (Zink, 2000; Zink *et al.*, 2001), where their origin, in contrast to the oceans, is still unknown. The investigation of the Eifel Maar lake as well as Lake Großer Treppelsee sediments, however, yielded no evidence of unsaturated alkenones.

An additional screening of the aromatic fractions yielded no significant distributions of the respective constituents. Even if a number of studies evaluated aro-

matic hydrocarbons as specific marker molecules for the depositional environment (Hughes *et al.*, 1995), no significant content was expected from that kind of young sediments as present in the areas under investigation. Investigating different settings, for example source rocks or crude oils, the distributions of several aromatic hydrocarbons may additionally serve as indicators for maturity (Radke and Welte, 1981; Radke *et al.*, 1982). Due to the less specific distribution in the present study, however, aromatic compounds were excluded from further investigation.

The results obtained from the detailed analysis of three compound specific lipid fractions will be discussed separately in the following sections.

5.2.1 Aliphatic Hydrocarbons

Three representative chromatograms that briefly visualise substantial differences in the hydrocarbon compositions are illustrated in *Fig. 5.9*. Numbers in chromatograms refer to *n*-alkane chain length, letter labelled peaks are listed in *Table 5.2*. The identified aliphatic hydrocarbons can be subdivided into *n*-alkanes, branched and/or unsaturated and cyclic compounds. The presentation of results in this chapter will be limited to this preliminary subdivision of aliphatic hydrocarbons; concentrations are given as the sum of the respective compounds. A more detailed evaluation also focussing on individual compounds will follow during the discussion of the origin of organic matter in *Chapter 6.2*.

Total amounts of all clearly identified and quantified aliphatic compounds vary between 80 – 1,670 µg/g TOC with a much sharper 25 to 75 % quartile between 340 – 770 µg/g TOC as illustrated in *Fig. 5.10*.

5.2.1.1 *n*-Alkanes

Alkanes with carbon numbers lower than *n*-C₁₅ were found in negligible concentrations throughout all three sedimentary profiles. The *n*-alkanes with a chain length from *n*-C₁₅ to *n*-C₃₃ constitute the majority of aliphatic hydrocarbons. Their percentages vary from 51 to 74 % of total aliphatic hydrocarbons. A maximum contribution is reached from *n*-C₂₇ to *n*-C₃₁ in most of the investigated sediments like it was previously reported for various terrestrial settings ([Cranwell, 1982](#); [Kawamura and Ishiwatari, 1985](#); [Wilkes *et al.*, 1999](#); [Schwark *et al.*, 2002](#)) and interpreted as land plant derived organic matter input. Due to the biosynthesis of *n*-alkanes from corresponding even chain carboxylic acids by decarboxylation ([Kolattukudy, 1980](#)) and the low degradation state of the investigated sediment profiles, odd *n*-alkanes are much more dominant than even numbered homologues, they make up between 40 – 65 % of aliphatic hydrocarbons whereas even *n*-alkane percentages vary between 6 – 26 %. Especially the observed pronounced predominance of odd numbered *n*-alkanes in the chain length range from *n*-C₂₇ to *n*-C₃₁ additionally points to terrestrial plant leaf waxes as important sedimentary organic matter sources ([Eglinton and Hamilton, 1967](#)).

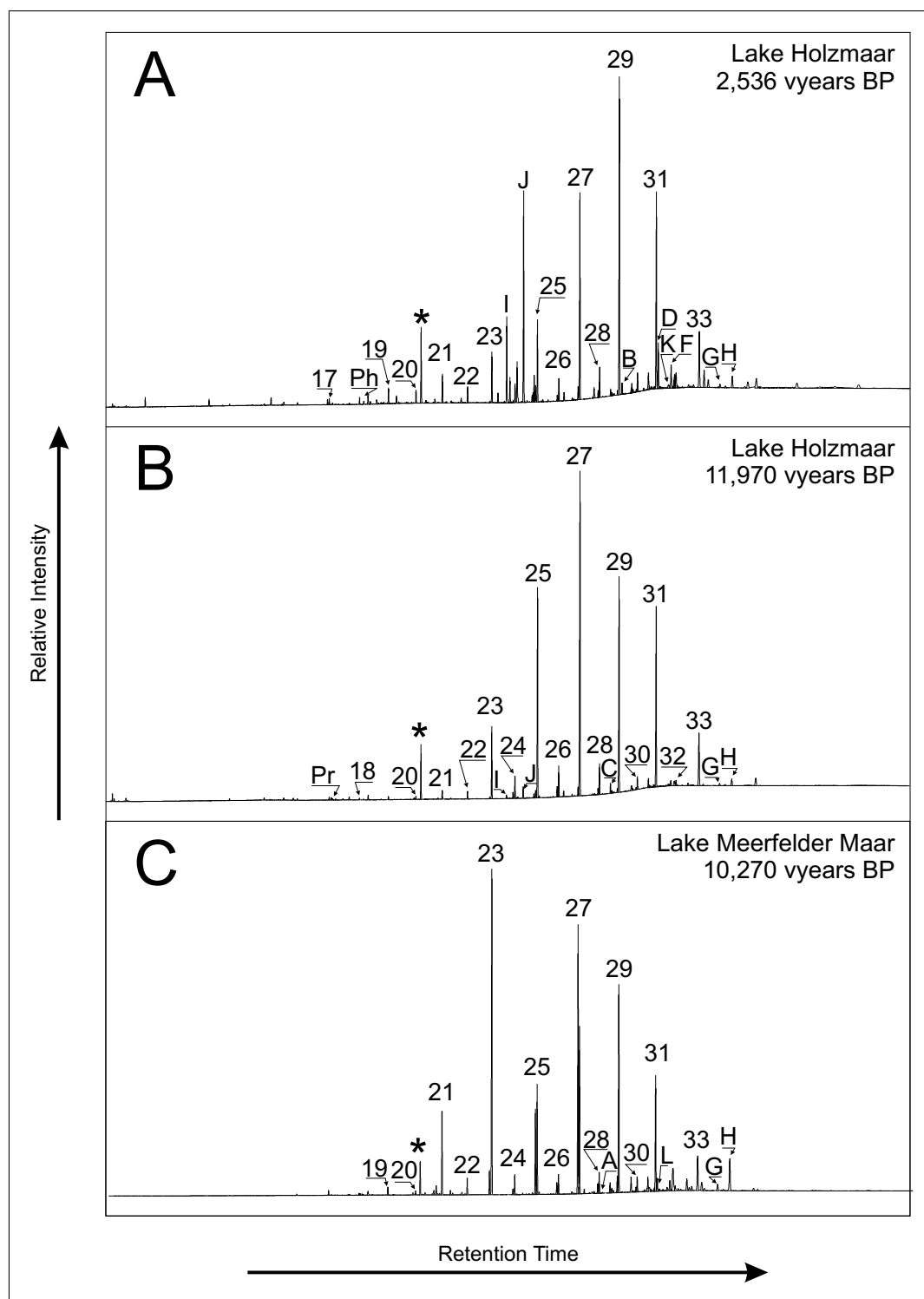


Figure 5.9: Exemplary chromatograms of aliphatic hydrocarbon fractions; numbers refer to chain length of *n*-alkanes; letters refer to compounds as listed in Table 5.2; Pr: pristane; Ph: phytane; asterisk: 5α-androstane as internal standard

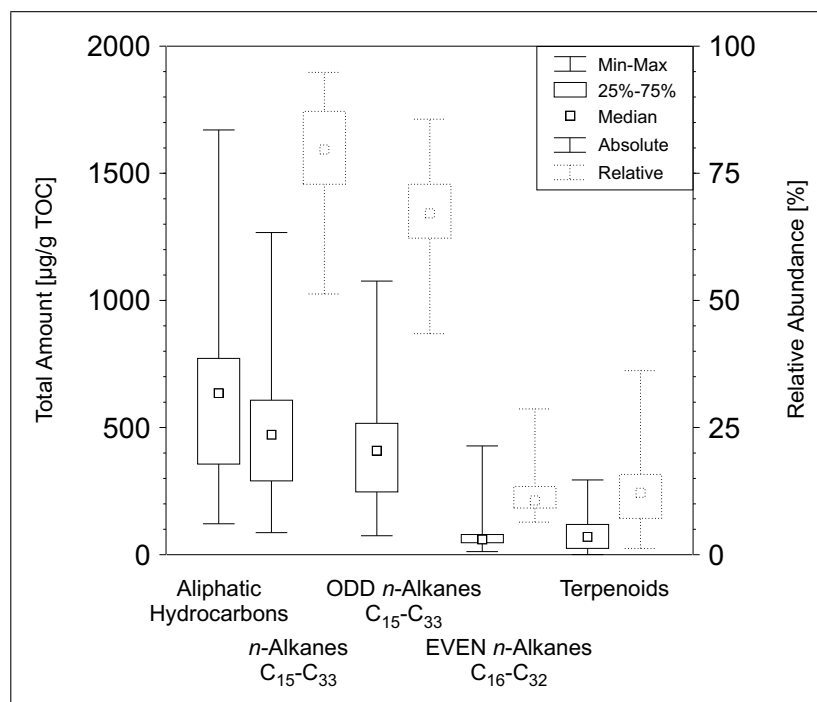


Figure 5.10: Total amounts (solid columns; left Y-axis) and abundances relative to detected compounds in sum (dashed columns; right Y-axis) of *n*-alkanes and terpenoids; *n*-alkanes are further subdivided to ODD- and EVEN-numbered homologues

Age- and/or depth related trends of relevant individual compounds will be discussed in *Chapter 6*, absolute concentrations are here assigned to groups referring to the structural fundamental units as introduced above. Results for each sample are listed in detail in *Appendix D*, *Tables D.5-D.16* for aliphatic hydrocarbons. Additionally, remarkable differences in the constituents group composition will be discussed detailed, however, limited to the dominant odd numbered homologues.

Summed concentrations of *n*-alkanes vary between 220 – 740 µg/g TOC in the **Lake Holzmaar** sedimentary sequence with percentages of odd-numbered derivatives ranging from 76 – 91 % relative to normal chain compounds (*cf. Fig. 5.11*). The uppermost section A of Lake Holzmaar, represented by four samples at 184, 1,311, 2,083 and 2,536 vyears BP is generally characterised by decreasing amounts of *n*-alkane concentrations from 530 µg/g TOC in the top sample to 450 µg/g TOC closely at the section A to B transition. The sections minimum of 400 µg/g TOC at 1.311 vyears BP is directly followed by a short term increase in the next 772 years, that is made up by enhanced abundances of homologues with

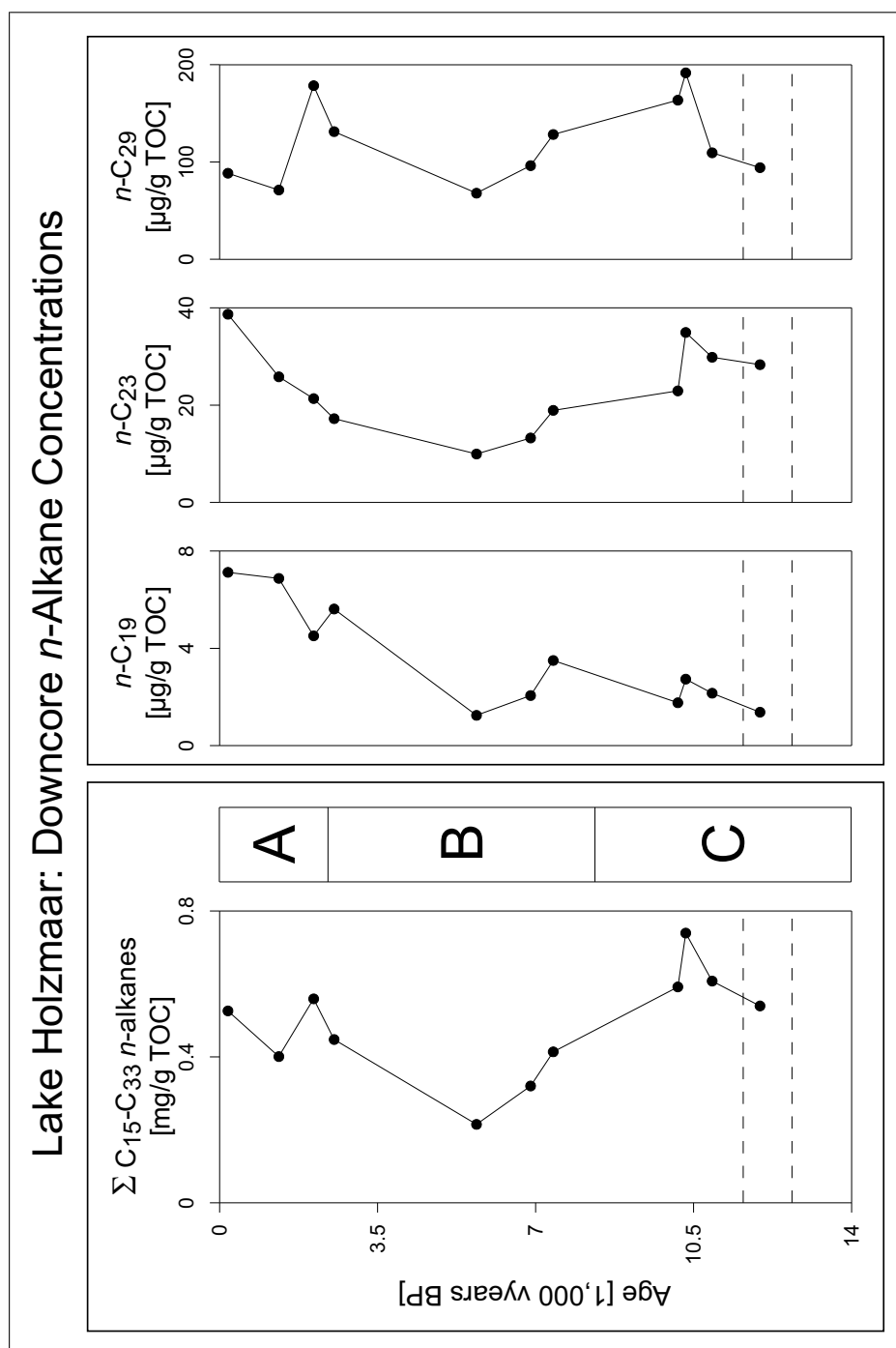


Figure 5.11: Summed downcore concentrations of n -C₁₅ \dots n -C₃₃ alkanes (left panel) and selected individual homologues as mentioned in the text (right panel) related to age for Lake Holzmaar; dashed lines indicate the Younger Dryas cold period

carbon numbers higher than 25, especially *n*-nonacosane. A depletion in shorter chain length compounds was observed in the same range of age with exception of a sharp peak of *n*-pentadecane, that, however, weakly affects summed alkane concentrations.

Middle Holocene section B, that was characterised by stable climatic conditions and high portions of allochthonous organic matter supply (Zolitschka and Negen-dank, 1998), is represented by three samples at 5,690, 6,888 and 7,390 vyears BP. This lithological zone is distinguished by reduced abundances in its upper half with the overall minimum of 220 µg/g TOC at 5,690 vyears BP, induced by a depletion in the whole homologous series of *n*-alkanes. With increasing age, concentrations of *n*-alkanes increase until the oldest sample of section B and further over the Holocene/Lateglacial transition.

However, relatively high abundance on top of the early Holocene/Lateglacial section C, represented by four samples between 10,150-11,970 vyears BP, is built up by enhanced concentrations of homologues beyond *n*-icosane, whereas decreasing concentrations were measured for the lighter homologues. With further increased age, the Lake Holzmaar overall maximum content of *n*-alkanes was measured at 10,325 vyears BP prior to another decrease towards the bottom of the profile. Despite this general trend, the concentration of *n*-pentacosane maximises 585 years later than the whole *n*-alkane series at 10,910 vyears BP. An additional observation is the outstanding increase of *n*-C₂₇, being the most abundant *n*-alkane in Lake Holzmaar profile during section C exclusively, whereas *n*-nonacosane dominates during middle Holocene and lower Subatlantic.

Changing to **Lake Meerfelder Maar**, variation width of summed *n*-alkane concentrations between 140 – 1,270 µg/g TOC is significantly higher as measured for Lake Holzmaar whereas percentages of odd-numbered homologues relative to *n*-alkanes between 60 – 92 % are well comparable (cf. Fig. 5.12).

The occurrence of *n*-alkanes is relatively uniform during the upper 10,000 years, including wide parts of Holocene sediments: Starting from 890 µg/g TOC, the Holocene maximum abundance in the uppermost sample, concentrations continuously decrease with exception of a slightly enhanced value at 6,290 vyears BP. The strongest depletion in *n*-alkane concentrations was measured between the two uppermost sediment samples, leading to a partial minimum at 1,910 vyears BP.

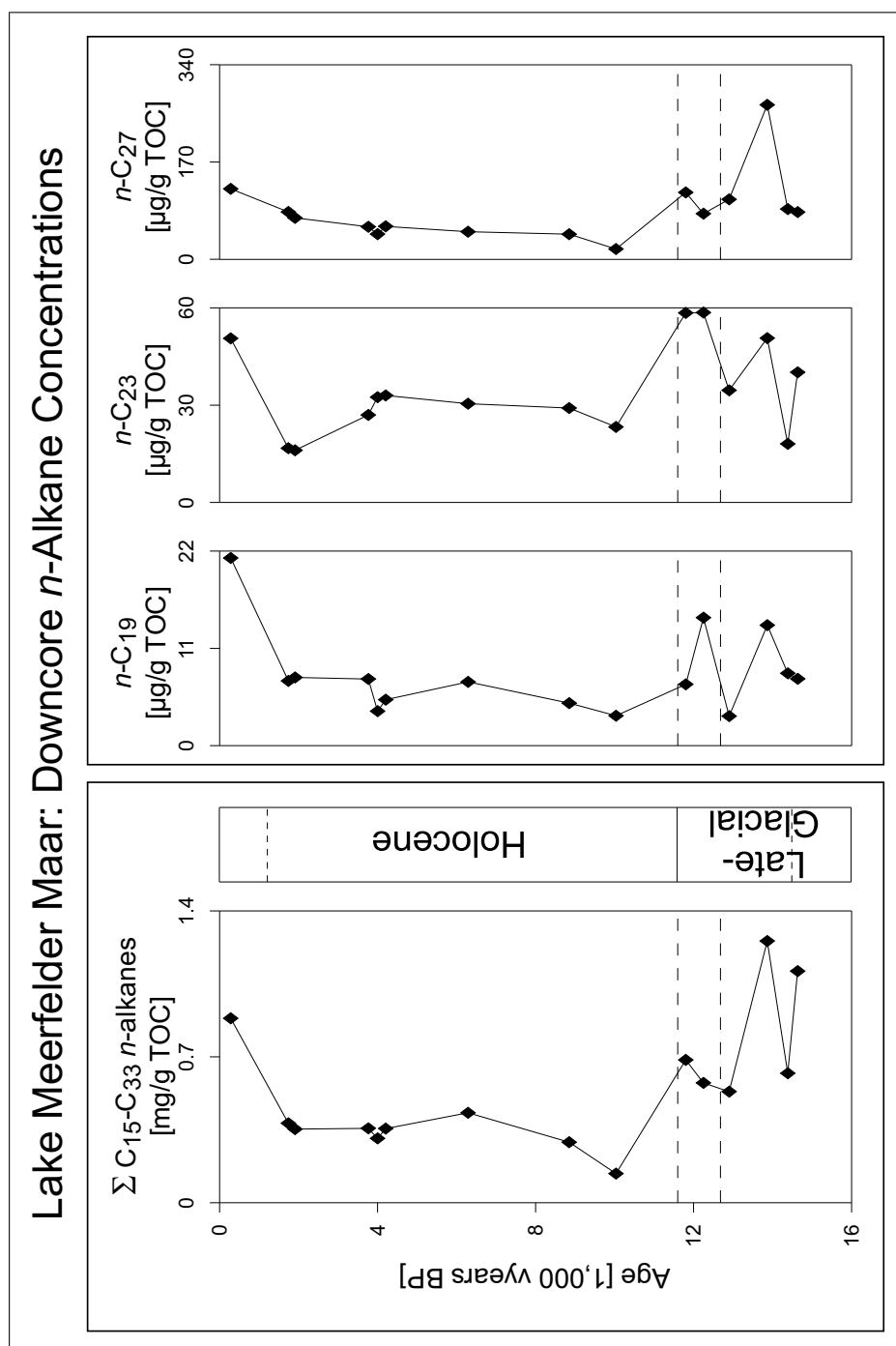


Figure 5.12: Summed downcore concentrations of $n\text{-C}_{15} \dots n\text{-C}_{33}$ alkanes (left panel) and selected individual homologues as mentioned in the text (right panel) related to age for Lake Meerfelder Maar; dashed lines indicate the Younger Dryas cold period; pointed lines in the stratigraphic column indicate the annually laminated core section

This date is in good temporal correlation to the beginning of annually laminated sediments as published by Zolitschka and Negendank (1998) and Brauer *et al.* (1999b).

With the exception of *n*-henicosane and *n*-tricosane whose absolute concentrations increase between 3,765-4,205 vyears BP, an additional significant depletion was measured for *n*-alkane abundances during this time. After further 1,185 years, the Lake Meerfelder Maar minimum of 60 µg/g TOC is reached. During early Holocene and Lateglacial, comparably high concentrations of long chain *n*-alkanes with a significant reduction during the Younger Dryas period were measured. However, this depletion was not observed uniformly for the entire homologous series of *n*-alkanes: Individual compounds in the carbon number range between 17-23 show a partial maximum abundance approximately in the middle of the Younger Dryas period at 12,250 vyears BP whereas the longer chain odd-numbered *n*-alkanes behave opposite, showing a partial minimum at the same time.

More marked variations of sedimentary *n*-alkane concentrations were observed during Lake Meerfelder Maars Lateglacial profile section below the Younger Dryas period: A maximum concentration of 1,260 µg/g TOC was found at 13,865 vyears BP, induced by strong enrichments trough the whole homologous series. Later on, a remarkably sharp minimum was detected at 14,365 vyears BP. This sample is very close to the lower end of the annually varved section of Lake Meerfelder Maar sedimentary sequence, dated to 14,500 vyears BP by Brauer *et al.* (1999b).

Towards the oldest sample, differences in *n*-alkane composition depending on chain length were found again: From the light-weight end to *n*-C₁₉, decreased concentrations were measured, contrasting to increased abundances of the remaining *n*-alkane group members with exception of *n*-heptacosane, whose absolute concentration decreases as mentioned for shorter chain length derivatives.

From Lake Meerfelder Maars second sample set, with a higher temporal resolution between 9,970 – 12,490 vyears BP (*Fig. 5.13*), relatively stable *n*-alkane occurrence was retrieved during the very early Holocene section. Summed concentrations vary between 140 – 710 µg/g TOC with most marked fluctuations during the upper 580 vyears. After 10,380 vyears BP, values slightly increase towards the beginning of the Younger Dryas with a period of enhanced alkane concentrations between 11,130 – 11,210 vyears BP. As already introduced during the

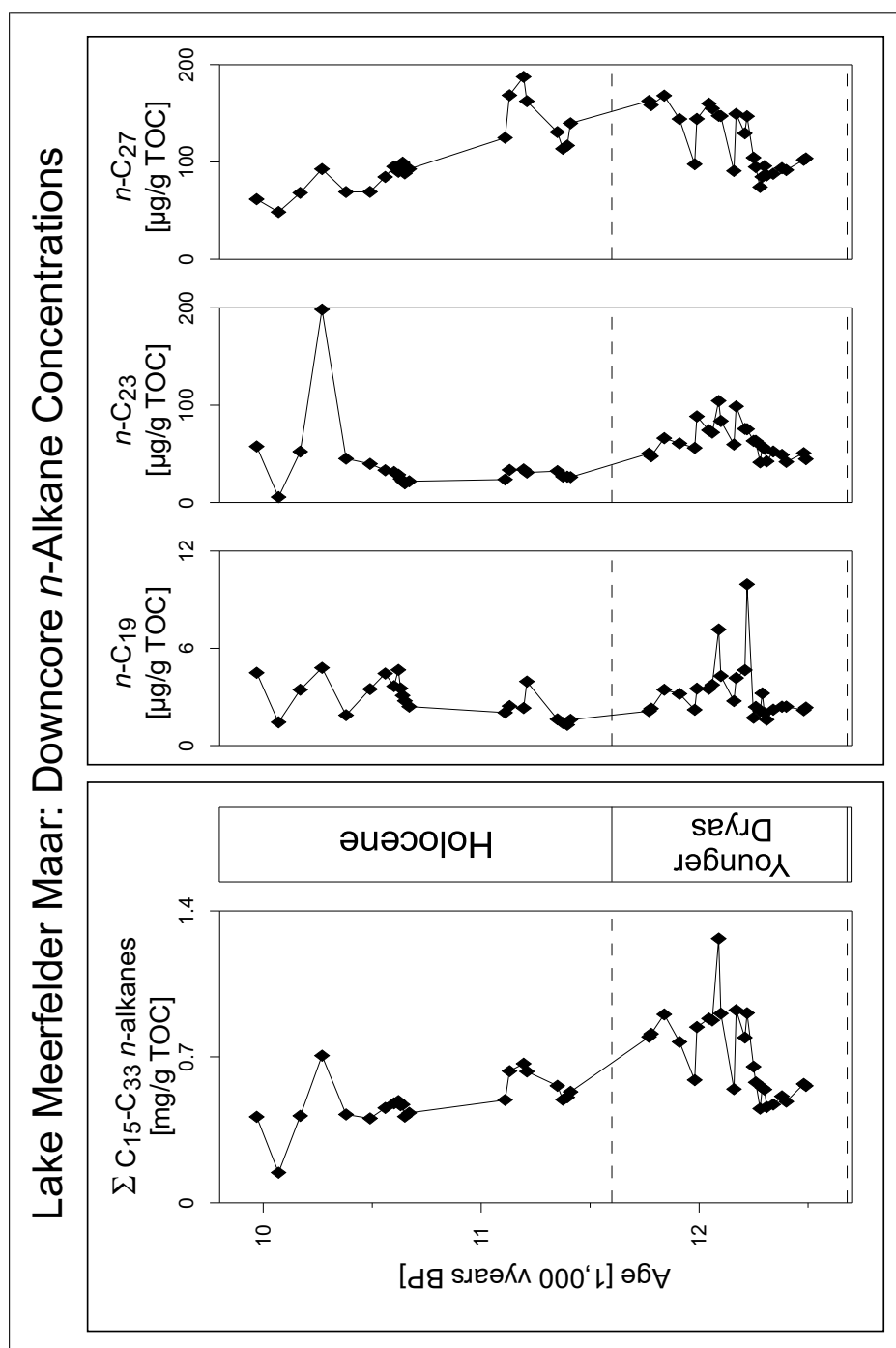


Figure 5.13: Summed downcore concentrations of n -C₁₅ ... n -C₃₃ alkanes (left panel) and selected individual homologues as mentioned in the text (right panel) related to age for Lake Meerfelder Maars high resolution sequence; dashed lines indicate the Younger Dryas cold period

description of the other sedimentary profiles, significantly differing contributions of individual homologues to the summed *n*-alkane concentration were detected: The early Holocene minimum abundance at 10,070 vyears BP is caused by a strong depletion in nearly all *n*-alkane concentrations, only *n*-heptacosane concentration is lowered slightly. The increase during the following 200 varve years was furthermore measured for all normal chain alkanes, however, highest slope by far was measured for *n*-tricosane whose absolute concentration is nearly quadrupled during the early Holocene maximum at 10,270 vyears BP in comparison to the preceding sample. Uniquely for the Lake Meerfelder Maar high resolution sequence, *n*-tricosane therefore becomes more abundant than *n*-pentacosane at this time.

After the stage of Holocene maximum abundance, a uniform reduction in *n*-alkane concentration was measured which is, however, not time synchronous for all homologues. The depletion persists until 10,380 vyears BP in the case of compounds lighter than *n*-icosane, whereas the heavier derivatives abundance reaches its partial minimum 110 varve years later.

Between 10,490 – 10,670 vyears BP, a short time oscillation of *n*-alkane distributions, starting with a slight increase was observed, showing temporal differences related to the *n*-alkane chain length in turn. Concentrations of the lightest investigated homologues including *n*-C₁₅ to *n*-C₁₉ increase until 10,620 vyears BP, whereas *n*-C₂₁ and *n*-C₂₃ continuously decrease instead of the oscillation observed for remaining alkanes. *n*-Pentacosane shows an oscillating behavior, however, maximising 20 varve years earlier compared to the shorter chain length homologues as described above. With further increasing chain length, variations become changed more general. An additional reduction was measured at 10,620 vyears BP in direct opposition to the sharp maximum abundances of the three lightest derivatives. The stage of maximum concentrations of long chain derivatives was dated to 10,630 – 10,640 vyears BP and is therefore latest among all detected *n*-alkanes. Within the sample section between 11,110 – 11,410 vyears BP, characteristically increasing concentrations were measured until 11,195 vyears BP prior to a significant reduction towards older samples. As already reported for the overlying sediments, individual compounds show different age related variations of their absolute concentration. Derivatives with carbon numbers up to *n*-C₁₉ maximise at 11,210 vyears BP, 15 years earlier as recognisable from the summed downcore plot in *Fig. 5.13*. With increasing chain length up to *n*-C₂₅, the dating of the

local maximum abundance shifts to 11,130 vyears BP, now 65 years later as illustrated in the summed downcore plot. The most dominating *n*-alkanes ranging from *n*-C₂₇ to *n*-C₃₁ mainly affect the summed downcore plot due to their high relative proportions compared to shorter chain length derivatives and maximise at 11,195 vyears BP in the case of *n*-C_{27–29} as well as 11,210 vyears BP in the case of *n*-C₃₁. Towards further increased age, absolute concentrations become decreased, however, the deepest samples of this subsection show slightly enhanced abundances of long chain homologues heavier than *n*-pentacosane. The most marked increase was measured for *n*-heptacosane.

Widely scattering *n*-alkane concentrations between 450 – 1,270 µg/g TOC were measured for Younger Dryas sediment samples. Divergences in maximum- and/or minimum abundances as well as their respective duration in relation to absolute ages during this important climatic epoch are better resolved in comparison to Lake Meerfelder Maars first profile and is described directly below.

The upper 70 varve years of Younger Dryas sediments (11,770 – 11,840 vyears BP) are characterised by increasing summed concentrations of *n*-alkanes, that are additionally higher as measured for overlying early Holocene sediment layers. With further increased age, a significant sinking was observed until a local minimum abundance at 11,980 vyears BP. Merely in the chain length range from *n*-C₁₅ to *n*-C₁₉, the onset of this depletion dates 70 varve years later but the minimum abundance is reached synchronously with the longer chain homologues.

The following sequence between 11,990 – 12,100 vyears BP shows increased *n*-alkane concentrations in sum again, including the Younger Dryas overall maximum of 1,270 µg/g TOC. During this chronologically sharply separated maximum, highest relative enrichments were measured for the shortest chain length homologues *n*-C₁₅ to *n*-C₁₉ whose absolute concentrations in sum are more than three times higher at this time compared to both adjacent samples. Absolute concentration of *n*-heptadecane moreover becomes higher than that of nonadecane, whereas concentrations in this chain length range increase with increasing chain length during remaining profile sections. Further interesting relationships between chain length and concentration were observed for the heaviest homologues between *n*-C₂₇ to *n*-C₃₁: heptacosane concentration maximises as most abundant *n*-alkane at 12,045 vyears BP and decreases with increasing age, whereas nonacosane is the most abundant homologue during the overall maximum 45 varve years later.

Synchronously for all detected *n*-alkanes, a sharp local minimum was determined

at 12,160 vyears BP prior to another rapid increase within the following ten varve years. This plateau persists with a slight depletion until 12,220 vyears BP. At this time a second very strong enrichment was determined especially for the chain length range from n -C₁₅ to n -C₁₉.

Further on, summed concentration is continuously reduced until 12,280 vyears BP, leading to the Younger Dryas overall minimum of 450 µg/g TOC in sum of all homologues. This state of relatively low n -alkane concentrations persists until the profiles bottom with exception of a short term enrichment for ten varve years between 12,290 – 12,300 vyears BP, where, however, absolute abundances are lower compared to the previously described stages of high abundances.

Downcore variations of n -alkane concentrations in sum for the **Lake Großer Treppelsee** sedimentary sequence are illustrated in *Fig. 5.14*. Average concentration of 220 µg/g TOC for summed n -alkanes in Lake Großer Treppelsee sedimentary profile is low compared to the Eifel Maar Lakes. Additionally, the variability between 90 – 320 µg/g TOC is lowest among the investigated archives with, moreover, lowest extremes. Lake Großer Treppelsee shows the most stable composition of long chain n -alkane subfraction: Within the short chain length range from n -C₁₅ to n -C₁₉, lowest concentrations between 0.1 – 14 µg/g TOC were measured for individual compounds with, deviatingly from the results previously reported for the Eifel Maar Lakes, higher abundances of n -heptadecane compared to n -nonadecane.

With increased chain length, abundances of homologues generally rise until n -nonacosane, the most abundant homologue in wide sections of the sedimentary record with a variation width from 20 – 90 µg/g TOC, whereas absolute concentrations of heavier alkanes are lower.

In relation to the core depth, a depletion in all homologues was observed for the uppermost section until 4.8 m depth below the sediment surface. With further increased core depth, n -alkane concentrations in sum continuously increase until 9.8 m depth, where a partial maximum abundance of n -alkanes was measured. Accordingly, [Giesecke \(1999\)](#) found single lighter layers at 9.3 – 9.7 m depth in between the calcareous mud ranging from 5.5 – 11 m profile depth. Between 10.7 – 12.6 m depth, significantly lowered n -alkane contents were measured, which are, however, not uniform for all homologues. Among the shortest chain length derivatives, n -pentadecane remains nearly constant whereas n -heptadecane and n -nonadecane behave proportionally in reverse. The longer chain length deriva-

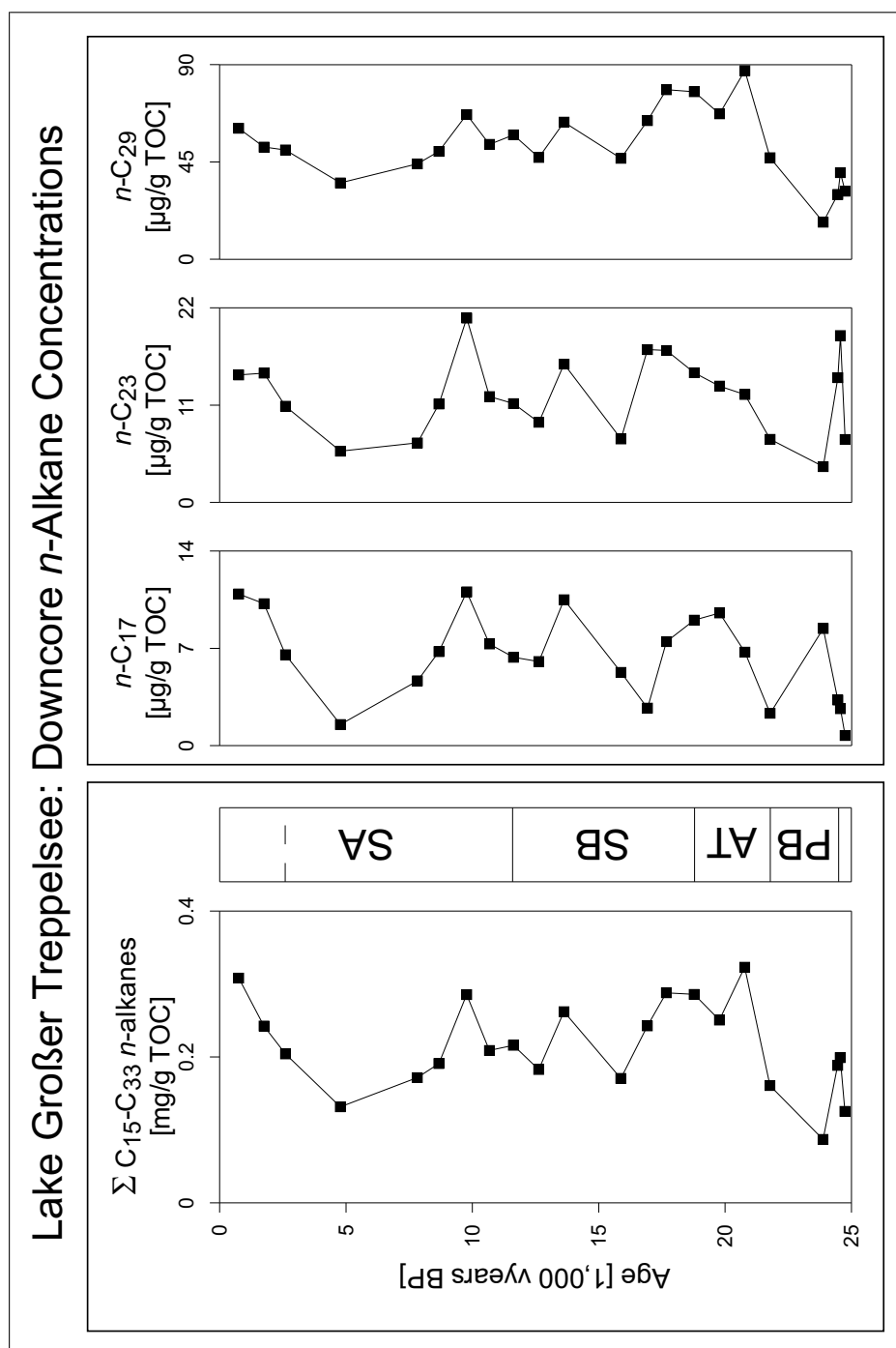


Figure 5.14: Summed downcore concentrations of $n\text{-C}_{15} \dots n\text{-C}_{33}$ alkanes (left panel) and selected individual homologues as mentioned in the text (right panel) related to profile depth of Lake Großer Treppensee; SA: Subatlantic; SB: Subboreal; AT: Atlantic; PB: Preboreal

tives abundances additionally decrease in this profile section, but *n*-heptacosane, *n*-nonacosane and *n*-tritriacontane show an intermediate enrichment at 11.6 m depth which is in good correlation to the beginning of lamination as published by Giesecke (1999).

Another partial maximum was measured at 13.6 m depth prior to the following short term reduction at 15.9 m depth. A relatively stable section characterised by constantly high abundances of *n*-alkanes was measured between 16.9 – 20.8 m profile depth. Considering individual compounds in this depth interval, significant differences of growth rates depending on chain length are recognisable. Below the minimum, concentrations of the lowest abundant homologues ranging from *n*-C₁₅ to *n*-C₁₉ are still lowered until 16.9 m below the sediment surface. On the other hand, longer chain derivatives are strongly enriched at the same depth in comparison to the local minimum of the summed *n*-alkane curve at 15.9 m depth.

With further increased depth, the shortest chain length derivatives reach their overall maximum abundance at 18.8 m, whereas a comparable maximum was found for the longer chain derivatives 1.1 m above. The overall maximum abundance of *n*-alkanes in Lake Großer Treppensee sedimentary sequence as illustrated in Fig. 5.14, that additionally marks the lower end of high *n*-alkane concentrations, is induced especially by high amounts of homologues heavier than *n*-C₂₃, whereas lighter derivatives are already lowered in the same depth.

Below 20.8 m depth, *n*-alkane concentrations are drastically reduced, the profiles overall minimum abundance was measured at 23.9 m where, on the other hand, the generally low abundant *n*-heptadecane shows a discrete maximum abundance with an absolute concentration 10-17 times higher than *n*-pentadecane and *n*-nonadecane, respectively. A last short term enrichment was found synchronously to the lower end of rhythmic lamination as published by Giesecke (1999) and is induced by strongest relative enrichments in medium chain length homologues between *n*-C₂₁ and *n*-C₂₅. The longer chain length derivatives are also enriched in this depth and further on show reversed abundances of *n*-heptacosane and *n*-nonacosane. The first named becomes most abundant *n*-alkane in Lake Großer Treppensee sedimentary sequence uniquely.

Table 5.2: Constituents of hydrocarbon fractions

Label*	Compound
A	cholestadiene
B	trinorhop-17(21)-ene
C	5 α -cholest-2-ene
D	hop-17(21)-ene
F	hop-13(18)-ene
G	homohop-30()-ene
H	β , β -homohopane
I	10 α -des-A-olean-13(18)-ene
J	A-lupane
K	fern-9(11)-ene
L	17 β , 21 α -norhopane

*Letters refer to labelled peaks in *Fig. 5.9*

5.2.1.2 Steroidal and Triterpenoidal Hydrocarbons

In addition to the *n*-alkanes described above, a number of cyclic terpenoids, namely hopane derived pentacyclic compounds and tetracyclic cholestanes/cholestenes as listed in *Table 5.2*, as well as 10 α -des-A-olean-13(18)-ene, A-lupane and fern-9(11)-ene, were identified within the hydrocarbon fractions. The structures of ten additionally detected terpenes could not be determined definitely.

The relative contribution of identified cyclic compounds to the sum of aliphatic hydrocarbons is low compared to the *n*-alkanes; summed amounts vary between 10 – 295 $\mu\text{g/g}$ TOC, representing a percentage between 1 – 36 % of quantified aliphatic hydrocarbons (*cf. Fig. 5.10*). The downcore variations of summed abundances are illustrated in *Fig. 5.15* for the two important groups of cholestanes/cholestenes and hopanes/hopenes. All homologues as listed in the table above were used for the summation, only in the case of Lake Großer Trepelsee, hop-17(21)-ene and 17 β ,21 α -norhopane were not detected continuously and therefore generally excluded from summation for that sedimentary profile.

Both, the concentrations and the variations of summed cholestanes/cholestenes, are low in **Lake Holzmaar** sediments (*cf. Fig. 5.15*; left panel) with the double unsaturated cholestadiene as lowest abundant derivative, followed by 5 α -cholest-

2-ene. The former compound shows insignificant age related variations around the average concentration of 0.3 $\mu\text{g/g}$ TOC, whereas enhanced abundances of the remaining compounds were measured at 2,536 vyears BP and, especially for 5 α -cholest-2-ene, at 7,390 vyears BP.

In contrast, bacteria related hopanoic biomarker concentrations are much higher, showing comparable age related variations with a stable composition during the Subatlantic and the middle Holocene. During the Subatlantic, abundances increase dramatically after a period of very low concentrations around 1,311 vyears BP. At 2,536 vyears BP, a significant maximum is reached synchronous to the Subatlantic to Holocene transition. Especially hop-17(21)-ene, hop-13(18)-ene and β,β -homohopane contribute in remarkable concentrations. With further increasing age, strongly reduced concentrations were measured towards the previously observed zone of minimum abundances around 5,690 vyears BP. Under contribution of the same three derivatives again, hopane concentrations reach their Lake Holzmaar overall maximum of 75 $\mu\text{g/g}$ TOC at 6,888 vyears BP, immediately followed by another decrease. This is obviously in contrast to the previously discussed *n*-alkane fractions, showing maximum abundances in the same range of age, but maxima were always reached at 7,390 vyears BP. At this time, hopane abundances are already lowered and remain decreasing until the Holocene to Lateglacial transition and further to the deepest sample inside the Younger Dryas cold period, in opposite to findings for *n*-alkanes again. Against this trend, trinorhop-17(21)-ene and hop-13(18)-ene show slight enhancements between 6,888 – 7,390 vyears BP and 7,390 – 10,150 vyears BP, respectively, without affecting the age-trend of the summed hopane fraction. Additionally, the relatively stable sorted contributions of each single compound to the hopane fraction is lost after 7,390 vyears BP. The earlier most important hop-17(21)-ene is strongest depleted during early Holocene and Lateglacial, whereas hop-13(18)-ene and β,β -homohopane are the most important constituents.

Varying around the average of 11 $\mu\text{g/g}$ TOC, summed cholestane/cholestene concentrations are about two times higher in the **Lake Meerfelder Maar** sedimentary profile (cf. *Fig 5.15*; middle panel). The most abundant derivative is 5 α -cholest-2-ene, whereas cholestadiene shows insignificant variations and lowest concentrations. Beside a slight enrichment in cholestadiene, the dominant 5 α -cholest-2-ene causes the enhanced cholestane/cholestene concentrations between

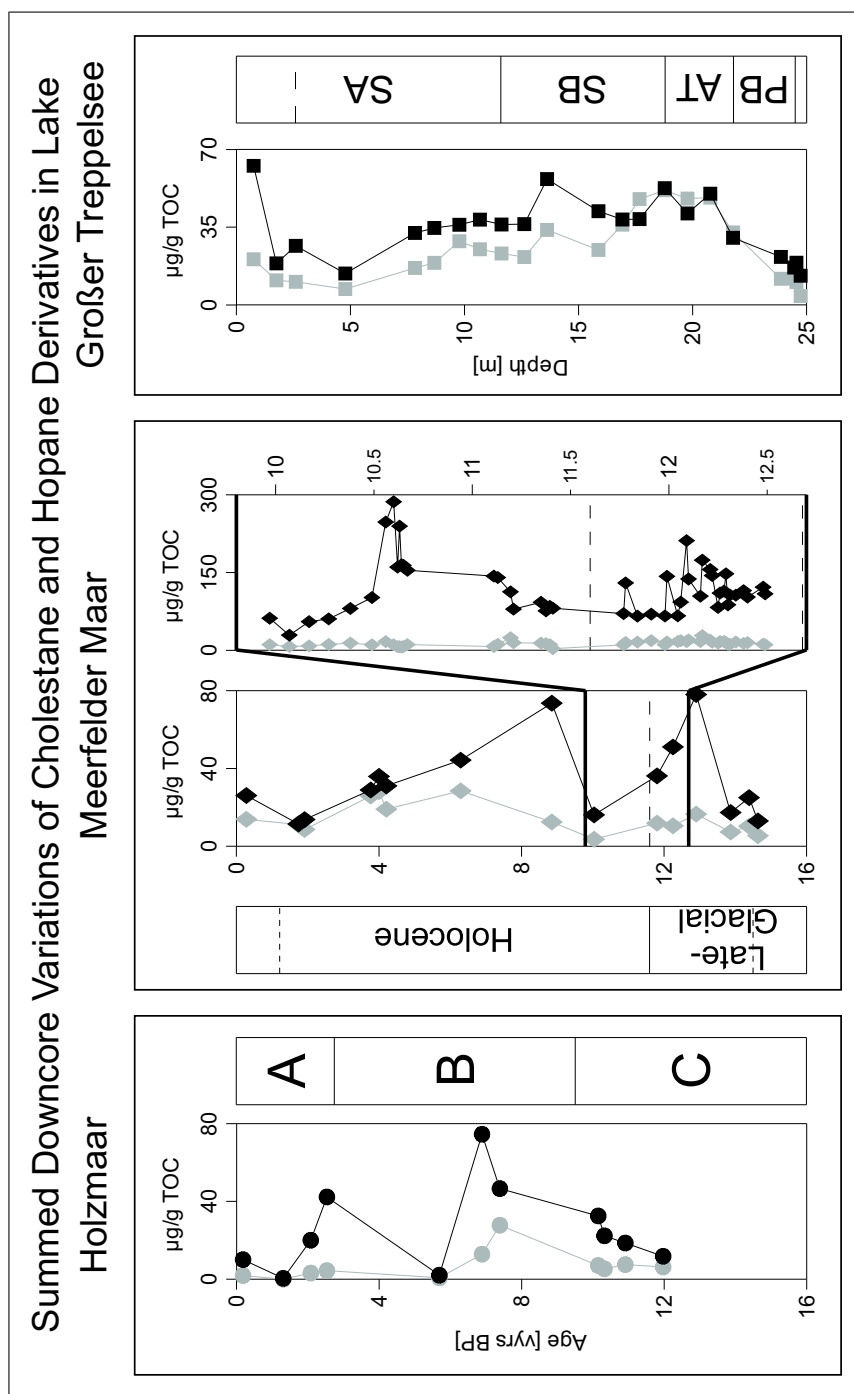


Figure 5.15: Summed cholestane + cholestene (gray symbols) and hopane + hopene (black symbols) concentrations for Lake Holzmaar (left plot), Lake Meerfelder Maar (middle plot) and Lake Großer Treppensee (right plot); dashed lines indicate the Younger Dryas period

3,765 – 6,290 vyears BP of 30 µg/g TOC on average. With further increased age, a major depletion of cholestanes was observed at 10,035 vyears BP in good agreement with the results, reported for *n*-alkanes. Towards the Younger Dryas, concentrations increase with a short term depletion during the cooler period itself until 12,900 vyears BP. The Lateglacial section is finally characterised by the lowest overall concentrations of cholestane derivatives.

Calculated to 30 µg/g TOC, average of summed hopane concentrations in Lake Meerfelder Maar sedimentary sequence is well comparable to that of Lake Holzmaar. Also weighing of included derivatives is similar. With the exception of hop-17(21)-ene, concentrations are firstly decreased in the uppermost profile segment. With the beginning of the laminated core section, in particular hop-17(21)-ene rapidly increases, showing a strong maximum at 4,000 vyears BP in direct opposition to strong depletions in short- and long chain *n*-alkanes. At 6,290 vyears BP, a significant decrease of β , β -homohopane, not affecting the enrichment of hopanes in sum, was observed. Within the next 2,560 years, hopane/ hopene concentrations further increase towards the Holocene maximum of 74 µg/g TOC in direct opposition to sinking cholestane/ cholestene abundances. Thus, Lake Meerfelder Maar does not show the characteristic minimum of hopane/ hopene distribution found for Lake Holzmaar and the Holocene maximum concentration was dated 1,962 later compared to Lake Holzmaar. Lake Meerfelder Maar Holocene maximum zone is directly followed by a decrease until 10,035 vyears BP, before another strong increase was measured during the Holocene to Lateglacial transition including the Younger Dryas cold period. This is again clearly in contrast to hopane/ hopene abundances in the Lake Holzmaar core. The profiles overall maximum concentration was found closely to the onset of the Younger Dryas low temperature period at 12,900 vyears BP before the Lateglacial is characterised by comparably low abundances.

The more detailed investigation of Lake Meerfelder Maar profile during early Holocene to Lateglacial transition shows an average cholestane concentration in the same range of magnitude whereas the hopane average concentration of 120 µg/g TOC is much higher during these times compared to the entire sedimentary sequence.

After a slight decrease between the two uppermost samples, cholestane/ cholestene concentrations continuously increase until 10,380 vyears BP. A characteristic os-

cillation, introduced by a slight depletion in summed cholestane/cholestene content and followed by a rapid enrichment and another depletion was detected within 180 varve years of sedimentation between 10,490 – 10,670 vyears BP. An additional sediment sequence with increased cholestane/cholestene content is obvious between during earliest Holocene between 11,130 – 11,395 vyears BP, where the maximum content of 30 µg/g TOC at 12,170 vyears BP.

A continuous increase in hopane/hopene concentrations from 30 – 100 µg/g TOC was detected from the sequences top sample until 10,490 vyears BP in contrast to closely scattering cholestane/cholestene abundances in sum. The slope of hopane/hopene enrichment is drastically increased during the following 110 varve years, finally reaching the overall detected maximum abundance of 290 µg/g TOC in sum of all detected derivatives at 10,600 vyears BP, obviously contrasting the relatively low cholestane/cholestene concentrations in the same range of time. Note, that in this range of age, where highest overall hopane concentrations were measured, no sample exists in the previously described lower resolved sample set. Thus, the temporary well separated stage of increased hopane/hopene abundances has no equivalent in this sample set, explaining the great difference in detected hopane/hopene maximum concentrations between both sample sets of Lake Meerfelder Maar. The underlying samples including the following 70 varve years until 10,670 vyears BP are in turn characterised by large fluctuations in hopane concentrations.

Whereas relatively stable abundances were measured towards the earliest Holocene, a further continuous depletion in summed hopane/hopene content was detected between 11,110 – 11,210 vyears BP prior to the Holocene/Younger Dryas transition where hopane/hopene composition remains constant.

The upper half of the Younger Dryas cold period is characterised by constant hopane/hopene concentrations between 11,770 – 12,045 vyears BP. These nearly constant downcore variations are interrupted by discrete maxima at 11,780 and 11,990 vyears BP, being more pronounced with increased varve age. The Younger Dryas maximum content of hopanes/hopenes in sum was measured at 12,090 vyears BP, prior to widely scattering concentrations in the underlying sediments. A relatively stable hopane/hopene composition, closely scattering around the average of 110 µg/g TOC was finally found for the early Younger Dryas section below 12,310 vyears BP.

As illustrated in *Fig. 5.15*; right panel, cholestane/cholestene concentrations in sum of the detected derivatives vary between 4 – 52 $\mu\text{g/g}$ TOC for the **Lake Großer Treppensee** sedimentary profile. The average of 25 $\mu\text{g/g}$ TOC is the highest measured in the present study. Ranging between 13 – 63 $\mu\text{g/g}$ TOC around the average of 34 $\mu\text{g/g}$ TOC, summed concentrations of hopanoic hydrocarbons are quite similar. The downcore variations of the summed concentrations are additionally well correlated to those of the cholestanes and cholestenes.

Generally decreasing content of both cholestanes/cholestenes as well as hopanoids was detected for the uppermost 5 m profile section of calcareous clays and silts without lamination. The underlying calcareous muds are characterised by increased concentrations until 9.78 m depth, that are continuously decreased in the following, interrupted by a short term maximum content at 13.63 m.

Highest abundances were measured for the rhythmically laminated calcareous muds below 15.88 m profile depth; the average concentration were determined as 49 $\mu\text{g/g}$ TOC and 46 $\mu\text{g/g}$ TOC between 17.68 – 20.78 m depth for cholestanes/cholestenes and hopanoids, respectively. Between 20.78 – 23.88 m, after [Giesecke \(1999\)](#) a profile section without general changes in sediment petrography, abundances of both compound subfractions are significantly lowered. Further decreased summed cholestane/cholestene as well as hopanoic hydrocarbon concentrations were also found for the lowermost samples where the sedimentary structure is disturbed by various sand layers ([Giesecke, 1999](#)).

5.2.1.3 Pristane and Phytane

Compared to the normal chain homologues, *iso*-alkanes are rarely found in higher plants ([Eglinton and Hamilton, 1963](#)). Nevertheless, two widespread and widely investigated acyclic diterpenoids of special interest in terms of organic matter preservation are pristane and phytane. Both of them are mainly diagenetic products of phytol, the alcohol unit in the side chain esters of chlorophyll ([Powell and McKirdy, 1973](#)). Beside this major source, tocopherols have been more recently found to be a potential precursor of pristane ([Goossens *et al.*, 1984](#)), which is then formed from the isoprenoidal side chain via an intramolecular rearrangement. Archaeobacteria may also be possible contributors of both compounds ([Chappe *et al.*, 1982](#); [Risatti *et al.*, 1984](#)). Considering only the phytol diagenesis as a source of pristane and phytane, one of these isoprenoids is formed preferentially depending

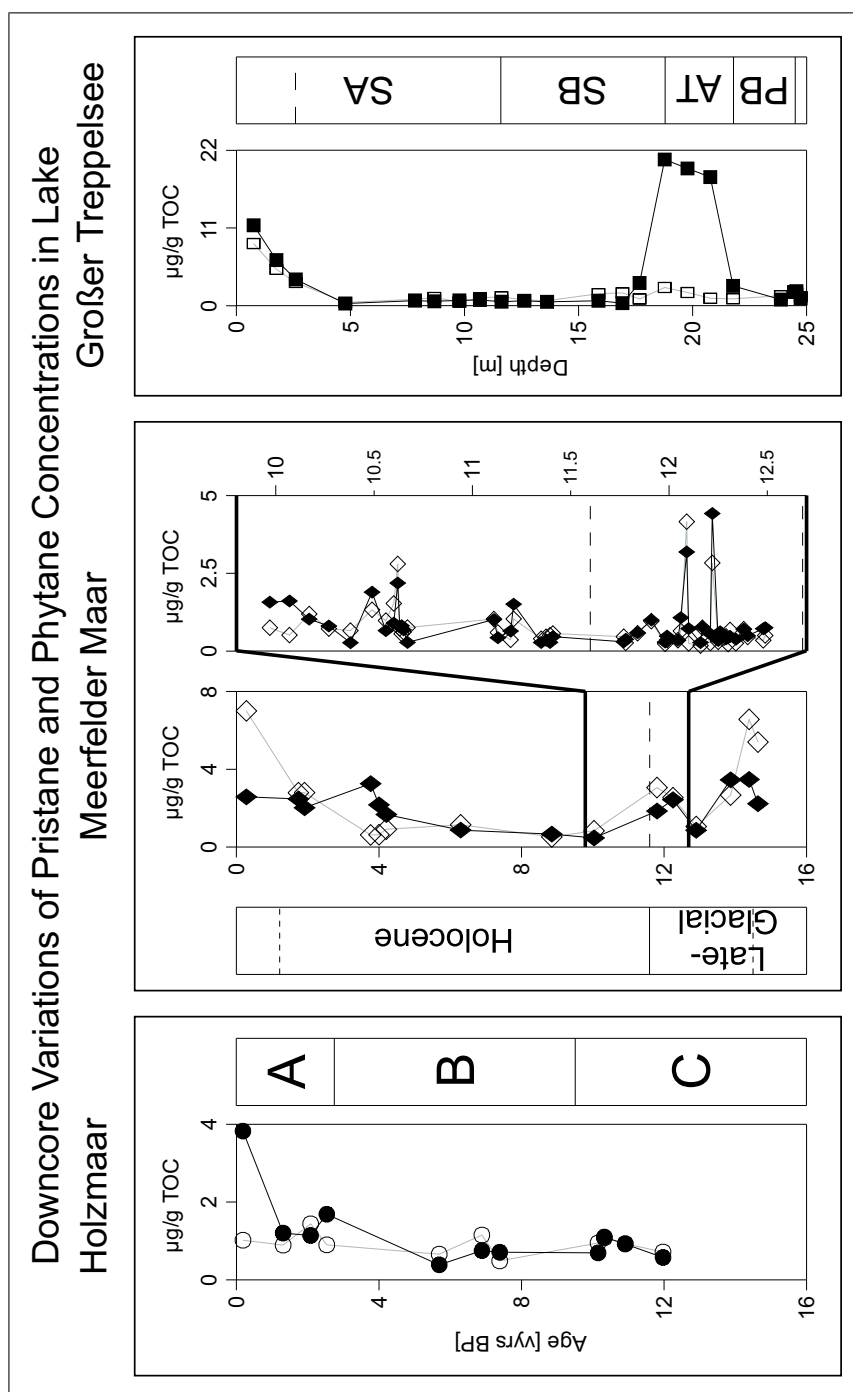


Figure 5.16: Downcore pristane (open symbols) and phytane (filled symbols) concentrations for Lake Holzmaar (left panel; circles), Lake Meerfelder Maar (middle panel; diamonds) and Lake Großer Treppensee (right panel; squares); dashed horizontal lines: Younger Dryas cold period

on the redox state during sedimentation and early diagenesis. Thus, the ratio of both compounds was widely used to infer the redox conditions and thus the preservation state of sedimentary records. *Didyk et al. (1978)* first suggested that Pr/Phy ratios lower than one point to anoxic environments whereas higher values were found to be typical for oxic conditions. Since that approach was also used in the present study to estimate the preservation state of the archives under investigation, the diagenesis of phytol as well as the relation between pristane and phytane will be discussed in the appropriate *Section 6.1*; the downcore variations of absolute abundances are briefly introduced at this point:

As obvious from *Fig. 5.16*, pristane concentrations vary from 0.5 $\mu\text{g/g}$ TOC to 1.5 $\mu\text{g/g}$ TOC for **Lake Holzmaars** sedimentary profile. Due to the high abundance of phytane in the top sample, a wider variation interval, ranging between 0.4 – 4.0 $\mu\text{g/g}$ TOC was determined.

Strongly decreasing phytane concentrations in contrast to stable downcore pristane concentrations were observed during Subatlantic (section A). At 2,083 vyears BP, merely pristane shows a moderately enriched concentration, being higher as that of phytane. After further 453 varve years, however, phytane concentrations become higher than those of pristane again.

Unsteady behavior was measured for both compounds during middle Holocene (section B): In its upper part from 2,536 to 5,690 vyears BP, concentrations of both compounds decrease with higher slope for phytane. Later on, both compounds become enriched, leading to a slight plateau at 6,888 vyears BP. Whereas pristane concentrations decrease towards section B's oldest sample, phytane abundance remains more stable over section B to C (Lateglacial) transition.

Concentrations of both compounds match very closely during the Lateglacial. A stage of slightly enhanced abundances was detected 10,325 vyears BP before concentrations of both compounds are continuously lowered until Lake Holzmaars profile bottom.

Ranging between 0.2 – 7.0 $\mu\text{g/g}$ TOC, the variation interval for both compounds is significantly wider for the investigated sedimentary sequence of **Lake Meerfelder Maar**. Highest overall abundance was measured for the top sample again; the more abundant compound, however, is pristane, clearly in contrast to Lake Holzmaar.

Absolute concentrations decrease during the upper Holocene profile section in gen-

eral. Beginning from the top sample, the dominating pristane concentrations are drastically reduced to reach values closely matching those of phytane between 1,740 – 1,910 vyears BP. A significantly differing downcore variation is obvious for both compounds with further increased varve age: the decreasing trend of pristane concentrations persists under similar slope until 4,000 vyears BP, whereas the Holocene maximum abundance of phytane was measured during this age interval.

Absolute concentrations match very closely from 6,290 vyears BP towards older samples, showing a slight tendency to lower values until 10,035 vyears BP. Towards the upper border of Younger Dryas cold period, another increase was measured for both compounds. Phytane concentration further increases during this period of lowered temperatures until 12,250 vyears BP to decrease in the following. Pristane concentration oppositionally decrease during the whole time interval.

Rising abundances of both compounds were detected before the Younger Dryas cold period until 13,865 vyears BP, before sediments become depleted in phytane concentration towards the profile bottom. Enrichment in pristane on the other hand persists for 520 additional varve years, a reduction was observed between the two oldest samples.

Considering the results from Lake Meerfelder Maars second sample set, dominating phytane concentrations were measured for the uppermost samples prior to closely matching abundances during early Holocene and Younger Dryas.

Simultaneously detected maxima are obvious at 10,490 and 10,620 vyears BP. The former is characterised by significantly enriched phytane abundance, pristane is more dominant during the latter. After a further slight enrichment in both compounds at 11,210 vyears BP, very stable composition of pristane and phytane on a relatively low level was observed during earliest Holocene and further on during the Younger Dryas period. Concentrations vary closely around the averages of 0.7 µg/g TOC and 0.8 µg/g TOC for pristane and phytane, respectively. However, two simultaneous significant maxima were observed for both biomarkers at 12,090 and 12,220 vyears BP. Maximum abundance change between both compounds: pristane dominates the former maximum whereas phytane is more dominant at the latter.

Compared to both Eifel Maar Lakes, less marked variations of pristane and phytane content were detected for **Lake Großer Treppensee** sediments. Average

concentrations are 1.9 $\mu\text{g/g}$ TOC and, more than twice as high, 4.5 $\mu\text{g/g}$ TOC, respectively. The huge difference between concentrations of pristane and phytane in this sedimentary sequence are, however, mainly caused by strongly differing concentrations for the three samples between 18.78 – 20.78 m depth (cf. *Fig. 5.16*, right panel), where the average phytane concentration is 20 $\mu\text{g/g}$ TOC. For both, over- and underlying samples, a very similar behavior was detected for both compounds.

Beginning with relatively high and slightly differing concentrations on the sediment surface, abundances of both compounds are continuously lowered until 4.78 m depth, where absolute concentrations match closely. According to [Giesecke \(1999\)](#), sedimentary composition changes from calcareous clay and silt to calcareous muds in this depth.

Towards the next sample, located 3.05 m below, both concentrations slightly increase and further remain relatively constant with pristane being the more abundant compound until 13.63 m depth, a profile segment nearly without any visible structuring.

A relatively weak enrichment in pristane concentrations was detected below 13.63 m profile depth in good correlation to the beginning of several rhythmic laminated core zones ([Giesecke, 1999](#)). For samples deeper than 16.93 m below the sediment surface, the core section is characterised by rhythmical lamination as already introduced, rapidly increasing phytane concentrations were measured up to the overall detected maximum of 20 $\mu\text{g/g}$ TOC at 18.76 m depth simultaneously to slightly increased pristane abundance of 3 $\mu\text{g/g}$ TOC. The stage of significantly enhanced phytane concentrations remains until 21.78 m profile depth before a rapid reduction within the following 2.1 m is obvious, leading to more closely matching pristane/phytane concentrations within the deepest core part.

5.2.1.4 Isotopic Composition of Aliphatic Hydrocarbons

Downcore $\delta^{13}\text{C}$ -values of odd-numbered *n*-alkanes in the chain length range from *n*-C₂₁ to *n*-C₃₃ for selected samples from both sample sets of Lake Meerfelder Maar are illustrated in *Fig. 5.17*. All data are presented in the usual delta notation as given in *Equation 5.1* relative to the Pee Dee Belemnite standard. A detailed data listing is available in *Appendix D, Tables D.17 to D.20*.

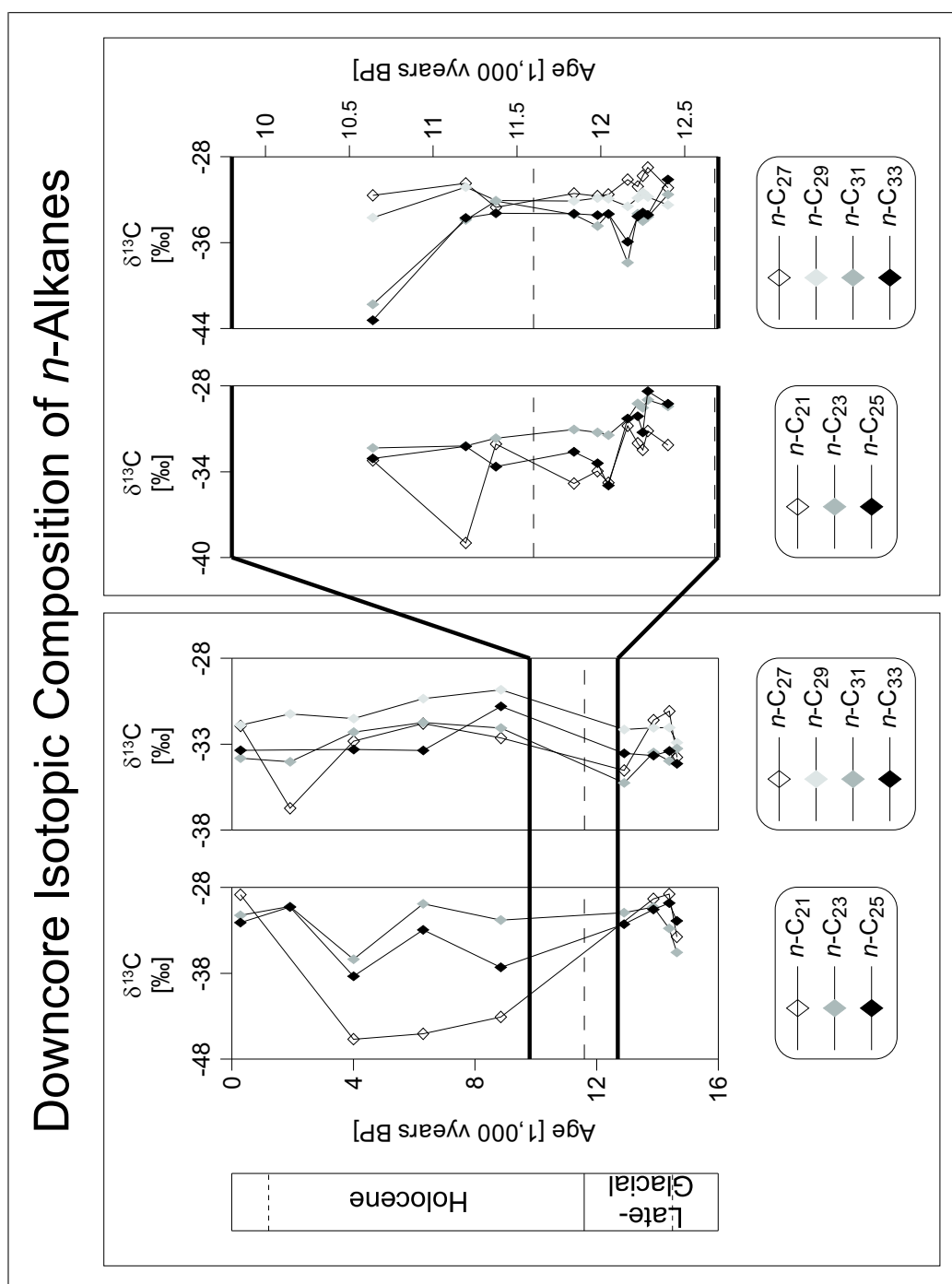


Figure 5.17: Downcore $\delta^{13}\text{C}$ -values for odd *n*-alkanes in Lake Meerfelder Maars sedimentary sequence for low (left box) and high (right box) resolved sample sets; each left plot: *n*-C₂₁ (open symbols), *n*-C₂₃ (gray symbols) and *n*-C₂₅ (black symbols); each right plot: *n*-C₂₇ (open symbols), *n*-C₂₉ (light gray symbols), *n*-C₃₁ (dark gray symbols) and *n*-C₃₃ (black symbols); dashed lines indicate the Younger Dryas cold period; dashed lines in the stratigraphic column indicate the section of annual sediment lamination

$$\delta^{13}C \text{ (‰)} = \left(\frac{R_{Sample}}{R_{Reference}} - 1 \right) * 10^3 \quad (5.1)$$

$$R = \frac{\delta^{13}C}{\delta^{12}C} \quad (5.2)$$

$\delta^{13}C$ -Values range from -54.9 ‰ to -28.3 ‰ for *n*-alkanes within the investigated chain length range; a slightly sharper variation width down to -45.7 ‰ is obvious for the plotted odd numbered homologues. Lightest values were found for the shortest chain homologue *n*-henicosane. The extremely low $\delta^{13}C$ values are limited to the age range between 4,000 – 8,850 vyears BP in excellent temporal correlation with the maximum abundances of this *n*-alkane. The lightest overall $\delta^{13}C$ -value of -54.9 ‰ was measured for the minor but well detectable *n*-C₂₈ homologue. Apart from the very negative $\delta^{13}C$ values of *n*-henicosane, these results are generally in good agreement with recently published compound specific carbon isotope data as published for example by Ficken *et al.* (1998a,b) for a Scottish montane peat bog and sediments of Lake Nkunga, Mt. Kenya, East Africa, respectively or by Huang *et al.* (1999) for sediments of Sacred Lake, Mt. Kenya, East Africa. Merely for the strikingly light values of the C₂₁ *n*-alkane, no comparable data are known from the present literature. Carbon isotope composition data of modern plants is additionally available from Ficken *et al.* (1998b), also including some data for *n*-henicosane, however, comparably low values were not observed.

During the Subatlantic, $\delta^{13}C$ of *n*-C₂₁ and *n*-C₂₇ are shifted to extremely light values first, whereas other homologues show only slightly increased (*n*-C₂₃, *n*-C₂₅, *n*-C₂₉) and/or decreased values. At 4,000 vyears BP, a significant minimum in *n*-tricosane and *n*-pentacosane isotopic values (-36.4 ‰ and -38.4 ‰, respectively) is obvious, whereas *n*-heptacosane is shifted back to a heavier value.

During middle Holocene until 8,850 vyears BP, $\delta^{13}C$ values of the *n*-C₂₁ alkane remain on an unusual light level of -44.6 ‰ on average, and also *n*-C₂₃ and, less pronounced, *n*-C₂₅ *n*-alkanes show slight depletions in $\delta^{13}C$. For the longer chain homologues finally similar and uniform $\delta^{13}C$ values between -29.8 ‰ and -33.4 ‰ were measured. Out of this group, *n*-C₃₃ is shifted from lightest values to second heaviest between 6,290 – 8,850 vyears BP.

Contrary shifts of isotopic values depending on *n*-alkane chain length are recognisable during the early Holocene and the Younger Dryas cold period: Homologues from *n*-C₂₁ to *n*-C₂₅ show increasing values whereas the longer chain odd-numbered derivatives commonly show decreasing ratios. At the lower bottom of the cold period, very similar values between -30.9 ‰ and -32.3 ‰ were detected for the short chain length *n*-alkane subgroup in contrast to a wide variation width from -32.2 ‰ to -35.3 ‰ for the longer chain length subgroup.

The shorter chain length *n*-alkanes are further characterised by very similar and increasing isotopic ratios during Lateglacial until 14,385 vyears BP, merely for *n*-tricosane decreased values were measured later than 13,865 vyears BP; a comparable decrease for *n*-C₂₁ and *n*-C₂₅ was found for the lowest sample.

More irregular behavior was detected for the longer chain length *n*-alkane subgroup: $\delta^{13}\text{C}$ -values of *n*-C₂₇ and *n*-C₃₁ alkanes drastically shift to heavier values below the Younger Dryas cold period until 13,865 vyears BP in contrast to nearly constant values for the remaining homologues. Towards the profiles bottom, also the isotopic composition of long chain *n*-alkanes shifts to lighter values that become very similar for each homologue with the oldest sample.

Recognisable from the higher resolved sample set (cf. *Fig. 5.17*; right panel), relatively stable isotopic composition in the chain length range from *n*-C₂₁ to *n*-C₂₅ was measured during the early Holocene with exception of the sharply lightened value of -39.0 ‰ for the C₂₁ *n*-alkane at 11,195 vyears BP. Beginning with extremely low $\delta^{13}\text{C}$ -values for *n*-C₃₁ and *n*-C₃₃ alkanes, longer chain *n*-alkanes show moderately (*n*-C₂₇, *n*-C₂₉) to strongly increasing (*n*-C₃₁, *n*-C₃₃) values during early Holocene.

In the upper part of Younger Dryas cold period, a relatively wide variation range from -34.8 ‰ to -31.1 ‰ was measured for the shorter chain homologues *n*-C₂₁ to *n*-C₂₅ in opposite to more similar values between -33.4 ‰ to -31.3 ‰ for longer chain *n*-alkanes. With further increasing age, two significant minima are obvious: *n*-C₂₁ and *n*-C₂₅ alkanes show low $\delta^{13}\text{C}$ -values at 12,045 vyears BP, whereas a comparably reduced $\delta^{13}\text{C}$ -values of *n*-C₃₁ and *n*-C₃₃ alkanes were detected 115 varve years later. Later than 12,160 vyears BP, a couple of varve years earlier as reported for the sharp shift in lipid biomarker concentrations, tendentially heavier $\delta^{13}\text{C}$ -values were measured for all investigated *n*-alkanes with heaviest compositions of -29.4 ‰ and -29.3 ‰ for *n*-tricosane and *n*-pentacosane.

5.2.2 Carboxylic Acids

Three exemplary chromatograms of acid fractions are illustrated in *Fig. 5.18*, numbers refer to the chain length of normal chain fatty acids and letter-labelled peaks are named in *Table 5.3*.

Acids can be subdivided again into *n*-fatty acids, branched and/or unsaturated and cyclic compounds. As already found for the relation between aliphatic hydrocarbons and *n*-alkanes, normal chain fatty acids within the chain length range from *n*-C₁₄ to *n*-C₃₂ clearly dominate the acid fractions (92 – 99 % relative to detected compounds in sum), however with a strong even over odd predominance, either maximising at *n*-hexacosanoic acid in wide parts of Lake Meerfelder Maar sequence or *n*-octacosanoic acid especially during stages of maximum fatty acid abundances in Lake Holzmaars sedimentary profile. This general composition of fatty acid fractions can also be inferred from exemplary chromatograms as illustrated in *Fig. 5.18* as well as from the relative composition of acid fractions as illustrated in *Fig. 5.19*. Decanoic to tridecanoic acid at the low molecular weight end as well as C₃₃ and C₃₄ *n*-fatty acids at the high molecular weight end of detectable fatty acids were also found, but in negligible concentrations and are therefore excluded from discussion.

In addition to the saturated normal chain homologues, a number of monounsaturated fatty acids was detected. Most prominent derivatives were the C_{16:1} and C_{18:1} acids, that were found in all three investigated profiles. Out of the bacteria derived branched fatty acids, *iso*-C₁₆ and *iso*-C₁₇ carboxylic acid were continuously detected.

A second important acid subgroup beside the normal chain homologues is made up by a variety of hopanecarboxylic acids. All of these compounds are early diagenetic products of hopanols and therefore typical markers for bacteria derived organic matter. Total amounts of all identified compounds vary between 179 – 3,959 µg/g TOC for investigated Eifel Maar Lake profiles.

5.2.2.1 Fatty Acids

Downcore variations of saturated *n*-fatty acids in sum as well as those of selected individual homologues for the investigated Eifel Maar Lake profiles are illustrated

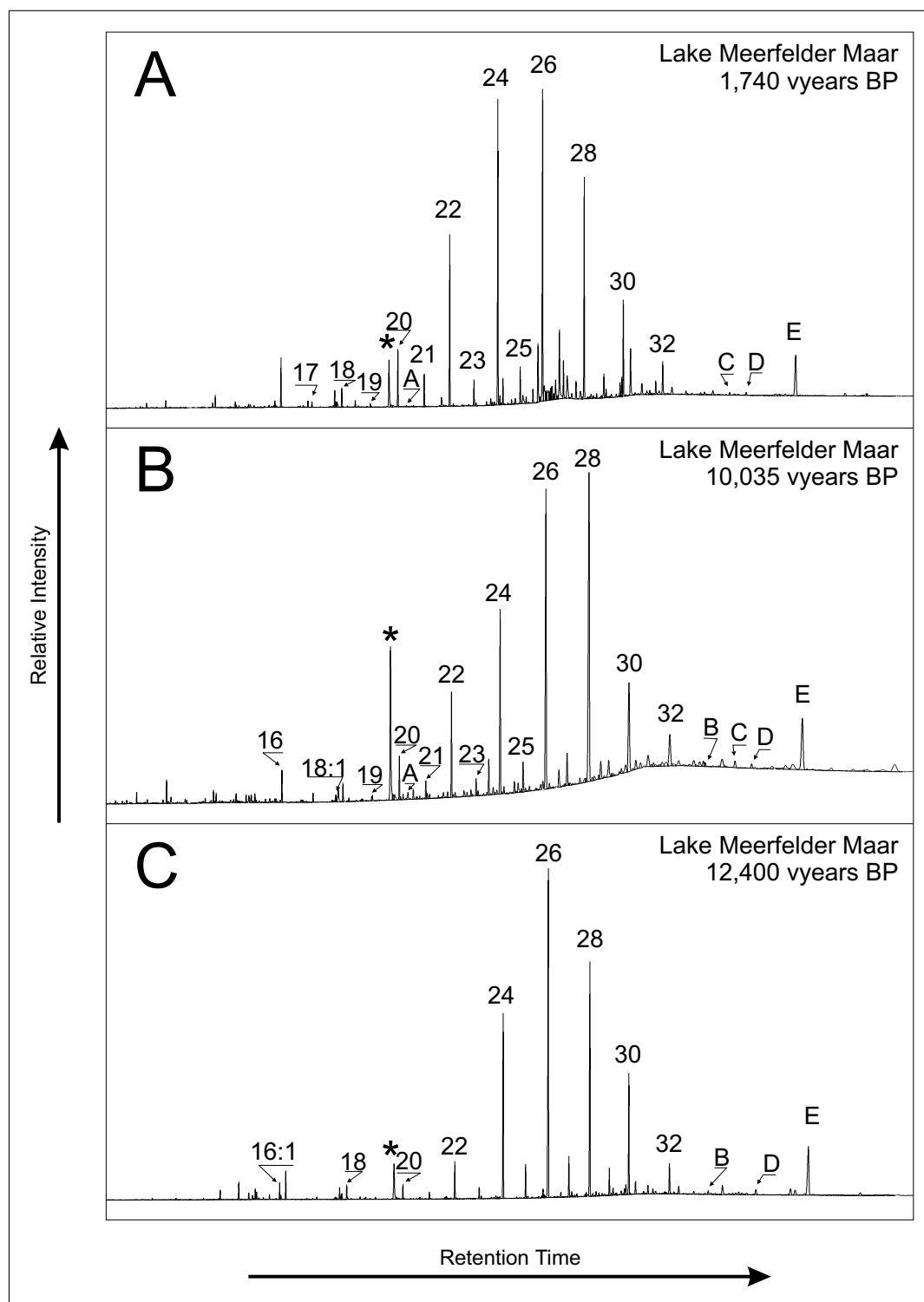


Figure 5.18: Exemplary chromatograms of acid fractions; numbers refer to chain length of *n*-fatty acids; letters refer to compounds as listed in Table 5.3; asterisk: *p*-*d*-icosanoic acid methyl ester as internal standard

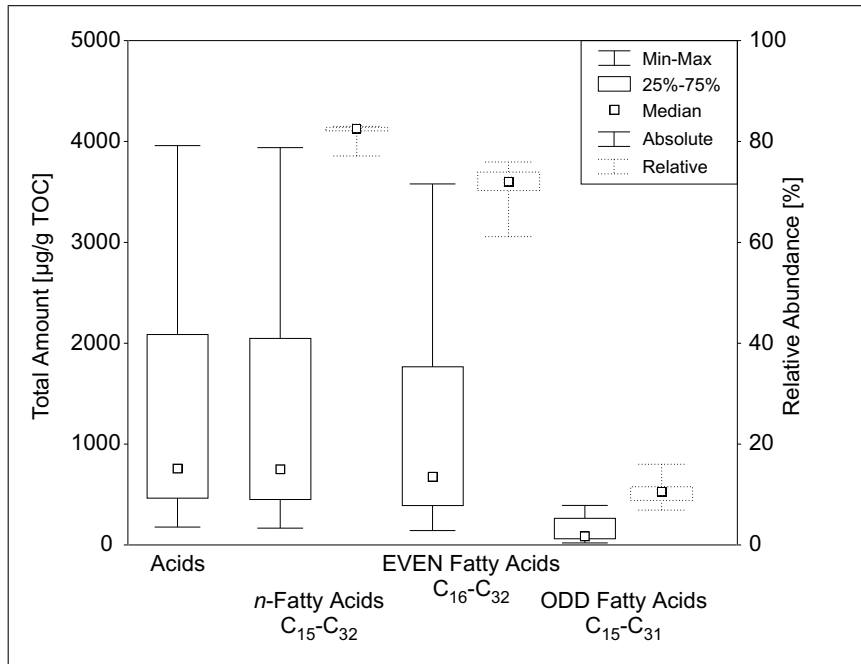


Figure 5.19: Total amounts and abundances of *n*-fatty acids relative to acids

in *Figs. 5.20, 5.22, 5.23*. Additionally, downcore concentrations of the C_{16:1} and C_{18:1} acids are shown in *Fig. 5.21*. Analogously to the previously discussed *n*-alkanes, single compounds are not discussed separately, the summed concentrations in the chain length range from *n*-C₁₆ to *n*-C₃₄ are used instead and downcore concentrations of selected homologues are illustrated. Nevertheless, important temporal differences of extremes depending on chain length as well as varying composition from single homologues at several varve ages will be described in detail. The complete data set is additionally available from *Appendix D, Tables D.21-D.29*.

As visible and in consistence with published data from other lacustrine archives (Ficken *et al.*, 1998a,b), absolute concentrations of normal chain fatty acids are clearly higher compared to the respective *n*-alkanes, varying between 180 – 3,970 µg/g TOC. Depending on the chain length of the homologues, absolute concentrations of individual derivatives higher than *n*-C₂₀ are higher in orders of magnitude compared to the lighter derivatives.

Absolute concentrations of observed unsaturated C_{16:1} and C_{18:1} acids are clearly lower, varying between 0.2 – 74 µg/g TOC with higher values for the heavier ho-

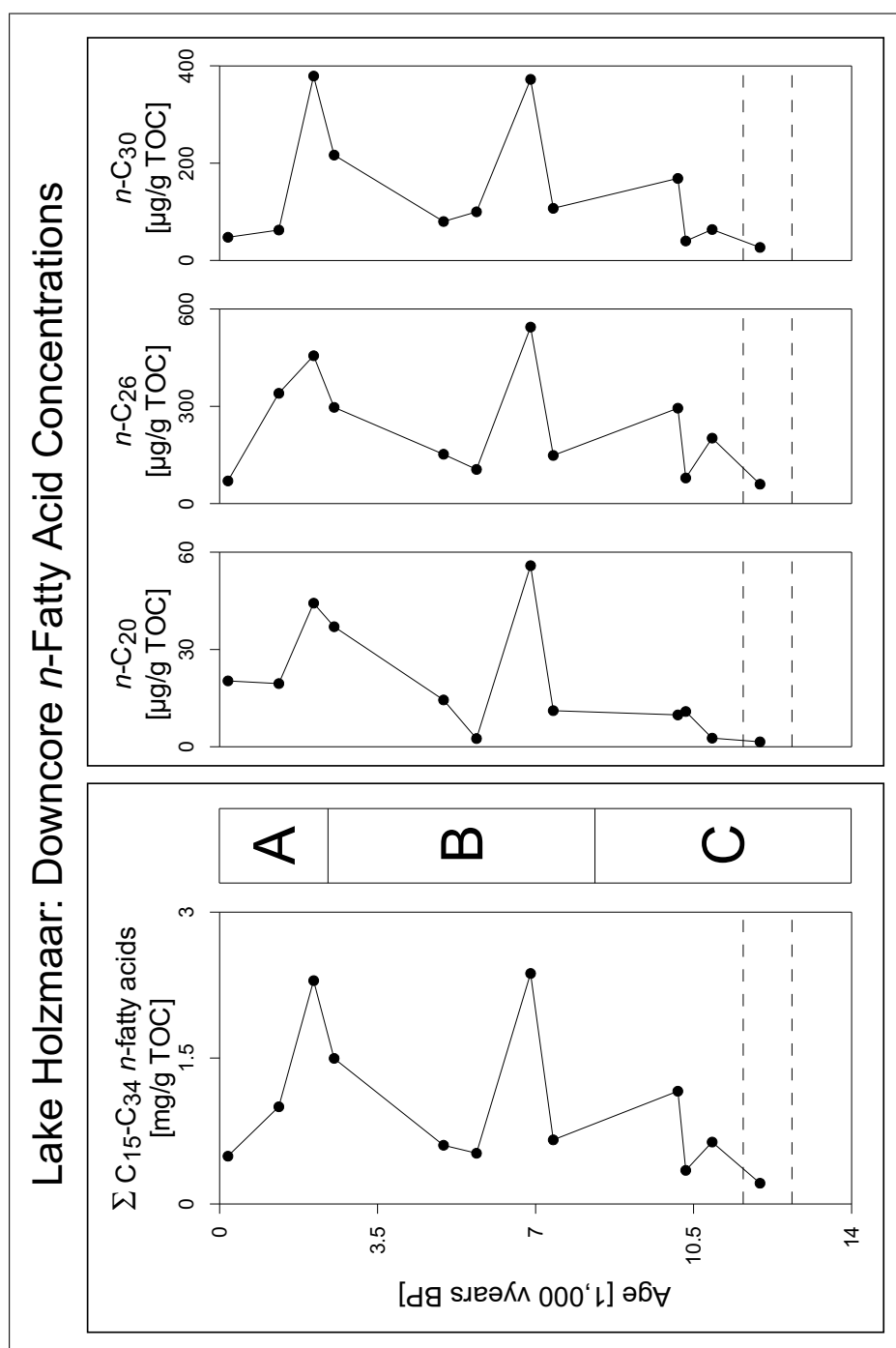


Figure 5.20: Summed downcore concentrations of $n\text{-C}_{15} \dots n\text{-C}_{34}$ fatty acids (left panel) and selected individual homologues as mentioned in the text (right panel) related to age for Lake Holzmaar; dashed lines indicate Younger the Dryas cold period

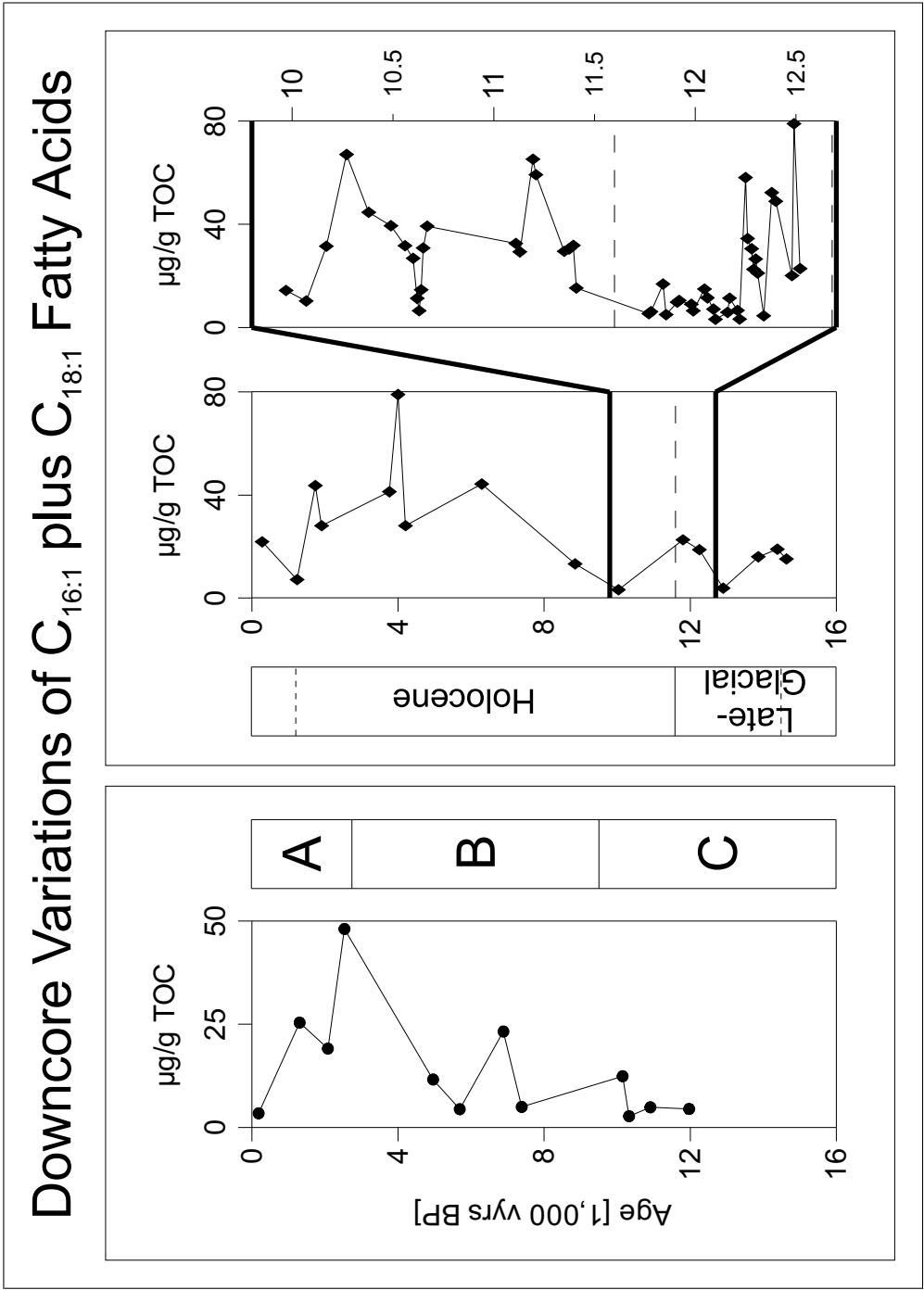


Figure 5.21: Summed downcore concentrations of $C_{16:1}$ and $C_{18:1}$ fatty acids; left plot: Lake Holzmaar; right plot: Lake Meerfelder Maar; dashed lines indicate the duration of the Younger Dryas period

mologue. Further lower concentrations, ranging between 0.2 – 11 µg/g TOC were finally detected for the 2- and 3-methyl fatty acids.

As obvious from *Fig. 5.20*, **Lake Holzmaars** Subatlantic section A is characterised by rapidly increasing amounts of fatty acids with increasing age. Consistent with the *n*-alkane data, the outstanding maximum contents of 2,374 µg/g TOC within this geological zone is reached at 2,083 vyears BP under a simultaneous enrichment of all homologues. Towards the Subatlantic to Holocene transition and further on until 5,690 vyears BP (middle Holocene), concentrations of fatty acid homologues are strongly depleted as already reported for aliphatic hydrocarbons; the summed concentration of 473 µg/g TOC is approximately four times lower compared to the Subatlantic maximum abundance.

Accordingly, increasing concentrations during Subatlantic section A were obtained for the C_{18:1} acid, whereas only slight enrichments in C_{16:1} content are obvious. The C_{18:1} acid shows a significant overall maximum at 2,536 vyears BP, later than the saturated fatty acids. Over the section A to B (middle Holocene) transition, concentrations decrease along with those of the *n*-fatty acids. With the exception of methylhexadecanoic acid, a Holocene minimum was observed for unsaturated and branched acids as reported for the saturated fatty acids at 5,690 vyears BP.

Whereas *n*-alkane concentrations continuously increase after this Holocene minimum stage, a sharply separated maximum with highest overall concentration of 2,431 µg/g TOC was observed directly in the next sample at 6,888 vyears BP. Significantly increased slopes were measured especially for *n*-C₂₆, *n*-C₂₈ and *n*-C₃₀ fatty acids. A synchronous maximum abundance is also obvious for unsaturated and branched derivatives. Highest enrichments were measured for the C_{18:1} acid, whereas the enrichment of other homologues was less pronounced. Slightly increasing abundances of all compounds were determined for the beginning of section C (early Holocene/Lateglacial).

During Lateglacial/early Holocene section C, most pronounced variations of the fatty acid composition in relation to chain length were detected. The uppermost sample at 10,150 vyears BP shows a slight enrichment in content of saturated as well as unsaturated and branched fatty acids under significant contribution of selected homologues: *n*-hexadecanoic acid becomes more abundant than *n*-icosanoic acid in contrast to *vice versa* behavior during the whole sedimentary sequence.

Relations of the longer chain derivatives remain stable, but hexacosanoic to triacosanoic acid show strong enrichments as already found for the Holocene maximum abundance. Also increased concentrations were measured for the $C_{16:1}$ and $C_{18:1}$ acids. The following 175 varve years are characterised by a rapid reduction of acid content with the exception of *n*-icosanoic acid, that is enriched compared to the previous sample prior to a drastic depletion during the lowermost profile section of Lake Holzmaars sedimentary sequence. These last 1,060 varve years show stable compositions of shortest normal chain as well as unsaturated and branched acids between *n*- C_{16} -*n*- C_{20} with *n*-icosanoic acid as lowest abundant homologue, uniquely for the complete profile. Longer chain length acids show a strong increase at 10,910 vyears BP caused by high proportions of *n*- C_{26} to *n*- C_{30} as found for earlier maxima. Towards the profiles bottom, decreased concentrations were also measured for this group of longer chain length fatty acids.

More pronounced as found for *n*-alkane distributions, average fatty acid concentration of 1,565 $\mu\text{g/g}$ TOC is remarkably higher in **Lake Meerfelder Maar** compared to the previously discussed Lake Holzmaar, also including a significantly higher variation width between 176 – 3,974 $\mu\text{g/g}$ TOC (*cf.* Fig. 5.22). Also the variation intervals for unsaturated (2.2 – 74 $\mu\text{g/g}$ TOC) and branched (0.7 – 6.4 $\mu\text{g/g}$ TOC) fatty acid content are generally enlarged in comparison to Lake Holzmaar. Additionally contrasting Lake Holzmaars sedimentary fatty acid composition, the most abundant homologue by far is *n*-hexacosanoic acid with the exception of one sample at 10,035 vyears BP, where *n*-octacosanoic acid is more dominant.

The uppermost and only partially laminated organic rich section is characterised by decreasing abundances of both normal chain as well as unsaturated and branched acid homologues, reaching a minimum time-synchronously at the beginning of regular lamination at 1,240 vyears BP. With increased age, strong increasing concentrations were measured first, that are slightly reduced between 1,740 – 1,910 vyears BP. This reduction, however, was found for shorter chain length compounds in the chain length range from *n*- C_{18} to *n*- C_{26} only with highest negative slope for *n*-icosanoic acid. During the Subatlantic/late Holocene between 1,910 – 4,000 vyears BP, fatty acid concentrations behave significantly different: Between *n*- C_{16} to *n*- C_{18} as well as *n*- C_{28} to *n*- C_{34} , concentrations are slightly decreased until 3,765 vyears BP to further rapidly increase until

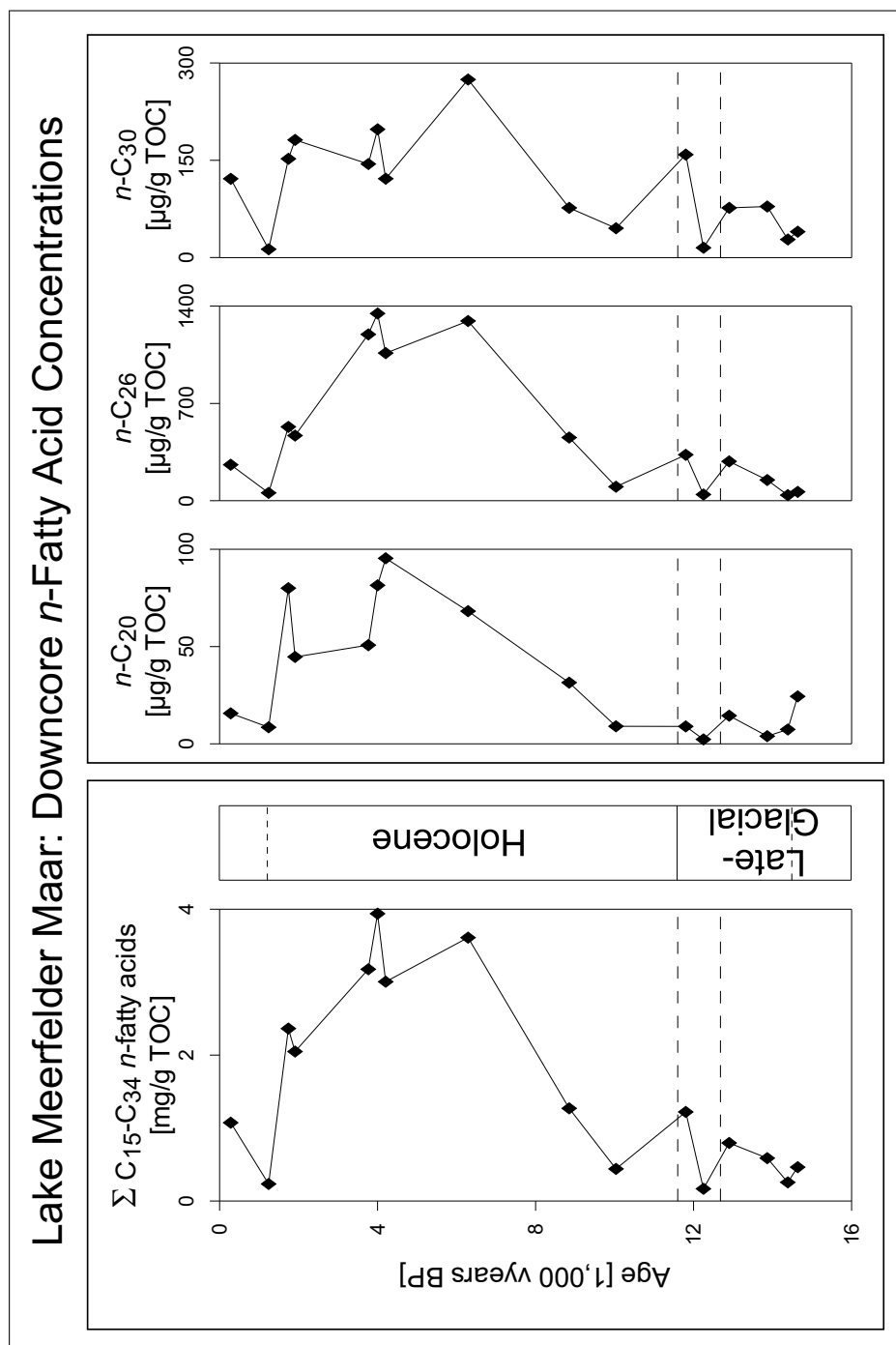


Figure 5.22: Summed downcore concentrations of n -C₁₅ \dots n -C₃₄ fatty acids (left panel) and selected individual homologues as mentioned in the text (right panel) related to age for Lake Meerfelder Maar; dashed lines indicate the Younger Dryas cold period; pointed lines in the stratigraphic column indicate the annually laminated core section

4,000 vyears BP. On the other hand, concentrations of remaining derivatives are strongly enriched during the whole age range until Lake Meerfelder Maars overall maximum fatty acid content at 4,000 vyears BP. Slightly increasing concentrations were finally detected for unsaturated and/or branched homologues too. Merely, octacosenoic acid shows a very strong enrichment during this age, maximising at 4,000 vyears BP.

With further increased age, fatty acid abundances are drastically reduced. *n*-Icosanoic- and *n*-docosanoic acid represent the only exception, showing an increasing trend for additional 205 varve years prior to the generally decreasing acid abundances, observed for all homologues until 10,035 vyears BP, the earliest Holocene sample. Among unsaturated and branched acids, relatively stable concentrations are obvious during the same range of age, and also the octacosenoic acid concentration is rapidly reduced after the Holocene maximum stage as described above.

During Lateglacial, relatively high concentrations of all compounds under investigation were measured at the upper border of the Younger Dryas cold period with high proportions of *n*-hexadecanoic, *n*-hexacosanoic and *n*-octacosanoic acid. Approximately during the middle Younger Dryas, at 12,250 vyears BP, the overall minimum abundance of normal chain fatty acids was determined, characterised by very low concentrations of all investigated fatty acid derivatives. Concentrations of unsaturated and branched homologues on the other hand continuously decrease during the Younger Dryas. Later on, concentrations of normal chain fatty acids become increased over the Lateglacial/ Younger Dryas transition (12,900 vyears BP) whereas the unsaturated and branched homologues minimise at this age. The enrichment in saturated fatty acids, however, is caused by strong slopes of the *n*-C₂₀, *n*-C₂₆ and *n*-C₂₈ acid content, whereas the remaining derivatives show inconsistent trends: *n*-C₁₆ and *n*-C₁₈ acids are slightly depleted, longer chain length homologues are slightly enriched below the Younger Dryas cold period.

The oldest samples are finally characterised by slightly reduced fatty acid contents under, in turn, irregular compositions from individual homologues in the short chain length range: *n*-hexacosanoic acid shows a significant enrichment at 13,865 vyears BP, whereas a significant depletion in *n*-icosanoic acid, the most abundant derivative in the chain length range from *n*-C₁₆ to *n*-C₂₀ during wide

ranges of the sedimentary profile, was detected at the same age. This constellation is restored in Lake Meerfelder Maars lowermost sample.

The investigation of Lake Meerfelder Maars second sample set with higher temporal resolution between the earliest Holocene and Younger Dryas cold period as illustrated in *Fig. 5.23* retrieved a variation width of *n*- fatty acid content very similar to that measured for the full-range and low resolved sequence as reported above. A partial maximum abundance of *n*-fatty acids as well as the unsaturated C_{16:1} and C_{18:1} homologues was detected at 10,270 vyears BP with an outstanding contribution of *n*-octacosanoic acid, whereas *n*-hexacosanoic acid is the most abundant homologue in underlying sediments.

The following 290 varve years are characterised by reduced fatty acid contents in general, that can be explained with the rapid depletion in *n*-octacosanoic acid after the detected maximum. Against this general trend, the unsaturated C_{18:1} becomes sharply enriched during this interval.

Between 10,560 – 10,670 vyears BP a very rapid fluctuation of acid concentrations was observed. Absolute concentrations first decrease from 2,190 µg/g TOC to 613 µg/g TOC in sum at 10,630 vyears BP to further increase to 2,537 µg/g TOC within only 20 varve years. The composition of fatty acid fractions is very stable during this time: *n*-hexacosanoic- and *n*-octacosanoic acid are the most abundant compounds by far, also showing highest variation width whereas downcore variations of the remaining homologues are much smoother, only showing the final enrichment clearly.

With increasing age, summed acid concentration is decreased first to further reach another stage of enriched abundances at 11,110 vyears BP. Until 11,210 vyears BP, absolute concentrations increase simultaneously for all investigated homologues and with constant composition; *n*-hexacosanoic and *n*-octacosanoic acid are the most abundant compounds.

The Younger Dryas period of cooler temperatures itself is characterised by a very significant bi-partitioning of fatty acid contents: The upper 450 varve years above 12,220 vyears BP show closely scattering concentrations around the average content of 661 µg/g TOC with maxima at 11,840 and 12,045 vyears BP. The lower 270 varve years below 12,250 vyears BP in contrast are characterised by a significantly higher average content of 2,266 µg/g TOC also including very strong and rapid fluctuations. Similar to the saturated fatty acids, unsaturated C_{16:1} and C_{18:1}

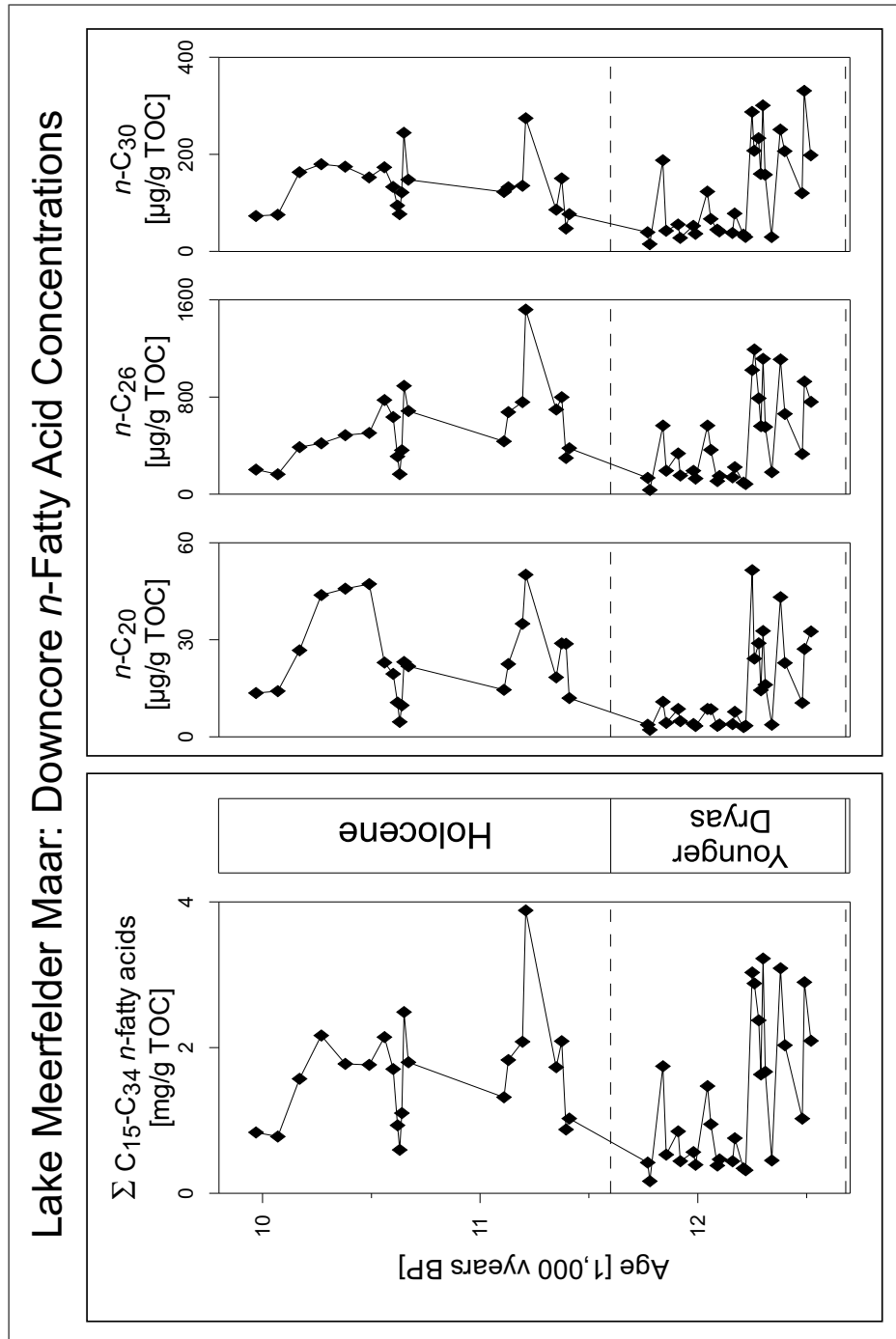


Figure 5.23: Summed downcore concentrations of $n\text{-C}_{15} \dots n\text{-C}_{34}$ fatty acids (left panel) and selected individual homologues as mentioned in the text (right panel) related to age for Lake Meerfelder Maars high resolution sequence; dashed lines indicate the Younger Dryas cold period

Table 5.3: Constituents of acid fractions

Label*	Compound
A	dehydroabietic acid
B	22 <i>R</i> -17 β (H),21 β (H)-hopanecarboxylic acid
C	22 <i>R</i> -17 α (H),21 β (H)-dihomohopanecarboxylic acid
D	22 <i>R</i> -17 β (H),21 β (H)-homohopanecarboxylic acid
E	22 <i>R</i> -17 β (H),21 β (H)-dihomohopanecarboxylic acid

*Letters refer to labelled peaks in *Fig. 5.18*

acids show the same age related behavior: Above 12,220 vyears BP, the average content in sum of 8.3 $\mu\text{g/g}$ TOC is significantly lower as below 12,250 vyears BP (35.1 $\mu\text{g/g}$ TOC).

5.2.2.2 Hopanoic Acids

Hopanoic compounds are early diagenetic products of hopanols, which are specific markers for bacterial activity. Thus, hopanoic acids may serve as indicators for bacterial activity in the investigated archives, even if the initial precursor itself was not identified. Out of the detected hopanecarboxylic acids as listed in *Table 5.3*, 22*R*-17 β (H),21 β (H)-dihomohopanecarboxylic acid was the most abundant homologue by far in all sediments, but concentration shifts during time occur simultaneously in the same direction for all hopanoic acids. The downcore variations of 22*R*-17 β (H),21 β (H)-dihomohopanecarboxylic acid concentrations for both investigated archives are illustrated in *Fig. 5.24*. The clear predominance of this hopanoic acid is believed to be typical for soils and young sediments as figured out by *Ries-Kautt and Albrecht (1989)*.

The concentrations of hopanoic acids in sum vary between 14 – 412 $\mu\text{g/g}$ TOC for **Lake Holzmaar**. The Subatlantic section A shows a continuous and strong increase in hopanoic acid abundances up to 246 $\mu\text{g/g}$ TOC. With the beginning of the middle Holocene section B, hopanoic acid concentrations in sum are rapidly shifted to significantly lower values, that show a slightly increasing trend with increasing age. This general trend, however, is interrupted by the overall maximum abundance at 6,888 vyears BP. Still relatively high concentrations were measured at the beginning of the Lateglacial/ early Holocene section C at 10,150 vyears BP. Later on, a clear shift to lower hopanoic acid concentrations is obvious between

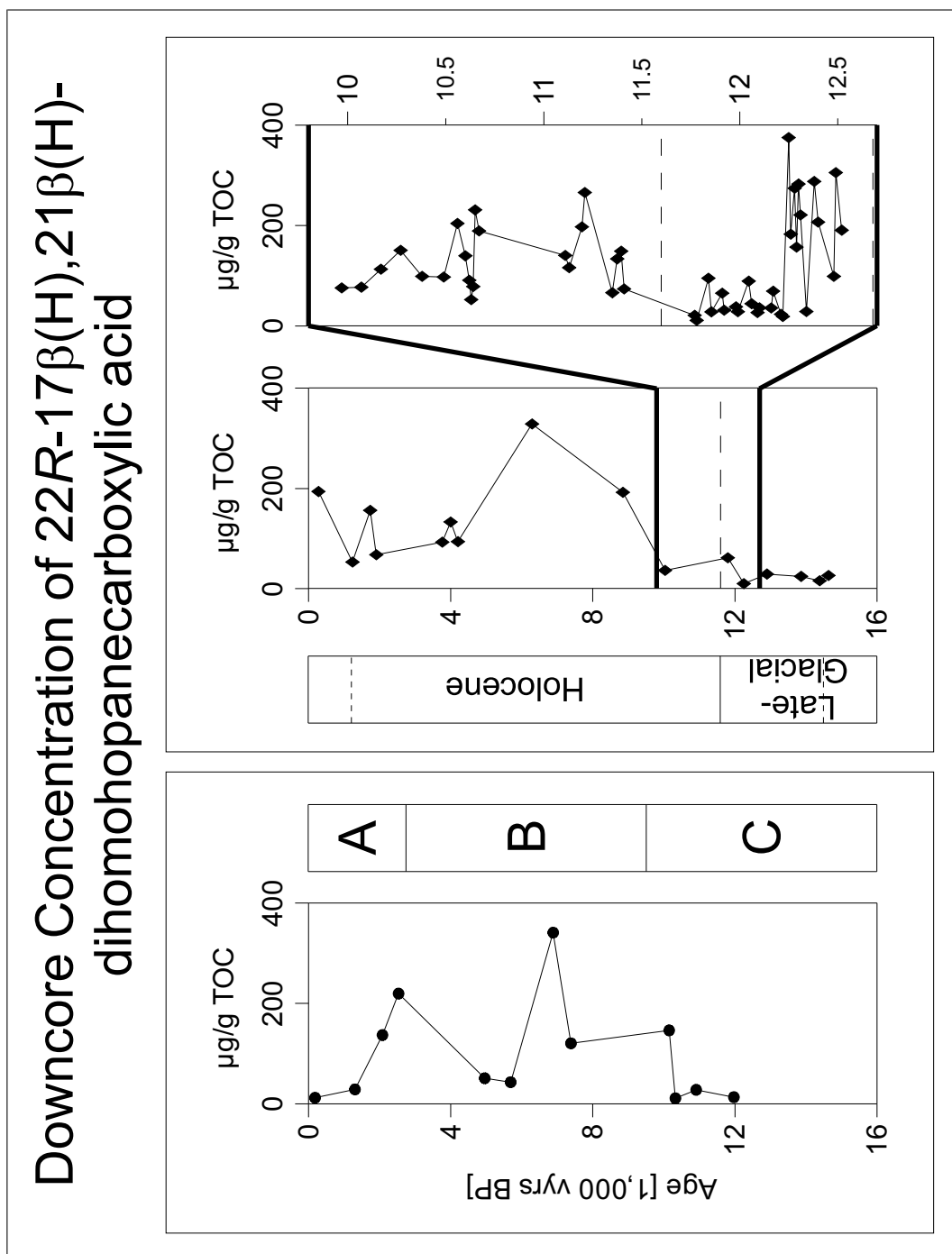


Figure 5.24: Downcore concentrations of 22*R*-17 β (H),21 β (H)-dihomohopanecarboxylic acid; left plot: Lake Holzmaar; right plot: Lake Meerfelder Maar; dashed lines indicate the Younger Dryas cold period

10,150-10,325 vyears BP. With further increasing age, values remain stable on a low level of 23 $\mu\text{g/g}$ TOC on average during the Lateglacial.

Variation width of hopanoic acid concentrations between 15 – 360 $\mu\text{g/g}$ TOC in **Lake Meerfelder Maar** sedimentary sequence is slightly narrower compared to Lake Holzmaar. Most abundant derivative during time is 22*R*-17 β (H),21 β (H)-dihomohopanecarboxylic acid in turn.

Rapidly scattering hopanoic acid concentrations were found for the uppermost samples of Lake Meerfelder Maar. Despite two single maxima, concentrations show a slightly increasing trend with increasing age during Subatlantic and late Holocene. This trend becomes enhanced below 4,205 vyears BP towards the overall maximum abundance at 6,290 vyears BP during the Holocene climate optimum. The maximum abundance of hopanoic acids in Lake Meerfelder Maar is as good correlated to that of Lake Holzmaar as the temporal resolution of both profiles allows.

Sediment samples older than the Holocene climate optimum are characterised by continuously lowered hopanoic acid abundances. A slight intermediate enhancement is obvious towards the beginning of the Younger Dryas cold period. During the Younger Dryas times, hopanoic acid concentrations are further reduced abruptly and remain on the lowest observed level during Lateglacial.

The more detailed investigation of the early Holocene/ Younger Dryas sequence of Lake Meerfelder Maar yields two significant stages of hopanoic acid abundances in relation to organic carbon content. Below 10,490 vyears BP a first rapid increase occurs, that is followed by another rapid reduction. The onset of the second increase was measured below 11,130 vyears BP; a partial maximum abundance is dated 80 varve years later. Summed hopanoic acid contents are further continuously reduced until the beginning of the Younger Dryas period and remain on a low level in older partition. Closely scattering concentrations around the average of 82 $\mu\text{g/g}$ TOC were measured between 11,770 – 12,220 vyears BP. A sharp increase in summed hopanoic acid concentrations in older samples is obvious as illustrated in *Fig. 5.24*. With exception of two single minima, summed concentrations remain on a higher level of 270 $\mu\text{g/g}$ TOC on average compared to the later Younger Dryas. This finding confirms the significant bi-partitioning of the Younger Dryas period of cooler temperatures into two separate stages as it was previously derived from various bulk geochemical as well as lipid data.

5.2.3 Alcohols and Sterols

Table 5.4: Constituents of alcohol fractions

Label*	Sterol	Number of C-Atoms
A	5 α (H)-Cholest-22(E)-ene-3 β -ol	27
B	Cholesterol	27
C	5 α -Cholestan-3 β -ol	27
D	5 α -Cholestan-3 α -ol	27
E	24-Methyl-5 β (H)-cholestan-3 β -ol	28
F	24-Methylcholesta-5,22(E)-dien-3 β -ol	28
G	24-Methyl-5 β (H)-cholestan-3 α -ol	28
H	23,24-Dimethylcholesta-5,22-dien-3 β -ol	29
I	23,24-Dimethylcholest-22(E)-en-3 β -ol	29
J	24-Methylene-5 α -cholestan-3 β -ol	28
K	24-R-Ethylcholest-5-en-3 β -ol	29
L	Stigmastanol	29
M	4,23,24-Trimethyl-5 α -cholest-22(E)-en-3 β -ol	30
N	Lanosterol	30
O	Tetrahymanol	
P	Diplopterol	

*Letters refer to labelled peaks in *Fig. 5.25*

Also the results presentation of alcohol fractions is initiated with three exemplary chromatograms being illustrated in *Fig. 5.25*. As well as in the previous sections, normal chain compounds are labelled by numbers, referring to the respective chain length. As illustrated in *Fig. 5.26*, this group is most dominant in the alcohol fractions with percentages between 53 – 90 % relative to the quantified compounds in sum. Absolute concentrations of *n*-alcohols vary between 165 – 2,191 $\mu\text{g/g}$ TOC for homologues in the chain length range from *n*-C₁₅ to *n*-C₃₂. The heaviest detected homologue was *n*-C₃₃ alcohol, however coeluting with another unidentified compound. It was therefore excluded from quantification. The most abundant homologue is *n*-hexacosanol; the chromatograms indicate a strong even over odd predominance.

Beside the normal chain compounds, a large variety of sterols was detected in the alcohol fractions. For better illustration, the appropriate retention range is displayed enlarged in *Fig. 5.25 B*; identified compounds are letter

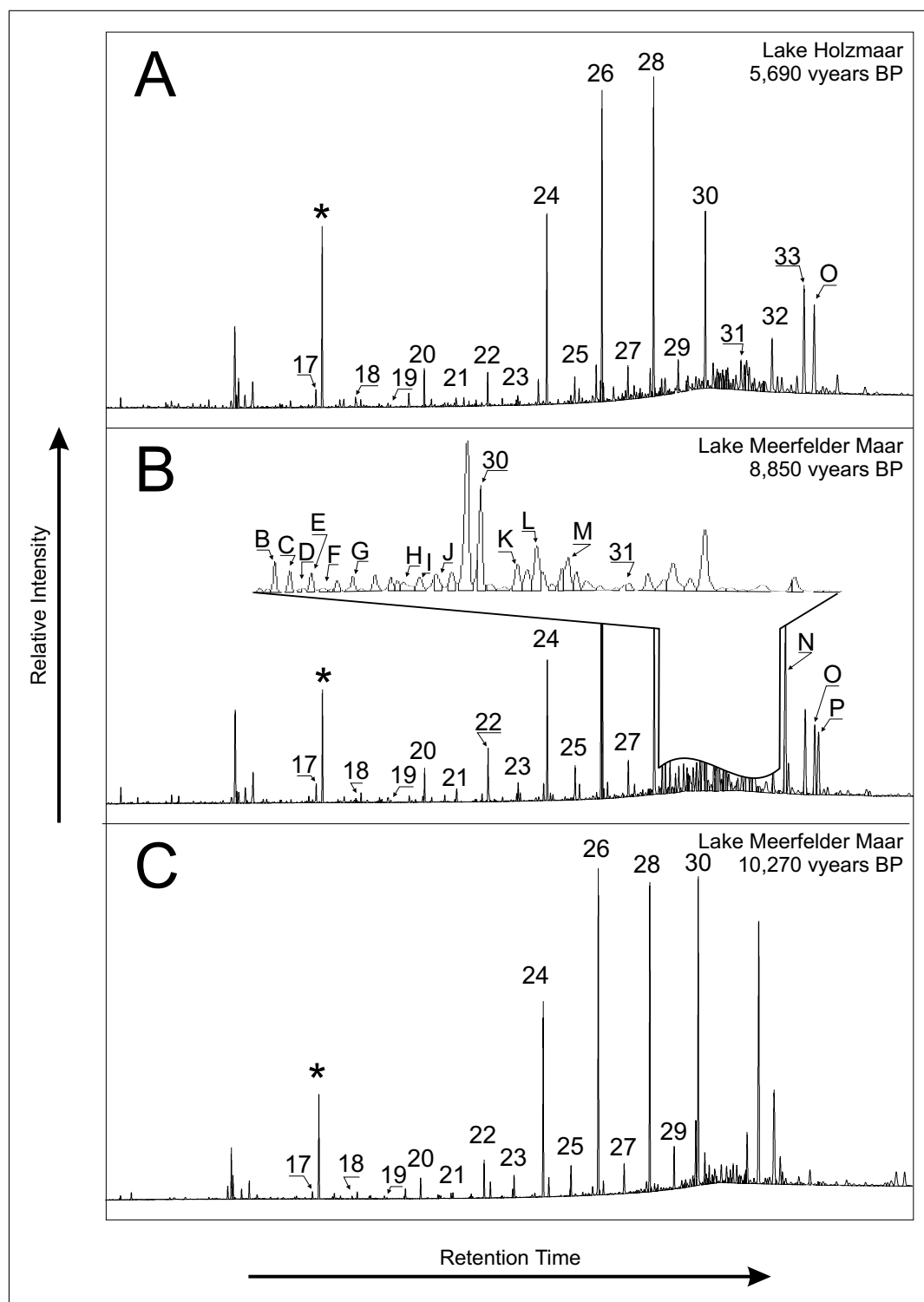


Figure 5.25: Exemplary chromatograms of alcohol fractions; numbers refer to chain length of *n*-alcohols; letters refer to compounds as listed in Table 5.4; asterisk: *p*-*d*-icosanoic acid methyl ester as internal standard

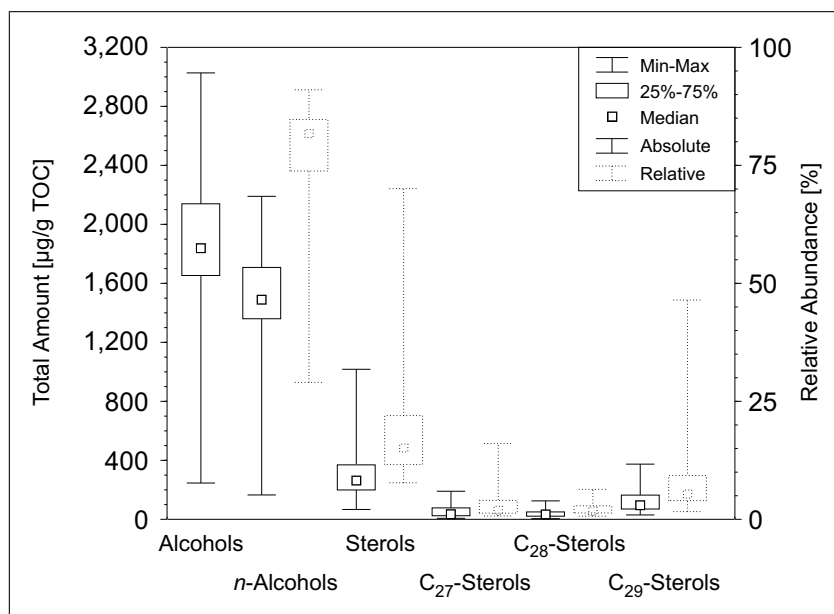


Figure 5.26: Total amounts (solid columns; left Y-axis) and abundances of *n*-alcohols and sterols relative to the sum of identified compounds (dashed columns; right Y-axis); concentrations and percentages of sterols are further subdivided to C₂₇, C₂₈ and C₂₉-sterols, percentages refer to identified compounds in sum in each case

labelled. The letters are assigned to individual compounds as listed in *Table 5.4*, where the number of carbon atoms is additionally specified for each sterol. Structures of identified compounds are illustrated in *Fig. B.3, Appendix B*.

As shown in *Fig 5.26*, absolute sterol concentrations in sum vary between 66 – 1,018 µg/g TOC. That corresponds to 7 – 71 % relative to all quantified compounds in this fraction. Out of the identified sterols, the subgroups of C₂₇- and C₂₈ sterols yield comparable percentages between 4.6 – 39.5 % and 3.8 – 32.3 % relative to sterols in sum, respectively. Considerably higher percentages between 13.0 – 66.3 % relative to sterols in sum were calculated for the heaviest detected subgroup of C₂₉ sterols. From this composition, an important terrestrial influence to the sedimentary organic matter of both Eifel Maar Lakes can be inferred; a more detailed interpretation will follow in *Chapter 6*.

In addition to the main constituents as introduced above, a minor proportion of the alcohols was made up by C₃₀ sterols (4,23,24-Trimethyl-5 α -(H)-cholest-22E-en-3 β -ol, Lanosterol), Tetrahymanol, Diplopterol and Homohopanol.

5.2.3.1 *n*-Fatty Alcohols

Downcore variations of the dominant *n*-alcohol subgroup in sum as well as of selected individual homologues are illustrated in *Fig. 5.27*. The presentation of results includes summarised concentrations of *n*-alcohols in the detected chain length range as mentioned above; a complete compilation of measured data is available as usual from *Appendix D, Tables D.30-D.38*.

Lake Holzmaars sedimentary sequence shows a general trend to lower *n*-alcohol content with increasing age (*cf. Fig. 5.27*). During the Subatlantic profile section A, a characteristic minimum abundance was detected at 1,311 vyears BP, whereas up- and underlying sediments show higher concentrations between 1,657 – 1,848 µg/g TOC. Merely the downcore concentrations of the *n*-C₃₂ behave mirror-like during this geological epoch. The second highest concentration was additionally measured closely to the section A to B (middle Holocene) transition at 2,536 vyears BP. These findings significantly differ from the results for *n*-alkanes and *n*-fatty acids, where comparable local maximum abundances were found during section A too, however, occurring 453 varve years earlier for both compound classes. The described minimum abundance during middle section A is furthermore in good temporal correlation to that reported for *n*-alkane distributions, showing a much bigger relative reduction as in case of *n*-alkanes.

In agreement with the previously reported results for *n*-alkanes and *n*-fatty acids, the upper part of section B is characterised by reduced concentrations with most marked depletions in *n*-hexacosanol to *n*-tricosanol. The turning point to increased concentrations was dated to 4,960 vyears BP, thus 730 varve years earlier than the respective inflection of *n*-alkanes and *n*-fatty acids.

Towards older samples, irregular behavior was measured for different homologues: Concentrations first increase uniformly until 6,011 vyears BP before *n*-octadecanol to *n*-octacosanol concentrations decrease whereas slightly increased abundances were measured for the remaining lighter and/or heavier derivatives. Generally increased summed concentrations can be taken from *Fig. 5.27* for the period between 7,194 – 7,631 vyears BP. This finding, however, is valid for homologues beyond *n*-C₂₀ only; lighter derivatives show dramatically lowered concentrations. Especially *n*-icosanol, that is more abundant than *n*-hexadecanol and *n*-octadecanol in overlying sediments, becomes the least abundant homologue in this period.

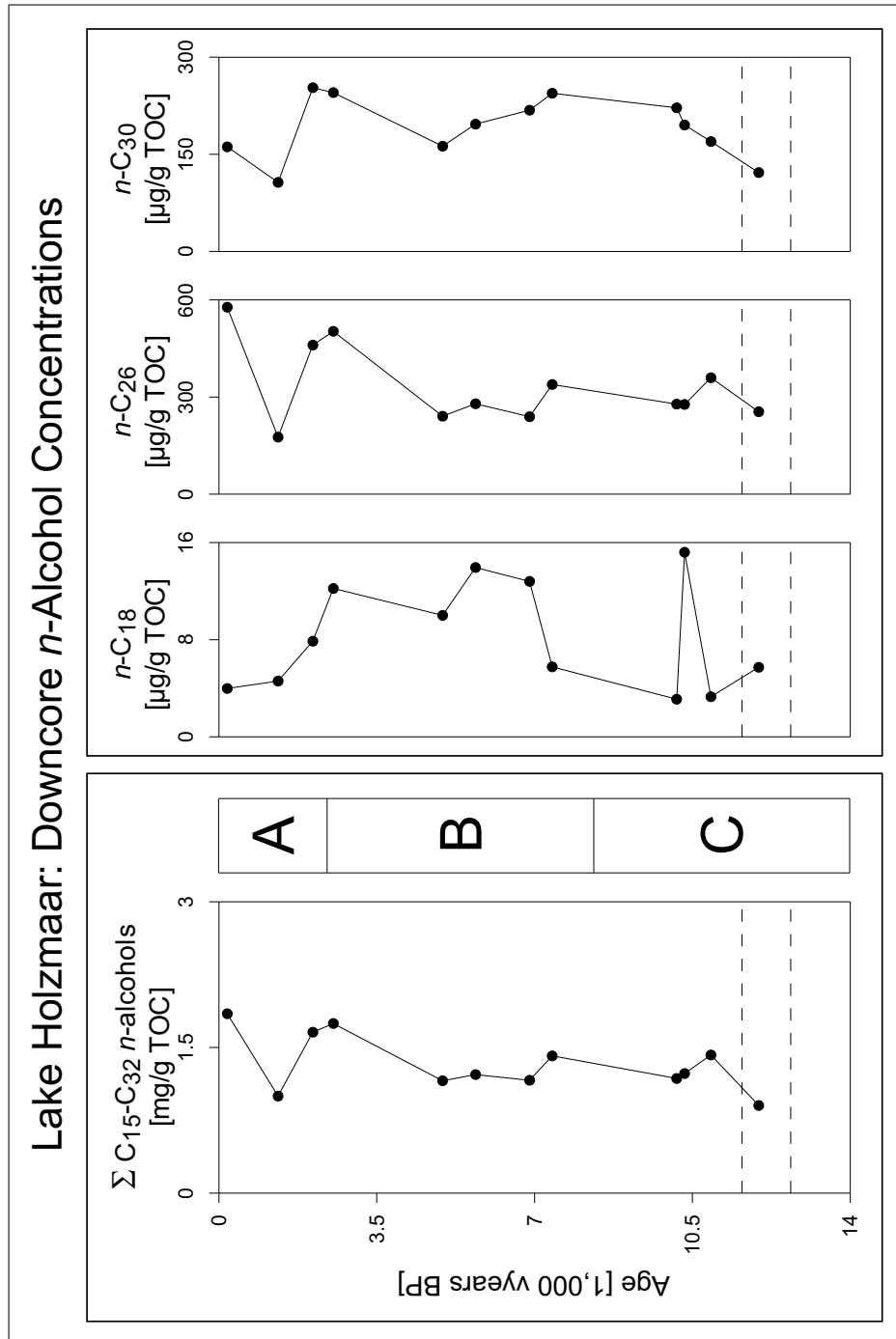


Figure 5.27: Summed downcore concentrations of n -C₁₅ \dots n -C₃₂ n -alcohols (left panel) and selected individual homologues as mentioned in the text (right panel) related to age for Lake Holzmaar; dashed lines indicate the Younger Dryas cold period

Over the sections B to C (Lateglacial/early Holocene) transition, *n*-tetracosanol and *n*-hexacosanol as well as *n*-dotriacontanol show further decreased concentrations but further dominate the summarised downcore concentration plot. This is clearly the opposite of normal chain compounds introduced during previous chapters, showing enhanced concentrations during early Holocene. A slight enrichment in *n*-alcohol concentrations was measured at 10,910 vyears BP, in this case 585 varve years later as a comparable enhancement reported for *n*-alkanes. The oldest sample of Lake Holzmaars investigated core section finally shows the lowest overall *n*-alcohol concentrations consistent with reduced concentrations of other normal chain compounds as described above.

Absolute concentrations of summed *n*-alcohols for the **Lake Meerfelder Maar** sedimentary sequence show a variation width between 174 – 2,191 µg/g TOC as illustrated in *Fig. 5.28*. Compared to Lake Holzmaar, the minimum concentration is considerably lower, whereas maximum concentrations are well comparable for both lakes.

Concentrations are firstly decreased from the profiles top to the beginning of annual sediment lamination as already found for all other normal chain compounds. At 1,740 and 1,910 vyears BP, sharply enriched abundances were measured prior to another decrease at 2,115 vyears BP, that was found to be the case for all homologues. A comparable sharply separated peak was not observed for the other two fractions of normal chain compounds.

Very similar to the results of *n*-fatty acid distributions, summed concentrations strongly increase from that time towards older samples until 6,290 vyears BP, merely the sharp peak of fatty acid abundances at 4,000 vyears BP could not be detected for *n*-alcohols. Beside the enriched total alcohol concentrations during the middle Holocene, significantly differing percentages of single homologues were detected as follows:

Concentrations of the two lightest homologues, hexadecanol and octadecanol are nearly constant throughout this epoch with the exception of a sharp enrichment of the first named derivative at 3,765 vyears BP. Concentrations of longer chain homologues show strongly enriched values, however, a slight depletion in C₂₂, C₂₄ and C₃*n*-alcohols was measured at 4,000 vyears BP. *n*-Icosanol reaches its middle Holocene maximum abundance at 4,205 vyears BP, whereas the more dominant longer chain homologues maximise 2,085 varve years later.

Between 6,290 – 8,850 vyears BP reduced abundances of *n*-alcohols were detected

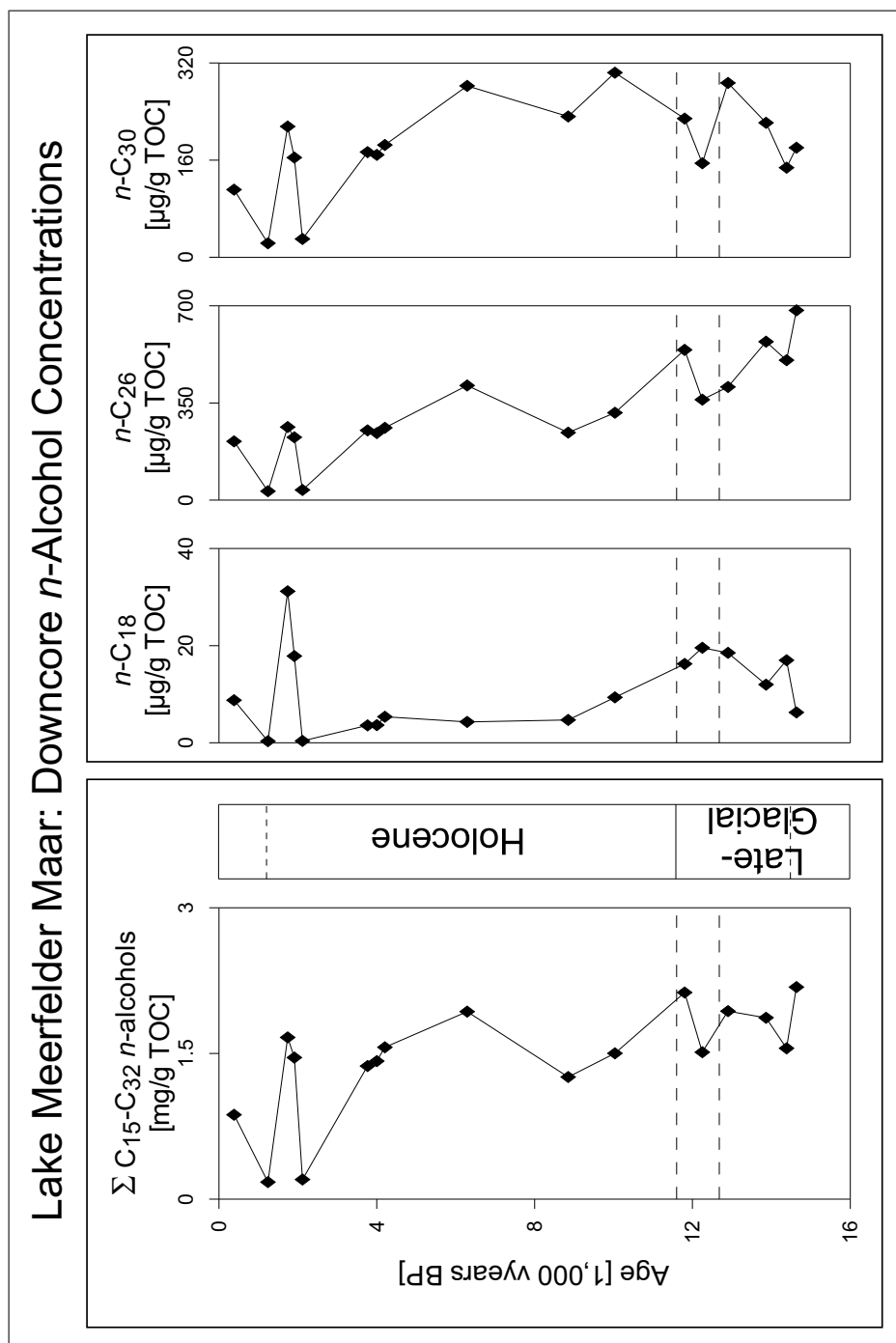


Figure 5.28: Summed downcore concentrations of $n-C_{15} \dots n-C_{32}$ n -alcohols (left panel) and selected individual homologues as mentioned in the text (right panel) related to age for Lake Meerfelder Maar; dashed lines indicate the Younger the Dryas cold period; pointed lines in the stratigraphic column indicate the annually laminated core section

with the exception of *n*-icosanol, showing an increasing concentration. Beginning with the next sample, alcohol concentrations increase towards the top sample of the Younger Dryas cold period where the second highest concentration was measured. A similar increase towards the Younger Dryas was found for fatty acid distributions, however, its onset was dated 1,185 varve years later.

During the Younger Dryas period of cooler temperature itself, *n*-alcohol concentrations are analogously to fatty acids decreased first to further increase towards the lower border of the cold period. During the lower Lateglacial, concentrations are stronger reduced as described for the fatty acids until the lower end of annual sediment lamination. A characteristic increase was finally measured for the oldest sample of Lake Meerfelder Maars sedimentary profile outside the laminated core section.

Investigating the higher resolved second sample set of Lake Meerfelder Maar, more detailed variations of *n*-alcohol abundances during the Younger Dryas and early Holocene were detected as shown in *Fig. 5.29* and described directly below:

The highest summed concentration was calculated at 9,970 vyears BP for the top sample before values decrease with increasing varve age. This general trend is interrupted by two stages characterised by enhanced abundances at 10,380 vyears BP as well as 11,130 vyears BP, persisting for 110 and 80 varve years, respectively. The latter named period is additionally in good temporal correlation with the results for fatty acids, but smaller by absolute concentration. With the beginning of the Younger Dryas, Lake Meerfelder Maars sedimentary profile is enriched in *n*-alcohol content. Summed concentrations are closely scattering around the average of 1,551 µg/g TOC, merely three significant minima at 12,090, 12,210 and 12,520 vyears BP were excluded from average calculation. The bi-partitioning of Younger Dryas could not be confirmed by *n*-alcohol distributions.

5.2.3.2 Sterols

Downcore variations of sterols, separated into C₂₇, C₂₈ and C₂₉ subgroups, are illustrated in *Fig. 5.30*. Individual sterols are used for summation as listed in *Table 5.4*; Absolute concentrations of individual sterols, normalised to TOC, are available from *Appendix D, Tables D.39 to D.47*.

As obvious from downcore plots, C₂₉ sterols are the most abundant sterol group

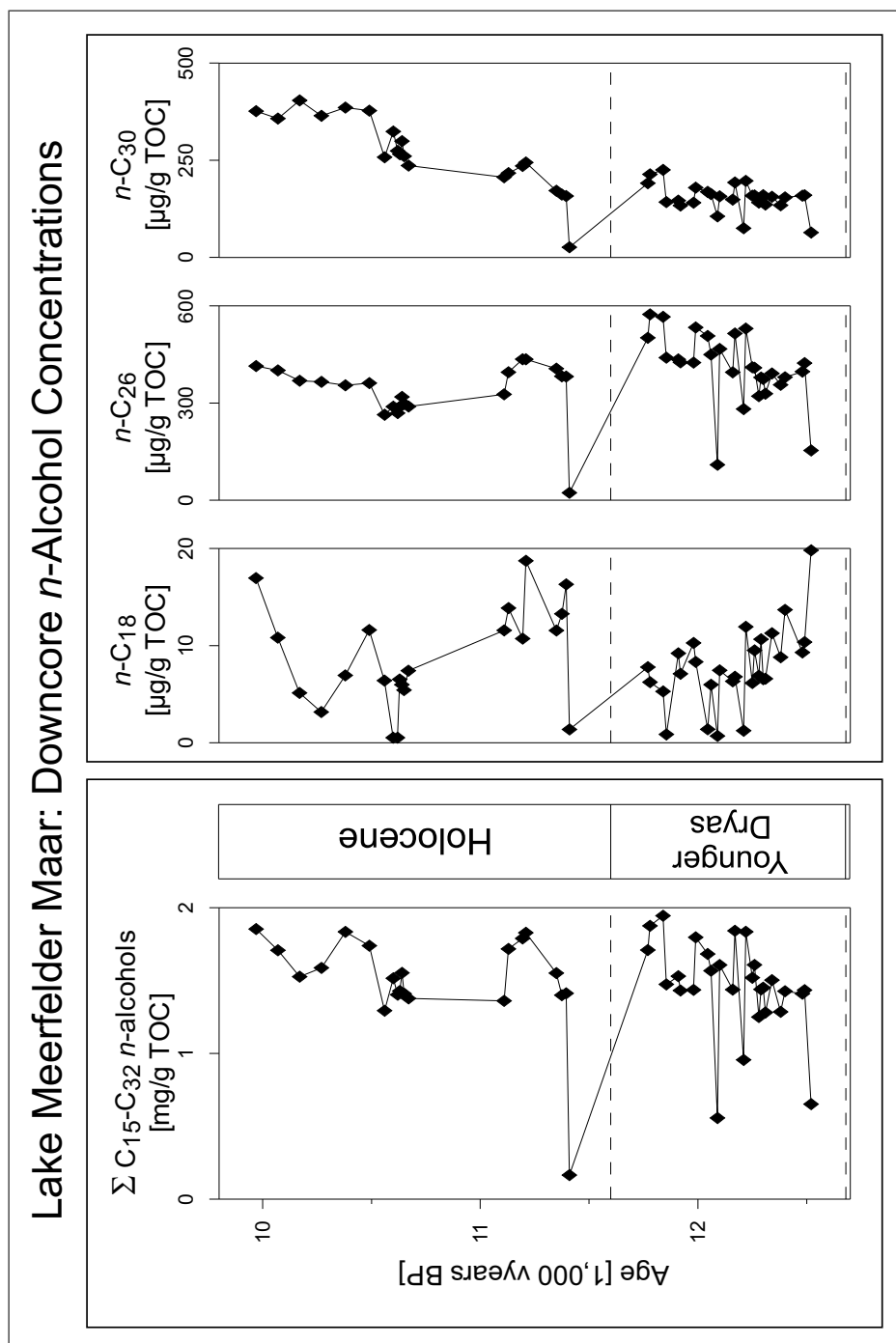


Figure 5.29: Summed downcore concentrations of $n\text{-C}_{15} \dots n\text{-C}_{32}$ n -alcohols (left panel) and selected individual homologues as mentioned in the text (right panel) related to age for Lake Meerfelder Maar's high resolution sequence; dashed lines indicate the Younger the Dryas cold period

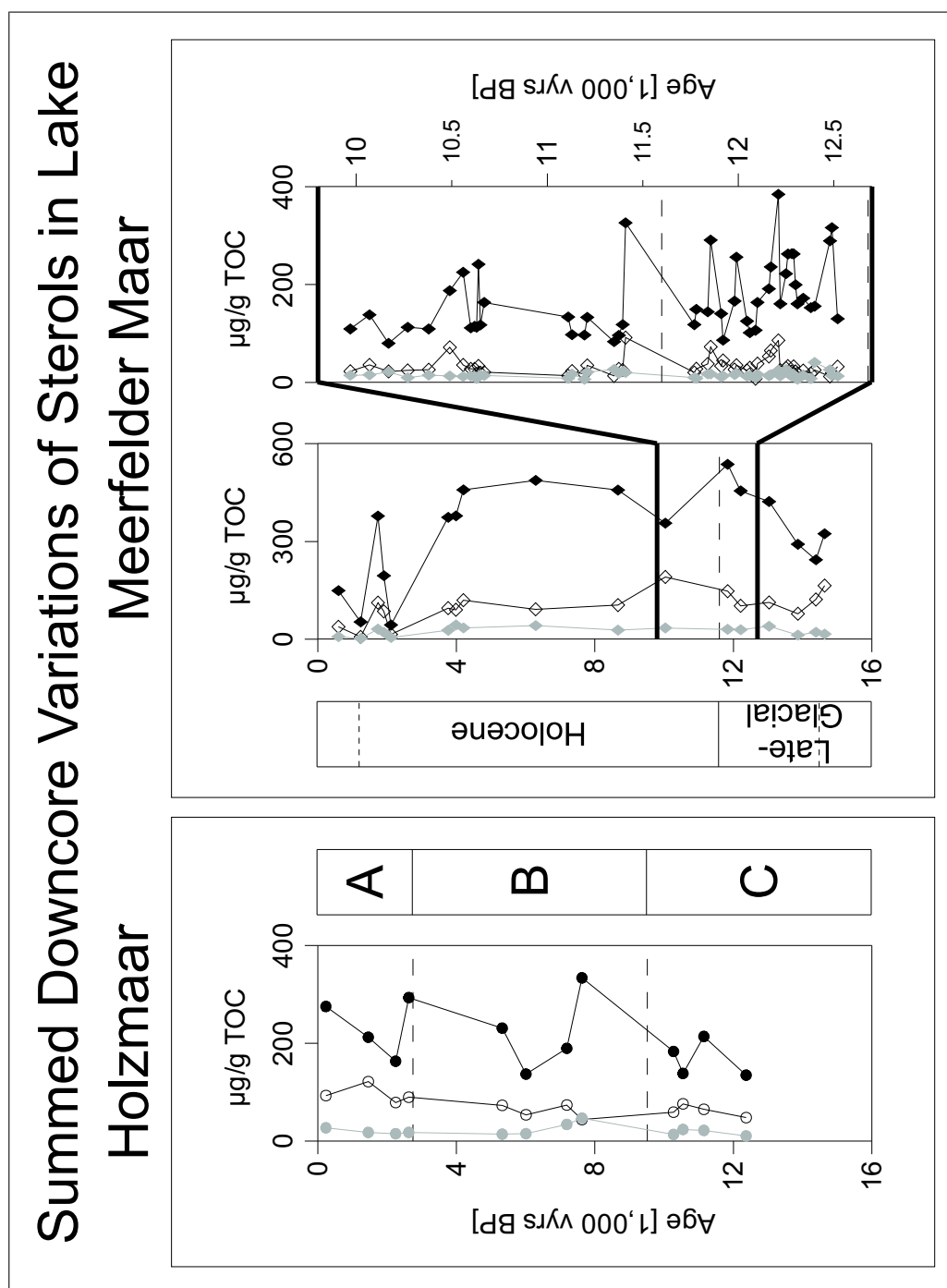


Figure 5.30: Summed downcore concentrations of sterols; left box: Lake Holzmaar (circles); right box: Lake Meerfelder Maar (diamonds) with low (left plot) and high (right plot) temporal resolution sample sets; open symbols: C₂₇ sterols; gray symbols: C₂₈ sterols; black symbols: C₂₉ sterols; individual sterols summarised to C₂₇, C₂₈ and C₂₉ subgroups as listed in *Table 5.4*; dashed lines indicate the Younger Dryas cold period; dashed lines in Lake Meerfelder Maar stratigraphic column indicate period of annual sediment lamination

in both more lakes during all geological zones, followed by C₂₇- and C₂₈ sterols in order of decreasing absolute concentrations.

Absolute sterol concentrations in sum vary between 212 – 513 µg/g TOC within **Lake Holzmaars** sedimentary profile. The uppermost section A (Subatlantic) shows continuously decreasing sterol concentrations with increasing age from the top sample until 2,083 vyears BP before a rapid increase was measured closely to the section A to B (middle Holocene) transition. Comparable downcore variations were observed for *n*-alcohols and aliphatic hydrocarbons too, the onset of increased abundances, however, was measured one sample above (770 varve years earlier). In contrast, fatty acids show reverse variations in total with increasing concentrations during section A and a rapid depletion during transition to section B.

Consistent with the previously presented results, section B (middle Holocene) is characterised by a significant reduction of absolute concentrations in its upper half. A well-marked minimum abundance of sterols was furthermore found at 5,690 vyears BP that is more pronounced as measured for fatty acids and in contrast to nearly constant *n*-alcohol concentrations in the same range of time.

The lower part of section B is characterised by rapidly increasing amounts of sterols consistent with other compound specific fractions; at 7,390 vyears BP, the summed concentrations of 512 µg/g TOC, representing Lake Holzmaars overall maximum sterol content, is approximately doubled in comparison to the minimum abundance 1,700 varve years earlier.

Changing from section B to C (Lateglacial), lowering sterol concentrations were measured until 10,325 vyears BP, obviously contrasting the age-related results for fatty acids and aliphatic hydrocarbons, whose abundances are enriched during the sections transition. The sediment samples between 10,150 – 10,910 vyears BP furthermore show interesting divergencies to the remaining compound classes: approximately in the middle of this interval, at 10,325 vyears BP, a local minimum of sterols was detected, continuing the decreasing trend since the middle Holocene prior to a short term enrichment at the intervals oldest sample. A comparable age related trend was observed for fatty acids whereas aliphatic hydrocarbons show a mirror-like behavior in this time and normal chain alcohol concentrations remain nearly constant. The oldest sample of Lake Holzmaars sedimentary profile finally shows lowest overall sterol concentration of 213 µg/g TOC.

Varying between 66 – 793 $\mu\text{g/g}$ TOC, the fluctuation width of sterol concentrations is considerably higher in **Lake Meerfelder Maars** sedimentary profile. The consideration of summed sterol subgroups separately yields especially increased concentrations of C_{29} sterols whereas concentrations of lighter molecular weight derivatives are more similar with less significant variations in C_{28} sterol abundances.

The upper non laminated profile segment is characterised by a lowering in absolute concentrations, resulting in a minimum abundance closely to the beginning of the annual lamination prior to a short term enrichment with a sharp peak at 1,740 vyears BP. A second minimum stage of sterol concentrations was measured 2,115 vyears BP before summed sterol concentrations rise drastically. Within 2090 varve years, summed concentrations of detected C_{29} sterols increase from 43 – 458 $\mu\text{g/g}$ TOC, whereas the C_{27} and C_{28} subgroups in sum show less dominant increases by factors 8.0 and 7.7, respectively. These downcore variations are in general very similar to those, observed for normal chain alcohols and fatty acids. The second minimum abundance, however, is additional to the results of fatty acid distributions in relation to age.

During the middle Holocene, sterol abundances remain nearly constant on the high level with the C_{29} derivatives as the by far most abundant subgroup. A slight reduction was observed between 8,670 – 10,035 vyears BP for C_{29} sterols in contrast to a mirror-like enrichment in C_{27} homologues. Thus, the period of relatively high sterol abundances persists for 2,380 varve years longer as detected for normal chain alcohols and acid compounds. The latter, contrary to *n*-alcohols and sterols, become not enriched during early Holocene.

The overall sterol maximum concentration of 793 $\mu\text{g/g}$ TOC in sum was determined in good temporal correlation to the upper border of the Younger Dryas period of cooler temperatures, caused by high values for the heaviest subgroup, whereas the two lighter sterol fractions are slightly depleted in comparison to the early Holocene. With further increasing age until 13,865 vyears BP, concentrations continuously decrease in case of the C_{27} subgroup and 520 varve years longer in case of the C_{29} sterols. Older samples are characterised by increased sterol concentrations in turn.

The described variations of sterol concentrations are clearly in contrast to those of normal chain alcohols and fatty acids during the Lateglacial, showing significant

maxima at both the upper and lower border of the Younger Dryas cold period. Also the highly significant maximum of *n*-alkane distributions at 13,865 vyears BP could not be confirmed for sterol abundances.

Considering Lake Meerfelder Maars higher resolved sample set between the early Holocene and Younger Dryas, generally increasing sterol abundances are obvious in the upper profile section after a slight reduction between 10,070 – 10,170 vyears BP. This trend is caused by the most dominant C₂₉ homologues, whereas nearly constant concentrations for both lighter subgroups were measured throughout the early Holocene, closely scattering around the average concentration of 32 µg/g TOC and 38 µg/g TOC for C₂₇- and C₂₈ sterols, respectively.

Later than 10,380 vyears BP, rapidly increasing concentrations of C₂₇- and C₂₈ sterols were detected. In case of the lighter C₂₇ subgroup, the enrichment is limited to a temporal sharply separated peak as a singular deviation from uniform abundances in relation to age as described above.

The most dominant C₂₉ subgroup in contrast shows continuously increasing concentrations in sum until 10,560 vyears BP. The next 110 varve years are characterised by very rapid fluctuations in C₂₉ sterol content: summed concentrations becomes strongly reduced from 225-112 µg/g TOC during the first 40 varve years of this period and then remain constant for additional 30 varve years (10,630 vyears BP). Only within the following 10 varve years, the concentration is shifted back to 241 µg/g TOC in sum, well comparable to the sample at the beginning of this rapid fluctuating period, to be further reduced within 10 varve years followed by a slight increase, measured at 10,670 vyears BP. A very similar behavior was already reported for normal chain fatty acids, whereas corresponding *n*-alcohols and *n*-alkanes show very constant abundances in the respective period. In the underlying sample sequence, beginning at 11,110 vyears BP, composition of the sterol fractions is uniform without remarkable extremes in all three subgroups for 385 varve years. Merely the last sample prior to the beginning of the Younger Dryas cold period shows strongly enhanced concentrations of C₂₇ and C₂₉ sterols by factor 3.6 and 2.8 in comparison to the overlying sample. This observation is in direct contrast to the results presented for fatty alcohol distributions, showing a depletion by a factor of 8.5 for the same sample.

With the beginning of the Younger Dryas cold period, sterol concentrations are reduced at first to further show rapidly varying abundances with a trend to slightly increased concentrations with increasing age. In contrast to fatty alcohol distributions, showing well marked minima during the Younger Dryas, outstanding maxima of sterol concentrations were measured at 11,855, 11,990, 12,210, 12,280 and 12,490 vyears BP. The significant bi-partitioning of Younger Dryas as reported for normal chain acid abundances could not be confirmed for sterol concentrations.

6 Discussion

Downcore concentrations of various compounds, detected in three lacustrine sedimentary archives and sorted by affiliation to general chemical compound classes, have been described up to this point. The results presented in the previous chapters strongly indicate variations in the composition of lipid fractions, that can be traced back to changing environmental conditions over geological time. Therefore, absolute contents of these compounds and/or ratios of two or more individual compounds will be evaluated as proxies for the reconstruction of environmental or climatic conditions using the known geological time scale.

Nevertheless, the initial composition of sedimentary particles is often inferred by various chemical and biological processes beginning during sinking through the water column and continuing during early diagenesis. A knowledge about the preservation state of the investigated organic matter is therefore certainly necessary to decide between varying organic matter compositions as possible results of changing environmental conditions or diagenetic effects and will be discussed prior to the actual evaluation of proxy parameters.

6.1 Preservation of Organic Matter

The first piece of evidence indicating good preservation of the investigated archives is that most Eifel Maar Lake sediments are annually laminated. Exceptions can be seen at shallow depths and in Lake Großer Treppensee between 11 – 25.5 m depth. These observations point to an absence of oxygen at the water/sediment transition during sedimentation and early diagenesis since bioturbation, e. g. of worms

and benthic organisms, would damage the layered structure otherwise. Relatively anoxic conditions, leading to good organic matter preservation can be further assumed from the unusual surface/ depth relation as mentioned in *Section 1.2.1* and listed in *Table 3.1* at least for the two Eifel Maar Lakes under investigation. However, a direct measurement of oxygen content is limited to very young sediments. Thus, previously established proxy parameters as TOC/ TS-, pristane/ phytane- and UR_{FA} ratios after [Wilkes *et al.* \(1999\)](#) will be used in the following to assess the preservation state of the investigated sedimentary archives.

Corresponding electron acceptors are necessary for oxidation processes of organic matter occurring during particle sinking through the water column and/ or after incorporation of these particles to the sedimentary body. Most common kinds of electron acceptors in lacustrine sedimentary systems are oxygen and sulphate. Nitrate and Fe^{3+} are of minor importance. Another chemical process changing the initial organic matter composition is fermentation. Additionally, methanogenesis may play an important role in organic matter degradation as shown for sediments of Lac du Bouchet, France by [Patience *et al.* \(1996\)](#).

6.1.1 TOC/ TS as Indicators of Preservation

Sulphate reduction being coupled to oxidation of sedimentary organic matter would be reflected in TOC/ TS ratios. As illustrated in *Figs. 5.1 and 5.2*, TOC/ TS ratios are relatively low (5.1 on average) throughout the Lateglacial and middle Holocene profile sections of the Lake Holzmaar profile. The ratios moreover do not show a significant differentiation between geological zones with the exception of rapid fluctuations during the early Holocene. Only the upper Subatlantic section shows significantly increased TOC/ TS ratios (9.8 on average), pointing to reduced organic matter loss by sulphate reduction. Similar results were obtained for the Lake Meerfelder Maar profile: Relatively low TOC/ TS ratios of 7.3 on average during Lateglacial with a trend to lower values in younger samples are only slightly higher as found for Lake Holzmaar. After low values at the Lateglacial/ Holocene transition, ratios become slightly increased during Holocene (10.2 on average) before relatively low ratios were calculated between 1,740-1,275 and at 420 years BP.

A more pronounced variation interval of TOC/TS ratios was measured for the Lake Großer Treppensee sedimentary sequence as it can be taken from *Fig. 5.4*. The lower 12 m are characterised by low values of 3.6 on average prior to rapid increase above 11.65 m profile depth (19.2 on average), the beginning of unlaminated sediments according to [Giesecke \(1999\)](#).

Beside these findings, the TOC content of investigated lake sediments exceeds the sulphur content by far. Thus, bacterial sulphate reduction, a prominent formation pathway of sedimentary sulphur components ([Rudd *et al.*, 1986](#)), might be strongly limited by the availability of sulphate. This is supported by low sulphate content of modern Eifel Maar Lakes between 20 – 25 mg/l for Lake Holzmaar and 13 – 21 mg/l for Lake Meerfelder Maar between 1979-1988 ([Scharf and Oehms, 1992](#)). Preliminary, a loss of the initial sedimentary organic matter to some extent cannot be excluded by interpreting TOC/TS ratios.

6.1.2 Unsaturated Fatty Acids as Indicators of Preservation

[Wilkes *et al.* \(1999\)](#) proposed a fatty acid unsaturation ratio (UR_{FA}) calculated from concentrations of stearic and oleic acid, based on the more rapid degradation of unsaturated fatty acids compared to saturated homologues ([Haddad *et al.*, 1992](#); [Meyers and Ishiwatari, 1993b](#)). In the case of organic matter degradation taking place to higher extent, [Wilkes *et al.* \(1999\)](#) expected a general downcore increase of the UR_{FA} ratio in consistency with the fast loss of unsaturated fatty acids observed in the uppermost anoxic sediments of a Japanese lake by [Kawamura *et al.* \(1980\)](#). They finally concluded a good preservation state of the sedimentary organic matter of Lago di Mezzano from the absence of an increasing trend of the UR_{FA} with increasing profile depth.

Downcore variations of the UR_{FA} are illustrated in *Fig. 6.1* for the investigated Eifel Maar Lakes. As obvious, the plots simply do not show a significant increase of the UR_{FA} with increasing age while average values are still lower compared to the study cited above. Moreover, the Subatlantic section A of Lake Holzmaars sedimentary sequence is characterised by a significantly decreasing ratio between the two uppermost samples. Simultaneously to the section A to B (middle Holocene) transition, a short term increase of the ratio is obvious prior to a following

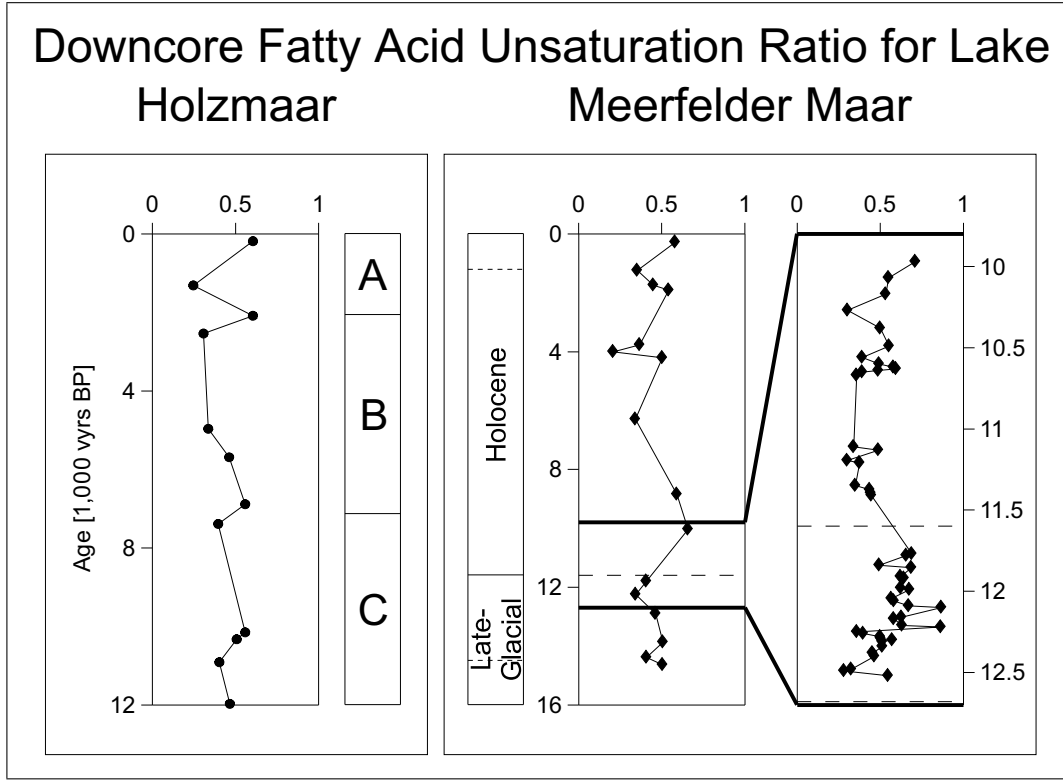


Figure 6.1: Downcore UR_{FA} ratio after Wilkes *et al.* (1999) for Eifel Maar Lakes; left panel: Lake Holzmaar (circles); right panel: Lake Meerfelder Maar (diamonds) including low (left plot) and high (right plot) temporal resolution sample sets; dashed horizontal lines: Younger Dryas cold period

reduction. Further slightly increasing ratios are visible during middle Holocene, especially between 4,960 – 6888 vyears BP. With the transition to the middle Holocene/Lateglacial section C, the UR_{FA} ratio is, however, shifted to lower values again.

Downcore UR_{FA} ratios of Lake Meerfelder Maars profile are closely similar to Lake Holzmaar with values centering on 0.5. Thus, the preservation state of Lake Meerfelder Maar sediments is obviously comparable to that of the Lake Holzmaar profile. The uppermost non-laminated core section (top to 1.2 m depth) is characterised by decreasing ratios, indicating a good preservation of organic matter. Slightly enhanced ratios are obvious with the beginning of annually laminated sediments (below 1.2 m depth). The general trend, however, points to lower UR_{FA} ratios, further supporting the good preservation state. Between 6,290 vyears BP and the beginning of the Younger Dryas cold period, another increase of the UR_{FA} was

observed, indicating a slightly deteriorated state of organic matter preservation. This partial trend, however, becomes negated during the period of cooler temperatures itself. Relatively low UR_{FA} ratios were finally detected for the lowermost samples during Lateglacial giving evidence for well organic matter preservation and supporting the usability of investigated sediments for evaluation of proxy parameters.

As obvious from the Lateglacial/Holocene transition with increased temporal resolution, a significant depletion in unsaturated $n\text{-C}_{18:1}$ fatty acid can be excluded for this major climatic transient too: The UR_{FA} ratio behaves relatively constant after a strong decrease between 9,970 – 10,270 vyears BP. Stages of enhanced ratios were detected between 10,560-10,670 as well as at 11,130 vyears BP, however, not showing a general trend. Moreover, generally decreasing UR_{FA} ratios were finally determined during the Younger Dryas cold period.

6.1.3 Pristane/ Phytane as Indicators of Preservation

A third parameter in the context of the estimation of organic matter preservation is the ratio between the two isoprenoids pristane and phytane, where the preferred formation of one compound depends on the redox state during sedimentation and early diagenesis.

As introduced in *Section 5.2.1.3*, both compounds can be derived from the diagenesis of phytol, the side chain in the chlorophyll molecule. A simplified pathway of the chlorophyll diagenesis after [Ikan *et al.* \(1975\)](#) is given in *Fig. 6.2*. Out of the intermediates of the pristane and phytane generation mentioned in this scheme, phytenic acid ([Boon *et al.*, 1975](#)), dihydrophytol ([Sever and Parker, 1969](#); [Ikan *et al.*, 1975](#)) and phytanic acid ([Blumer and Cooper, 1967](#)) have been reported to occur in recent sediments. As a result of simulated diagenesis of sediments, [Ikan *et al.* \(1975\)](#) and [de Leeuw *et al.* \(1977\)](#) unanimously found that dihydrophytol is formed under reducing conditions whereas phytenic acid is formed under oxidising conditions. Based on these results, the ratio of the diagenetic products pristane and phytane was used to estimate the redox conditions during sinking and early diagenesis of organic matter, and [Didyk *et al.* \(1978\)](#) first suggested that pristane/phytane ratios lower than one point to anoxic environments whereas higher values were found to be typical for oxic conditions.

Contrastingly, [Horsfield \(1978\)](#) argued, that this general approach is ambiguous

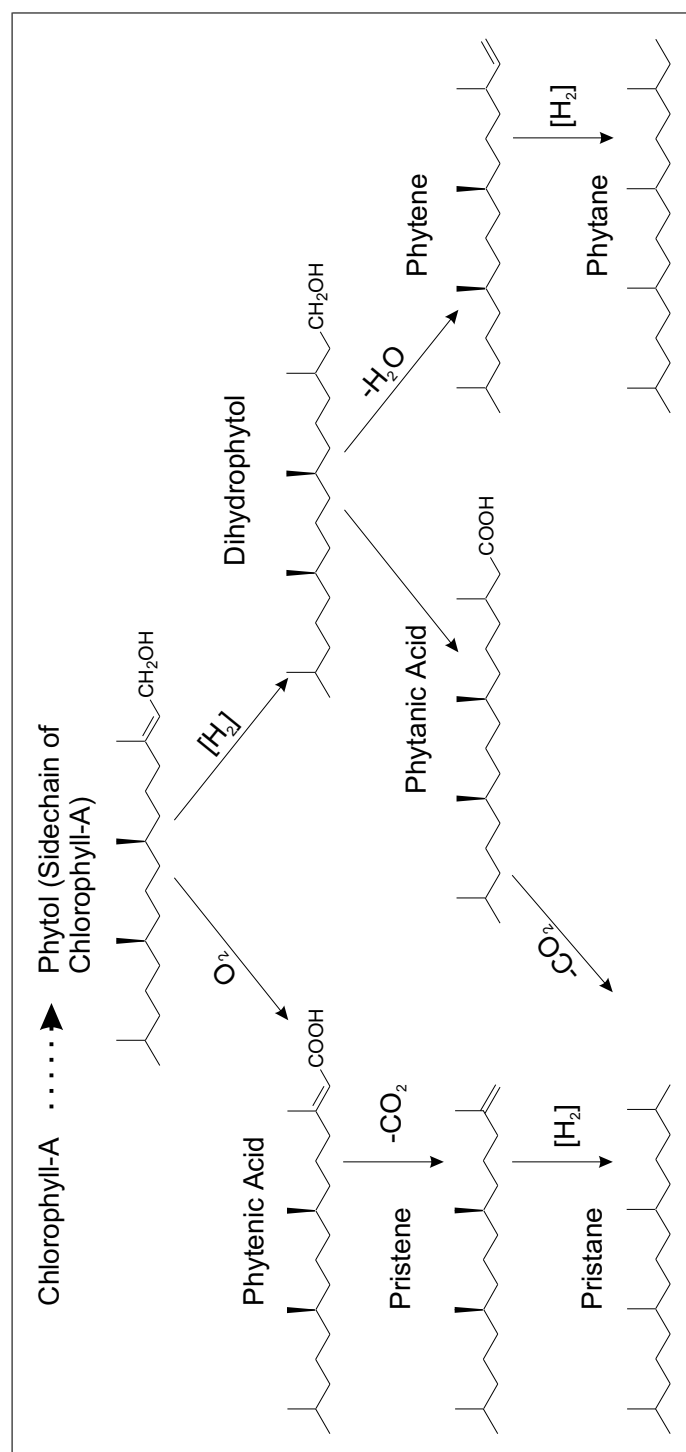


Figure 6.2: Phytol sedimentary diagenesis, simplified after Ikan *et al.* (1975)

since most sediments have upper oxidising and lower reducing layers and thus suggested to interpret low pristane/phytane ratios with a short residence in the oxidising layer and *vice versa* higher ratios with a longer residence. The application of pristane/phytane ratios becomes further limited due to other sources than phytol as mentioned in *Section 5.2.1.3*. Additionally, Volkman and Maxwell (1986) do not recommend to use this parameter for the reconstruction of the environment for samples of low thermal maturity as investigated in the present study. Some evidence exists for a dependency between thermal maturity and pristane/phytane ratios. ten Haven *et al.* (1987) indicate increasing ratios with increasing maturity. Hughes *et al.* (1995) on the other hand found only little and no systematic variation in pristane/phytane ratios in relation to maturity in several sets of oils. However, maturity is urgently assumed to be low for the samples investigated in the present study in comparison to e.g. oil field studies. Another limitation consists of the dependency of the pristane/phytane parameter from the lake salinity as indicated by ten Haven *et al.* (1987). Accordingly, low ratios may also point to a hypersaline sedimentation environment due to effects of variable salinity on halophilic bacteria. Additionally, increasing salinity leads to an intensified density stratification of the water body resulting in reduced oxygen content at the water/sediment interface which further implies reduced pristane/phytane ratios (Peters and Moldowan, 1993).

Despite all these limitations, a comparison between the two similar Eifel Maar Lakes should be possible without problems if the results of the previously discussed parameters in relation to the preservation state are kept in mind. The illustration in *Fig. 6.3* shows very equal ratios for both maar lakes closely around unity in wide ranges of age and, additionally, comparable age related variations in both cores. The oldest samples of the Lake Meerfelder Maar sequence are characterised by comparably high ratios that are continuously reduced to 0.77 at 13,865 vyears BP. This date is in good correlation to the lower border of sediment varving; Brauer *et al.* (1999a) found continuous one-year layers until 14,000 vyears BP. The missing of annual lamination as well as the higher pristane/phytane ratios point to more oxic conditions in older samples under which enhanced bioturbation prevents the preservation of single year sediment layers.

After the Younger Dryas cold period, ratios decrease in Lake Holzmaar with a short-term increase at 10,150 vyears BP whereas they increase again in Lake

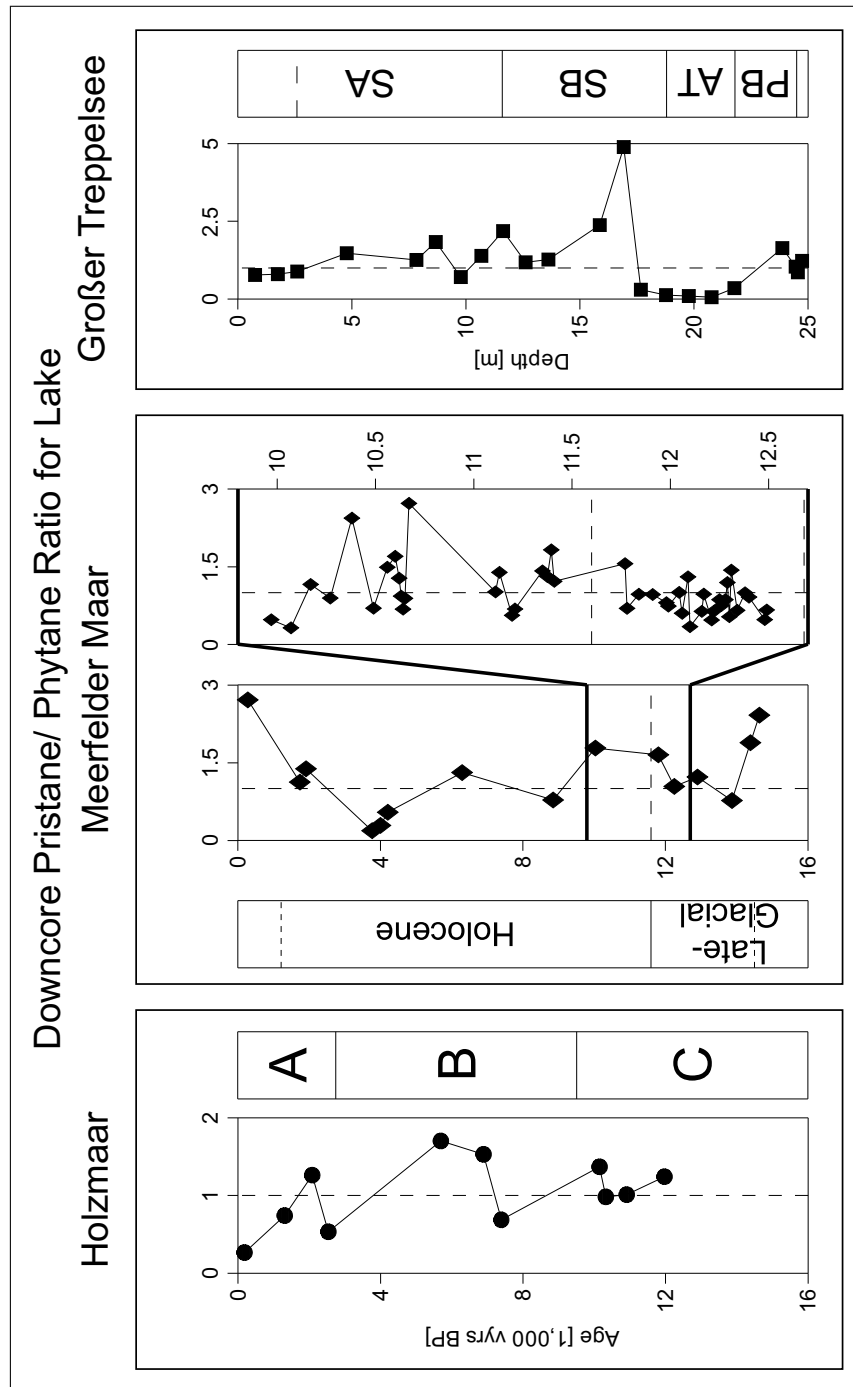


Figure 6.3: Downcore pristane/phytane ratios for Eifel Maar Lakes (left and middle plot; circles: Lake Holzmaar; diamonds: Lake Meerfelder Maar) and Lake Großer Treppensee (right plot); dashed horizontal lines: Younger Dryas cold period; dashed vertical lines: $Pr/Phy = 1$

Meerfelder Maar profile. From approximately 10,100 vyears BP, a major decrease of the Pristane/Phytane ratio until 2,536 vyears BP and 3,765 vyears BP was observed for Lake Holzmaar and Lake Meerfelder Maar, respectively. This trend is interrupted by a plateau of more dominant pristane concentrations at approximately 6,300 vyears BP in both lakes again. The period between 8,850 – 3,765 vyears BP of Lake Meerfelder Maar is characterised by strikingly low ratios of 0.6 on average. The only exception from this general behavior is one sample approximately in the middle of this range. The lowest overall values of 0.2 on minimum are obvious for the three uppermost samples of this interval. These findings suggest an excellent preservation of the sedimentary organic matter. As described during *Section 5*, the same range of age is also characterised by lipid distributions that clearly differ from those of sediments above and below, e.g. increased *n*-heneicosane and *n*-tricosane abundances, decreased $\delta^{13}\text{C}$ isotope ratios of the same homologues, increased abundances of cholestane and, more pronounced, hopane derivatives, increased abundances of *n*-fatty acids in sum as well as single unsaturated C_{16:1} and C_{18:1} fatty acids and finally increased sterol abundances, especially of the C₂₉ homologues. Thus, an organic matter contributing community, that significantly differs from both, older and younger times of the Lake Meerfelder Maar, must be expected for this range of time. The lack of comparably differing lipid distributions in the sedimentary record of Lake Holzmaar on the other hand points to a local phenomenon in the catchment of Lake Meerfelder Maar that is not primary controlled by climatic conditions. A more important reason for the unique differences in the organic matter composition of both maar lake records must be seen in the different morphology as introduced in *Section 3.1*, determining a different vegetation development. The sources of sedimentary organic matter will be evaluated during the following sections, allowing a more detailed differentiation between both maar lake records.

Remarkable differences in Pristane/Phytane ratios between the Maar Lakes were calculated for the uppermost profile sections: Lake Holzmaar is characterised by ratios as low as 0.27, whereas Lake Meerfelder Maar shows a strong increase up to 2.71 between 1,900 – 280 vyears BP. Also within this upper section, interpretation of the increasing Pristane/Phytane ratios with more oxic conditions is supported by Brauer *et al.* (1999a), who found only partly varved sediments in this profile segment. Lake Holzmaar in contrast shows annual lamination until the profiles top with organic rich varves especially in the uppermost part (Haj-

das *et al.*, 1995; Zolitschka, 1998; Stockhausen and Zolitschka, 1999), pointing to enhanced organic matter preservation under anoxic conditions.

Pristane/phytane ratios are relatively uniform throughout the whole sequence under investigation, again closely scattering around unity. A generally good preservation of the sedimentary organic matter can therefore be assumed for this archive too. A remarkable feature are, however, the very low ratios of 0.2 on average between 21.78 – 17.68 m profile depth, well correlated to the laminated core section. They initially suggest a further improved preservation state. Note, however, that unproportionately high phytane concentrations were measured for the same samples (*cf.* Fig. 5.16), clearly exceeding the concentration of both compounds in sum in remaining samples. Thus, an additional source of phytane must be taken in account beside the good preservation state of the sedimentary organic matter since the respective core section is not characterised by an increased amount of organic matter content (*cf.* Fig. 5.4).

Summary: Laminated structure of Eifel Maar Lake sediments and Lake Großer Treppelsee sediments between 25.5 – 11 m depth indicates enhanced preservation under more anoxic conditions since bioturbation can be excluded. Nevertheless, a partial loss of organic matter to some extent due to bacterial sulphate-reduction can not be excluded from TOC/TS ratios throughout all three investigated sedimentary profiles. Two more specific parameters, the UR_{FA} ratio after Wilkes et al. (1999) as well as downcore variations of pristane/phytane ratios on the other hand point to a good preservation state of organic matter from Eifel Maar Lakes and Lake Großer Treppelsee under relatively anoxic conditions. An important finding is the improved preservation state of sediments from Lake Meerfelder Maar between 8,850 – 3,765 vyears BP and of Lake Großer Treppelsee between 21.78 – 17.68 m profile depth.

It can therefore be concluded, that the investigated sedimentary organic matter is well preserved in general, being not overprinted by diagenetic transformations by high extend. So far, investigated sediments represent variations in the composition of organic matter contributors, that are related to environmental and/or climatic changes in the respective catchment areas.

6.2 Origin of Organic Matter in the investigated Lake Sediments

Variations of lipid biomarker distributions analysed in sedimentary sequences of the two Eifel Maar Lakes and Lake Großer Treppensee indicate variations of biological sources being related to fluctuations in environmental and climatic conditions since significant variations in organic matter content were detected in dependency to geological profile sections as reported in *Chapter 5*. Therefore, several compounds and/or compound classes will be assigned to discrete organic matter sources and/or source groups in the following.

6.2.1 Normal Chain Compounds as Source Indicators

Well-known and specific sources of sedimentary lipids are needed to reconstruct proportions of different vegetation types in limnic systems and the surrounding catchment areas. Variable contributions of these vegetation types during time allow inferences to environmental and/or climatic conditions. Despite the specific sources of individual normal chain compounds as introduced in *Section 1.3*, entire mixtures of normal chain compounds out of the alkane, acid and alcohol fractions will be evaluated in the present section in order to detect general changes in the composition of the sedimentary organic matter as well as their potential linkage to environmental and/or climatic shifts.

Various publications dealing with normal chain biomarker distributions were published in the past for differentiation between terrestrial and aquatic source organisms (Ficken *et al.*, 1998a,b; Wilkes *et al.*, 1999; Ficken *et al.*, 2000; Schwark *et al.*, 2002). Generally, short and medium chain odd numbered compounds in case of aliphatic hydrocarbons and even numbered compounds in case of fatty acids and alcohols with carbon numbers between 15-25 are associated with aquatic sources, where shorter derivatives originate from lacustrine algae in contrast to mainly macrophytic plants as sources of the longer chain derivatives, especially out of the *n*-alkanes (Ficken *et al.*, 2000, 2002).

Compounds with carbon numbers between 27-33 mainly originate from cuticular waxes of higher land plants (Cranwell, 1973b). According to Brincat *et al.* (2000),

Table 6.1: CPI for *n*-alkane distributions in investigated profiles

	CPI_{HC}	CPI_{HC}^{SC}	CPI_{HC}^{MC}	CPI_{HC}^{LC}
Lake Großer Treppelsee	5.96 ± 1.27	2.97 ± 2.74	3.41 ± 0.99	6.37 ± 1.35
Lake Holzmaar	8.55 ± 1.98	1.65 ± 0.40	4.65 ± 1.79	9.58 ± 2.23
Lake Meerfelder Maar	7.54 ± 1.42	1.29 ± 0.47	4.65 ± 1.44	8.58 ± 1.86

the respective group of *n*-alkanes can be further subdivided into different source classes: high relative amounts of *n*-C₂₇ point to a dominant forest vegetation, whereas a higher relative contribution of *n*-C₃₁ is typical for a dominant vegetation of herbs and shrubs.

A first criterion to distinguish between sources of normal chain compounds are Carbon Preference Indices (CPI). CPI calculated from absolute *n*-alkane concentrations are listed in *Table 6.1*, formulas are given in *Appendix A.1*. Like reported from previous studies, average CPI values between 6.0 and 8.5 are typical for dominant organic matter supply from cuticular waxes of higher plants; the marked dominance of odd-numbered homologues is caused by the decarboxylation pathway of *n*-alkanes from corresponding fatty acids with carbon atom numbers being increased by one (Kolattukudy, 1980). Moreover, a significant dependence of CPI from *n*-alkane chain length is obvious from *Table 6.1*: As listed, values increase with chain length from lowest values for short chain homologues to maxima at *n*-C₂₇ - *n*-C₃₁ alkanes. The dominating last named group of *n*-alkanes obviously causes the high CPI values of the whole *n*-alkane series in sum. This initially points to different sources of the respective chain length groups of *n*-alkanes. The chain length ranges used for calculation were adopted from Ficken *et al.* (2000) and citations therein, proposing aquatic algae, submerged and emergent macrophytes as well as higher land plants as the respective groups of source organism in the case of *n*-alkanes. Respective chain length ranges were increased by one for *n*-fatty acids as well as *n*-alcohols.

Table 6.2: CPI for *n*-fatty acid distributions in Eifel Maar Lakes

	CPI_{FA}	CPI_{FA}^{SC}	CPI_{FA}^{MC}	CPI_{FA}^{LC}
Lake Holzmaar	7.11 ± 1.29	3.53 ± 2.22	11.01 ± 8.32	7.24 ± 1.35
Lake Meerfelder Maar	7.78 ± 2.50	5.14 ± 2.19	7.31 ± 2.15	8.03 ± 2.77

Table 6.3: CPI for *n*-fatty alcohol distributions in Eifel Maar Lakes

	CPI_{FA}	CPI_{FA}^{SC}	CPI_{FA}^{MC}	CPI_{FA}^{LC}
Lake Holzmaar	10.62 ± 2.85	0.91 ± 0.40	7.54 ± 2.37	6.58 ± 4.19
Lake Meerfelder Maar	6.93 ± 1.80	1.66 ± 0.92	6.86 ± 1.74	4.29 ± 1.69

The marked predominance of even-numbered fatty acids (71 – 93 % of total acids; $CPI_{FA} = 7.70 \pm 2.25$ on average of all samples) is slightly higher as the OEP calculated for *n*-alkanes. Listed values are typical for both plant and animal derived fatty acids due to their unique biosynthesis from C_2 units derived from glucose under presence of enzymes, coenzymes and carrier-proteins, initially leading to palmitate (Killops and Killops, 1993). Diversification occurs by further addition of C_2 units on a similar pathway and, in the case of plants, by enzymatic dehydrogenation, leading to conjugated unsaturated fatty acids. Energy is yielded by hydrolysis of glycerides and successive loss of C_2 units from the acid chain (β -oxidation). However, in bacteria and mainly in plants, oxidation is performed by loss of single carbon atoms from the acid chain, leading to the odd numbered derivatives (α -oxidation). However, CPI values are not as chain-length dependent as found for *n*-alkanes previously (*cf.* Table 6.2). Thus, CPI indices after Wilkes *et al.* (1999) are very similar in both Maar Lakes. Within the short chain subgroup, ranging from C_{13} to C_{19} , slightly lowered values were calculated, that are significantly lowest in Lake Holzmaar. A remarkably high average of 11.01 was calculated for the mid-range between C_{19} - C_{25} in Lake Holzmaar profile, above all caused by highest values between 4,960 – 7,390 vyears BP ranging from 11.5–36.7. This temporary shift of CPI values preliminary indicates a changed fatty acid source during that time. The long chain subgroup, ranging from C_{25} - C_{31} finally shows values that are not as much higher, compared to shorter chain length subgroups, as found for *n*-alkane CPI indices.

CPI indices of fatty alcohols are listed in Table 6.3. The highest overall indices were found over the complete medium and long chain length range of Lake Holzmaar sedimentary sequence whereas the respective value of Lake Meerfelder Maar is lower than that determined for *n*-alkanes and *n*-fatty acids. Calculated to more specific chain length ranges, low indices were measured for the short chain length range similar to those of *n*-alkanes. CPI indices are also closely comparable to those of fatty acids within the medium and long chain length range with the ex-

ception of the relatively low value for long chain homologues in the Lake Meerfelder Maar profile.

Cluster analysis after the Ward-Method using squared Euclidian distances (cf. *Section 4.7*) was performed for each compound class separately in order to detect dependencies between normal chain compounds of different chain length more precisely. Clusters for single compounds show similarities between contributions of these compounds throughout the profiles and therefore point to similar sources or source groups. The resulting dendrograms with clusters for odd numbered *n*-alkanes as well as even numbered *n*-fatty acids and *n*-alcohols are shown in *Fig. 6.4*. Respective data of all three archives have been used for calculation of dendrograms to ensure the data base being as wide as possible since the goal of that kind of analysis is to test similarities in occurrence of several individual compounds, that rather depend on discrete groups of source organisms than on a special archive or geological setting.

For all of the three investigated compound specific fractions, short chain compounds are well separated into single clusters. Note, however, that absolute concentrations of individual compounds do not necessarily affect this result; decisive criterion for assignment are synchronous changes in absolute concentrations of several compounds during time for combination of individual compounds into clusters.

In more detail, the three lightest derivatives of *n*-alkanes form a main cluster with a relative similarity of 84 %. This grouping confirms a uniform contribution of short chain *n*-alkanes from a discrete source. This is in agreement with the results published by [Nishimoto \(1974\)](#); [Weete \(1976\)](#), indicating the algal origin of the short chain *n*-alkane homologues.

Grouping of several *n*-alkane homologues is more complicated within the mid-chain length range: *n*-Alkanes with carbon numbers 21 and 23 are combined to a subgroup with a relative similarity of 83 % between both members. According to [Barnes and Barnes \(1978\)](#); [Cranwell \(1984\)](#); [Ogura *et al.* \(1990\)](#); [Viso *et al.* \(1993\)](#); [Ficken *et al.* \(1998a\)](#) and [Ficken *et al.* \(2000\)](#), this group of individual aliphatic hydrocarbons is derived from macrophytes and should also contain *n*-pentacosane. According to the last named publication, *n*-alkane distributions of macrophytes maximise at *n*-C₂₃ to *n*-C₂₅ in case of submerged and floating species, a chain length range not typical of higher plant leaf waxes ([Kolattukudy *et al.*](#),

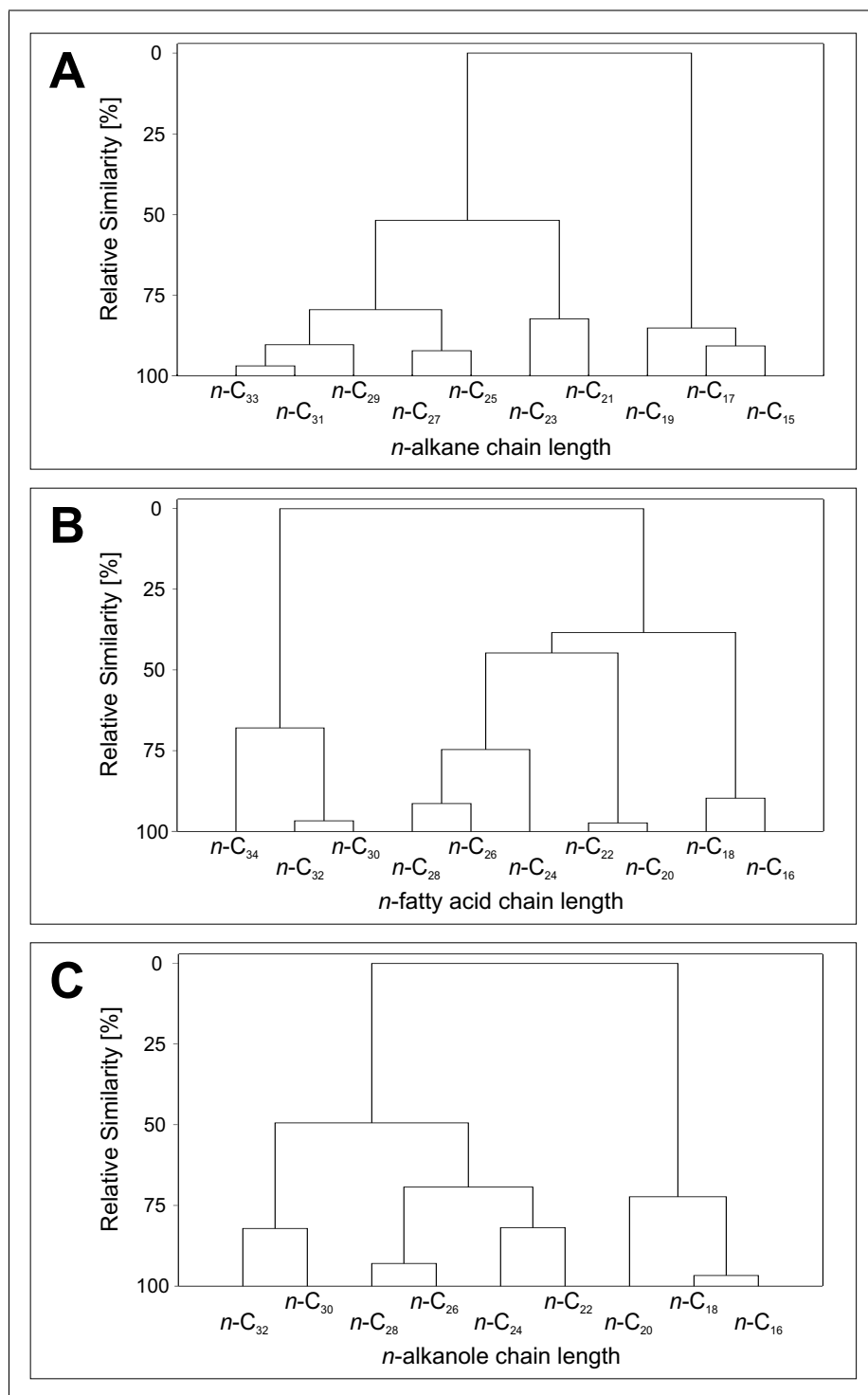


Figure 6.4: Cluster diagram for saturated *n*-alkanes (A), *n*-fatty acids (B) and *n*-alkanoles (C), clusters for chain length using data from all investigated archives

1976), as well as at $n\text{-C}_{27}$ to $n\text{-C}_{29}$ in case of emergent species. Abundances of $n\text{-pentacosane}$ throughout the investigated sedimentary profiles, however, is more similar (92 %) to $n\text{-heptacosane}$, also a common source indicator for tree-leaves (Cranwell, 1973b), especially birch leaf-waxes as determined from correlation between pollen data and lipid distributions by Schwark *et al.* (2002). The present investigation therefore shows, that a separation of source organisms based on concentrations of $n\text{-alkanes}$ is difficult, especially in case of the border-compound $n\text{-pentacosane}$ with submerged macrophytes and emergent macrophytes and/or land plants as possible source organisms. Nevertheless, $n\text{-C}_{21}$ and $n\text{-C}_{23}$ $n\text{-alkanes}$ in relation to $n\text{-alkanes}$ in sum seem to confidentially reflect percentages of sedimentary organic matter supply originating from submerged macrophytes whereas the $n\text{-C}_{25}$ homologue should be used carefully for distinction between source classes due to the emergent macrophytes and land plants being potential source classes. The last sub-cluster, summarising the longest chain length homologues heavier than $n\text{-C}_{25}$, shows a relative similarity of at least 83 %. These compounds are allocated to higher land plants (Eglinton and Hamilton, 1967) such as grasses, herbs, shrubs and trees. Additionally, selected emergent species of macrophytes such as *Phragmites communis* and *Juncus effusus* are also known to show $n\text{-alkane}$ patterns similar to land plants (Barnes and Barnes, 1978; Cranwell, 1984), maximising at $n\text{-C}_{27}\text{--}n\text{-C}_{29}$. Consistent with Brincat *et al.* (2000), $n\text{-heptacosane}$ as a marker compound for forest vegetation is well separated within the highest chain length sub-cluster whereas the longer chain derivatives $n\text{-nonacosane}$ and $n\text{-untriacontane}$ show relative similarities of 92 %, representing a herbaceous vegetation type.

For cluster analysis of normal chain fatty acids a highly specific cluster was separated for the short chain homologues $n\text{-hexacosanoic}$ and $n\text{-octacosanic}$ acid, further confirming the algal origin as published by Ficken *et al.* (1998b). In contrast to $n\text{-alkane}$ clusters, the shortest chain length compounds also show similarities to longer chain homologues, that are, however, less significant (38 %).

A well partitionated splitting was retrieved for fatty acids in the mid-chain length range. A discrete sub-cluster is formed by $n\text{-C}_{20}$ and $n\text{-C}_{22}$ homologues with a relative similarity of 97 % between both homologues and less important similarities of 38 % and 45 % to neighboring sub-clusters of shorter and longer chain length range, respectively. This is, considering the biochemical formation of $n\text{-alkanes}$ by

decarboxylation of *n*-fatty acids, clearly in opposition to the results of *n*-alkane cluster analysis where corresponding homologues are assigned to clusters with no similarity between them. *n*-Tetracosanoic acid, according to Ficken *et al.* (1998b) also a suitable proxy for macrophyte derived organic matter, is more similar assigned to the long chain length range up to *n*-octacosanoic acid. *n*-Hexacosanoic and *n*-octacosanoic acid behave very similar (91 %), whereas the relative similarity of both acids to tetracosanoic acid is lower (75 %). This finding furthermore confirms the unclear assignment in the middle chain length range, considering *n*-tetracosanoic acid being equivalent to *n*-triaicosane on the biochemical decarboxylation pathway; emergent macrophytes or land plants are respective organic matter sources in turn.

n-Hexacosanoic- and *n*-octacosanoic acid on the other hand belong to the long chain length range, being typical proxy markers for land plant vegetation. More significantly as found for *n*-alkanes, long chain fatty acids are further subdivided, the longest chain length homologues above the *n*-C₂₈ fatty acid show no similarity to the previous cluster. This finding more significantly than the *n*-alkane dendrogram supports the partitioning of long chain compounds to derive from different sources since *n*-C₂₈ to *n*-C₃₀ fatty acids are well comparable to the *n*-alkanes with carbon atom number being decreased by one due to the decarboxylation pathway.

Finally, even numbered fatty alcohols in the chain length range from *n*-C₁₆ to *n*-C₃₂ were combined into groups with respect to similarities in changing concentrations during time by cluster analysis. The most specific cluster was calculated for short chain homologues from *n*-hexadecanol to *n*-icosanol with relative similarities of 97 % and 72 %.

Assignment of mid chain *n*-alcohols is unspecific compared to the previously discussed compound specific fractions. A good correlation was found for *n*-docosanol and *n*-tetracosanol content (82 %). A next subcluster is formed by *n*-hexacosanol and *n*-octacosanol, typical proxies for land plant derived organic matter supply, with relative similarities of 93 % between the compounds themselves. Also the assignment to the neighboring subcluster of the two shorter chain length fatty alcohols still retrieves a good relative similarity of 69 %.

As already reported, the long chain length range is subdivided into groups confirming discrete terrestrial plants as source organisms.

Table 6.4: Chain length ranges of *n*-alkyl lipids, representing different organic matter sources

Compound Class	Representing organic matter supply of		
	Algae	Macrophytes	Land Plants
<i>n</i> -Alkanes	<i>n</i> -C ₁₅ – <i>n</i> -C ₁₉	<i>n</i> -C ₂₁ – <i>n</i> -C ₂₃	<i>n</i> -C ₂₇ – <i>n</i> -C ₃₁
<i>n</i> -Fatty Acids	<i>n</i> -C ₁₆ – <i>n</i> -C ₁₈	<i>n</i> -C ₂₀ – <i>n</i> -C ₂₂	<i>n</i> -C ₂₈ – <i>n</i> -C ₃₂
<i>n</i> -Fatty Alcohols	<i>n</i> -C ₁₆ – <i>n</i> -C ₁₈	<i>n</i> -C ₂₂ – <i>n</i> -C ₂₄	<i>n</i> -C ₂₈ – <i>n</i> -C ₃₂

Summary:

The grouping of algal and land plant derived *n*-alkyl lipids could be proved by cluster analysis, but there are some difficulties detecting macrophyte derived contribution to the sedimentary organic matter: *n*-henicosane and *n*-tricosane are clearly grouped together, whereas *n*-pentacosane shows more similar abundance variations to the land plant derived *n*-C₂₇ alkane. Comparable results were also obtained from cluster analysis of both other investigated lipid fractions. Therefore, the established ratio for *n*-alkanes derived from submerged and floating macrophytes as recently published by Ficken et al. (2000) was modified in this study to include only the *n*-C₂₁ and *n*-C₂₃ alkanes. It is proposed to reflect submerged macrophyte derived organic matter supply since variations of *n*-pentacosane abundances could not be clearly separated from other abundant *n*-alkanes, that are surely known to derive from higher land plants. Analogous chain length ranges, indicative for discrete organic matter sources, were defined based on the results of cluster analysis as listed in Table 6.4

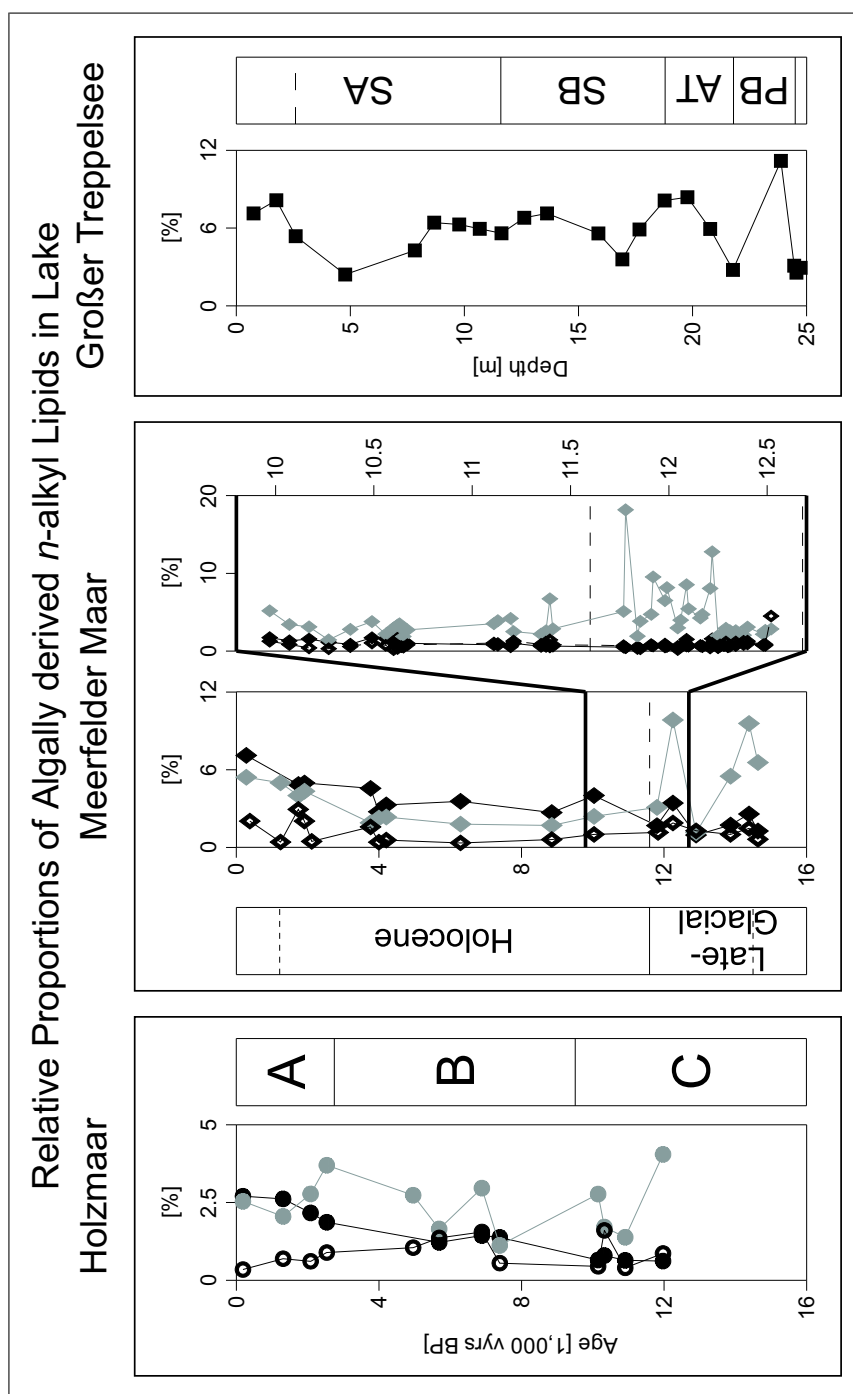


Figure 6.5: Downcore percentages of algal derived normal chain alkyl lipids; left panel (circles): Lake Holzmaar; middle panel (diamonds): Lake Meerfelder Maar including both, low and high resolution sample sets; right panel (squares): Lake Großer Treppensee; open symbols: *n*-alcohols; grey symbols: *n*-fatty acids; black symbols: *n*-alkanes; percentages are calculated from chain length ranges as listed in Table 6.4 in relation to the whole detected chain length range of the respective *n*-alkyl fraction

Contributions of the organic matter sources inside and surrounding the investigated lakes to the sedimentary matter as well as time-related variations will be reconstructed in the following based on the assignment of normal chain compounds to discrete organic matter sources as described above.

Relative abundances of aquatic algally derived *n*-alkyl lipids is low for all three investigated lipid fractions and, moreover, in all three investigated sedimentary archives. However, a quantitative comparison especially of short chain *n*-alkyl lipids, mainly originating from algal material, should be handled carefully. Meyers *et al.* (1980, 1984) reported a proportional depletion in short chain *n*-C₁₆ and *n*-C₁₈ fatty acids and alcohols relative to longer chain homologues during sinking of particles during the water column and incorporation into the sedimentary matter. Analogously, Kawamura *et al.* (1987) reported reduced *n*-C₁₇ alkane content, also an algal biomarker, in surficial sediments compared to particles collected from sediment traps.

Despite the generally good preservation state of the archives under investigation as figured out in *Section 6.1*, an estimation of algal contribution to the sedimentary organic matter based on relative proportions of short chain *n*-alkyl lipids therefore seems to lead to an underestimation of these sedimentary organic matter sources. Additionally, reduced relative abundances were detected with increasing age especially for the Eifel Maar Lakes, probably indicating a preferred diagenetic loss of short chain derivatives during time.

Lowest abundances were calculated for **Lake Holzmaars** sedimentary sequence, ranging between 0.6 – 4.4 % with a general trend to lower values with increasing age as illustrated in *Fig. 6.5, left panel*. Relative abundances of normal chain fatty acids are higher compared to *n*-alkanes, whereas no significant variations were detected in relation to the geological zones.

A nonuniform contribution of short chain compounds is obvious during the oldest section C of the profile. Short chain *n*-alkane abundances point to relatively stable autochthonous contribution. Fatty acid abundances on the other hand show highest overall percentages in the lowermost sample in temporal correlation to the end of the Younger Dryas cold period that are further significantly reduced. The following strong increase of autochthonously derived fatty acids towards the Lateglacial/Holocene transition is in opposition to slightly reduced abundances of the respective *n*-alkane homologues.

Whereas short chain fatty acid percentages are clearly reduced after the Lateglacial/Holocene transition, *n*-alkane abundances point to slightly elevated autochthonous productivity. A partial maximum contribution, that is most pronounced for fatty acids, is obvious at 6,888 vyears BP prior to another reduction, consistently detected for all investigated compound classes.

After generally increasing abundances of autochthonously derived compounds towards the Holocene/Subatlantic transition, behavior of investigated compound classes differs towards the profiles top. Whereas short chain *n*-alkane abundances suggest a continuous rise of autochthonous organic matter sources, fatty acids indicate a reduction between 2,536 – 1,311 vyears BP; an increased importance of autochthonous productivity can be confirmed for the uppermost sample only.

Generally higher percentages of short chain *n*-alkyl lipids are obvious from *Fig. 6.5, middle panel* for **Lake Meerfelder Maars** sedimentary sequence, varying between 1.2 – 10.5 %. This finding preliminary indicates an increased autochthonous productivity in that lake during time. Moreover, variations in percentages of short chain homologues are very similar for all investigated compound classes, differences between *n*-alkanes and *n*-fatty acids as discussed for Lake Holzmaar before could not be detected. Clearly in contrast to the findings for Lake Holzmaar, the relative abundances of short chain *n*-alkanes are higher than those of *n*-fatty acids during wide parts of the profile. Age related variations are, however, less specific in Lake Meerfelder Maar, showing continuously increasing percentages of algal derived compounds with decreasing age.

Most pronounced variabilities are obvious from Lateglacial and Younger Dryas samples. During the Lateglacial, highest overall short chain fatty acid percentages point to an increased importance of algally derived sedimentary organic matter during this period of relatively cold and dry conditions. This suggestion is also supported by slightly increased abundances of short chain homologues out of the other compound specific fractions. The strong influence of autochthonously derived organic matter becomes reduced during Allerød and Bølling, the first periods of ameliorated climatic conditions after the Lateglacial, to reach its overall minimum as obtained from all compound specific fractions directly with the beginning of the Younger Dryas cold period. A reverse development occurred during this period of deteriorated climatic conditions itself: Percentages of short chain *n*-alkyl lipids show a highly significant maximum abundance at 12,250 vyears BP, approximately in the middle of the Younger Dryas. Thus, an increased propor-

tion of autochthonously derived sedimentary organic matter must be taken into account. A further reduced dominance of short chain compounds simultaneously with the Younger Dryas/ Holocene transition points to reduced autochthonous productivity in Lake Meerfelder Maar at the outgoing Younger Dryas.

Autochthonously derived *n*-alkane proportions increase during the early Holocene and until 10,035 vyears BP whereas short chain fatty acid percentages decrease below the values of *n*-alkanes in this range of time. The overlying Holocene sediments are characterised by a very stable composition from short chain homologues of all investigated compound classes. This finding indicates stable environmental and/ or climatic conditions during this time until 4,000 vyears BP. A significantly improved contribution of algae to the sedimentary organic matter can be inferred from short chain homologues of all investigated compound classes above this date until the profiles top. However, a diagenetic loss of short chain compounds in older samples must also be taken into account.

The investigation of the Lateglacial/ Holocene transition with improved temporal resolution basically confirms these findings. The changed dominance between algally derived *n*-fatty acids and *n*-alkanes, however, is not included in this sample set. Its absolute date is probably later as inferred from the first sample set due to the high integration width of each sample out of this set.

Percentages of short chain homologues out of all investigated compound classes are very low during the older part of the Younger Dryas period. Beginning at 12,220 vyears BP, a sharp increase of short chain fatty acids confirms the increased importance of algally derived organic matter as retrieved from the lower resolved profile before. An increase was also observed for the short chain *n*-alkanes. It is, however, less pronounced, again in agreement with the previously discussed profile. Short chain fatty acid percentages remain on an elevated level of 7.3 % on average until 11,780 vyears BP, close to the Younger Dryas/ Holocene transition. Beside the high average of short chain fatty acids, rapid fluctuations are obvious from *Fig 6.5*, including the overall maximum of 19.4 %. These observations give a strong evidence for a significant bi-partitioning of the Younger Dryas cold period as it has been proposed by [Schwark *et al.* \(2002\)](#) based on longer chain *n*-alkane abundances and pollen data of Lake Steisslingen, Germany.

The beginning of the Holocene is further characterised by low percentages of short chain homologues, suggesting a reduced priority of autochthonous organic matter supply during times of ameliorated climatic conditions.

Lake Großer Treppensee finally shows highest overall percentages of short chain algally derived *n*-alkanes of 8.05 % on average, indicating a more important autochthonous productivity compared to the Eifel Maar Lakes.

The overall maximum contribution of autochthonous organic matter is obvious from *Fig. 6.5, right panel* at 23.88 m depth during Preboreal after relatively low percentages during the Younger Dryas. The maximum abundance is directly followed by the overall minimum. Overlying laminated sediments are characterised by a continuous enrichment in algally derived proxy compounds until 19.78 m profile depth, that is reduced in the following. The partly laminated Subboreal and lower Subatlantic sediments are characterised by a continuously increased importance of autochthonous organic matter as it can be inferred from short chain *n*-alkanes. This trend is reversed above 8.68 m profile depth. The upper Subatlantic samples are finally characterised by increased supply from autochthonous organic matter, a feature as consistently observed for the Eifel Maar Lakes. A slight depletion must be considered only between the two uppermost samples.

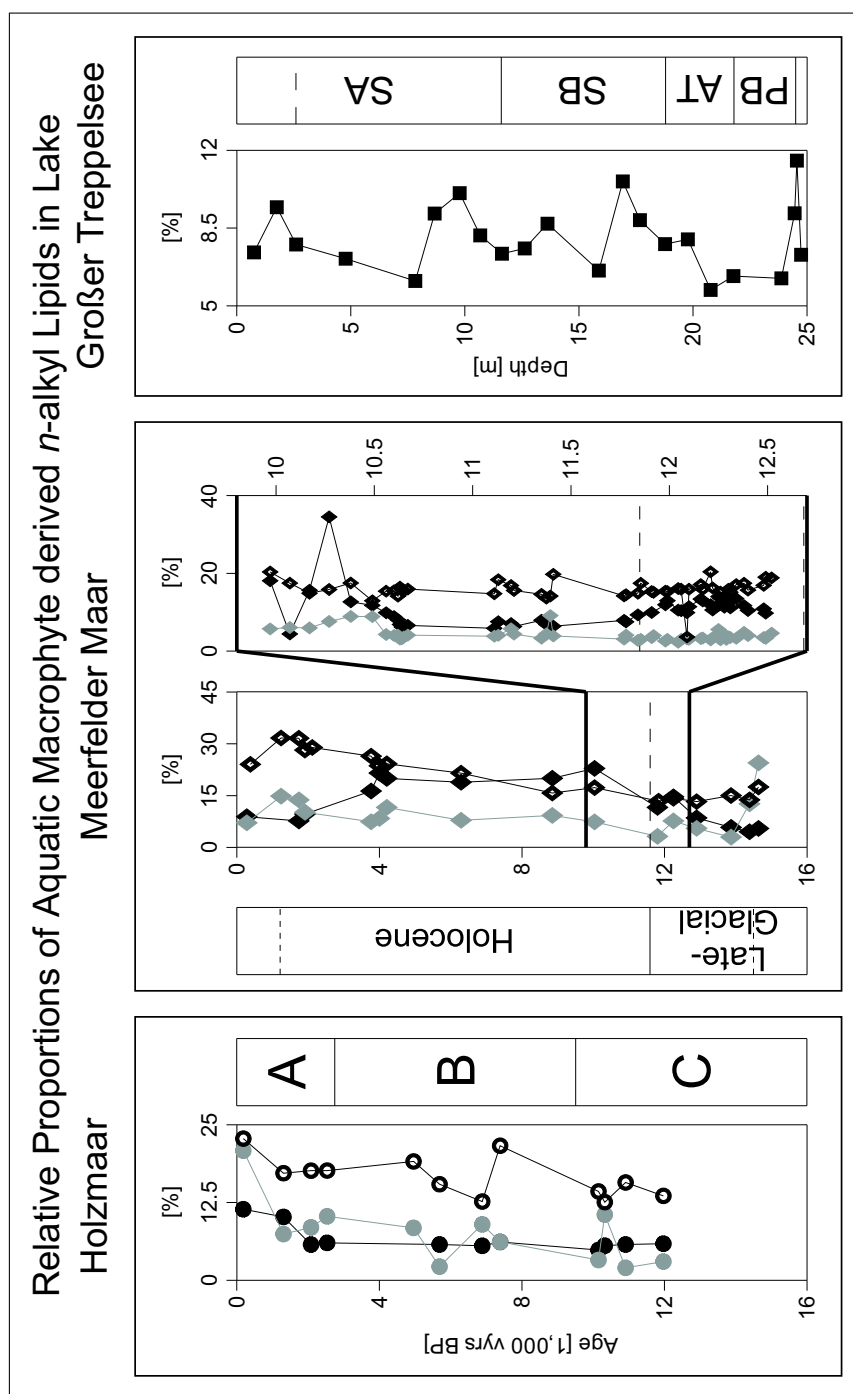


Figure 6.6: Downcore percentages of aquatic macrophyte derived normal chain alkyl lipids; left panel (circles): Lake Holzmaar; middle panel (diamonds): Lake Meerfelder Maar including both, low and high resolution sample sets; right panel (squares): Lake Großer Treppensee; open symbols: *n*-alcohols; grey symbols: *n*-fatty acids; black symbols: *n*-alkanes; percentages are calculated from chain length ranges as listed in Table 6.4 in relation to the whole detected chain length range of the respective *n*-alkyl fraction

Varying between 2 – 35 %, aquatic macrophyte derived proxy-compounds are more abundant. This general feature is valid for all compound specific fractions under investigation. Downcore profiles of mid-chain *n*-alkyl lipids are illustrated in *Fig. 6.6*. In contrast with the previously reported results for the short chain lipid group, the most dominant compound is changing frequently between the three included lipid fractions.

A stable contribution of macrophytes to **Lake Holzmaars** sedimentary sequence during the Younger Dryas and the transition to the early Holocene can be inferred from stable mid chain *n*-alkyl lipid percentages *cf. Fig. 6.6, left panel*. Merely a slight enrichment in *n*-fatty acid abundances points to a temporally enhanced growth of macrophytes at 10,325 vyears BP. The middle Holocene profile section B is further characterised by stable percentages of mid chain *n*-alkanes on a relatively low level of 6 % on average. This is despite the increased *n*-alkane concentrations in sum over the Lateglacial/Holocene transition and the general trend of decreased total *n*-alkane concentrations during the middle Holocene (*cf. Fig. 5.11*). Thus, a constantly low sedimentation of macrophyte derived organic matter can be assumed. Fatty acid distributions on the other hand suggest a remarkable variability: The generally increasing trend with decreasing age is interrupted by a sharp fluctuation between 6,888 – 4,960 vyears BP. The sharply defined maximum abundance of total fatty acids (*cf. Fig. 5.20*) at the lower end of this interval, however, does not affect the relative proportion of mid chain fatty acids. Secondly, the maximum of aquatic macrophyte derived fatty acids is temporally well correlated to a minimum abundance of total fatty acids, clearly indicating reduced organic matter sedimentation under simultaneously increased relevance of macrophytes as sedimentary organic matter sources during the outgoing Lateglacial.

Most marked variations of macrophyte derived *n*-alkyl lipid percentages for Lake Holzmaar were detected during the Subatlantic section A. Percentages of mid chain *n*-fatty acids slightly decrease first to show a rapid increase from 7.7 – 23 % between the two top samples. On a lower level, *n*-alkane distributions confirm this increase. Its onset, however, dates 772 varve years earlier. An increased contribution of aquatic macrophytes to the sedimentary organic matter of Lake Holzmaar can therefore be assumed for most recent sediments.

Generally increased aquatic macrophyte derived *n*-alkyl lipid percentages are obvious from *Fig. 6.6, middle panel* for **Lake Meerfelder Maars** sedimentary sequence. Highest overall *n*-fatty acid percentage out of the mid chain length range was detected for the lowermost sample, that is, however, in opposition to low fatty acid concentrations in sum (*cf. Fig. 5.22*).

With decreasing age, percentages continuously decrease during the Lateglacial until 13,865 vyears BP. The *n*-alkanes show a very slightly increasing trend instead. Simultaneously increasing percentages of mid chain homologues above 13,865 vyears BP towards the Younger Dryas and Holocene indicate an establishment of macrophytes as important organic matter sources. As also reported for short chain homologues, which are typical for algally derived organic matter, a partial maximum of macrophyte contribution to the sedimentary organic matter is obvious during the Younger Dryas period of cooler conditions.

The increasing trend of macrophyte derived proxy compounds persists over the Lateglacial/ Holocene transition until 10,035 vyears BP. From this time, contribution of macrophytes to the sedimentary organic matter remains nearly constant on a comparably high level with the *n*-alkanes showing the highest percentages out of the mid chain homologues of 21 % on average.

A reverse trend can be concluded for sediments above 4,205 vyears BP from decreased mid chain *n*-alkane percentages. Fatty acids contrastingly further indicate macrophytes as important organic matter contributors.

The separate investigation of the Lateglacial/ Holocene transition yields very uniform percentages of aquatic macrophyte derived *n*-alkyl lipids ranging between 2 – 35 %. The maximum values were calculated for *n*-alkanes during the early Holocene exclusively (*Fig. 6.6, middle panel*).

The Younger Dryas period of cooler conditions is characterised by a very stable contribution of macrophyte derived mid chain fatty acids around the average of 4 %. The percentages of corresponding *n*-alkanes are slightly higher. The down-core variation of absolute normal chain fatty acid concentrations in sum as well as percentages of algally derived short chain homologues retrieved a significant bi-partitioning of the Younger Dryas period, indicating changing organic matter supply to the lake sediment. The composition of sedimentary organic matter from macrophytes on the other hand is not influenced by these changing quantities since mid chain *n*-alkyl percentages are very stable during the whole Younger Dryas. A varying dominance of macrophyte growth can merely inferred from slightly de-

creasing mid chain *n*-alkanes above 11,990 vyears BP.

The constant percentages of mid chain homologues persist nearly free of variation over the Younger Dryas/Holocene transition until 10,640 vyears BP. Based on mid chain *n*-alkyl lipid percentages, this date marks a significant increase in macrophyte growth in Lake Meerfelder Maar, confirming the Holocene stage of increased macrophyte abundance as inferred from the lower resolved sample set before.

The sedimentary sequence of **Lake Großer Treppelsees** shows most irregular variations of aquatic macrophyte derived *n*-alkanes between 5 – 12 %, the sharpest observed variation interval (*cf. Fig. 6.6, right panel*).

A local maximum was observed at 24.56 m profile depth during the Younger Dryas. This result gives evidence for a prominent contribution of aquatic macrophytes to the sedimentary organic matter during the Younger Dryas period while previously established forest vegetation was opened due to reduced temperatures (Giesecke, 1999). The overlying sediments of the Preboreal and Atlantic, which have been found to contain high proportions of algally derived organic matter (*cf. Fig 6.5*), are characterised by *vice versa* low percentages of macrophyte derived mid chain homologues in contrast to high absolute concentrations of *n*-alkanes in sum. Enhanced growth of macrophyte populations is obvious during late Atlantic and Subboreal; an outstanding maximum of mid chain *n*-alkanes was measured at 16.93 m profile depth.

After the transition to the Subatlantic, percentages of mid chain *n*-alkanes are rapidly shifted to lower values, indicating a generally decreased influence of this vegetation type to the sedimentary organic matter of Lake Großer Treppelsee as matchingly detected for algae too. The generally lowered percentages are, however, despite a slight increasing trend with decreasing depth, suggesting a continuous reestablishment of macrophytes.

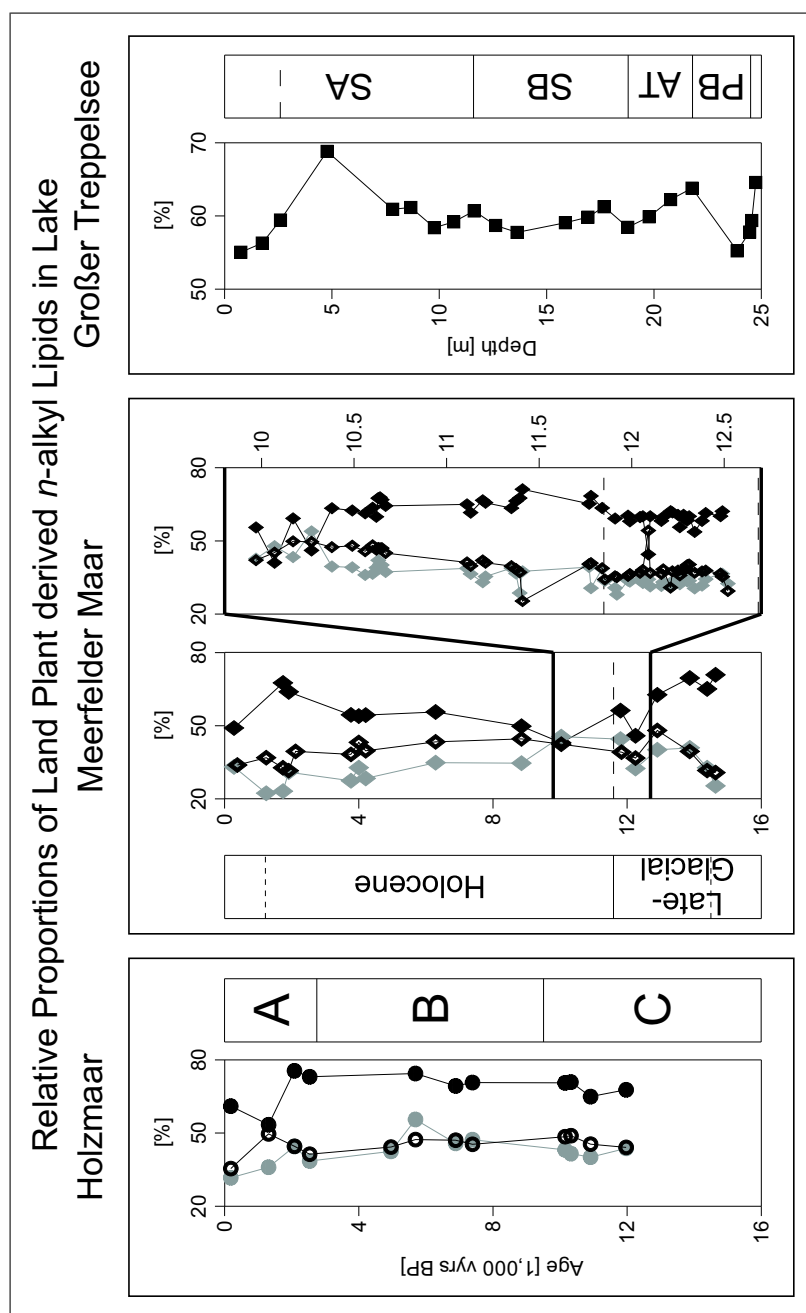


Figure 6.7: Downcore percentages of land plant derived normal chain alkyl lipids; left panel (circles): Lake Holzmaar; middle panel (diamonds): Lake Meerfelder Maar including both, low and high resolution sample sets; right panel (squares): Lake Großer Treppensee; open symbols: *n*-alcohols; grey symbols: *n*-fatty acids; black symbols: *n*-alkanes; percentages are calculated from chain length ranges as listed in *Table 6.4* in relation to the whole detected chain length range of the respective *n*-alkyl fraction

Ranging from 36 – 80 %, land plant derived long chain *n*-alkyl lipids within the chain length ranges as listed in [Table 6.4](#) are the most important subgroup in all three investigated sediment cores by far as obvious from [Fig. 6.7](#). This gives a strong evidence for land plants from catchment areas surrounding the investigated lakes being the most important contributors to the sedimentary organic matter during time. Moreover, the variations of long chain *n*-alkyl lipids in relation to sedimentation age clearly fit to the vegetation development as reconstructed using pollen analysis data by [Litt and Stebich \(1999\)](#); [Litt et al. \(2001\)](#) for the Eifel Maar Lakes and [Giesecke \(1999\)](#) for Lake Großer Treppensee. Vegetation reconstruction of Eifel Maar Lakes was carried out on a different time slice compared to this study, focussed on the Younger Dryas/Holocene transition. An overlap between 14,600 – 11,600 vyears BP, however, ensures a correlation of both results.

The highest overall contribution of land plants among the investigated archives can be assumed for **Lake Holzmaar** from long chain alkyl lipid percentages between 43 – 76 % relative to the respective series of homologues in sum *cf.* [Fig. 6.7, left panel](#).

Beginning within the outgoing Younger Dryas cold period, decreasing long chain *n*-alkane percentages point to reduced land plant vegetation as it would be expected during this geological epoch due to reduced temperatures. The constant long chain *n*-fatty acid content on the other hand indicates a stable contribution from land plant vegetation to the sedimentary organic matter. Their relative contribution to the fatty acid content in sum decreases above 10,910 vyears BP under simultaneous enrichment of long chain *n*-alkanes. An equal contribution of long chain homologues to the respective compound fraction on a very high level (68 – 71 %) is reached closely to the beginning of middle Holocene profile section B at 10,150 vyears BP.

The further very constant and similar percentages of long chain homologues between 67 – 76 % support stable environmental conditions without significant changes in the terrestrial vegetation composition as it was found from sedimentological investigations by [Zolitschka and Negendank \(1998\)](#). The authors additionally argue for a prominent sedimentation of autochthonous organic matter. Contrastingly, a dominant proportion of sedimentary organic matter, derived from terrestrial land plant vegetation must be taken into account based on the high relative abundances of long chain *n*-alkyl lipids. Additionally, a selective degradation of short chain homologues on a high level can be excluded for this lithological

zone due to the continuous annually sediment lamination, reflecting stable and oxygen-poor limnological conditions at the sediment/ water boundary.

Significantly reduced abundances of long chain fatty acids were calculated above 5,690 vyears BP whereas long chain *n*-alkane percentages remain constant until the beginning of the Subatlantic section A, where opposite variations of investigated lipid classes are obvious: Land plant derived fatty acid percentages are continuously increased with decreasing age between 2,536 – 1,311 vyears BP whereas long chain *n*-alkane proportions indicate a dramatic reduction of land plant vegetation in Lake Holzmaars catchment area. A slight enrichment in long chain *n*-alkanes on the other hand was found between the top samples, whereas long chain fatty acids are depleted in the same order of magnitude like reported for *n*-alkanes approximately 700 varve years earlier. Thus, a reduced influence of terrestrial organic matter to the sediment can be assumed for the Subatlantic.

In contrast to the findings for aquatic macrophyte derived *n*-alkyl lipids, long chain homologues are less dominant in the sedimentary sequence of **Lake Meerfelder Maar** in comparison to Lake Holzmaar *cf.* Fig. 6.7, *middle panel*. Beginning at the Lateglacial, rapidly and very strongly increasing long chain fatty acid percentages from 36 % to 76 % demonstrate a fundamental establishment of land plant vegetation in the catchment area of Lake Meerfelder Maar after the last European glaciation. Land plant derived *n*-alkane percentages on the other hand show a slight enrichment between 10,910 – 10,325 vyears BP in contrast to slight depletions in the remaining interval above the Lateglacial and below the Younger Dryas cold period.

Long chain *n*-alkyl lipids of all investigated compound fractions indicate deteriorated climatic conditions for the growth of land plant vegetation during this period itself by significantly decreased rates in relation to the respective series of homologues. A following amelioration of climatic conditions can be derived from increased proportions above 12,250 vyears BP. This date, however, still falls into the the time of the Younger Dryas, extending from 12,680 – 11,600 vyears BP (Brauer *et al.*, 1999a). An increase of land plant vegetation proxies at this time gives another evidence for a partitioning of this geological period as it has been already documented by the variations of the total fatty acid content as well as bulk geochemical parameters.

Exactly mirror-like to the mid chain *n*-alkanes, the percentages of long chain *n*-alkyl lipids further decrease at the Younger Dryas/ early Holocene transition.

That points to a shifting vegetation composition towards more aquatic plants and less dominant terrestrial vegetation of herbs, shrubs and trees. Similar to the mid chain homologues, middle Holocene sediments reflect stable climatic conditions by low variability of the percentages of long chain derivatives where highest proportions were determined for fatty acids. Still mirror-like to the mid chain *n*-alkanes, a slight Holocene maximum of land plants can be derived from the maximum proportion of long chain homologues at 6,290 vyears BP in direct opposition to the slightly reduced mid chain percentage at the same time.

More unsteady variations were furthermore found for the youngest sediments during the Late Holocene/Subatlantic. Lowered long chain fatty acid proportions above 3,765 vyears BP might reflect less prominent sedimentation of land plant derived organic matter whereas long chain *n*-alkane percentages on the other hand still increase until 1,910 vyears BP.

More detailed reconstruction of the terrestrial vegetation development can be derived from the second sample set of Lake Meerfelder Maar. Closely scattering long chain *n*-alkyl lipid proportions are obvious within the Younger Dryas period. A slight enrichment in long chain *n*-fatty acid proportions above 12,400 vyears BP could be interpreted with a moderately growing terrestrial vegetation. This stage persists until 12,260 vyears BP before values are abruptly reduced from 74 – 57 % within only 40 varve years. The continuously increasing importance of land plant vegetation can be derived from increasing proportions of long chain *n*-alkyl lipids above 12,090 vyears BP, still within the Younger Dryas period. The absolute varve age of this onset, however, differs for the investigated compound classes: Long chain fatty acids show a prominent excursion to higher percentages just above this date, that will be short-term negated again. Simultaneously increased proportions for all compound fractions were detected above 11,920 vyears BP that is still below the upper time-border of the Younger Dryas period.

Early Holocene variations of land plant derived long chain *n*-alkyl percentages show low variation width with long chain *n*-fatty acids having the highest relative proportions. In addition, changes in percentages are contrary for the investigated compound fractions up to 10,380 vyears BP. Very rapid fluctuations in long chain *n*-alkane percentages above this date could explain an unstable terrestrial vegetation contribution to the sedimentary organic matter. Finally, none of the lipid classes reflects prominently increased land plant derived organic matter sedimentation as it would be expected from a substantial amelioration of climatic

conditions after the Younger Dryas cold period. This remark is valid for land plant vegetation forms in sum, a more detailed differentiation into different plant groups will follow below.

More uniform and closely scattering variations of long chain *n*-alkanes between 55 – 69 % are obvious for Lake Großer Treppensee from *Fig. 6.7*.

A reduction of terrestrial vegetation during the Younger Dryas and Preboreal can be inferred from less dominant long chain homologues in good agreement with pollen data from [Giesecke \(1999\)](#). Their percentages become suddenly increased further in agreement with the cited author with the beginning of the Atlantic. A moderate reduction of land plant derived sedimentary organic matter point to slightly less important terrestrial vegetation during this period itself. The beginning of the Subboreal marks another sharp increase, that is, however, further reduced with decreasing age. The highest enrichment by amount between late Subatlantic stage I points to the most prominent establishment of land plant vegetation in Lake Großer Treppensees catchment area but a peak of comparable significance is not obvious from pollen data during this time. Subatlantic stage II is finally characterised by diminishing long chain alkyl proportions to lowest overall values.

Varying proportions of homologues in the long chain length range are an additional useful tool to specify contributing land plant vegetation in more detail. Two approaches are known from recent literature:

- [Brincat *et al.* \(2000\)](#) used depth variations in relative abundances of C₂₇- and C₃₁ *n*-alkanes of a Lake Baikal, southeastern Siberia, sedimentary sequence to distinguish between herbaceous vegetation during the Lateglacial on the one hand and forest vegetation during the Holocene on the other hand. Consistent with pollen data from the same archive, dominant C₂₇ percentages represent a forest vegetation, whereas higher C₃₁ proportions point to a herbaceous vegetation type as a prominent organic matter source.
- [Schwark *et al.* \(2002\)](#) used a ternary plot of relative C₂₇-, C₂₉- and C₃₁ *n*-alkane concentrations to differentiate changes in land plant derived organic matter input to sediments of Lake Steisslingen, southwestern Germany. Especially concentrations of the C₂₇ *n*-alkane have been found to be well correlated to the betula population as reconstructed from pollen data.

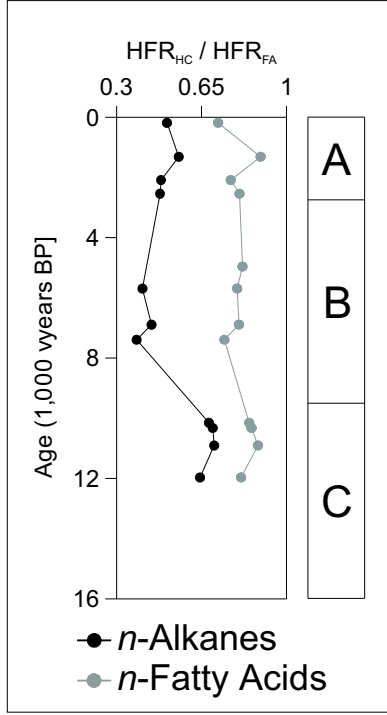


Figure 6.8: Downcore variations of HFR_{HC} (black symbols) and HFR_{FA} (grey symbols) for Lake Holzmaars sedimentary sequence

Both, the C_{27} vs. C_{31} n -alkane ratios and ternary plots of long chain n -alkane and n -fatty acid percentages are illustrated in *Figs. 6.8 – 6.14* for all investigated archives separately. The original calculation of the long chain n -alkane ratio was, however, modified to the Herbaceous vs. Forest Ratio for Hydrocarbons (HFR_{HC}) as given in *Equation 6.1* in order to normalise calculated data on a 0-1 scale. Based on the commonly accepted genesis of n -alkanes from corresponding fatty acids with one more carbon atom, a similar ratio is suggested for n -fatty acids as given in *Equation 6.2* (HFR_{FA}); its relation to the n -alkane ratio will be discussed in the following. The ternary plot of long chain n -alkanes as used by [Schwark et al. \(2002\)](#) was additionally adopted to the long chain fatty acids by increasing the respective carbon numbers by one.

$$HFR_{HC} = \frac{C_{27}}{C_{27} + C_{31}} \quad (6.1)$$

$$HFR_{FA} = \frac{C_{28}}{C_{28} + C_{32}} \quad (6.2)$$

Downcore variations of the HFR_{HC} and HFR_{FA} as well as ternary plots of long chain n -alkanes and n -fatty acids for **Lake Holzmaar** are illustrated in *Figs. 6.8*

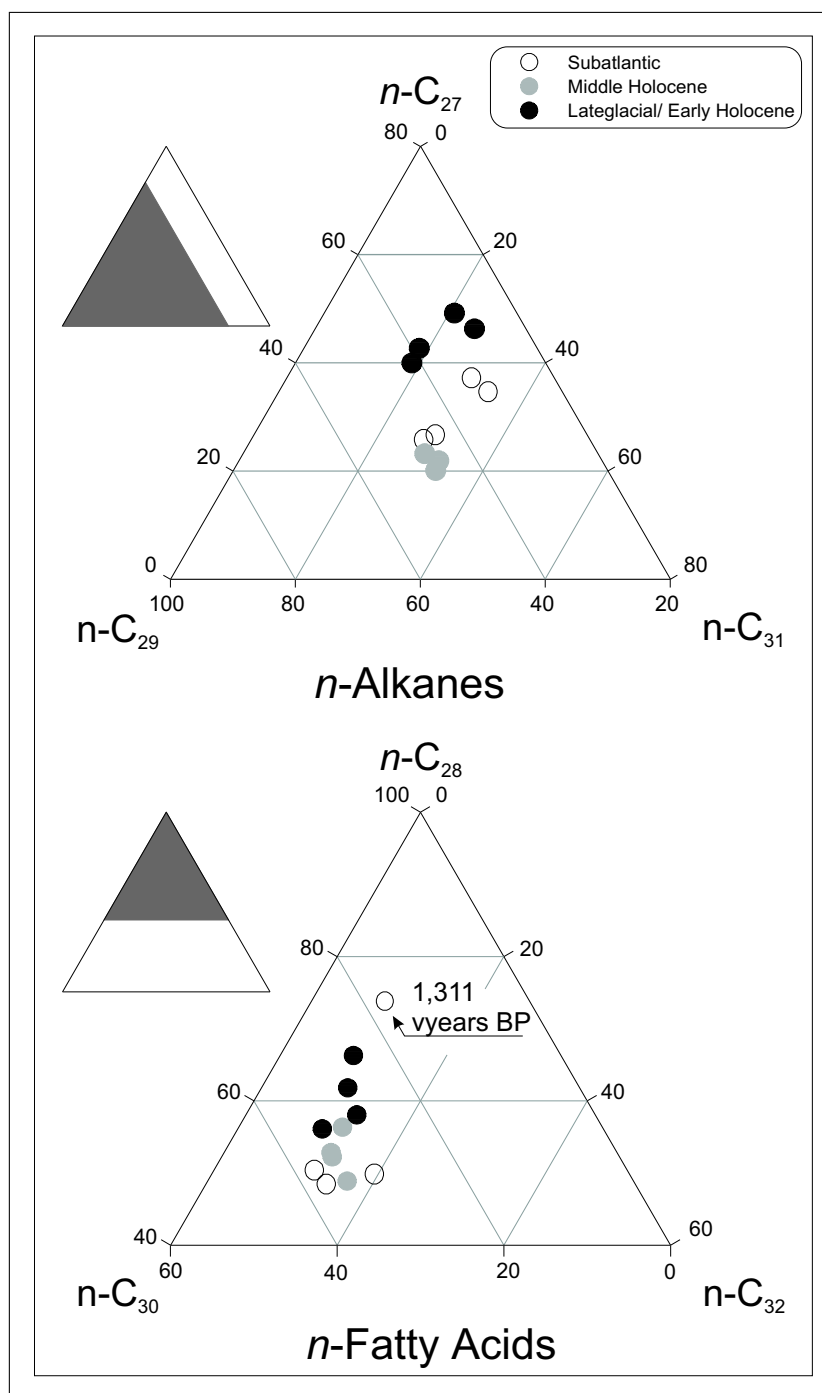


Figure 6.9: Ternary diagrams of long chain *n*-alkanes and *n*-fatty acids of Lake Holzmaar; open symbols: Subatlantic; grey symbols: middle Holocene; black symbols: Lateglacial to early Holocene; the upper left schematics illustrate the plot areas selected for magnification out of an usual ternary plot with axes on a 0-100 scale

and 6.9, respectively. Higher ratios were generally determined for HFR_{FA} whereas variations of both data are well correlated in relation to age. The ternary plot of long chain *n*-alkanes visualises a good separation of integrated geological ages whereas a less specific separation becomes obvious from the respective long chain fatty acids.

The Younger Dryas cold period is included with the lowermost sample being characterised by relatively high ratios of HFR_{HC} and HFR_{FA} . With further decreasing ages, both ratios become increased during the early Holocene, indicating an increased establishment of forest vegetation due to the ameliorated climate in comparison to relatively cold temperatures during the underlying Younger Dryas. With the beginning of the middle Holocene section B, HFR_{HC} and HFR_{FA} become slightly decreased. Also a clear separation of both sample groups is obvious from the ternary diagram of *n*-alkanes. Compared to the older Lateglacial/early Holocene, middle Holocene samples are significantly enriched in C_{31} *n*-alkane and depleted in C_{27} *n*-alkane proportion whereas less specific variations for the C_{29} *n*-alkane proportion relative to this group of long chain homologues in sum are obvious. Even if the separation between the stratigraphic sections is weaker in the case of long chain *n*-fatty acids, these compounds show comparably reduced proportions of the *n*- C_{28} homologue whereas the proportions the *n*- C_{32} fatty acid are relatively uniform throughout the whole sedimentary sequence of Lake Holzmaar. With further decreasing age, the investigated middle Holocene core section is characterised by stable HFR_{HC} and HFR_{FA} values, confirming the stable environment during this geological era.

More characteristic variations are obvious for the youngest Subatlantic profile section. Corresponding samples plot between the areas of older samples in the ternary plot of *n*-alkanes with widest variations for individual samples. Both, the HFR_{HC} and HFR_{FA} synchronously indicate a maximum establishment of forest vegetation during the Subatlantic at 1,311 vyears BP, whereas a clear reduction was found towards the youngest sample. This finding is confirmed by the ternary plot of long chain fatty acids, where the highest overall proportion of the *n*- C_{28} homologue was found at 1,311 vyears BP whereas the remaining Subatlantic samples show lowest overall percentages of that homologue (*cf.* Fig. 6.9). Beside changing environmental or climatic conditions, however, a human influence must be taken into account for this reduction of tree vegetation during the youngest times. Haaren (1992) for example report on homogeneous farming in the Eifel

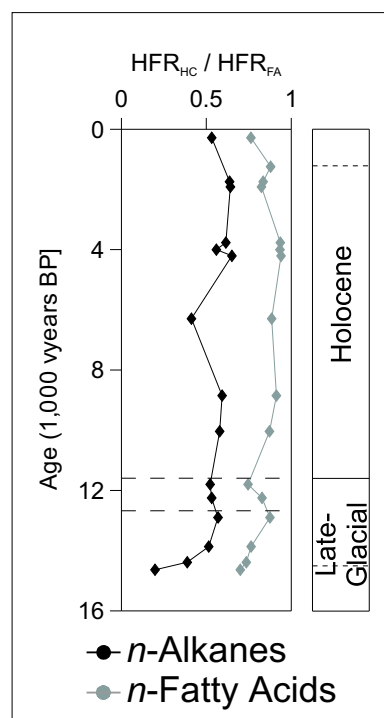


Figure 6.10: Downcore variations of HFR_{HC} (black symbols) and HFR_{FA} (grey symbols) for Lake Meerfelder Maar sedimentary sequence

region from about 1,400 A.D. until up to the 20th century. A major deforestation, however, was excluded due to the missing of settlements in the vicinity of Lake Holzmaar.

Also generally higher HFR_{FA} compared to HFR_{HC} were calculated for **Lake Meerfelder Maar** during the Lateglacial and the Holocene as illustrated in *Fig. 6.10*. Both parameters strongly increase from the lowermost sample during Bølling and Allerød until the beginning of the Younger Dryas period with most significant enrichments in HFR_{HC} from 0.2-0.6. Consistently, a major depletion in C_{31} and enrichments in C_{27} n -alkane percentages with decreasing varve age are obvious from the ternary plot of long chain n -alkanes (*cf. Fig. 6.11*). A very similar behavior was consistently observed for the respective homologues out of the n -fatty acids, showing the Lateglacial maximum abundance of the n -octacosanoic acid with the beginning of the Younger Dryas at 12,900 vyears BP. This clearly indicates a change in the composition of terrestrial organic matter sources from a tundra-like vegetation towards an establishment of forests during these initial warming periods.

The lowering in HFR_{FA} and, less significantly, HFR_{HC} ratios during the Younger

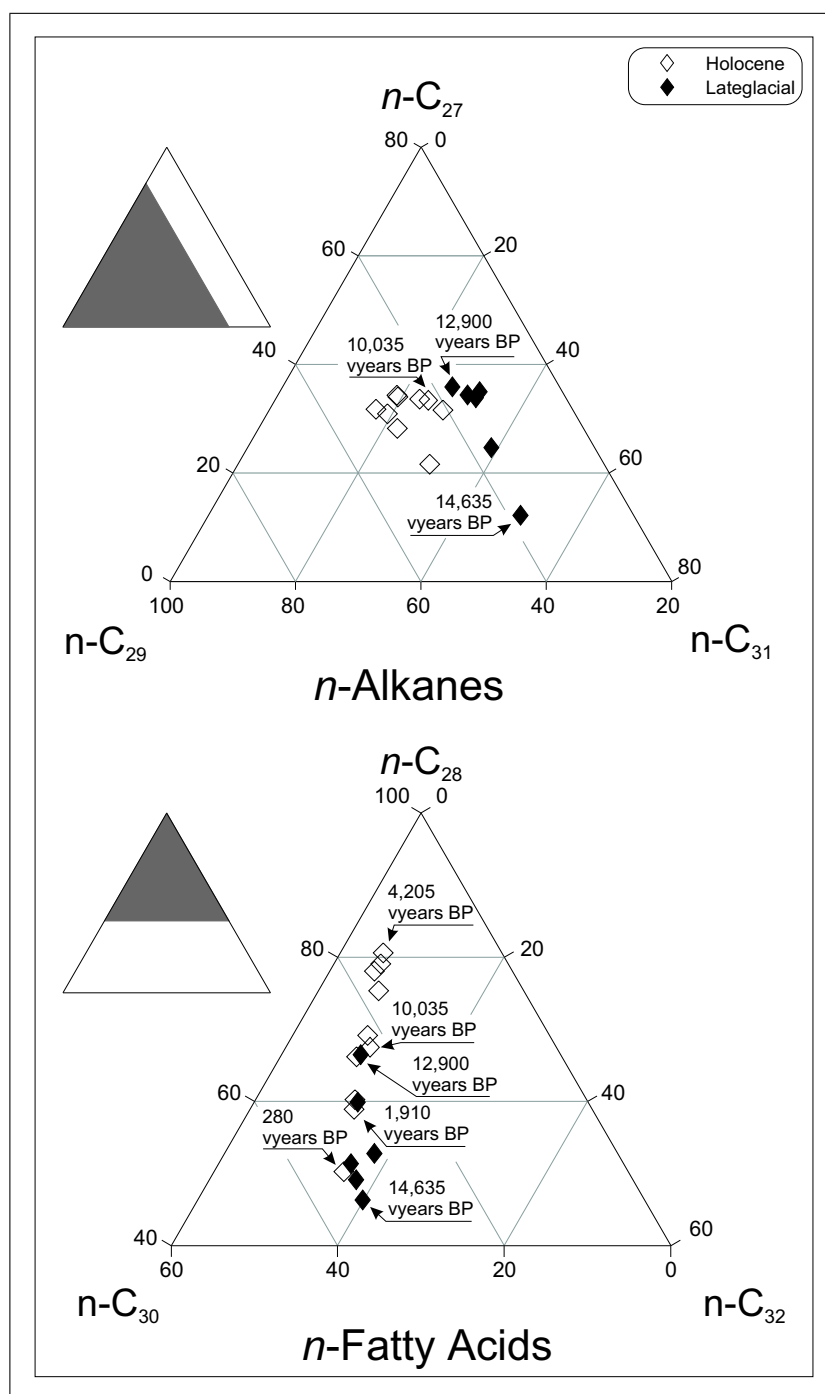


Figure 6.11: Ternary diagrams of long chain n -alkanes and n -fatty acids of Lake Meerfelder Maar; open symbols: Holocene; black symbols: Lateglacial; the upper left schematics illustrate the plot areas selected for magnification out of an usual ternary plot with axes on a 0-100 scale

Dryas period gives evidence for lowered temperatures, resulting in less dominant tree growth in the catchment areas and at least a partial reestablishment of open grass- and shrub vegetation forms.

A following climate amelioration can be derived from increased ratios simultaneously to the beginning of the early Holocene above 11,800 vyears BP. This result is also supported by the good separation of Holocene samples from earlier ones in the ternary plots of long chain homologues. In contrast to the establishment of forest vegetation in general after the Lateglacial, indicated by significantly increased C_{27} *n*-alkane percentages, a major enrichment in relative abundances of the C_{29} *n*-alkane characterises the Younger Dryas/early Holocene transition. Following Schwark *et al.* (2002), this points to an increased growth of conifers, whereas *n*-alkane distributions originating from deciduous tree species like *Betula* maximise at the C_{27} *n*-alkane.

During the Holocene, relatively stable values for both parameters on a high level were calculated, indicating stable climatic conditions. A significant minimum of HFR_{HC} is obvious at 6,290 vyears BP, whereas HFR_{FA} values initially do not support at least a major reduction of forest establishment in Lake Meerfelder Maars catchment. More clearly, the ternary plot of long chain *n*-fatty acids yields a remarkable variability of the relative proportions, especially of the C_{28} and C_{32} homologues during the Holocene. Accordingly, relatively high proportions of *n*-octacosanoic acid between 70 – 80 % were determined for earlier Holocene samples between 10,035 – 3,765 vyears BP.

A substantial loss of forest vegetation forms is finally retrieved from synchronously lowered HFR_{HC} and HFR_{FA} values during the uppermost 1,127 varve years. In agreement, the ternary plot of long chain fatty acids yields low relative abundances of the C_{28} acid between 50 – 66 % with the lowest value for the top sample and *vice versa* increased abundances of the C_{30} acid, indicating a reduction of forest vegetation forms above 1,910 vyears BP. This thesis is further supported by relatively high proportions of the heaviest fatty acid homologue, which is believed to represent herbaceous vegetation, again in the top sequence above 1,910 vyears BP. As already reported for Lake Holzmaar, a human influence seems to be a valid explanation since Haaren (1992) reports a major deforestation around Lake Meerfelder Maar. Note in this context, that two villages are situated directly in the alluvial zone of Lake Meerfelder Maar (*cf.* Section 3.1.2 and Fig. 3.5) whereas settlements around other maar lakes are often outside the catchment areas. Ad-

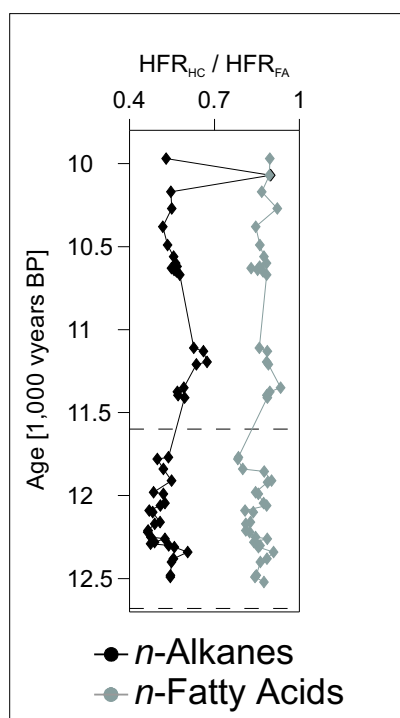


Figure 6.12: Downcore variations of HFR_{HC} (black symbols) and HFR_{FA} (grey symbols) for the high resolution sequence of Lake Meerfelder Maar

ditionally, the absence of a continuous lamination during the uppermost profile section (*cf.* dashed horizontal lines in stratigraphic column of *Fig. 6.10*) points to enhanced bioturbation due to oxygen supply to the water/sediment surface. This causes a worsening in organic matter preservation in this section.

More clearly as the variations of land plant derived *n*-alkyl lipids during the Younger Dryas and the transition to the Holocene in general, the HFR_{FA} - and, more significantly, the HFR_{HC} ratio show the previously already introduced bipartitioning of the Younger Dryas period (*Fig. 6.12*). Especially the sharp decrease of the HFR_{HC} above 12,340 vyears BP indicates a rapid change in the composition of terrestrial organic matter contributors to more herbaceous vegetation forms. Accordingly, the ternary plots (*Fig. 6.13*) well separate between the early- and late Younger Dryas, where samples from the latter are characterised by higher C_{31} and lower C_{29} *n*-alkane percentages. This and the further continuous increase of the HFR_{HC} as well as the high variability of relative C_{27} *n*-alkane proportions during the late Younger Dryas (above 12,210 vyears BP) and the early Holocene indicate a substantial change in climatic conditions in addition to the changed course of the brook Meerbach as proposed by Brauer *et al.* (1999a), flow-

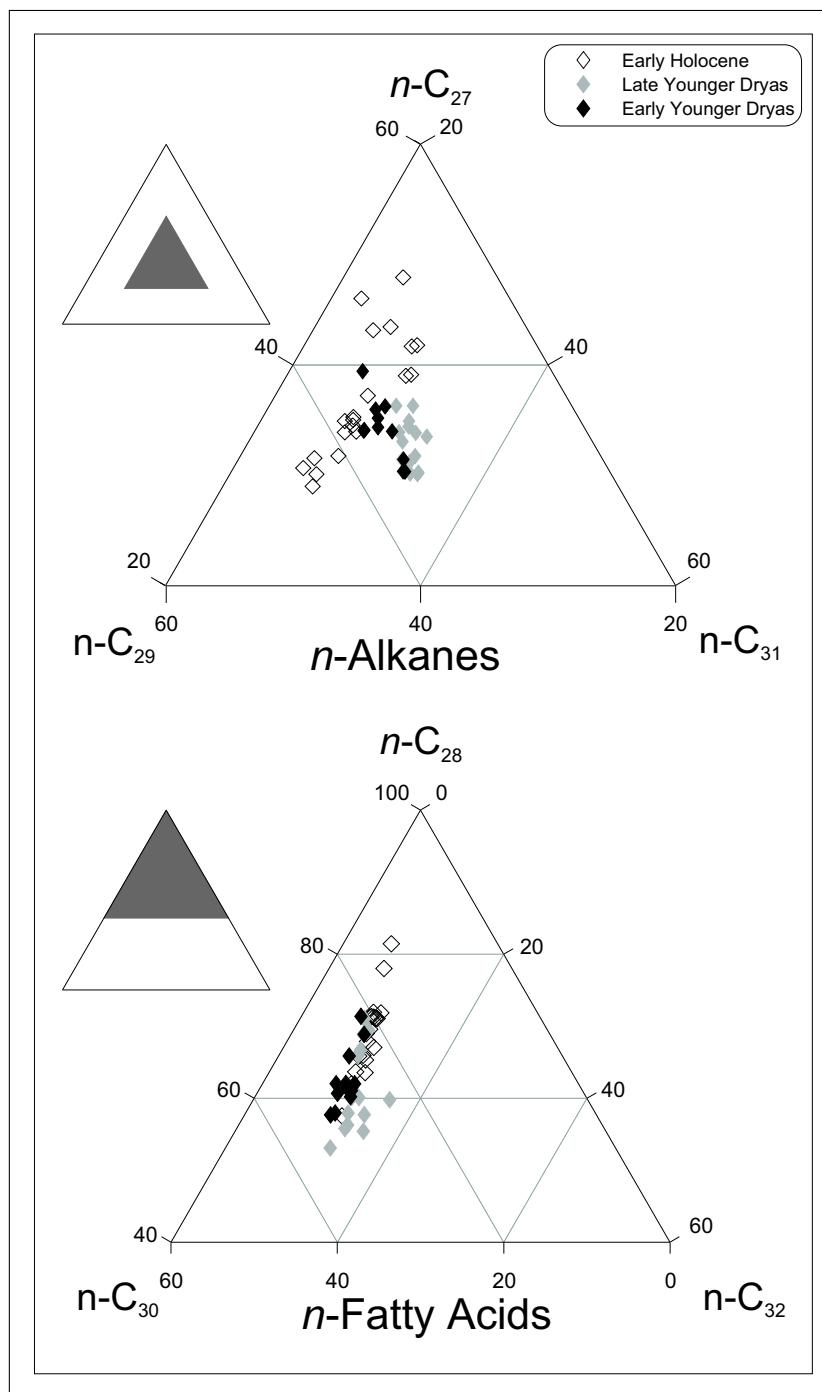


Figure 6.13: Ternary diagrams of long chain *n*-alkanes and *n*-fatty acids for the high resolution sequence of Lake Meerfelder Maar; open symbols: early Holocene; grey symbols: late Younger Dryas; black symbols: early Younger Dryas; the upper left schematics illustrate the plot areas selected for magnification out of an usual ternary plot with axes on a 0-100 scale; note, that one *n*-alkane data point was omitted from illustration due to plotting outside the magnification area

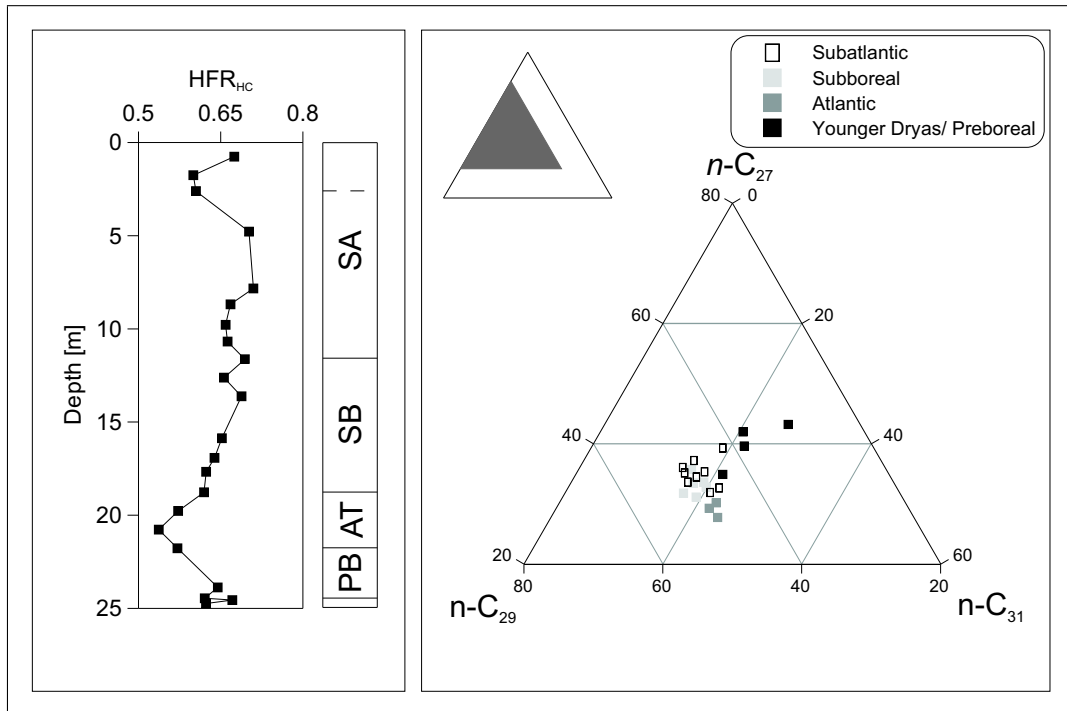


Figure 6.14: Downcore variations of HFR_{HC} (left panel) and ternary plot of long chain n -alkanes (right panel) for the Lake Großer Treppensee sedimentary sequence; open symbols: Subatlantic; light grey symbols: Subboreal; dark grey symbols: Atlantic; black symbols: Younger Dryas/Preboreal; the upper left schematic illustrates the plot area selected for magnification out of an usual ternary plot with axes on a 0-100 scale)

ing through Lake Meerfelder Maar only during the late Younger Dryas. Opposite trends of both HFR ratios were retrieved during the early Holocene. After matchingly increasing significance of tree *vs.* herbaceous vegetation types, the HFR_{FA} indicates a reduced dominance above 11,350 vyears BP, whereas HFR_{HC} ratios further increase. A *vice versa* trend is obvious above 11,130 vyears BP.

Weakest variations between 0.5-0.7 were calculated for the HFR_{HC} of the Lake Großer Treppensee profile. Also the ternary plot of relative long chain n -alkane percentages shows weaker variations of the included samples; geological ages are moderately separated (*cf.* Fig. 6.14). Best marked, the oldest Younger Dryas/Preboreal samples are separated from the remaining younger sample groups. Included stratigraphic sections, however, can be well recognised from the downcore plot of HFR_{HC} too:

Relatively high HFR_{HC} ratios were calculated for the oldest samples, probably including the late Younger Dryas and Preboreal. Overlying Atlantic samples are

characterised by slightly reduced ratios, indicating a less significant change in the terrestrial vegetation composition towards herbs and shrubs. More significantly, the ternary plot of long chain *n*-alkanes shows a shift between both sample groups. Compared to the older Younger Dryas/Preboreal, overlying Atlantic samples are characterised by decreased relative C₂₇- and *vice versa* increased C₂₉ *n*-alkane abundances, whereas the relative contribution of C₃₁ *n*-alkane remains nearly constant. As recently deduced by Schwark *et al.* (2002), this could be interpreted with a constant ratio between forest *vs.* herbaceous vegetation forms. The changed predominance of the two shorter chain length homologues, however, points to more enhanced coverage with conifer-type trees and reduced growth of betula species in Lake Großer Treppelsees catchment during the Atlantic in comparison to the older Younger Dryas/Preboreal.

Slightly increasing HFR_{HC} during the Subboreal indicates a further change in terrestrial vegetation composition, benefiting forest vegetation type *vs.* reduced coverage of herbs and shrubs. The interpretation of the *n*-alkane ternary plot yields no additional information due to nearly unchanged C₂₉ *n*-alkane percentages. Thus, increasing betula-type seems to be the most marked feature during the Subboreal.

A short-term reversal in the HFR_{HC} was finally observed closely to the Subatlantic I/II transition after no significant change is obvious across the Subboreal/Subatlantic boundary. Also no specific change in the long chain *n*-alkane composition could be retrieved from the ternary diagram. This indicates a stable terrestrial vegetation composition under relatively constant environmental and climatic conditions in the catchment area of Lake Großer Treppelsee.

Additional information about the sources of sedimentary organic matter can be retrieved from the *n*-alkane isotope composition that was determined for selected samples of **Lake Meerfelder Maar** as presented in *Chapter 5.2.1.4*.

The carbon isotopic composition of plants is primarily controlled by the composition of carbon dioxide used for photosynthesis while two fractionating processes have to be distinguished: (i) the fractionation during the reversible uptake and diffusion of CO₂ into the plant and (ii) the fractionation during the photosynthesis itself. Photosynthesising plants can be subdivided into two groups: About 90 % of the present-day plants use the so called C₃ pathway, where *ribulose biphosphate carboxylase oxygenase* reacts with carbon dioxide. The carbon is subsequently reduced to form carbohydrates and the initial enzyme is recovered. In general, $\delta^{13}\text{C}$

isotope fractionations ranging from -20 ‰ to -30 ‰ are expected for this kind of plants. Smaller isotope fractionation is expected from so called C₄ plants (e.g. several grasses), which use *phosphoenol pyruvate carboxylase* for carbon fixation (Hoefs, 1997). Under unlimited carbon dioxide supply, the fractionation during enzymatic carbon fixation is the controlling factor, resulting in $\delta^{13}\text{C}$ ratios between -17 ‰ to -40 ‰ (O'Leary, 1981). A third group of plants is characterised by the *Crassulacean acid metabolism (CAM)* which can use both the C₃ and C₄ pathway.

As summarised by van der Meer *et al.* (2001b), other carbon fixation cycles are used by various bacteria. Accordingly, sulfur- and other bacteria use the reversed tricarboxylic acid cycle for the fixation of carbon dioxide, anaerobic bacteria and archaea were reported to use the acetyl-CoA pathway in several modifications and the 3-hydroxypropionate pathway was finally proposed to function in *Chloroflexus aurantiacus*, a green non-sulfur bacterium, and in autotrophic Crenarchaeota (Menendez *et al.*, 1999). In contrast to the relatively strong ^{13}C depletion during photosynthesis as described above, carbon fixation using these pathways results in more moderate ^{13}C depletions. van der Meer *et al.* (2001b,a) summarised $\delta^{13}\text{C}$ depletions between 2-14 ‰ in comparison to the source carbon during the reversed tricarboxylic acid cycle and the 3-hydroxypropionate pathway in contrast to 20-30 ‰ in the case of the more common C₃, C₄ pathways. The authors further reviewed differences in carbon isotope effects between bulk cell material and lipids. In contrast to the previously reported depletion in ^{13}C of lipids during the C₃, C₄ pathways, the tricarboxylic acid cycle was reported to be characterised by an ^{13}C enrichment of straight chain lipids relative to the bulk cell material (van der Meer *et al.*, 1998).

In addition to these biochemical isotope effects, carbon isotope fractionation also occurs due to the inorganic CO_{2(g)}, CO_{2(aq)}, H₂CO₃, HCO₃⁻ and CO₃²⁻ equilibria of the global carbon cycle prior to the autotrophic fixation of carbon dioxide. Highest fractionation by amount is known between CO_{2(aq)} and HCO₃⁻ (Hoefs, 1997).

In the case of strictly aquatic carbon fixation, the most common source is dissolved carbon dioxide. Assuming an unlimited carbon dioxide supply to the water body (equilibrium), carbon isotope fractionation between atmosphere and water can be neglected (Mook *et al.*, 1974). Thus, carbon fixated by algae is expected to be

undistinguishable from that fixated by C₃ plants.

A chain length based source assignment of *n*-alkanes was presented above. Considering isotope composition of the respective homologues, however, causes difficulties in the case of aquatic plants since emergent and floating species use different carbon pools for photosynthesis. Whereas emergent macrophytes can use atmospheric CO₂, submerged macrophytes do not have access to this pool and behave more similar to algae. Potential carbon sources are ambient CO₂, biogenic CO₂, volcanic CO₂, co-methanogenic CO₂ and bicarbonate from rock weathering (Ficken *et al.*, 1998b), where the latter source seems to be negligible due to the low TIC content in the profile of Lake Meerfelder Maar. Thus, the measured $\delta^{13}\text{C}$ composition of aquatic plant and algally derived biomarkers is influenced by both the composition of source carbon and biotic fractionation (Keeley and Sandquist, 1992). Additionally, *n*-alkanes assigned to plant groups as source organisms are still derived from a variety of different species, producing the same homologues. Thus, the measured isotope composition is a mixture from contributing species, probably contributing with different carbon isotope signatures. Moreover, single leaves may show a wide range of isotope values (Ficken *et al.*, 1998a, and citations therein).

Considering the compound specific isotope data of the Lake Meerfelder Maar profile as introduced in *Section 5.2.1.4*, no specific variations of the $\delta^{13}\text{C}$ values are obvious for the longer chain length range of odd numbered *n*-alkanes (C₂₇–C₃₃). Single values are between -29.8 to -35.3 ‰ within the expected range with no significant age related variations. A single exception was detected for the *n*-C₂₇ alkane at 1,910 vyears BP, showing a slightly lighter $\delta^{13}\text{C}$ value. Thus, an assignment of these data to changing paleoenvironmental and/or paleoclimatic conditions remains difficult. This general behavior of compound specific isotope composition was also determined for the samples out of the profile section with higher temporal resolution, merely the two heaviest homologues (C₃₁, C₃₃) are slightly more depleted in ^{13}C at 12,160 and 10,640 vyears BP.

Clearly in opposition to these findings, the lighter *n*-alkanes show a stage of drastic depletion in ^{13}C between 8,850 – 4,000 vyears BP with an average of -37 ‰ for the C₂₁ – C₂₅ *n*-alkanes and lowest overall values down to -46 ‰ for *n*-henicosane. Additionally, the stage of light isotopic values of *n*-henicosane is temporally well correlated to the maximum abundance of the same compound. Despite no com-

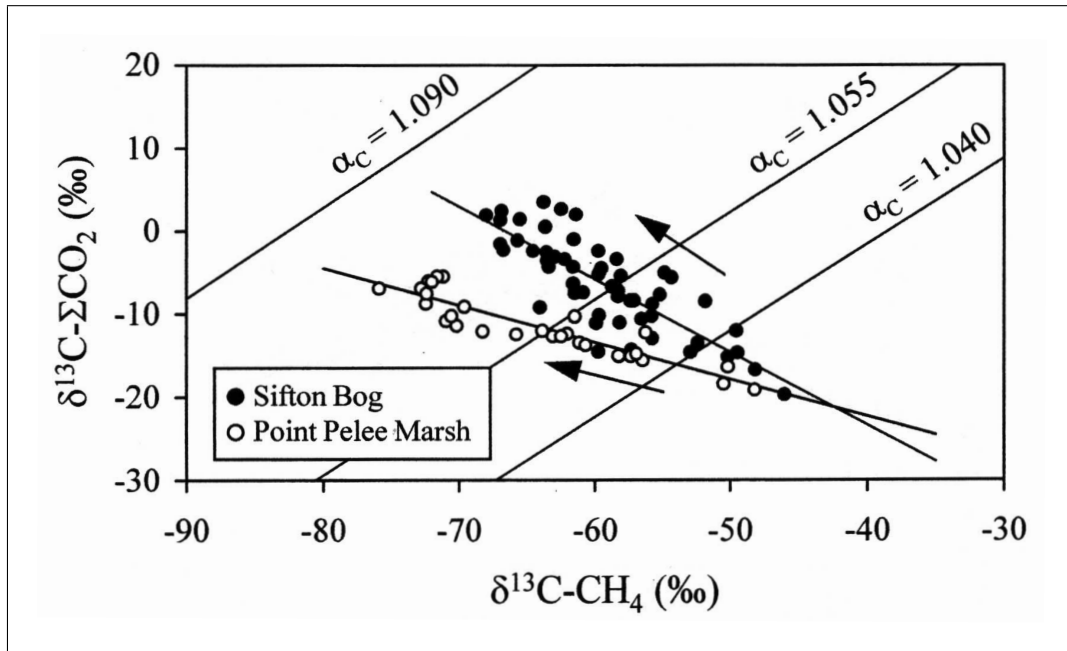
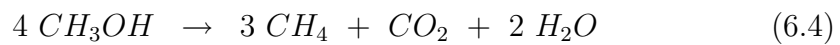
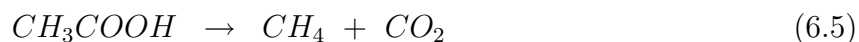


Figure 6.15: Type I relation between CH_4 and CO_2 stable carbon isotopic composition in anaerobic environments after [Hornibrook et al. \(2000\)](#)

parable data showing that kind of ^{13}C depletion being available, these results indicate a significant change in the composition of the organic matter contributing community.

The only source for carbon being depleted in ^{13}C as found for the C_{21} *n*-alkane in Lake Meerfelder Maar is microbial methanogenesis, the last step of anoxic organic matter degradation that occurs in the absence of alternative electron acceptors like nitrate or sulfate. [Hoefs \(1997\)](#) recognised two pathways: CO_2 reduction occurs preferentially in sulfate-free marine sediments, whereas fermentation e.g. of acetate is more common in freshwater sediments. It should be noted that this is a general observation and that both processes can occur in each environment. The gross-equations for methanogenesis using carbon dioxide as well as methanol and acetic acid, that were formed during earlier stages of anoxic organic matter degradation, are given below:





A general prerequisite for the fermentation pathway to take place is the absence of oxygen to enable the growth of methanogenic bacteria. The elevated preservation state of the sedimentary organic matter of Lake Meerfelder Maar between 8,850 – 4,000 vyears BP as figured out using e.g. pristane/ phytane ratios (*cf. Section 6.1.3, Fig. 6.3*) as well as the preservation of annually separated varve layers give evidence that such conditions can be assumed during that time. In either case of methanogenesis, methane is extremely depleted in ^{13}C ; -110 ‰ to -60 ‰ are known for marine sediments (CO_2 reduction) as well as -65 ‰ to -50 ‰ for freshwater sediments (acetate fermentation) (Whiticar and Faber, 1986).

Additionally, the enzymatic fermentation pathway also yields carbon dioxide (*cf. Equations 6.4 and 6.5*). Hornibrook *et al.* (2000) investigated the relations between the stable carbon isotopic compositions of methane and carbon dioxide in two anaerobic environments, the Stifton Bog and the Point Pelee Marsh, both situated in southwestern Ontario, Canada. As a result, $\delta^{13}\text{C}\text{-CH}_4$ values decrease whereas $\delta^{13}\text{C}\text{-CO}_2$ values *vice versa* increase with increasing sample depth (*cf. Fig. 6.15*). This observation was attributed to a transition from aceticlastic methanogenesis to a predominance of the CO_2 reduction pathway or methanogenesis using autotrophically formed acetate. A second type of relation being characterised by increasing values of both $\delta^{13}\text{C}\text{-CH}_4$ and $\delta^{13}\text{C}\text{-CO}_2$ with increasing depth was detected in wetland soils due to an early dependence of methanogens on porewater CO_2 (*cf. Fig. 6.16*).

Even if the data set acquired during the present study does not allow a more detailed assessment on the methanogenesis that obviously took place in Lake Meerfelder Maar, it can be concluded from the study cited above that $\delta^{13}\text{C}\text{-CO}_2$ values in anaerobic environments are usually higher than those of methane; Hornibrook *et al.* (2000) obtained values between -75.9 to -46.0 ‰ for $\delta^{13}\text{C}\text{-CH}_4$ and -19.7 to -1.0 ‰ for $\delta^{13}\text{C}\text{-CO}_2$. Similar results were previously published by Whiticar (1999) who also found the discrimination between $\delta^{13}\text{C}\text{-CH}_4$ and $\delta^{13}\text{C}\text{-CO}_2$ to be relatively constant. Assuming similar conditions in Lake Meerfelder Maar, a subsequent utilisation of methanogenesis derived carbon by plants using the C_3 or C_4 pathway would result in $\delta^{13}\text{C}$ values further decreased by 20-25 ‰ due to the ^{12}C preference of these processes and thus be a potential explanation for the mea-

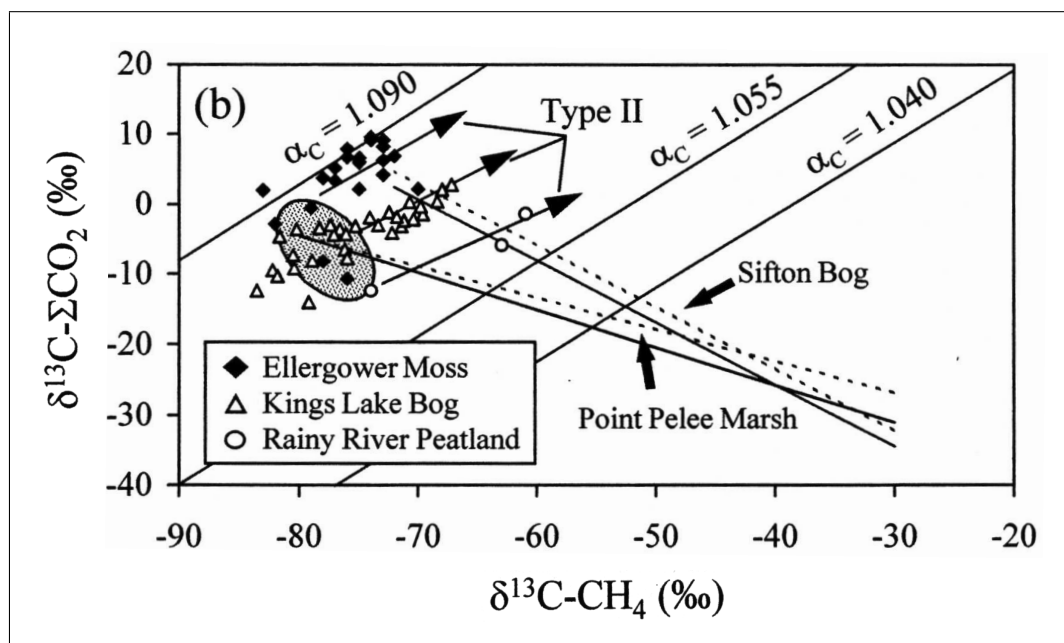


Figure 6.16: Type II relation between CH_4 and CO_2 stable carbon isotopic composition in wetland soils after [Hornibrook et al. \(2000\)](#)

sured light isotopic composition of *n*-henicosane. A carbon fixation using the less common bacterial pathways as described above on the other hand seems to have not occurred due to the weaker isotope effects that had to be expected otherwise. Thus, the assignment of *n*-henicosane to aquatic macrophytes as organic matter source seems to be the most reasonable explanation. No evidence was found from the present literature indicating aquatic algae or photosynthetic bacteria being a source of *n*-henicosane. This is also in consistency with the present study, where no age related similarities between *n*-henicosane concentrations on the one hand and concentrations of shorter chain length homologues on the other hand were observed (*cf.* [Fig. 6.4](#)). At least a weak similarity of *n*-henicosane concentrations to the more typical biomarkers of algae and photosynthetic bacteria in the shorter chain length range is, however, expected if these organisms would be the sources of *n*-henicosane.

Another important observation are the relatively light $\delta^{13}\text{C}$ values for the light *n*-alkanes as determined from samples out of the higher resolved sample set. Above 12,160 vyears BP, the low $\delta^{13}\text{C}$ values of the C_{21} and C_{25} *n*-alkanes give strong

evidence for a partitioning of the Younger Dryas period as it has been previously inferred, especially from the short chain length fatty acid abundances.

6.2.2 Steroids and Triterpenoids as Source Indicators

6.2.2.1 Sterols as Source Indicators

The detection of various sterol derivatives allows the quantification of different source organism types since different biosynthetic pathways occur in land plants and algae on the one hand and animals and fungi on the other hand leading to different sterol compositions in the respective organism types as it is illustrated in *Fig. 1.10* after [Killops and Killops \(1993\)](#).

Structural differences in naturally occurring tetracyclic alcohols (saturation state, methyl groups on the basic carbon skeleton as well as the side-chain, stereochemistry) lead to a large variety of distinctive sterols ([Mackenzie *et al.*, 1982](#); [Brassell *et al.*, 1983](#); [Volkman, 1986](#)).

In general, C₂₇- and C₂₉ sterols are reported to originate from higher land plants, especially from their leaf waxes ([Huang and Meinschein, 1976](#); [Nishimura and Koyama, 1976](#)). Cholesterol, a C₂₇ sterol, was found to be a major constituent of algal sterols that is not dominant in sterol fractions of land plant derived organic matter ([Nishimura and Koyama, 1977](#); [Rieley *et al.*, 1991](#)). In a similar way, [Huang and Meinschein \(1979\)](#) argue that major differences exist between C₂₇- and C₂₉ sterol contribution of zooplankton and higher plants, respectively. C₂₈ sterols were found to show less significant variations, probably due to the origin from terrestrial as well as aquatic sources ([Meyers, 1997](#)). In more detail, Cholesterol as a prominent compound in all investigated sterol fractions originates from zooplanktonic sources in both aquatic and terrestrial organisms ([Wardroper *et al.*, 1978](#)). The brassicasterol is of special interest in connection with the source assignment of sedimentary organic matter since this compound has been found to be a major constituent of some diatom derived sterol fractions ([Volkman, 1986](#)). Another important proxy for autochthonous organic matter is the C₃₀ homologue dinosterol (dinosterol). It was found to be the major sterol component in many dinoflagellates ([Boon *et al.*, 1979](#)) and therefore used for the reconstruction of primary productivity ([Ariztegui *et al.*, 1996](#); [Wilkes *et al.*, 1999](#)). The C₃₀ sterol 24-*R*-ethylcholest-5-en-3 β -ol, that was detected in high concentrations is finally reported to be derived from higher land plants and thus represents terrestrial organic matter supply to the sediment ([Huang and Meinschein, 1979](#); [Volkman,](#)

Table 6.5: Homologues used for ternary plots of C₂₇- to C₃₀ sterols

Number of Carbon Atoms	Included Homologues
C ₂₇	5 α -(H)-cholest-22(E)-en-3 β -ol cholesterol
C ₂₈	brassicasterol 24-methylene-5 α -cholestan-3 β -ol
C ₂₉	stigmastanol β -sitosterol
C ₃₀	dinosterol

1986).

On the other hand, the mentioned variety of individual compounds, that often differ only in little detail from each other, bears risk for source assignment as figured out by Volkman (1986) since many potential sources are still undefined.

Nevertheless, Huang and Meinschein (1976, 1979) used a ternary plot of C₂₇-, C₂₈- and C₂₉ sterol percentages to show a major shift between land plants and algae as sources of sedimentary organic matter whereas bacteria can be neglected as sources of sterols. These organisms do not synthesise sterols themselves but utilise them as electron donors (Eyssen *et al.*, 1973). Thus, an effect on the carbon number distribution of sterols is not expected due to bacterial activity. In addition to their own measurements of sterol compositions of plankton and sediments from the Gulf of Mexico and the associated estuarine system, Huang and Meinschein (1979) enlarged their data base by sterol data from Meinschein and Kenny (1957); Attaway *et al.* (1971); Pryce (1971) and Nishimura and Koyama (1977).

Extending the basic carbon number based assignment of sterols to respective sources, Schulte (1997) suggested to summarise C₂₈ and C₃₀ homologues. This suggestion was based on the finding, that algae and cyanobacteria may also be sources of C₂₉ sterols and further that C₃₀ homologues, especially dinosterol, as proxies for aquatic sterols are neglected from the initial interpretation. A modification of the ternary plot using C₂₈+C₃₀ instead of C₂₈ sterols as illustrated in Fig. 1.11 B was therefore suggested; the distinction was limited to mainly marine and terrestrial sources.

Based on this framework, Figs. 6.17, 6.18 and 6.19 illustrate these relations for

the maar lake sediments that were investigated during the present study. Each figure is subdivided into two subfigures: each upper (A) diagram illustrates the ternary plot after Huang and Meinschein (1979) and each lower (B) that one after the modification as suggested by Schulte (1997). Sterol homologues that were used for calculation are listed in Table 6.5. These are the same as in the study published by Huang and Meinschein (1979) with the exceptions of the missing campesterol and the added dinosterol in the case of the lower plots to ensure comparability. As expected from previously discussed data of other compound classes, the diagrams indicate a terrestrial nature of the sedimentary organic matter under investigation. Beside the large variation width between individual samples, a complete separation of the included geological ages is not possible based on sterol distributions. A more detailed description follows below:

The Lateglacial/early Holocene samples of **Lake Holzmaar** (*cf.* Fig. 6.17) are significantly depleted in C₂₉ sterols, indicating a small input of terrestrial vegetation residues during that time. With the beginning of the middle Holocene, the relative contribution of C₂₉ sterols clearly increases under decreasing proportions of the lighter C₂₇ homologues, giving evidence for the development of land plant vegetation in Lake Holzmaars catchment area. The obvious variation in C₂₈ sterol percentages is finally of reduced significance since respective sources are of both aquatic and terrestrial origin (Huang and Meinschein, 1979; Meyers, 1997). The latter, however, reported some selected algal derived sterol compositions to consist nearly completely of C₂₈ sterols. The inclusion of the C₃₀ dinosterol essentially improves the separation of the geological zones that are part of the sedimentary profile of Lake Holzmaar (*cf.* Fig. 6.17 B). With one exception at 11,970 vyears BP, the respective samples of the Lateglacial/early Holocene profile section show relatively high proportions of this homologue and thus clearly plot in the region typically for mainly aquatic derived organic matter. This obviously reflects an increased importance of primary productivity in Lake Holzmaar during this time in comparison to younger samples. Relatively unspecific separation was yielded for the younger middle Holocene and Subatlantic samples. Both sample series, however, fall into the area of more terrestrial derived organic matter, indicating the establishment of land plant vegetation after the cooler glacial conditions.

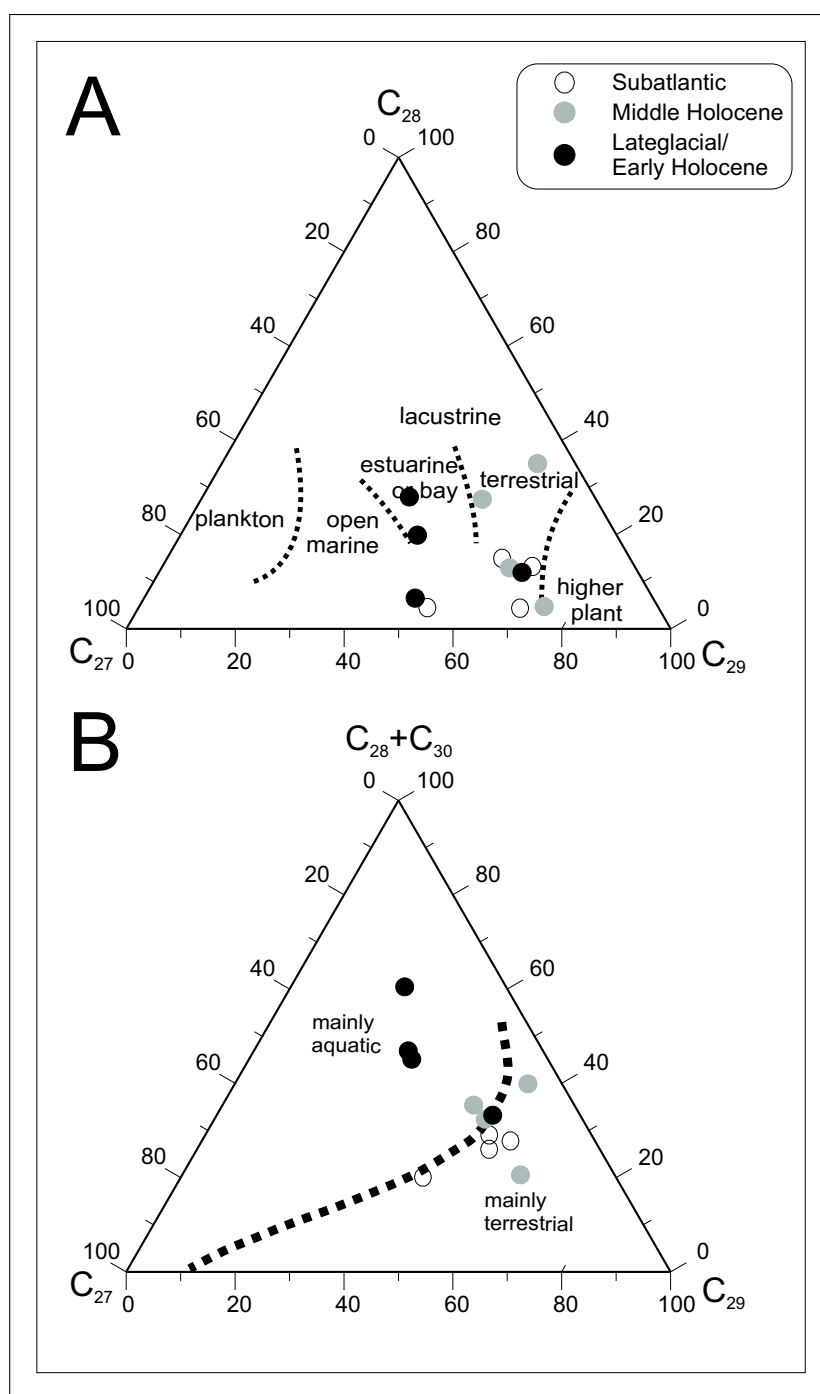


Figure 6.17: Ternary plots of sterols after [Huang and Meinschein \(1979\)](#) (A) and [Schulte \(1997\)](#) (B) for Lake Holzmaar

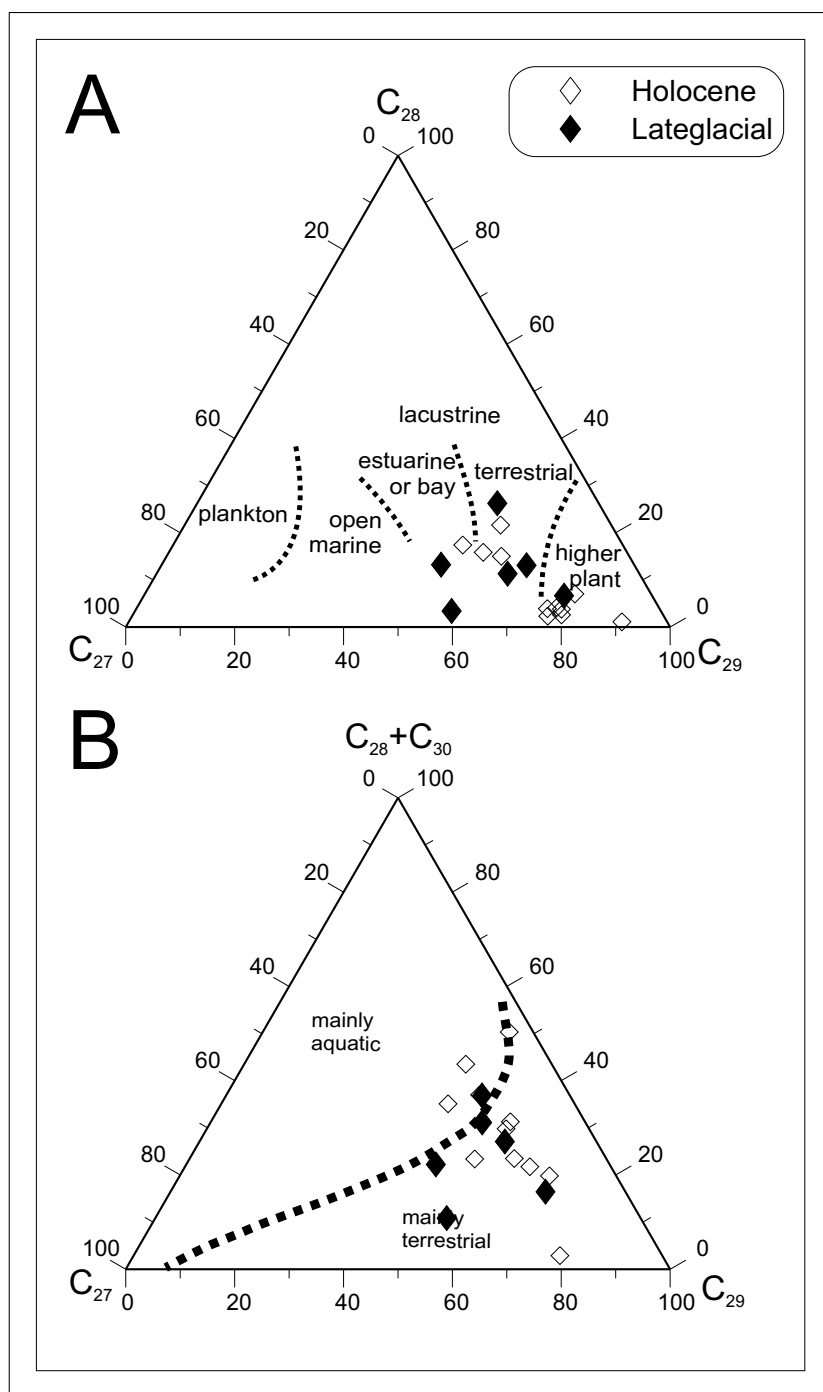


Figure 6.18: Ternary plots of sterols after Huang and Meinschein (1979) (A) and Schulte (1997) (B) for Lake Meerfelder Maar

More significantly as for Lake Holzmaar, most of the **Lake Meerfelder Maar** samples plot in the terrestrial region of sterol distributions. Contrastingly to the first described archive, no separation of Lateglacial samples due to reduced C₂₉ sterol abundances in comparison with the C₂₇ homologues is obvious from the ternary plot in (*cf.* *Fig. 6.18*), probably pointing to more developed terrestrial vegetation forms in its catchment area during glacial ages. Especially the Holocene sediments of Lake Meerfelder Maar are drastically depleted in C₂₈ sterols. The inclusion of dinosterol yields, in contrast to the previously described Lake Holzmaar, no significant improvement of the ternary sterol plot. Even if all samples plot slightly closer to the C₂₈+C₃₀ corner, the separation of included geological zones becomes not improved by this measure.

The increased temporal resolution of Lake Meerfelder Maars second sample set yielded no results divergent to those obtained from the full range profile as described above. The majority of samples falls into the terrestrial and/ or land plant area of the ternary plot in turn (*cf.* *Fig. 6.19*), and no significant separation of Lateglacial/ early Holocene samples is obvious. Additionally, the bi-partitioning of the Younger Dryas period between 12,250 – 12,220 vyears BP as inferred from various bulk geochemical as well as lipid data cannot be reproduced from any of the detected sterol-type compounds or ratios between them. The inclusion of dinosterol however, yields a considerable variability in the C₃₀ sterol percentages as visible from *Fig. 6.19 B*. The Younger Dryas samples are thus identified to be of mainly aquatic nature whereas a shift to terrestrial sources becomes obvious for the transition to the Holocene. Note, however, that this separation is relatively weak, a more specialised interpretation of dinosterol abundances will follow later below.

More detailed information about similarities between sterol abundances were yielded from cluster analysis as illustrated in *Fig. 6.20*. As already introduced for normal chain compounds, data from all investigated archives are used for calculation.

As obvious, significant similarities are not limited to sterol homologues with the same carbon number. At first, the homologues Cholesterol (B), 24-methyl-5 β (H)-cholestan-3 α -ol (G), 24-ethylcholestan-3 β -ol (L), 5 α -cholestan-3 β -ol (C) and brassicasterol (F), two C₂₇, two C₂₈ and one C₂₉ homologues, show the highest overall similarities between 94 % and 78 %. A second highly significant

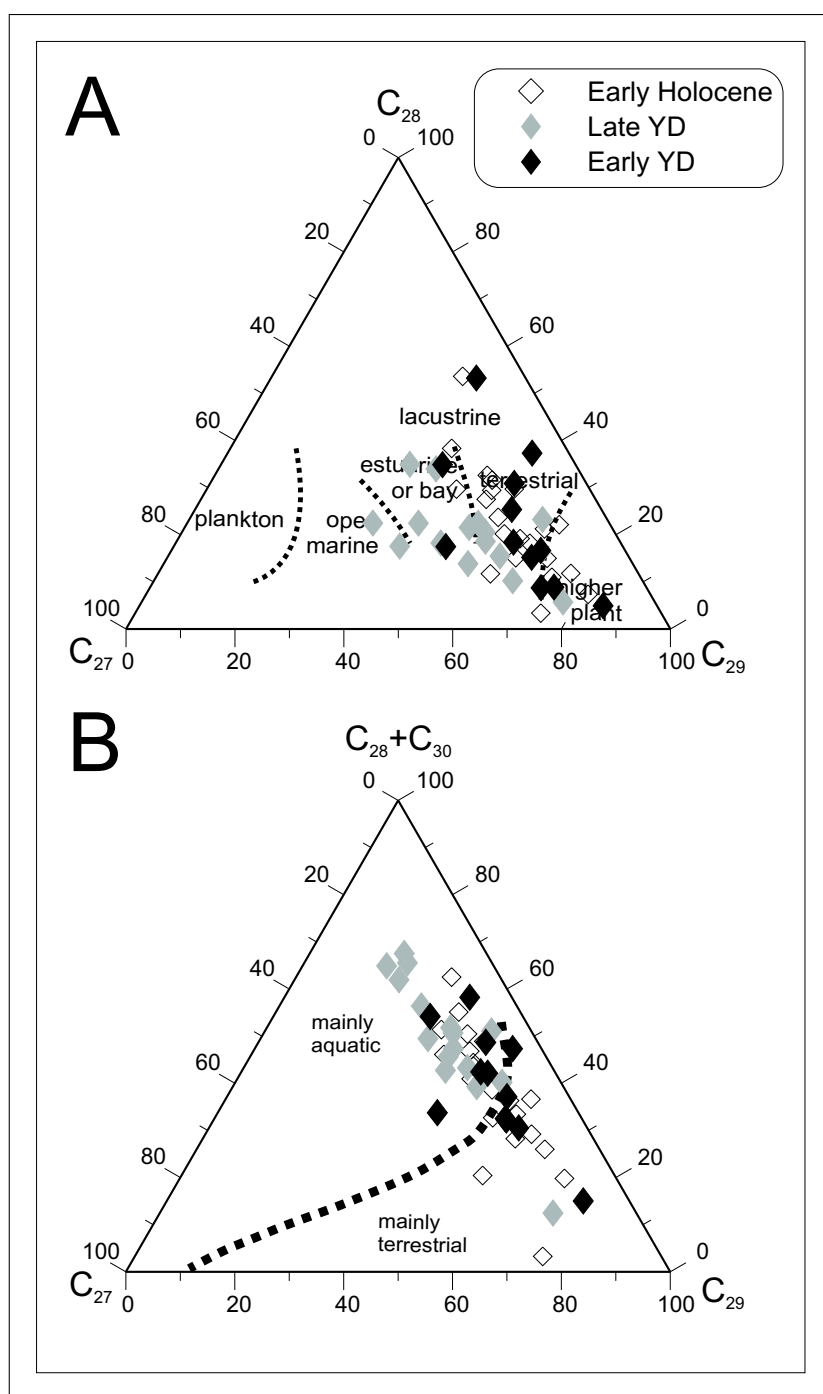


Figure 6.19: Ternary plots of sterols after Huang and Meinschein (1979) (A) and Schulte (1997) (B) for Lake Meerfelder Maar (high resolution sequence)

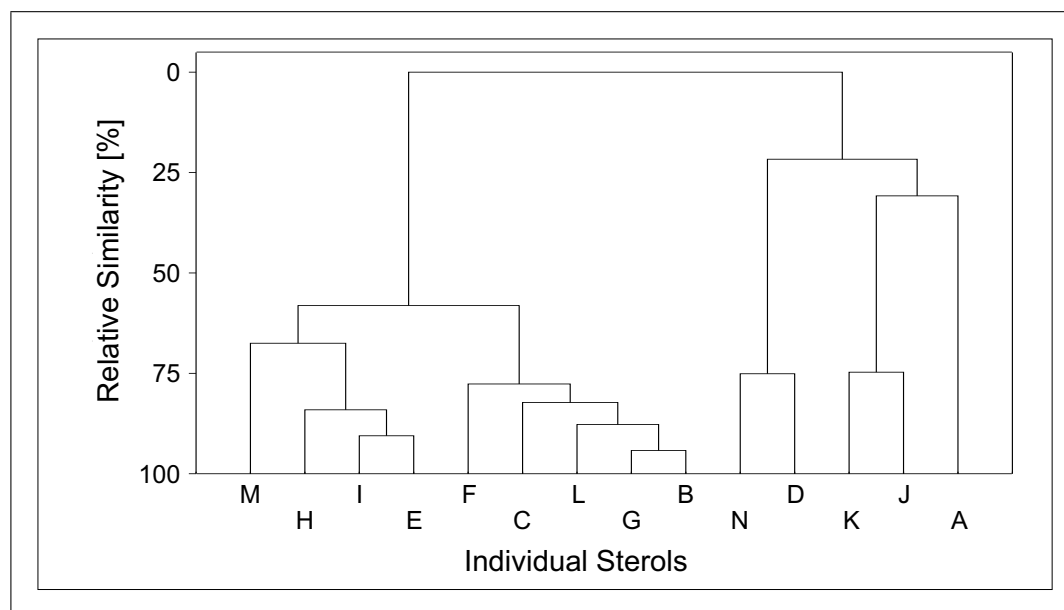


Figure 6.20: Cluster diagram for individual sterols using data from all investigated archives; letter labels are assigned to sterols as listed in [Table 5.4](#)

group is made up by the C_{28} and C_{29} sterols 24-methyl-5 β (H)-cholestan-3 β -ol (E), 23,24-dimethylcholesta-22(E)-en-3 β -ol (I) and 23,24-dimethylcholesta-5,22-dien-3 β -ol (H) with relative similarities of 91 % and 84 % while a similarity of 67 % to dinosterol (M), a C_{30} sterol and the last member of this sub-cluster, is less specific. The relative similarity between these two sub-clusters is still 58 %.

The second main-cluster is formed with generally lower relative similarities between individual compounds. 5 α -cholestan-3 α -ol (D) and lanosterol (N) form a first sub-cluster; the similarity between both compounds is 75 %. While the first named compound is a mainly algally derived C_{27} sterol, the latter has been reported as being an intermediate in sterol biosynthesis by animal and fungi ([Killops and Killops, 1993](#); [Barrero *et al.*, 1998](#)) and was also analysed in human serum ([Phillips *et al.*, 1999](#)). The latex of *Euphorbia lathyris* was finally shown to synthesise lanosterol ([Giner and Djerassi, 1995](#)). However, it is unusual to detect this sterol in lacustrine sediments (*cf.* [Fig. 1.10](#)). A second sub-cluster is made up by the homologues 24-methylene-5 α -cholestan-3 β -ol (J) and 24-*R*-ethylcholest-5-en-3 β -ol (K) with the same relative similarity of 75 % between both sterols. Less significant, 5 α (H)-cholest-22(E)-ene-3 β -ol (A) is combined to this group with a rel-

ative similarity of 31 % whereas further reduced similarity of 22 % is obvious to 5 α -cholestan-3 α -ol (D) and lanosterol (N).

These findings clearly demonstrate that no sharp separation exists between the sterol groups containing 27 and 29 carbon atoms for the investigated archives. On the other hand, similarities between individual sterol homologues are clearly consistent with the previously proposed intermediate attitude of C₂₈ compounds (Huang and Meinschein, 1979; Meyers, 1997) due to biological sources from both aquatic and terrestrial ecosystems. This is confirmed by the absence of sub-clusters, containing both, C₂₇ and C₂₉ sterols with the only exception of 24-ethylcholestan-3 β -ol (L) that is assigned to the sub-cluster with highest similarity. Beside this exception, representatives of both sterol groups show similarities only between themselves and/or C₂₈ sterols. The results of the cluster analysis presented in this study additionally give no evidence for significant similarities in C₂₈ and C₃₀ sterol abundances. Even if brassicasterol (C₂₈) and dinosterol (C₃₀) are known to originate from autochthonous organic matter producers, they are members of different sub-clusters with a relatively low similarity of 58 % between them. In the same way, the typical land plant derived C₂₉ compounds 24-ethylcholestan-3 β -ol and 24-*R*-ethylcholest-5-en-3 β -ol (both C₂₉) are members of the two main clusters with lowest similarity between them. So far, the basic carbon number based assignment of sterols to groups of source organisms needs to be handled cautiously. A source assignment using more specific distributions of individual sterols will follow directly below.

Ariztegui *et al.* (1996) inferred variations of primary productivity in Lake St. Moritz from dinosterol (dinosterol) concentrations. Wilkes *et al.* (1999) used a ATR_{ST} similarly with the sterols 4,23,24-Trimethyl-5 α -cholesta-5,22-dien-3 β -ol, 24-*R*-ethylcholest-5-en-3 β -ol and 24-ethylcholestan-3 β -ol being additionally included for the reconstruction of aquatic *vs.* terrestrial productivity in a 34,000 vyears BP sediment core from Lago di Mezzano, central Italy.

Downcore variations of both the dinosterol concentrations and the ATR_{ST} values for the investigated archives are illustrated in *Fig. 6.21*. Divergent from the cited study, the 5-dehydrodinosterol was not detected in the investigated sediment samples and therefore excluded from calculation. It is clear that both parameters are well correlated.

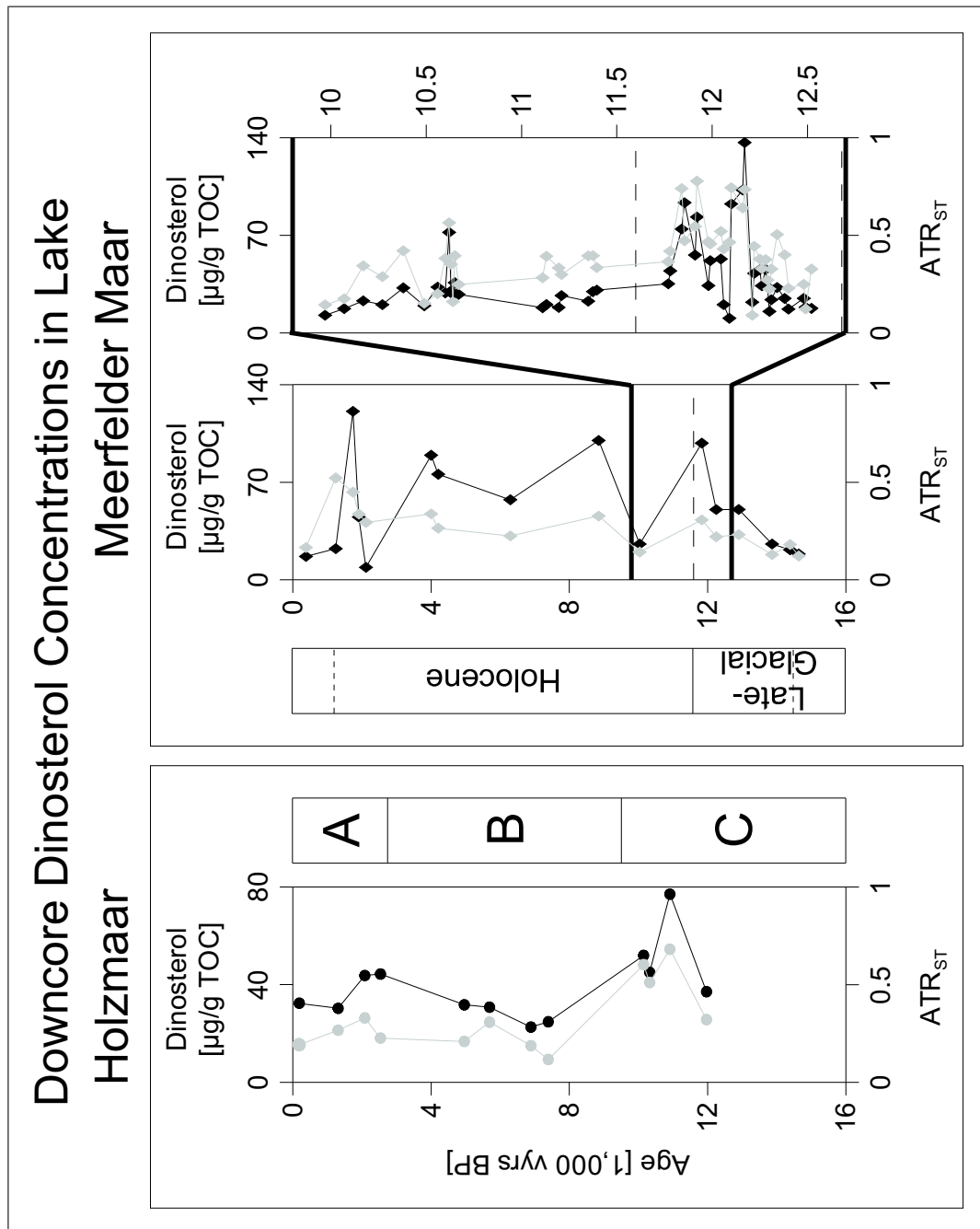


Figure 6.21: Downcore variations of dinosterol concentrations (black graphs) and ATR_{ST} ratios (grey graphs) for Lake Holzmaar (left box) and Lake Meerfelder Maar (right box), including both low (left plot) and high (right plot) temporal resolution sample sets; data points for Lake Meerfelder Maar at 3,765 and 11,410 vyears BP were removed because dinosterol was not detected in these samples

Dinosterol concentrations vary between 22 – 77 µg/g TOC in the **Lake Holzmaar** profile. A strong increase in the dinosterol concentration and the ATR_{ST} ratio is observed during the Lateglacial and early Holocene section C from the profiles bottom until 10,150 vyears BP. As this trend is in general agreement with increasing TOC content as well as Rock-Eval HI parameters, an increased autochthonous productivity can be assumed for Lake Holzmaar at the outgoing Lateglacial and transition to the Holocene. Moreover, increased autochthonous productivity can also be inferred from algally derived *n*-alkanes.

A significantly reduced primary productivity can be assumed for the beginning of middle Holocene profile section C from reduced dinosterol concentration in relation to TOC as well as in relation to the C_{29} sterol concentrations (ATR_{ST}). Another increase of autochthonous organic matter supply can be inferred from increased parameters beginning at 7,390 vyears BP, as good correlated to the beginning of the Holocene climatic optimum (approximately 8,000 – 6,000 years BP, [Zolitschka *et al.* \(2003\)](#)) as possible from the investigated sample sets temporal resolution. Highest slopes of increasing dinosterol as well as ATR_{ST} are obvious until the upper border of the Holocene climatic optimum. Later on, concentrations of dinosterol further increase. The nearly constant ATR_{ST} ratios on the other hand suggest an simultaneous increase in land plant derived organic matter supply to the sediment of Lake Holzmaar.

The uppermost Subatlantic section A is finally characterised by reduced dinosterol concentrations and ATR_{ST} ratios, probably reflecting less important autochthonous productivity in comparison to terrestrial derived sedimentary organic matter.

Ranging between 8 – 137 µg/g TOC, variation width of dinosterol concentration is remarkably higher for the sedimentary sequence of **Lake Meerfelder Maar**. Beginning with the lowermost samples, intensified autochthonous lake productivity can be inferred from increasing dinosterol concentrations as well as ATR_{ST} values during Bølling and Allerød. This trend is in clear consistency with simultaneous enrichments in organic carbon content as well as Rock-Eval HI values. Thus, the climate amelioration at the outgoing Lateglacial and during the first warming periods is well reflected in dinosterolas well as ATR_{ST} data.

During the intermediate cooling of the Younger Dryas period dinosterol concentration as well as its relation to terrestrial vegetation derived homologues remain constant first. This suggests an interrupt in increasing autochthonous productivity

due to the temporary cooling. During the late Younger Dryas on the other hand, a sharp increase in dinosterol abundance between 12,250 – 11,833 vyears BP might refer to increased autochthonous productivity. This is clearly in opposition to reduced organic carbon content and HI values, which indicate a worse quality of sedimentary organic matter due to reduced primary productivity. Relative proportions of algally derived normal chain lipids (cf. *Fig. 6.5*) contrastingly also point to increased algal productivity during the late Younger Dryas.

The Younger Dryas/Holocene transition is characterised by a rapid reduction of dinosterol concentrations first whereas short chain *n*-alkyl lipid distributions give no evidence for reduced algal productivity and also TOC and HI data remain stable during the transition. A rapid increase in dinosterol concentrations relative to both organic carbon content and C₂₉ sterols above 10,035 vyears BP indicates enhanced primary productivity during ameliorated Holocene climatic conditions. This behavior remains stable during the mid Holocene climate optimum and further until 4,000 vyears BP. This is also supported by continuously increased organic carbon content and HI values as inferred from Rock-Eval pyrolysis, and also the content of short chain *n*-alkyl lipids remains nearly constant during that age interval indicating stable climatic conditions.

Above 4,000 vyears BP, further increased ATR_{ST} ratios reflect an additional increase in autochthonous productivity that is in consistence with the bulk organic geochemical data as well as short chain lipid abundances.

Using the higher resolved sample sequence including the Younger Dryas and Lateglacial/Holocene transition only, a more precise record of primary productivity during times becomes obvious as follows:

Relatively low dinosterol concentrations and ATR_{ST} ratios (0.3 on average) and also low data fluctuation width characterise the earlier Younger Dryas period from its beginning until 12,210 vyears BP. With increased age, a significant increase was found especially for the ATR_{ST} values (0.5 on average), whereas absolute dinosterol concentrations show a large fluctuation interval. This trend is in general agreement with short chain fatty acid data whereas *n*-alkanes do not show significant variations during the Younger Dryas. The onset of increased short chain fatty acid percentages and decreased organic carbon and hydrocarbon content, however, was found between 12,250 – 12,220 vyears BP, whereas the sharply separated onset of higher ATR_{ST} values falls slightly younger between 12,210 – 11,170 vyears BP.

During youngest times of the Younger Dryas, dinosterol data indicate an abrupt reduction of the primary productivity that persists over the Younger Dryas/Holocene transition and further on during early Holocene stages with a slight trend to lower values with decreasing age. An exception from that general trend are significantly enhanced dinosterol concentrations and ATR_{ST} values between 10,650 – 10,380 vyears BP, the so called *boreal oscillation*, which is, less marked, also reflected in reduced organic carbon contents and increased short chain *n*-alkyl lipid percentages.

Another potential proxy marker for autochthonous productivity is brassicasterol, originating from diatoms (Volkman, 1986; Killops and Killops, 1993; Meyers, 1997). Downcore concentrations of this compound are illustrated in *Fig. 6.22*. Additionally, a diatom *vs.* terrestrial ratio for sterols DTR_{ST} was formulated analogously to the ATR_{ST} ratio used by Wilkes *et al.* (1999). A detailed sedimentological investigation of Lake Meerfelder Maar sediments was published by Brauer *et al.* (1999a) that will be used for comparison.

Very low brassicasterol concentrations were measured throughout the profile of **Lake Holzmaar**, and also the consequently low values of the DTR_{ST} ratio indicate a less dominant autochthonous contribution in comparison to higher plants to the sedimentary organic matter. Nevertheless, both the brassicasterol concentrations and the DTR_{ST} ratios slightly distinguish between included geological ages. Beginning during the Lateglacial, increasing values argue for increased diatom growth in Lake Holzmaar due to ameliorated climatic conditions and increasing temperatures at the outgoing glacial ages and during the first warming periods, Bølling and Allerød. Above 10,325 vyears BP, reduced diatom growth can be inferred from lowering brassicasterol and DTR_{ST} ratios over the sections C/B transition. This result is in good agreement with the previously discussed reduced autochthonous productivity as inferred from dinosterol and ATR_{ST} values, consistently pointing to reduced primary productivity. An onset of increased diatom growth can be inferred from brassicasterol concentrations above 5,690 vyears BP, furthermore in agreement with the findings for dinosterol as already reported. These results obviously demonstrate an increased primary productivity during the Holocene climate optimum. The less marked increase in DTR_{ST} ratios on the other hand indicates that organic matter supply from terrestrial higher plants increased in a comparable way as autochthonous organic matter contribution. Thus, both

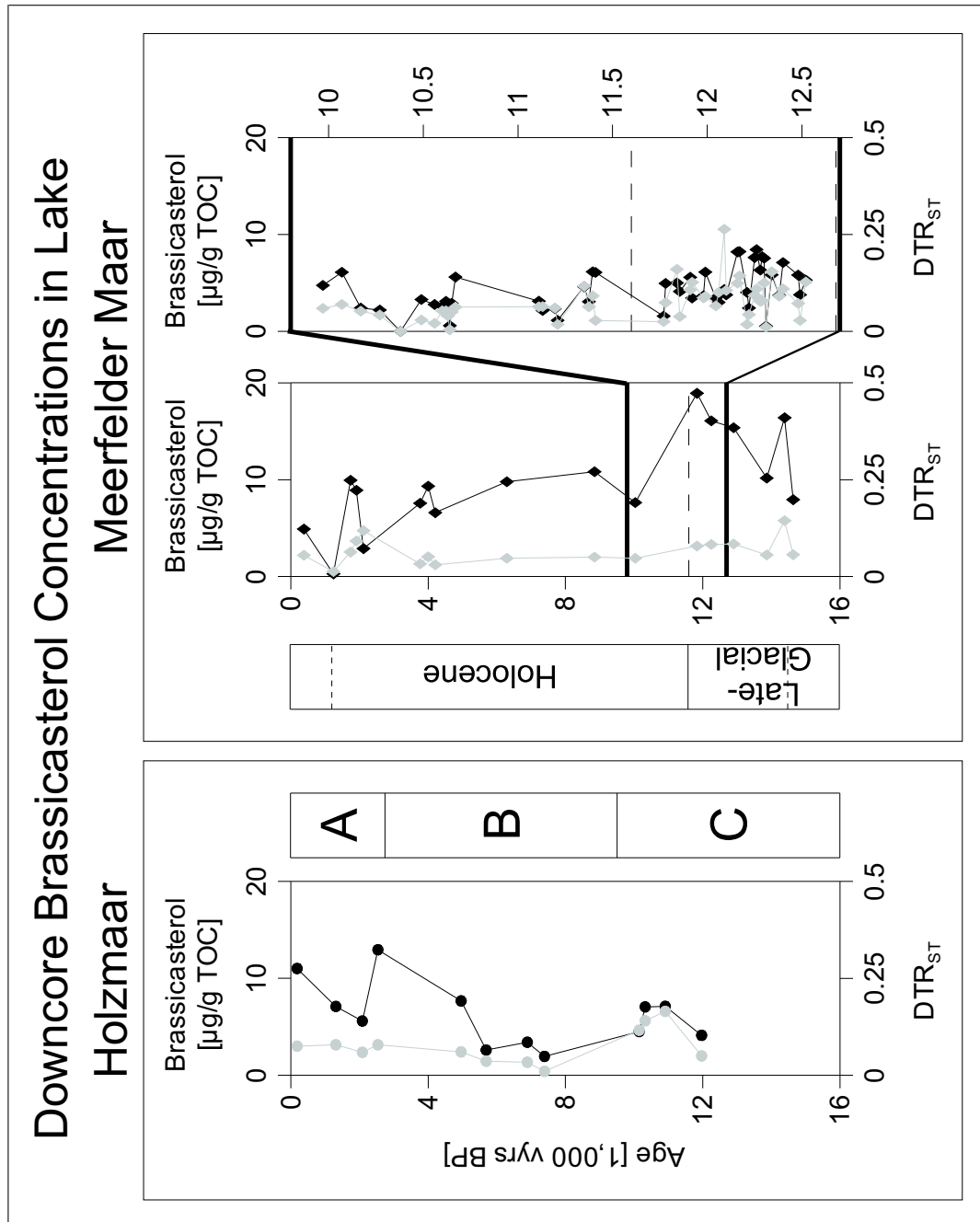


Figure 6.22: Downcore variations of brassicasterol concentrations (black graphs) and DTR_{ST} ratios (grey graphs) for Lake Holzmaar (left box) and Lake Meerfelder Maar (right box), including both low (left plot) and high (right plot) temporal resolution sample sets

vegetation forms obviously gained from climatic conditions during that time. Concentrations of brassicasterol are further increased over the upper border of Holocene climate optimum. An abrupt lowering, however, was found between 2,536 – 2,083 vyears BP, where relatively constant DTR_{ST} ratios further indicate a stable ratio between diatom- and terrestrial plant derived organic matter. A similar shift of reduced dinoflagellate growth was previously inferred from decreasing dinosterol abundances. This shift, however, was dated between 2,083 – 1,311 vyears BP. So far, a reduction in primary lake productivity seems to have occurred during Subatlantic. Based on the data presented here, dinoflagellates were concerned first, whereas the diatom growth was reduced with time-delay. The uppermost samples of Lake Holzmaar finally give evidence for a significant enrichment in organic matter derived from autochthonous organisms. This increase, however, may also be triggered by eutrophication, caused by human activity.

Also closely matching similarity between dinosterol concentrations and ATR_{ST} ratios on the one hand and brassicasterol concentrations and DTR_{ST} ratios on the other hand were retrieved for the **Lake Meerfelder Maar** sequence. Last named parameters are as low as reported for Lake Holzmaar.

A general increase in diatom derived brassicasterol concentration is obvious for the lowermost profile section from the Lateglacial during Bølling and Allerød and further during Younger Dryas period. A partial maximum abundance of brassicasterol was additionally detected at 14,385 vyears BP. Further in analogy to Lake Holzmaar, brassicasterol data of Lake Meerfelder Maar suggest a depletion in autochthonous organic matter supply during the early Holocene. The period between 8,850 – 3,765 vyears BP, representing the Holocene climate optimum, is characterised by enhanced diatom contribution inferred from brassicasterol concentration. This is in agreement with the interpretation of dinosterol concentrations as discussed above. The uppermost Subatlantic part of Lake Meerfelder Maars profile is characterised by decreasing amounts of dinosterol which reflects less dominant autochthonous productivity. As reported for dinosterol data, the Subatlantic depletion is interrupted by a sharp peak of enrichment between 1,740 – 1,910 vyears BP.

The higher temporal resolution of Lake Meerfelder Maar yields an interesting difference between dinosterol and brassicasterol data as follows:

The early Younger Dryas period seems to be characterised by a continuously en-

hanced autochthonous bioproductivity as it is recognisable from increasing brassicasterol concentrations. Short-term interruptions of this general trend were measured at 12,310 and 12,220 vyears BP. Above 12,160 vyears BP, however, brassicasterol concentrations become clearly lowered for the remaining late Younger Dryas. This finding supports a reduced primary productivity as it has been proposed from the decreased bulk organic geochemical parameters (TOC, HI) as well as short chain fatty acid distributions. The dating of this reduction on the other hand shows a time delay: based on TOC and HI data, the shift would be expected above 12,250 vyears BP. So far, diatoms are supposed to be minor organic matter contributors during the late Younger Dryas whereas dinosterol data indicate a large fluctuation of dinoflagellates around 12,160 vyears BP and further continuously enhanced growth during the upper Younger Dryas.

The reconstruction of brassicasterol based diatom populations in Lake Meerfelder Maar is in good consistency with the results published by Brauer *et al.* (1999a). Only a few planktonic diatoms (*Stephanodiscus*) were detected in summer sediment layers during late Allerød. A significant increase of diatoms was detected with the onset of the Younger Dryas, leading to monospecific diatom layers. The dominant autochthonous productivity was explained with eutrophication by surface run-off due to forest collaps as a result of decreasing temperatures. This state was found to change abruptly at 440 years after the beginning of the Younger Dryas. Regular diatom blooms are missed from younger sediments and the significantly decreased brassicasterol concentrations are in consistency with these results. Less precise consistency must be, however, considered for sediments younger than the Younger Dryas: Whereas brassicasterol concentrations remain on a relatively low level over the Younger Dryas/Holocene transition, Brauer *et al.* (1999a) report layers of planktonic diatoms during the Preboreal. Note in this context that all biomarker concentrations are normalised to TOC content. Thus, increasing amounts of organic matter from different sources such as land plants as inferred from pollen data (Litt and Stebich, 1999; Litt, 2000) during Preboreal, lead to a dilution of autochthonously derived sterol compounds in relation to TOC content.

Based on the obvious differences between brassicasterol and dinosterol abundances as introduced above, a DBR ratio is suggested to reconstruct varying contributions of diatoms *vs.* dinoflagellates (*cf. equation 6.6*). Downcore variations are illustrated for both sedimentary archives in *Fig. 6.23*.

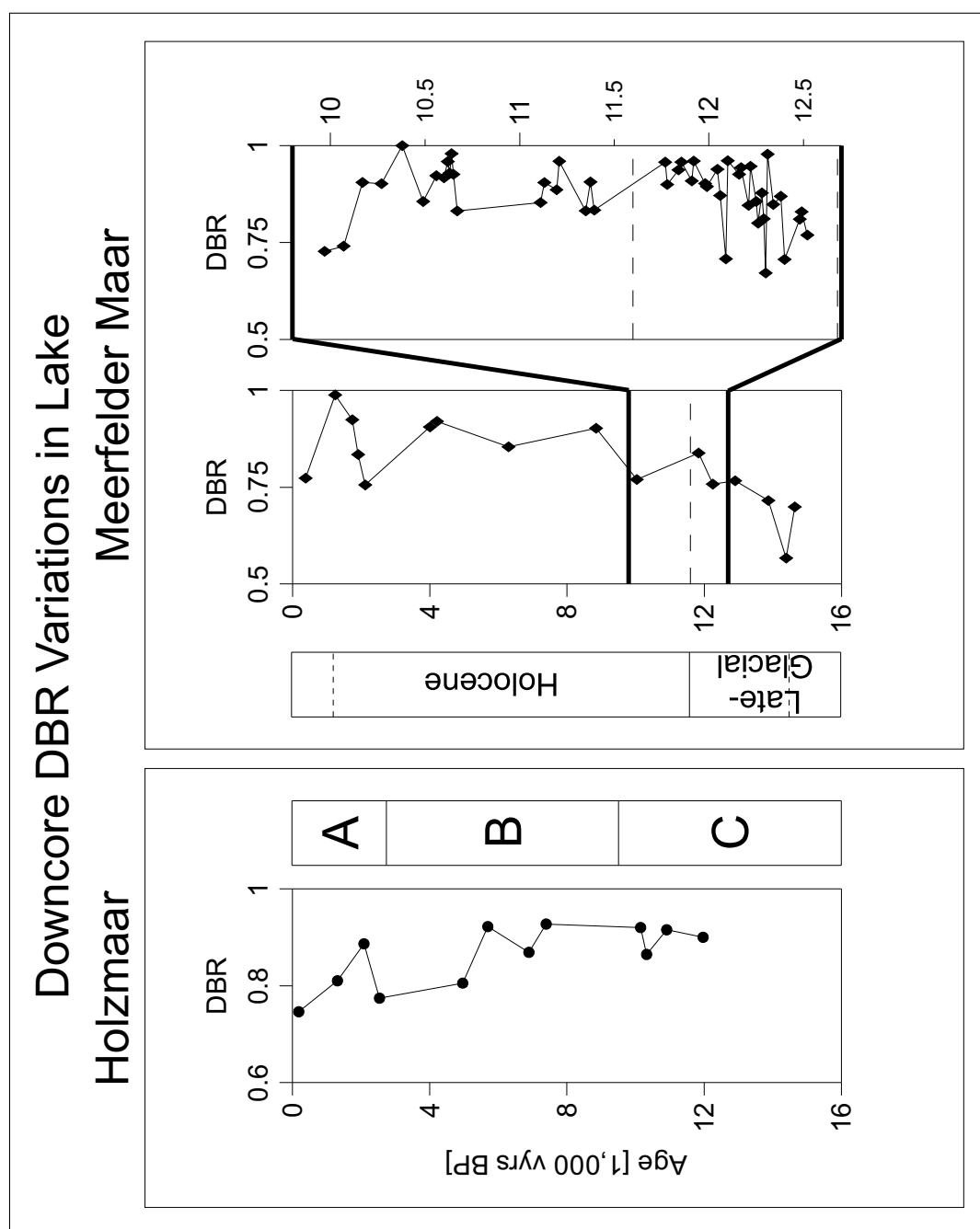


Figure 6.23: Downcore variation of the DBR ratio; left plot: Lake Holzmaar; right plot: Lake Meerfelder Maar; note, that samples at 3,765, 10,380 and 11,410 vyeears BP of Lake Meerfelder Maars sedimentary sequences were omitted from illustration since at least one sterol was not detected

$$DBR = \frac{dinosterol}{dinosterol + brassicasterol} \quad (6.6)$$

For **Lake Holzmaar**, highest overall ratios on a relatively constant level were calculated during the Lateglacial and early Holocene up to 7,390 vyears BP. Above this date, decreasing ratios indicate a shift to less dominant dinoflagellate populations and a *vice versa* more dominant organic matter contribution from diatoms. In the case of **Lake Meerfelder Maar**, increasing ratios during the Lateglacial towards the Younger Dryas period indicate in consistency with the results of [Brauer *et al.* \(1999a\)](#) a reduction of diatom blooms.

Despite these general observations, a more specified link to environmental and/or climatic conditions remains difficult to establish since both organism types exist in a wide variety of species. In their review, [Schrenk-Bergt *et al.* \(1998\)](#) for example report on diatoms being widespread organisms, contributing about 25 % of the Earth's primary productivity ([Willén, 1991](#)); 6,000 species in 200 genera are known to live under a broad range of environmental conditions, e. g. of the pH factor, of the trophic state, of the water temperature, of the water chemistry, of the water depth, of the salinity, of the SiO₂ availability and of the light intensity. Keeping in mind, that the described sterol homologues are not reported to be capable to certainly distinguish between individual species, it seems complicated to trace variations of these compounds back to the environment these organisms lived at.

6.2.2.2 Cholestane- and Hopane Derivatives as Source Indicators

Beside the normal chain compounds as discussed in *Chapter 6.2.1*, relevance of cholestane and hopane derivatives out of the hydrocarbon and acid fractions will be discussed in this section.

Wilkes *et al.* (1999) suggested a BTR_{FA} ratio of $22R-17\beta(H),21\beta(H)$ -dihomohopancarboxylic acid *vs.* C_{26} fatty acid to estimate proportion of bacteria derived sedimentary organic matter and/or extent of bacterial reworking of primary organic matter during early diagenesis or pedogenesis. The ratio is based on the generally accepted origin of hopane derivatives from bacteria derived hopanols by diagenetic transformation whereas the saturated long chain fatty acids are typical constituents of land plant derived organic matter (*cf. Section 6.2.1*).

Downcore variation of BTR_{FA} ratios after Wilkes *et al.* (1999) as well as a similar ratio, formed from summed hopanoic acid concentration *vs.* C_{28} - C_{32} saturated fatty acids as assigned to land plants as respective organic matter sources by cluster analysis(*cf. Table 6.4*) are illustrated in *Fig. 6.24*. Based on these findings, hopanoic hydrocarbons were tested for usability in the same way. A BTR_{HC} ratio was used by Wilkes *et al.* (1999). This parameter was extended analogously to the respective acids to include summed hopanoic hydrocarbons *vs.* land plant derived *n*-alkanes in the chain length range from C_{27} – C_{31} as inferred from cluster analysis (*cf. Table 6.4*). The downcore variations of both ratios are illustrated in *Fig 6.25*.

Both acid related parameters are well correlated for the sedimentary sequence of **Lake Holzmaars**, ranging between 0.1 – 0.4. Slightly lower values in the range between 0 – 0.3 were calculated for the hydrocarbon related parameters which are well correlated in turn. The lithological zones after Zolitschka and Negendank (1998) can be well distinguished by all parameters with the most clear trends for the hydrocarbon ratios. Beginning during the Lateglacial, generally lowest values were calculated for section C. With decreasing age, all parameters are abruptly shifted to higher values in the early and middle Holocene above 10,325 vyears BP. Characteristic maxima are obvious between 7,390 – 6,888 vyears BP with the acid related parameters maximising first. All values further remain on a relatively high level during the middle Holocene profile section B; merely one exception is made up by a significant minimum in hydrocarbon related ratios at 5,690 vyears BP, where generally very low concentrations of hopanoic hydrocar-

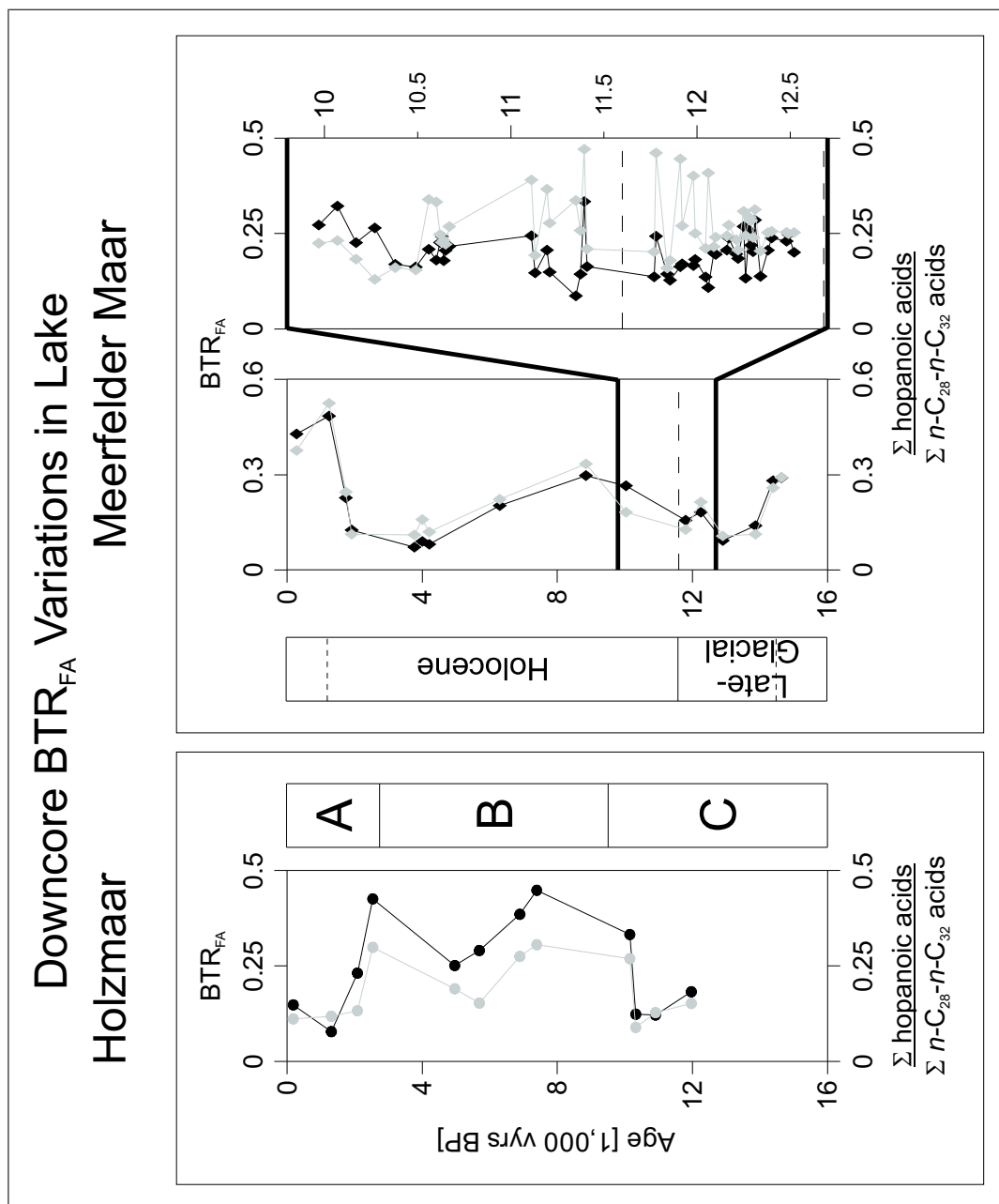


Figure 6.24: Downcore variation of BTR_{FA} ratio (black graph) and summed hopanoic acid concentration *vs.* summed $C_{28}-C_{32}$ saturated fatty acids (grey graph); left plot: Lake Holzmaar; right plot: Lake Meerfelder Maar

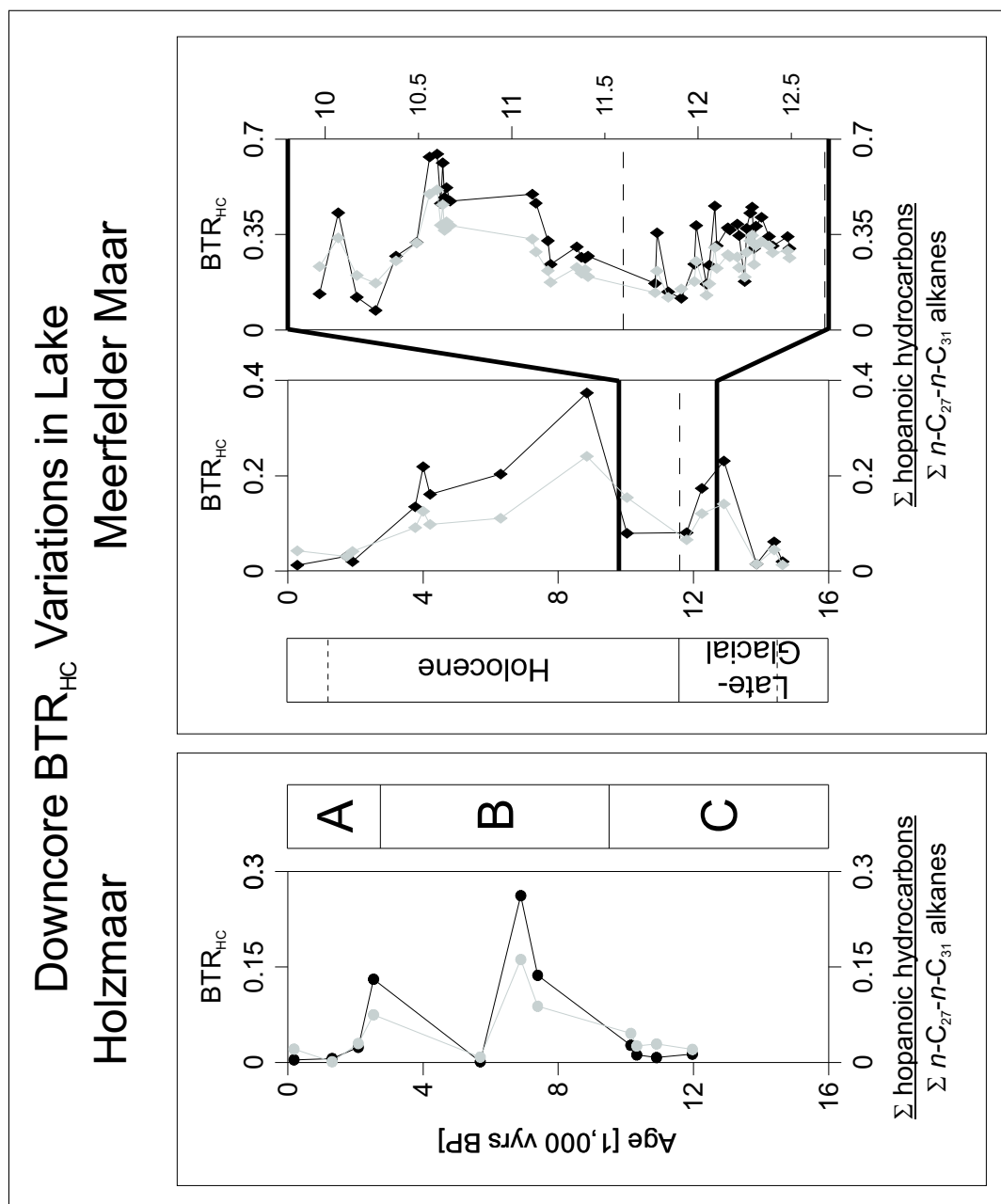


Figure 6.25: Downcore variation of BTR_{HC} ratio (black graph) and summed hopanoic hydrocarbons vs. summed C₂₇-C₃₁ n-alkanes (grey graph); left plot: Lake Holzmaar; right plot: Lake Meerfelder Maar

bons were measured. These results verify an enhanced bacterial activity compared to glacial ages. Assuming a prominent proportion of bacteria being autochthonous organic matter contributors, this confirms the enhanced sedimentation of autochthonous organic matter during the middle Holocene as inferred from sedimentological results published by [Zolitschka and Negendank \(1998\)](#). Thus, hopanoic biomarkers seem to reflect autochthonous organic matter proportions better than short and normal chain lipids since these compounds are relatively instable against diagenetic attack.

A general trend to lower values between 7,390 – 4,960 vyears BP, the period of Holocene optimum, demonstrates the good climatic conditions for development of land plant vegetation to disadvantage of relative proportions of autochthonously synthesised organic matter. A reverse trend is finally obvious for the youngest investigated Subatlantic profile section: continuously lowering values for both acid and hydrocarbon related parameters indicate a reduced quantity of bacteria derived organic matter.

BTR_{FA} as well as BTR_{HC} ratios are in the same range of magnitude for the sedimentary profile of **Lake Meerfelder Maar**. During the Lateglacial, continuously decreasing acid related ratios give evidence for reduced bacterial activity due to lowered temperatures. Contrastingly, the concentrations of hopanoic hydrocarbons in relation to long chain *n*-alkanes suggest an appreciable growth of bacteria populations above 13,865 vyears BP. All hopanoid related ratios remain on a relatively low level during the Younger Dryas. In the case of BTR_{FA} ratios, a partial maximum is obvious during the cooling period itself. Later on, increasing ratios during the early Holocene indicate a continuous growth of bacteria communities in consistency with the findings for Lake Holzmaar. This trend persists until 8,850 vyears BP matchingly for parameters from both compound classes and thereafter shows a reversal. As already argued during the description of Lake Holzmaar, this might indicate reduced autochthonous organic matter production during the Holocene Optimum, where land plant vegetation benefits from warm temperatures.

The results for the uppermost Subatlantic age are partially in contrast to the findings for Lake Holzmaar: Since 1,910 vyears BP, rapidly increasing acid related ratios might suggest increasing proportions of bacterially derived organic matter and/ or degree of bacterial reworking. The BTR_{HC} ratios on the other hand be-

have very similar as described for Lake Holzmaar showing continuously decreasing values towards the profiles top.

The more detailed investigation of sediments out of the higher resolved sample set during the Younger Dryas/ Holocene transition yields differing results. The values of the BTR_{FA} as well as the BTR_{HC} are closely scattering. Nevertheless, a slight trend to lower ratios is obvious for both parameters during the upper section of the cold period (*cf.* Fig. 6.24). Values of the BTR_{FA} shift from 0.22 to 0.17 on average above 12,250 vyears BP; 0.35 and 0.29 on average were calculated for BTR_{HC} . The same shifts were also observed for the extended ratios. Merely for the hopanoic acids *vs.* long chain *n*-alkane ratio, four samples out of the upper Younger Dryas show increased values, which are caused by relatively high concentrations of the less important 22*R*-17 β (H),21 β (H)-hopanecarboxylic acid.

Even if these changes occur not as abrupt as observed for other bulk organic geochemical and lipid data, the results prove a decreased importance of bacteria as organic matter contributors in relation to land plants during the upper Younger Dryas. Note in this connection, that absolute hopanoic acid and hydrocarbon concentrations show a shift to lower values during upper Younger Dryas period more clearly as the ratios used in this section in order to rate bacterial activity against land plant derived organic matter influx.

Inconsistent changes in bacterial *vs.* terrestrial activity can be inferred from hopane derivatives *vs.* long chain *n*-alkyl lipid ratios during the early Holocene. The marked variation as observed especially for medium chain length fatty acids around 10,500 vyears BP has no equivalent in hopanoic *vs.* long chain fatty acid content whereas hydrocarbon related ratios strongly suggest dominant bacterial activity between 11,130 – 10,560 vyears BP.

6.3 Paleoenvironmental Implications

Various bulk geochemical as well as lipid biomarker data have been discussed during the past sections especially regarding their utility as proxy-data for reconstructing paleoenvironmental and paleoclimatic conditions. Despite the fact that mainly ubiquitous lipids were detected in both Eifel Maar Lakes as well as Lake Großer Treppelsee, many individual compound abundances and ratios of several lipids were found to well distinguish between the geological ages as they were included in the investigated profiles of at least the last 15,000 years before present. Moreover, significant trends of land plant vegetation on the one hand and autochthonous bioproductivity on the other hand have been found during single epochs. All these data need to be merged to a whole in the following in order to reconstruct depositional histories of the areas under investigation as precisely as possible. Due to their small geographic distance, the similar geological setting as well as similar climatic conditions that can be assumed for the investigated Eifel Maar Lakes, they will be discussed together. A separate section will deal with the reconstruction of the paleoenvironment for Lake Großer Treppelsees catchment area.

6.3.1 Eifel Maar Lakes

Bulk organic geochemical parameters as well as lipid data are available for the last 12,480 and 14,685 calendar years from Lake Holzmaars and Lake Meerfelder Maars sedimentary profile sections, respectively. Thus, the Lake Holzmaar profile begins in the middle of the Younger Dryas cold period, whereas the last Glacial Age is included for Lake Meerfelder Maar.

Generally low productivity is expected during glacial ages due to the cold and/or dry climate. Low TOC content and low HI values were measured for the respective profile section of Lake Meerfelder Maar. As figured out for Lago di Mezzano by Wilkes *et al.* (1999), these data reflect glacial conditions. These authors as well as Ramrath *et al.* (1999), investigating the same sedimentary archive, further interpret high OI values as an indicator of significantly increased surface-runoff due to reduced evapotranspiration of terrestrial vegetation coverage. OI values measured for Lake Meerfelder Maar during the glacial period are clearly lower

as found for Lago di Mezzano and the wide scattering representing lake level fluctuations is not obvious. Lipid biomarker distributions that represent terrestrial organic matter supply, especially long chain fatty acids, supportingly indicate an appreciable land plant derived organic matter influx. The ratio between the C₂₇ and C₃₁ *n*-alkanes for the glacial samples indicates a steppe-like vegetation of herbs and shrubs. Based on these findings, a moderate autochthonous productivity and an open steppe-like plant vegetation in the catchment rather than higher plants and trees can be assumed during the Lateglacial period of cool and/or dry climate conditions.

A rapid climate amelioration is known to have occurred after the deglaciation during Bølling (13,700 – 13,550 vyears BP) and Allerød (13,400 – 12,700 vyears BP); both stages are interrupted by the Older Dryas. This development is preliminary reflected in increasing organic carbon content as well as HI values above 13,865 vyears BP, documenting a benefit of bioproductivity from increased temperatures and/or precipitation. The sharply reduced TOC/TN ratios reflect a growing importance of allochthonous production to the disadvantage of autochthonously produced biomass more clearly.

This thesis is in good agreement with reduced abundances of algally derived lipids (*n*-alkanes, *n*-fatty acids) and *vice versa* increasing abundances of macrophyte and, more marked, land plant derived lipid biomarkers. Moreover, the C₂₇ *vs.* C₃₁ *n*-alkane ratio as well as the corresponding ratio of fatty acids with carbon numbers being increased by one correspondingly reflect a significant change in the terrestrial vegetation composition from dominant herbs and shrubs to more established forests. Further in agreement to this assumption, also summed concentrations of C₂₉ sterols continuously increase above 14,385 vyears BP, indicating increasing amounts of terrestrial plant derived organic matter to the lake sediment.

These interpretations are generally supported by studies of [Litt and Stebich \(1999\)](#); [Litt \(2000\)](#) and [Litt *et al.* \(2001\)](#) who published pollen diagrams for the investigated Eifel Maar Lakes. Accordingly to the findings of this study, a major increase in *betula*, a pioneer tree, was found after approximately 14,100 vyears BP during the outgoing Lateglacial and Meiendorf. Gramineae, a herb species, on the other hand reach a maximum abundance at approximately 14,400 vyears BP and further continuously decrease. After approximately 13,550 vyears BP, the authors additionally detected an increasing number of

pinus pollen further indicating a benefit of land plant vegetation from improved climate conditions.

The climate development after the Lateglacial to Holocene optimum conditions via Bølling and Allerød occurred not continuously, it was interrupted by an intermediate cooling, the Younger Dryas period, that is still under strong investigation. Due to the significant changes during this stage, it will be discussed in detail in a separate section below using the temporally higher resolved sample set. However, it may already be stated that a significant and temporally well marked shift in the sedimentary organic matter composition can be referred from both bulk organic geochemical parameters and lipid fraction compositions. Decreasing content of organic carbon as well as lowered HI values indicate lower quantity and quality of sedimentary organic matter in both Eifel Maar Lakes correspondingly. The abundances of normal chain lipids further support a maximum stage of autochthonous productivity and *vice versa* reduced contribution from terrestrial plants during the Younger Dryas. Terrestrial derived organic matter sources also vary during this time as obvious from the C_{27}/C_{31} *n*-alkane ratio.

The Younger Dryas cooling is directly followed by the Holocene age when generally ameliorated climate conditions including both increased temperatures and precipitation, are typical. Central Europe was covered by closed forests, especially during the so-called Holocene climate optimum (approximately 8,000 – 6,000 vyears BP) and first human activity is detectable through changes in the vegetation composition as well as archeological finds (Zolitschka *et al.*, 2003). Beside the bulk organic geochemical parameters, lipid data are available for both Eifel Maar Lakes from that time on.

Rapid enrichments in organic carbon content and HI values as well as depletions in OI values from Rock-Eval pyrolysis argue for a general increase of bioproductivity and an improvement of sedimentary organic matter for both Eifel Maar Lakes. In general, this development is also reflected in lipid biomarker data. However, major differences between both lakes can be derived from various individual compounds. Since climate conditions are supposed to be very similar due to the small geographical distance between both archives, differences in lipid composition, resulting from varying autochthonous and/or land plant vegetation, need to be caused by differences in size or morphology of the respective catchment areas. Unfortunately, pollen data for comparison with lipid distributions are not avail-

able for that age.

Proportions of short chain *n*-alkyl lipids, that are known to derive mainly from autochthonous organisms, are reduced in relation to respective homologues in sum in comparison to older ages, especially in the case of fatty acids, and are essentially constant throughout the Holocene. A slight trend to increased abundances with decreasing age is obvious for Lake Holzmaar only. This might indicate a stable autochthonous productivity on a relatively low level under stable climate conditions of warm temperatures and humid precipitation circumstances.

More specific biomarkers on the other hand propose pronounced variations of primary productivity in both maar lakes. Relations between bacteria derived hopanoic and land plant derived long chain fatty acids demonstrate a stage of high bacterial activity for Lake Holzmaar between 7,390 – 2,083 vyears BP, that is, however, on a low level as inferred from normal chain homologues. The rise occurs sharply at the lower border and the Holocene optimum stage is characterised by a well defined reduction of the BTR_{FA} ratio, being in good consistency with the proposed maximum abundance of land plants. Very similar, rising bacterial activity is obvious during the early Holocene for Lake Meerfelder Maar. Above the maximum of the BTR_{FA} ratio at 8,850 vyears BP, bacterial activity is reduced and land plant derived organic matter is *vice versa* reduced during the Holocene optimum. Out of the sterol fractions, sterols dinosterol and brassicasterol have been further evaluated as proxies for autochthonous organic matter production since these compounds mainly originate from dinoflagellates and diatoms, respectively. In case of Lake Holzmaar, reduced dinosterol concentrations at the beginning of the Holocene age, that are well correlated to their relative proportion in comparison to land plant derived sterol homologues, point to a sharp reduction of dinoflagellate population in that lake. Contrasting relations were found for Lake Meerfelder Maar. An equivalent behavior was also detected for brassicasterol. Interestingly, both marker molecules consistently indicate a sharp growth of the respective source organism populations above 7,390 vyears BP in Lake Holzmaar, slightly time-delayed to the onset of the Holocene climate optimum. Both parameters reach a partial maximum around 2,300 vyears BP in good temporal correlation to the beginning of the Subatlantic age. Slightly deviating, an increase of both biomarker concentrations proofs enhanced autochthonous productivity of Lake Meerfelder Maar, however between 8,850 – 4,000 vyears BP.

Also stable proportions were found for *n*-alkyl homologues in the mid-chain range as they are found to be typical for aquatic macrophytes. Nearly no variation is obvious for *n*-alkanes whereas fatty acids show a slight trend to increased proportions with decreased age. This finding, however, is strictly limited to Lake Holzmaar; the completely different behavior for Lake Meerfelder Maar indicates a massive growth of aquatic macrophytes in this lake. The temporal interval of mid-chain *n*-alkane maximum abundances lies between 10,035 – 4,000 vyears BP and is most expressed for *n*-alkanes, but enrichments were also found for mid chain fatty acids. Thus, enhanced mid-chain *n*-alkyl lipid proportion of Lake Meerfelder Maar are well correlated to the maximum abundance stage of sterol biomarkers typical for autochthonous productivity as deduced above.

Adding the isotope composition of *n*-alkanes during the Holocene to the current interpretation yields further important information about organic matter contributors to Lake Meerfelder Maars sedimentary record as follows: Beginning with the early Holocene $\delta^{13}\text{C}$ values of *n*-hencicosane shift to extremely light values; -43.1 ‰ to -45.7 ‰ were measured between 8,850 – 4,000 vyears BP. Also the next odd-numbered homologue *n*-tricosane shows a depletion in ^{13}C that is, however, not as marked as for *n*-C₂₁ and an additional enrichment was detected at 6,290 vyears BP. *n*-Pentacosane finally shows an intermediate ^{13}C depletion at 4,000 vyears BP only. Measured isotope composition, especially of *n*-hencicosane cannot be explained by fractionation during carbon fixation in plants; no comparable data are available from the present literature. Thus, methanogenesis was suggested to have occurred and have been the source of ^{13}C depleted carbon. (*cf.* Section 6.2.1).

If the ^{13}C depleted hencicosane of Lake Meerfelder Maar has been biosynthesised from sources resulting from methanogenesis, other proxy-parameters should give evidence for increased microbial activity during the same time. As illustrated in Fig. 6.26, the downcore HI values point to sedimentary organic matter of higher quality between 10,310 – 3,765 vyears BP. The average content of volatile hydrocarbons in that range of age is 364 mg/g TOC in contrast to only 221 mg/g TOC on average for the remaining under- and overlying samples. This observation primarily reflects a higher autochthonous productivity in the lake. Further supporting this thesis, the content of unsaturated fatty acids, especially that of the

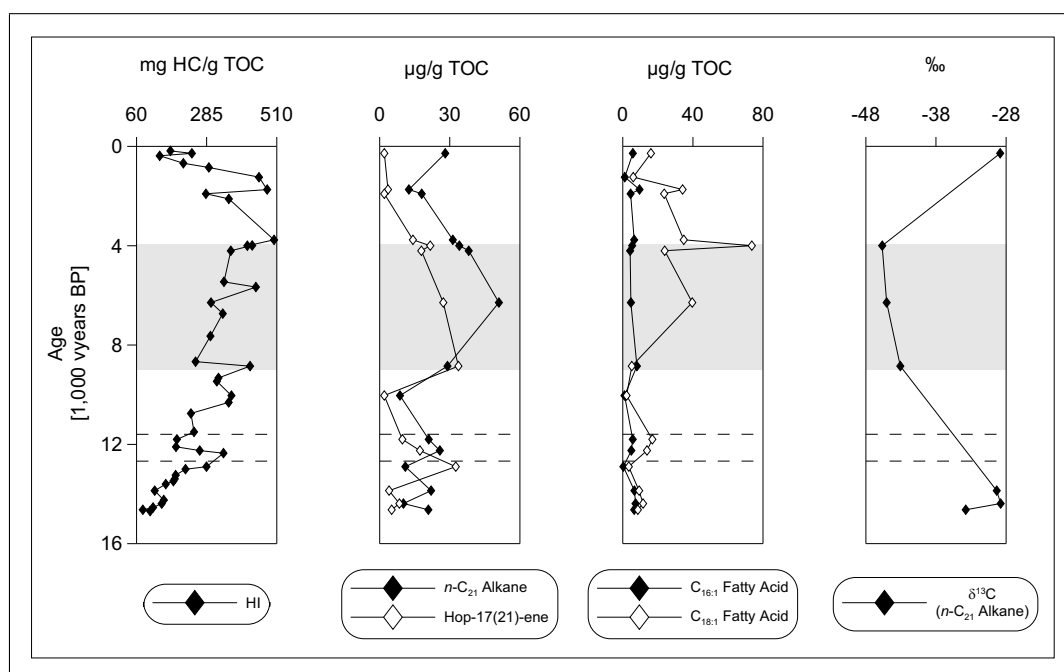


Figure 6.26: Downcore variations of selected parameters indicating the significant change in the organic matter composition in Lake Meerfelder Maar during the middle Holocene; dashed lines indicate the duration of the Younger Dryas cold period

$C_{18:1}$ fatty acid, show strongly enriched concentrations during that interval (*cf.* *Fig. 6.26*). The concentration of the ^{13}C depleted C_{21} *n*-alkane is finally strongly increased during that time ($36.7 \mu\text{g/g TOC}$ *vs.* $17.8 \mu\text{g/g TOC}$ on average) in, moreover, good temporal correlation to hop-17(21)-ene concentration. The latter is proposed to originate from hop-22(29)-ene, an initial C_{30} triterpenoid (Farri-*mond and Telnaes, 1996*). Thiel *et al.* (1999) found this compound to originate from bacterial productivity. Since hop-17(21)-ene has not been reported to be found in specific bacterial species, the authors argued for methanotrophic bacteria that are known to synthesise the precursor molecule hop-22(29)-ene as source organisms.

An increased autochthonous productivity in Lake Meerfelder Maar under strong oxygen consumption, resulting in methanogenesis taking place, as well as the extensive growth of macrophytes point to an extensive shallow water zone. Due to the special morphometry of the Lake Meerfelder Maar volcanic crater (*cf.* *Fig. 3.2*), it can be influenced by minimum lake level fluctuations. Only an increase by 1 m compared to the present day lake level leads to a significantly enlarged

shallow water zone. This would be a preferred habitat for aquatic macrophytes, which would utilise methanogenesis derived carbon for photosynthesis and therefore contribute strongly $\delta^{13}\text{C}$ depleted C_{21} *n*-alkanes as observed. Thus, an increased lake level must be considered for Lake Meerfelder Maar at least between 8,850 – 3,765 vyears BP compared to the present-day conditions which would be in agreement with sedimentological investigations of the same archive (Brauer, pers. comm.).

The distribution of unsaturated fatty acids, especially the $\text{C}_{18:1}$ homologue, which have been evaluated to reflect autochthonous organic matter contribution, show increasing trends in both Eifel Maar Lakes beginning approximately with the end of the period of Holocene climate optimum conditions. This trend persists until 2,536 vyears BP, just into the Subatlantic profile section, in case of Lake Holzmaar. Slightly different, Lake Meerfelder Maar maximum abundance occurred 4,000 vyears BP and may still be caused by the high lake level. Nevertheless, concentrations remain on a high level above this date, pointing to high autochthonous matter contribution during Holocene/Subatlantic transition. This, the increasing dinosterol and brassicasterol concentrations with decreasing age as well as the reduced land plant derived biomarker concentrations (long chain *n*-alkyl lipids) can be interpreted with cooler and/or dryer conditions after the Holocene climate optimum.

This finding is further supported by bacteria derived biomarker distributions. Based on the BTR_{FA} ratios for both Eifel Maar Lake archives, minimum values during the Holocene climate optimum indicate high allochthonous productivity under warm and/or wet conditions, whereas the younger Holocene sequence is in turn characterised by increasing values, indicating a change to more cold and/or dry conditions, benefitting the autochthonous productivity. In case of Lake Meerfelder Maar, a probable overprint is obvious again during the stage of assumed higher lake levels during Holocene.

Substantial differences in organic matter composition between the investigated archives were detected during the most recent Subatlantic profile sections. A correlation to climate and/or environmental conditions, however, is difficult, since increasing human activities probably overprint the climate induced changes of autochthonous and allochthonous bioproductivity.

In general, reduced organic carbon content as well as HI values above

2,686 vyears BP and 3,765 vyears BP for Lake Holzmaar and Lake Meerfelder Maar, respectively, are interpreted as sedimentation of less organic material in lower quality. This interpretation is further supported by simultaneously increased OI values for both maar lakes, pointing to enhanced surface run-off as noted by Wilkes *et al.* (1999). This assumption is consistent with the enhanced amounts of clastic sediment material as published by Zolitschka and Negendank (1998) and Brauer *et al.* (1999a) for both Eifel Maar Lake archives during the Subatlantic. Beside this general correspondence between the investigated sedimentary records, the evaluation of lipid biomarker distributions of these youngest sediment sections yielded remarkable differences as described in the following:

As inferred from normal chain lipid distributions, a slight increase in autochthonous productivity can be assumed for both archives, that is more distinct for Lake Meerfelder Maar. Contrasting results were merely found for Lake Holzmaar, where short chain fatty acids show a pronounced maximum abundance at the Holocene/Subatlantic transition, while concentrations are strongly reduced during the overlying samples; the increasing trend was limited to the period between the two uppermost samples. Also the more specific sterol biomarkers show the same general trend, but both, dinosterol and brassicasterol, show significant maximum concentrations at 2,536 – 2,083 vyears BP in Lake Holzmaar as well as between 1,910 – 1,740 vyears BP in Lake Meerfelder Maar sedimentary sequence, pointing to significantly enhanced contribution from dinoflagellates and diatoms, respectively. Since the increase of both sterol concentrations occurred nearly constant beginning from from Holocene climate optimum in Lake Holzmaar, a general reduction of autochthonous productivity can be assumed above this date. Lake Meerfelder Maar shows an equivalent trend, the increase of sterols dinosterol and brassicasterol, however, occurs not continuous during Holocene to Subatlantic, is probably overprinted by effects of the lake level fluctuation is figured out above; the behavior at the Holocene/Subatlantic transition, however, is quite similar. Thus, a general shift of climatic conditions can be inferred for this transition. Since markers for autochthonous productivity rapidly decrease, the change seems to be orientated to warmer and/or wetter conditions.

The loss of land plant derived normal chain *n* alkyl lipids above approximately 2,000 vyears BP on the other hand probably seems to be interpretable by human induced deforestation. This hypothesis would be supported by the age related variations of the *n*-alkane ratios, giving evidence for a change in land plant vegetation

to more dominant herbs and shrubs as allochthonous organic matter contributors simultaneously for both lakes in that range of time.

Summary: Up to now, various biomarker parameters have been demonstrated to reflect enhanced bioproductivity at the transition from glacial ages to the Holocene and especially during the stage of Holocene climate optimum conditions, affecting both autochthonous and allochthonous bioproductivity. Moreover, some of these proxy-compounds have been evaluated to describe substantial differences in the sediment composition of both Eifel Maar Lakes, that can not be triggered by varying climate and/or environmental conditions since these conditions need to be at least very similar for both archives. Including the morphometry of investigated maar craters, these parameters reflect changes of the lake level of Lake Meerfelder Maar. Only little variation in water depth leads to immensely changes in the extension of the shallow water zone and thus to substantial changes in the composition of the organic matter contributing organisms in this lake and its surrounding catchment area.

Also sharp changes in organic matter composition were detected during the Holocene/Subatlantic transition, being initiated with a sharp peak of autochthonous productivity, that points to relatively cold and/or dry conditions, which are further ameliorated during Subatlantic as evidenced by reduced autochthonously derived proxy-markers.

6.3.1.1 The Lateglacial to Holocene Transition

The climatic conditions during the Lateglacial to Holocene transition are still under discussion. A rapid warming is known to have occurred after the last European glaciation during Allerød and Bølling. This climate amelioration, however, was not continuous until the Holocene optimum. Rather, an intermediate cooling is represented by the Younger Dryas period. Reasons for this period are discussed controversially in the literature: The deglaciation after the Lateglacial resulted in changed North Atlantic Ocean circulation as inferred from $\delta^{14}\text{C}$ by Goslar *et al.* (1999). On the other hand, a change in solar activity, that might have affected central European climate, has also been taken in account (Goslar *et al.*, 2000). Climatic conditions during the Younger Dryas and consequences for vegetation development are still under strong investigation.

Based on sedimentological and pollen data, Brauer *et al.* (1999a) determined its duration between 12,680 – 12,665 vyears BP and 11,640 – 11,590 vyears BP which is in good correlation to similar works cited therein. Its beginning was explained with major changes in the North Atlantic Ocean Thermohaline Circulation (THC) due to melt water pulses from icebergs as inferred from $\delta^{14}\text{C}$ variations, drastically affecting climatic conditions (Goslar *et al.*, 1999). Merely, an anomalous behavior during the middle Younger Dryas remained without explanation. More recently (Goslar *et al.*, 2000) relevated this finding and explained changing $\delta^{14}\text{C}$ content by varying solar activity. Thus, deep ocean circulation during the Younger Dryas might be similar to the present-day conditions. Additionally, van Geel *et al.* (1999) and Renssen *et al.* (2000) found the change in $\delta^{14}\text{C}$ being too abrupt to be caused by changed North Atlantic Ocean circulation, which is expected to affect more drowsy. The latter study also identified the Younger Dryas being part of an approximately 2,500 year quasi-cycle recorded in $\delta^{14}\text{C}$ date that must be caused by solar activity. Apart from that, Lowell *et al.* (1995); Thompson *et al.* (1995) and Bard *et al.* (1997) found evidence for the Younger Dryas having occurred also on southern hemisphere. This can not be caused by the THC of the Northern Atlantic Ocean only.

In contrast to the widely available literature about reasons and duration of the late Pleistocene climate cooling during the Younger Dryas, only little is known about vegetation response to the changed conditions. Brauer *et al.* (1999b) found

Table 6.6: Parameters, partitioning the Younger Dryas period

Parameter (Average)	Above 12, 220 vyears BP	Below 12, 250 vyears BP
TOC [%]	1.49	3.59
TIC [%]	0.54	1.29
TS [%]	0.26	0.68
HI [mg HC/ g TOC]	209	344
Summed <i>n</i> -alkanes [mg/ g TOC]	0.844	0.531
Σ C ₂₇ -C ₃₁ <i>n</i> -alkanes [μ g/ g TOC]	434.72	272.96
C _{16:1} +C _{18:1} fatty acids [μ g/ g TOC]	8.31	35.07
Summed hopanoid acids [μ g/ g TOC]	81.62	269.76
brassicasterol [μ g/ g TOC]	4.49	5.80

a highly specific bi-partitioning of the Younger Dryas period in an earlier and later stage based on sedimentological investigation. Because of the lack in a synchronous vegetation signal retrieved from pollen data, the authors explained the observed subdivision of the Younger Dryas by changes in local hydrological conditions. During the early Younger Dryas, soil erosion may have resulted in eutrophication leading to increased primary production. The sedimentological changes in the late Younger Dryas might be due to a changed course of the Meerbach stream, which after 12, 240 vyears BP may have drained into the lake and thereby increasing the catchment. This could have been triggered by an increase in precipitation. Two studies of Mid-European settings (Lake Ammersee, Lake Steisslingen; [von Grafenstein *et al.* \(1999\)](#); [Schwark *et al.* \(2002\)](#)), however, found climate related changes in the terrestrial vegetation composition. The authors of the latter study, for instance, reported that the relative proportion of the C₂₇ *n*-alkane correlates well with birch pollen and shows a local maximum in the middle of the Younger Dryas; *n*-C₂₇ is generally lower in the early Younger Dryas compared to the late Younger Dryas. A similar variability of *n*-C₂₇ is not observed in Lake Meerfelder Maar, again in agreement with the pollen data which do not provide evidence for vegetation changes here. However, these observations provide common evidence for a significant variability of organic matter in lake sediments during the relatively short Younger Dryas period caused by climatic variations as explained in the following:

Various measured parameters showing significant shifts during the Younger Dryas period are listed in [Table 6.6](#). All bulk organic geochemical parameters as listed

there show a shift to lower values between 12,250 – 12,220 vyears BP, two neighboring samples. These results preliminary give evidence for a significant change in the organic matter composition at this time. Reduced organic carbon content and HI values point to a reduced autochthonous productivity and lower quality of the sedimentary organic matter during the later stage of the Younger Dryas. This behavior is reflected by that of a number of biomarker parameters as listed in *Table 6.6*: The concentrations of algally and bacteria derived unsaturated C_{16:1} and C_{18:1} fatty acids are sharply lowered between 12,250 – 12,220 vyears BP and also their abundance in relation to the respective saturated homologues, especially in the case of the C_{16:1} fatty acid, show the same trend. Further supporting this hypothesis, the bi-partitioning is very clearly reflected in hopanoic acid concentrations. Between the two neighboring samples between 12,250 – 12,220 vyears BP, concentrations are sharply lowered, most marked for the most abundant homologue dihomohopanecarboxylic acid. This gives a strong evidence for sharply reduced bacterial activity at this time in Lake Meerfelder Maar.

Out of the detected sterols, reduced abundances above 12,250 vyears BP could be determined for brassicasterol, indicating reduced productivity of diatoms, whereas dinosterol concentrations contrary show now significant variation at the detected transition border and, moreover, an increasing trend during the overlying late Younger Dryas period, giving evidence for an increasing growth of dinoflagellates.

Beside the proxy-markers typically for autochthonous organic matter contribution to the lake sediment, proportions of land plant derived *n*-alkyl lipids indicate an increasing contribution from land plants to the sedimentary organic matter especially above 11,910 vyears BP, slightly after the proposed change of climatic conditions, what could be explained with a necessary time delay between changing environmental conditions on the one hand and vegetation response on the other hand. An event in vegetation response during the middle Younger Dryas as found by *Schwark et al. (2002)* based on both, C₂₇ *n*-alkane concentration as well as birch pollen numbers, can not be confirmed for Lake Meerfelder Maar. In the actual study, concentrations of that homologue as well as of the heavier homologues show nearly constant concentrations on a relatively low level below 12,250 vyears BP and further become continuously enriched during late Younger Dryas as illustrated in *Fig. 6.27*. Despite the lack in correlating vegetation signals as inferred from pollen analysis as published by *Brauer et al. (1999b)*, this finding is in a general consistency with the pollen diagram from *Litt et al. (2001)*, at least indicating

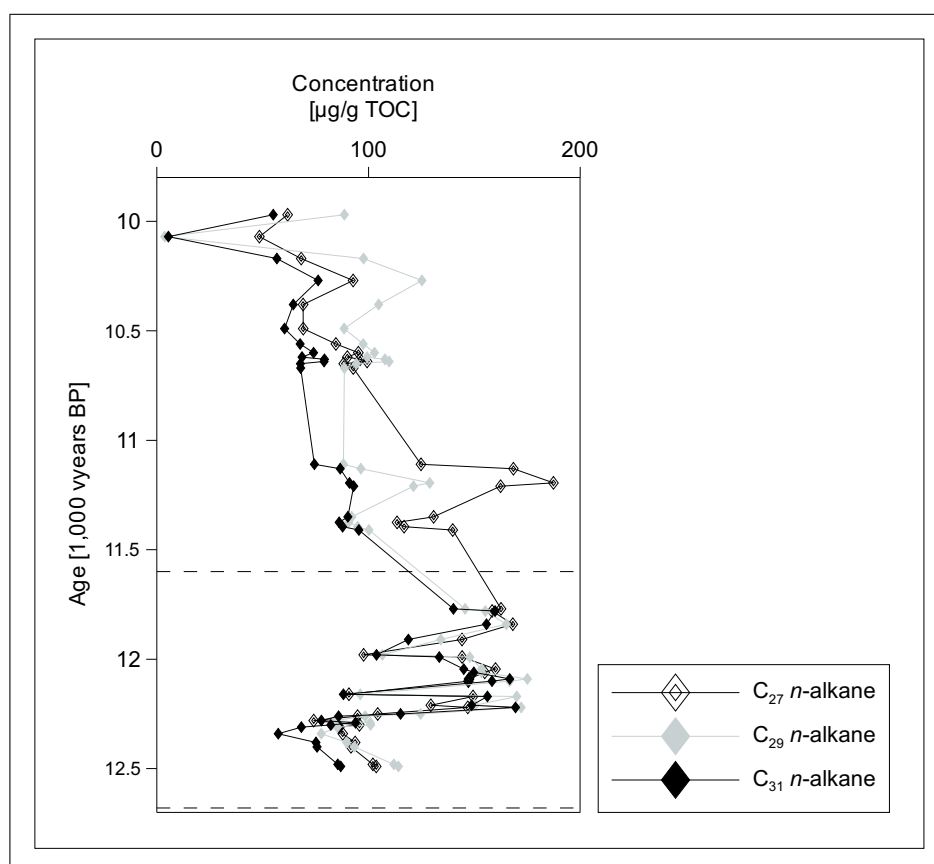


Figure 6.27: Downcore C₂₇ (open symbols), C₂₉ (gray symbols) and C₃₁ (black symbols) *n*-alkane concentrations for Lake Meerfelder Maar during the Younger Dryas period as indicated by dashed lines and transition to the early Holocene

increased tree and shrub abundances during late Younger Dryas in the catchment. Thus, ameliorating climate conditions benefitting terrestrial vegetation forms must be considered for this period.

Summary: Based on the findings about Younger Dryas vegetation development, the decreasing autochthonous lake productivity and the increase in terrestrial derived biomarker abundances, warmer and/or more humid conditions can be assumed for the later sub-period of the Younger Dryas. Land plants and especially tree vegetation forms benefit from increased atmospheric temperatures. Moreover, assumed more humid conditions are in consistency with the proposed higher precipitation (Brauer et al., 1999b). Triggered by higher precipitation, the Meerbach stream might have drained into Lake Meerfelder Maar beginning from late Younger Dryas due to an increased water level and thus have enlarged the catchment area, furthermore increasing allochthonous organic matter supply to the sediment. In this case, the drainage into the lake occurred suddenly, explaining the rapid shift in many parameters as described. The change in climatic conditions occurred gradually, explaining the continuous shifts, e.g. in long chain n-alkyl lipid increase

6.3.2 Lake Großer Treppensee

Paleoclimatic interpretation for investigated Lake Großer Treppensee sediments is based on a less wide data base since lipid biomarker distributions beside the bulk organic geochemical data are limited to aliphatic hydrocarbon distributions.

Nevertheless, just bulk organic geochemical data well reflect the lithozones as published by Giesecke (1999): The Younger Dryas cold period is probably included with the lowermost samples since a comparable dating as used for the Eifel Maar Lake sediments is not available, no precise particulars are possible. Low organic carbon content, HI parameters and strongly decreasing long chain *n*-alkane concentrations on the one hand and increasing inorganic carbon content on the other hand between the three lowermost samples, however, point to a less dominant terrestrial vegetation as it would be expected during stages of lower temperatures. Especially the increasing TIC values additionally indicate enforced surface run-off. Probable sources of the needed water supply could be the last deglaciation, leading to increased water gauge of the Schlaube stream.

Increasing organic carbon content and, more marked, HI parameters at least during the Preboreal and Atlantic point to increased autochthonous productivity and/or increased quality of deposited organic matter. This is generally supported by time-synchronously increased *n*-alkane abundances. More specific, enrichments, especially in short chain homologues as well as time synchronously in summed cholestane concentrations, substantiate enhanced autochthonous organic matter contribution during the Atlantic, whereas mid-chain *n*-alkanes, typically for aquatic macrophytes as respective sources, show a distinct maximum during the Younger Dryas and further remain on the lowest overall level during Preboreal and Atlantic.

Terrestrial vegetation forms are reduced during the Younger Dryas due to cooler or dryer temperatures; a rapid onset of enhanced growth can clearly be inferred above 23.9 m profile depth. As inferred from C_{27} vs. C_{31} *n*-alkane ratios, this enrichment in terrestrial vegetation forms, however, is due to enhanced growth of herbs and shrubs. A continuous increase of tree vegetation can be retrieved above 19.8 m profile depth during the middle Atlantic and further Subboreal. Synchronously, also macrophyte derived *n*-alkanes increase whereas lowered short chain *n*-alkane and cholestane (above 18.8 m) concentrations indicate reduced autochthonous productivity. Thus, a significant amelioration of the climate towards higher tempera-

tures and/or more humid conditions must be considered during middle Atlantic and early Subboreal stages.

Another shift in environmental or climatic conditions is obvious from bulk organic geochemical parameters as well as aliphatic hydrocarbon distributions during the early Subatlantic above 16.9 m profile depth. Beside nearly constant organic carbon content, HI values are rapidly decreasing. Contrarily, short chain *n*-alkane concentrations as proxies for autochthonous productivity slightly increase above this point, whereas aquatic macrophytes as organic matter sources seem to be drastically reduced after a sharp growth during the Atlantic and also land plant derived long chain *n*-alkane proportions show slight depletions. Later on parameters remain relatively stable until 9.8 m below the sediment surface.

In the opposite direction as described during the last paragraph, changes in bulk organic geochemical data as well as aliphatic hydrocarbon distributions are obvious above this depth. Reduced short and medium chain *n*-alkane concentrations as well as a significant enrichment in land plant derived long chain homologues indicate a benefit of terrestrial vegetation from ameliorated climate conditions. Beside increasing TOC contents, this is, however, not supported by changes in HI values.

The uppermost Subatlantic section is finally characterised by deteriorated conditions, since long chain *n*-alkanes decrease. Moreover, the C₂₇ vs. C₃₁ *n*-alkane ratio gives evidence for a shift from terrestrial vegetation forms towards more dominant herbs and shrubs. Beside the increase in autochthonous derived proxies, a human influence e.g. by deforestation can not be excluded.

7 Summary and Conclusions

With the growing understanding of human influence on the Earth system, an increasing number of scientific investigations focuses on vegetation responses to changing environmental and/or climatic conditions. A detailed prediction, how e.g. increasing atmospheric temperatures affect the composition of terrestrial and aquatic vegetation composition, however, remains difficult without a detailed knowledge of comparable changes during the past.

A number of archives recording changes in environmental and/or climatic conditions under varying temporal integration and resolution have been evaluated up to now. Changing conditions are, however, not recorded directly. Measured proxy-parameters need to be interpreted and correlated to environmental and climatic parameters.

Lacustrine sedimentary archives are generally regarded as excellent archives in terms of paleolimnology. Sediments of two maar lakes, a special form of crater lakes, have been selected as sedimentary records for the study presented here. The lipid compositions of Lake Holzmaar and Lake Meerfelder Maar sediments have been evaluated with respect to varying proportions of autochthonous and allochthonous organic matter contribution. In a second step, detected changes in organic matter contributing sources were correlated to environmental and climatic changes. In order to overcome the regional scale of this investigation, sediments from Lake Großer Treppensee, eastern Brandenburg, were added to this study and investigated under the same programme. A selected section of Lake Meerfelder Maar sedimentary profile including the Younger Dryas cold period and transition to the early Holocene was finally analysed under highest achievable temporal resolution to detect vegetation response to climatic change in high detail.

Bulk organic geochemical parameters (TOC, TIC, TS, TN, HI, OI) were measured as fundamental data. Lipids were extracted using a flow blending method and further separated into compound specific fractions using a semi-preparative liquid-chromatographic separation procedure. The fractions of aliphatic hydrocarbons, carboxylic acids and alcohols plus sterols were inventoried by means of gas chromatography (GC) and gas chromatography-mass spectrometry (GC-MS). GC-MS was performed in order to identify individual compounds by interpretation of mass spectra and comparison with authentic standards and/or literature data; GC was performed for quantification of these compounds.

A compelling prerequisite for the connection between lipid distributions and environmental and/or climatic conditions is a good preservation of the investigated sedimentary matter. Using three different parameters, TOC/TS, Pristane/Phytane and UR_{FA} ratios, it could be confirmed that the investigated sedimentary records are well preserved. A partial loss of organic matter could not be excluded, however, the organic matter composition was found to be not overprinted by diagenetic effects by far. It was therefore concluded, that changes in the lipid composition are related to changes in the organic matter contributing community in and around the investigated lakes as a result of changing environmental and/or climatic conditions.

At next, detected lipids were assigned to their respective source- and/or source organism groups. In the case of normal chain lipids, the generally accepted assignment to aquatic sources and land plants could be confirmed by cluster analysis. Based on this analysis, the recently suggested marker molecules of aquatic macrophytes in the middle chain length range, however, had to be modified due to a slightly different assignment of the respective homologues.

The application of these findings to the investigated sedimentary profiles identified a prominent contribution of higher land plants to the sedimentary organic matter fractions of all three profiles, that developed after the last Glacial. Important differences in aquatic macrophyte growth were further found between the two Eifel Maar Lakes. The investigation of selected long chain homologues further allowed a specification of changes in the contribution of herbs and shrubs *vs.* trees during times.

After the primary production seemed to be underrepresented as organic matter source from the detected normal chain lipids, a more reliable reconstruction was allowed by the composition of several sterol homologues in the sedimentary records. In addition to the more general approach based on carbon numbers of detected individual sterols, known compound specific parameters were applied and modified in the present study.

The changing composition of the organic matter contributors in and around the investigated lakes was finally used as a framework to assess the development of environmental and/or climatic conditions in the respective catchment areas. Beside the reconstruction of the climate amelioration at the late Glacial/early Holocene transition and further towards the Holocene climate optimum, that was shown to effect both autochthonous and allochthonous productivity, a regional phenomenon of Lake Meerfelder Maar became obvious from various biomarker parameters. Accordingly, a slightly increased lake level during the Holocene climate optimum seems to have caused an extensive shallow water zone. The consequently changed composition of the ecosystem was shown to be reflected in the biomarker composition.

The investigation of the temporally high resolved core section of Lake Meerfelder Maar finally substantially supported the recent discussion on climatic change during the Younger Dryas period of cooler temperatures, which was former seen to be homogeneous. The data of the investigated profile section yielded a significant and sharp shift in the composition of the sedimentary organic matter during the Younger Dryas. A supposed change of the Meerbach stream into Lake Meerfelder Maar during the late Younger Dryas might explain the abrupt shifts. The more continuous shifts of other proxy compounds, however, also support a climatically driven change of the vegetation in the catchment area of Lake Meerfelder Maar. A comparison with sediments from other maar lake sediments thus may be useful to separate local phenomena from climatic change and to support the ongoing discussion on the Younger Dryas climate.

Bibliography

- Ariztegui, D., Chondrogianni, C., Lami, A., Guilizzoni, P., Lafargue, E., 2001. Lacustrine organic matter and the Holocene paleoenvironmental record of Lake Albano (central Italy). *Journal of Paleolimnology* 26(3), 283–292.
- Ariztegui, D., Farrimond, P., McKenzie, J. A., 1996. Compositional variations in sedimentary lacustrine organic matter and their implications for high Alpine Holocene environmental changes: Lake St. Moritz, Switzerland. *Organic Geochemistry* 24, 453–461.
- Attaway, D. H., Haug, P., Parker, P. L., 1971. Sterols in five coastal spermatophytes. *Lipid* 6, 687–691.
- Bard, E., Rostek, F., Sonzogni, C., 1997. Interhemispheric synchrony of the last deglaciation inferred from alkenone palaeothermometry. *Nature* 385, 707–710.
- Barnes, M. A., Barnes, W. C., 1978. Organic compounds in lake sediments. In: Lerman, A. (ed.), *Lakes: Chemistry, Geology, Physics*. Springer-Verlag, Berlin, 127–152.
- Barrero, A. F., Oltra, J. E., Poyatos, J. A., Jiménez, D., Oliver, E., 1998. Phycomysterols and Other Sterols from the Fungus *Phycomyces blakesleeanus*. *Journal of Natural Products* 61, 1491–1496.
- Barrett, S. M., Volkman, J. K., Dunstan, G. A., LeRoi, J.-M., 1995. Sterols of 14 species of marine diatoms (Bacillariophyta). *Journal of Phycology* 31, 360–369.

- Berner, R. A., 1989. Biochemical cycles of carbon and sulfur and their effect on atmospheric oxygen over Phanerozoic time. *Paleogeography, Paleoclimatology, Paleoecology* 73, 97–122.
- Blumer, M., Cooper, W. J., 1967. Isoprenoid acids in recent sediments. *Science* 158, 1463–1464.
- Blumer, M., Guillard, R. R. L., Chase, T., 1971. Hydrocarbons of marine phytoplankton. *International Journal on Life in Oceans and Coastal Waters* 8, 183–189.
- Bonani, G., Susan, D., Niklaus, T., Suter, M., Housley, R., Bronk, C., van Klinken, G., Hedges, R., 1992. Altersbestimmung von Milligrammproben der Ötztaler Gletscherleiche mit der Beschleunigermassenspektrometrie-Methode (AMS). In: Höpfel, F., Platzner, W., Spindler, K. (eds.), *Der Mann im Eis*, Bd. 1. Veröffentlichung der Universität Innsbruck, 108–116.
- Bond, G., Showers, W., Cheseby, M., Lotti, R., Almasi, P., deMenocal, P., Priore, P., Cullen, H., Hajdas, I., Bonani, G., 1997. A pervasive millennial-scale cycle in North Atlantic Holocene. *Science* 278, 1257–1266.
- Boon, J. J., Rijpstra, R. I. C., de Lange, F., de Leeuw, J. W., Yoshioka, M., Shimizu, Y., 1979. Black Sea sterol - a molecular fossil for dinoflagellate blooms. *Nature* 277, 125–127.
- Boon, J. J., Rijpstra, W. I. C., de Leeuw, J. W., Schenk, P. A., 1975. Phytanic acids in sediments. *Nature* 258, 414–416.
- Bordowskiy, O. K., 1965a. Accumulation of organic matter in bottom sediments. *Marine Geology* 3, 33–82.
- Bordowskiy, O. K., 1965b. Sources of organic matter in marine basins. *Marine Geology* 3, 5–31.
- Brassell, S. C., 1993. Applications of biomarkers for delineating marine paleoclimatic fluctuations during the Pleistocene. In: Engel, M. H., Macko, S. A. (eds.), *Organic Geochemistry*. Plenum Press, New York, 699–738.
- Brassell, S. C., Eglinton, G., Marlowe, I. T., Pflaumann, U., Sarnthein, M., 1986. Molecular stratigraphy: a new tool for climatic assessment. *Nature* 320, 129–133.

- Brassell, S. C., Eglinton, G., Maxwell, J. R., 1983. The geochemistry of terpenoids and steroids. *Biochemical Society Transactions* 11, 575–586.
- Brauer, A., Endres, C., Günter, C., Litt, T., Stebich, M., Negendank, J. F. W., 1999a. High resolution sediment and vegetation responses to Younger Dryas climate change in varved lake sediments from Meerfelder Maar, Germany. *Quaternary Science Reviews* 18, 321–329.
- Brauer, A., Endres, C., Negendank, J. W. F., 1999b. Lateglacial calendar year chronology based on annually laminated sediments from Lake Meerfelder Maar, Germany. *Quaternary International* 61, 17–25.
- Brincat, D., Yamada, K., Ishiwatari, R., Uemura, H., Naraoka, H., 2000. Molecular-isotopic stratigraphy of *n*-alkanes in Lake Baikal Holocene and glacial age sediments. *Organic Geochemistry* 31, 287–294.
- Brovkin, V., Levis, S., Loutre, M. F., Crucifix, M., Claussen, M., Ganopolski, A., Kubatzki, C., Petoukhov, V., 2003. Stability analysis of the climate-vegetation system in northern high latitudes. *Climatic Change* 57, 119–138.
- Chappe, B., Albrecht, P., Michaelis, W., 1982. Polar lipids of archaebacteria in sediments and petroleums. *Science* 217, 65–66.
- Clark, R. C., Blumer, M., 1967. Distribution of *n*-paraffins in marine organisms and sediment. *Limnology and Oceanography* 12, 79–87.
- Claussen, M., Brovkin, V., Ganopolski, A., Kubatzki, C., Petoukhov, V., Rahmstorf, S., 1999a. A new model for climate system analysis. *Env. Mod. Assmt.* 4, 209–216.
- Claussen, M., Kubatzki, C., Brovkin, V., Ganopolski, A., Hoelzmann, P., Pachur, H. J., 1999b. Simulation of an abrupt change in Saharan vegetation at the end of the mid-Holocene. *Geophysical Research Letters* 24, 2037–2040.
- Collister, J. W., Rieley, G., Stern, B., Eglinton, G., Fry, B., 1994. Compound-specific $\delta^{13}\text{C}$ analyses of leaf lipids from plants with differing carbon dioxide metabolisms. *Organic Geochemistry* 21, 619–627.
- Cranwell, P. A., 1973a. Branched-chain and cyclopropanoid acids in a recent sediment. *Chemical Geology* 11, 307–313.

- Cranwell, P. A., 1973b. Chain length distribution of *n*-alkanes from lake sediments in relation to post-glacial environmental change. *Freshwater Biology* 3, 259–265.
- Cranwell, P. A., 1974. Monocarboxylic acids in lake sediments: Indicators, derived from terrestrial and aquatic biota, of paleoenvironmental trophic levels. *Chemical Geology* 14, 1–14.
- Cranwell, P. A., 1976. Decomposition of aquatic biota and sediment formation: lipid components of 2 blue-green algal species and of detritus resulting from microbial attack. *Freshwater Biology* 6, 481–488.
- Cranwell, P. A., 1982. Lipids of aquatic sediments and sedimenting particulates. *Prog. Lipid Res.* 21, 271–308.
- Cranwell, P. A., 1984. Lipid geochemistry of sediments from Upton Broad, a small productive lake. *Organic Geochemistry* 7, 25–37.
- Cranwell, P. A., Eglinton, G., Robinson, N., 1987. Lipids of aquatic organisms as potential contributors to lacustrine sediments - II. *Organic Geochemistry* 11, 513–527.
- Dansgaard, W., Johnson, S. J., Clausen, H. B., Dahl-Jensen, D., Gundestrup, N. S., Hammer, C. U., Hvidberg, C. S., Steffensen, J. P., Sveinbjórnsson, A. E., Jouzel, J., Bond, G., 1993. Evidence for general instability of past climate from a 250-kyr ice-core record. *Nature* 364, 218–220.
- Dansgaard, W., Johnson, S. J., Clausen, H. B., Langway, C. C., 1971. Climatic record revealed by the Camp Century ice core. In: Turekian, K. (ed.), *The late Cenozoic glacial ages*. Hartford, Conn., 37–56.
- de Leeuw, J. W., Simoneit, B. R., Boon, J. J., Rijpstra, W. I. C., de Lange, F., v. d. Leeden, J. C. W., Correia, V. A., Burlingame, A. L., Schenk, P. A., 1977. Phytol derived compounds in the geosphere. In: Gomez-Angulo, J. A., Campos, R. (eds.), *Advances in Organic Geochemistry*. Enadisma, Madrid, 61–80.
- Didyk, B. M., Simoneit, B. R. T., Brassell, S. C., Eglinton, G., 1978. Organic geochemical indicators of palaeoenvironmental conditions of sedimentation. *Nature* 272, 216–222.

- Doerffel, K., Eckschlager, K., Henrion, G., 1990. Chemometrische Strategien in der Analytik. Deutscher Verlag für Grundstoffindustrie, Leipzig.
- Eglinton, G., Hamilton, R. J., 1963. The distribution of alkanes. In: Swain, T. (ed.), Chemical Plant Taxonomy. Academic Press, London.
- Eglinton, G., Hamilton, R. J., 1967. Leaf epicuticular waxes. Science 156, 1322.
- Espitalié, J., Deroo, G., Marquis, F., 1985. La pyrolyse Rock-Eval et ses applications. Deuxième partie: Interprétation des paramètres. Rev. Inst. Fr. Pét. 40, 755–784.
- Espitalié, J., Laporte, J. L., Madec, M., Marquis, F., Leplat, P., Paulet, J., Boutefeu, A., 1977. Méthode rapide de caractérisation des roches mères, de leur potentiel pétrolier et de leur degré d'évolution. Rev. Inst. Franç. Pétr. 32, 23–42.
- Eyssen, H. J., Parmentier, G. C., Compennolle, F. C., De Pauw, G., Piessens-Deuff, M., 1973. Biodegradation of sterols by *Eubacterium* ATCC 21, 408–Nova species. European Journal of Biochemistry 36, 411–421.
- Farrimond, P., Telnaes, N., 1996. Three series of rearranged hopanes in Toarcian sediments (northern Italy). Organic Geochemistry 25, 165–177.
- Ficken, K. J., Barber, K. E., Eglinton, G., 1998a. Lipid biomarker, $\delta^{13}\text{C}$ and plant macrofossil stratigraphy of a Scottish montane peat bog over the last two millenia. Organic Geochemistry 28, 217–237.
- Ficken, K. J., Li, B., Swain, D. L., Eglinton, G., 2000. An *n*-alkane proxy for the sedimentary input of submerged/floating freshwater aquatic macrophytes. Organic Geochemistry 31, 745–749.
- Ficken, K. J., Street-Parrot, F. A., Perrott, R. A., Swain, D. L., Olago, D. O., Eglinton, G., 1998b. Glacial/interglacial variations in carbon cycling revealed by molecular and isotope stratigraphy of Lake Nkunga, Mt. Kenya, East Africa. Organic Geochemistry 29, 1701–1719.
- Ficken, K. J., Wooller, M. J., Swain, D. L., Street-Perrott, F. A., Eglinton, G., 2002. Reconstruction of a subalpine grass-dominated ecosystem, Lake Rutundu, Mount Kenya: a novel multi-proxy approach. Paleo 177, 137–149.

- Filley, T. R., Freeman, K. H., Bianchi, T. S., Baskaran, M., Colarusso, L. A., Hatcher, P. G., 2001. An isotopic biogeochemical assessment of shifts in organic matter input to Holocene sediments from Mud Lake, Florida. *Organic Geochemistry* 32, 1153–1167.
- Fuhrmann, A., 2003. Geochemical Indicators of Paleoenvironmental and Paleoclimatic Change in Ancient and Recent Lake Deposits: Facies Models, Facies Distributions and Hydrocarbon Aspects. Ph.D. thesis, Technische Universität Berlin.
- Fuji, N., 1992. Palynological investigation of Core 323-PC1 from Lake Baikal, southeastern Siberia. In: Horie, S., Toyoda, K. (eds.), *International Project on Paleolimnology and Late Cenozoic Climate Newsletter*, volume 6. 103–115.
- Ganopolski, A., Kubatzki, C., Claussen, M., Brovkin, V., Petoukhov, V., 1998. The influence of vegetation-atmosphere-ocean interaction on climate during the mid-Holocene. *Science* 280, 1916–1919.
- Gelpi, E., Oro, J., Schneider, H. J., Bennett, E., 1968. Olefins of high molecular weight in two microscopic algae. *Science* 161, 700–702.
- Gelpi, E., Schneider, H., Mann, J., Oro, J., 1970. Hydrocarbons of geochemical significance in microscopic algae. *Phytochemistry* 9, 603–612.
- Giesecke, T., 1999. Pollenanalytische und sedimentchemische Untersuchungen zur natürlichen und anthropogenen Entwicklung im Schlaubetal. Ph.D. thesis, Humboldt-Universität zu Berlin, Fachbereich Geographie.
- Giner, J. L., Djerassi, C., 1995. A reinvestigation of the biosynthesis of lanosterol in *Euphorbia lathyris*. *Phytochemistry* 39(2), 333–335.
- Goad, L. J., 1981. Sterol biosynthesis and metabolism in marine invertebrates. *Pure and Applied Chemistry* 51, 837–852.
- Goossens, H., de Leeuw, J. W., Schenck, P. A., Brassell, S. C., 1984. Tocopherols as likely precursors of pristane in ancient sediments and crude oils. *Nature* 312, 440–442.
- Goslar, T., Arnold, M., Tisnerat-Laborde, N., Czernik, J., Więckowski, K., 2000. Variations of Younger Dryas atmospheric radiocarbon explicable without ocean circulation changes. *Nature* 403, 877–879.

- Goslar, T., Wohlfarth, B., Björck, S., Possnert, G., Björck, J., 1999. Variations of atmospheric ^{14}C concentrations over the Allerød-Younger Dryas transition. *Climate Dynamics* 15, 29–42.
- Griffiths, M., 1978. Specific blue-green algal carotenoids in sediments of Esthwaite Water. *Limnology and Oceanography* 23, 777–784.
- Haaren, C. v., 1992. The development of landscape around the maar lakes. *Arch. Hydrobiol. Beih. Ergebn. Limnol.* 38, 11–32.
- Haddad, R. I., Martens, C. S., Farrington, J. W., 1992. Quantifying early diagenesis of fatty acids in a rapidly accumulating coastal marine sediment. *Organic Geochemistry* 19, 205–216.
- Hajdas, I., Zolitschka, B., Ivy-Ochs, S. D., Beer, J., Bonani, G., Leroy, S. A. G., Negendank, J. W., Ramrath, M., Suter, M., 1995. AMS Radiocarbon Dating Of Annually Laminated Sediments from Lake Holzmaar, Germany. *Quaternary Science Reviews* 14, 137–143.
- Halbfass, W., 1896. Die noch mit Wasser gefüllten Maare der Eifel. *Verhandlungen des naturhistorischen Vereins der preußischen Rheinlande und Westfalens* 53, 310–335.
- Halbfass, W., 1897. Tiefen- und Temperaturverhältnisse der Eifelmaare. Dr. A. Petermann's Mitteilungen aus Justhus Perthes' geographischen Anstalt 43, 149–153.
- Harvey, H. R., Eglinton, G., O'Hara, S. C. M., Corner, E. D. S., 1987. Biotransformation and assimilation of dietary lipids by *Calanus* feeding on a dinoflagellate. *Geochimica et Cosmochimica Acta* 51, 3031–3040.
- Hedges, J. I., Clark, W. A., Quay, P. D., Richey, J. E., Devol, A. H., Santos, U. d. M., 1986. Composition and fluxes of particulate organic material in the Amazon River. *Limnol. Oceanogr.* 31, 717–738.
- Hedges, J. I., Ertel, J. R., Leopold, E. B., 1982. Lignin geochemistry of a Late Quaternary sediment core from Lake Washington. *Geochimica et Cosmochimica Acta* 46, 1869–1877.

- Hedges, J. I., Mann, D. C., 1979. The characterization of plant tissues by their lignin oxidation products. *Geochimica et Cosmochimica Acta* 43, 1803–1807.
- Herbin, G. A., Robins, P. A., 1968. Studies on plant cuticular waxes – III. The leaf wax alkanes and hydroxy acids of some members of the Cupressaceae and Pinaceae. *Phytochemistry* 7, 1325.
- Hoefs, J., 1997. *Stable Isotope Geochemistry*, volume 4. Springer.
- Holton, R. W., Blecker, H. H., Onore, M., 1964. Effect of growth temperature on the fatty acid composition of blue-green algae. *Phytochemistry* 3, 595–602.
- Holton, R. W., Blecker, H. H., Stevens, T. S., 1968. Fatty acids in blue-green algae: Possible relation to phylogenetic position. *Science* 160, 545–547.
- Hornibrook, E. R. C., Longstaffe, F. J., Fyfe, W. S., 2000. Evolution of stable carbon isotope compositions of methane and carbon dioxide in freshwater wetlands and other anaerobic environments. *Geochimica et Cosmochimica Acta* 64(6), 1013–1027.
- Horsfield, B., 1978. . Ph.D. thesis, Newcastle Upon Tyne University, England.
- Horsfield, B., Curry, D. J., Bohacs, K., Littke, R., Rullkötter, J., Schenk, H. J., Radke, M., Schaefer, R. G., Carroll, A. R., Isaksen, G., Witte, E. G., 1994. Organic geochemistry of freshwater and alkaline lacustrine sediments in the Gree River Formation of the Washakie Basin, Wyoming, U.S.A. In: *Advances in Organic Geochemistry 1993*, volume 22. Elsevier Science Ltd., 415–440.
- Huang, W.-Y., Meinschein, W. G., 1976. Sterols as source indicators of organic materials in sediments. *Geochimica et Cosmochimica Acta* 40, 323–330.
- Huang, W.-Y., Meinschein, W. G., 1979. Sterols as ecological indicators. *Geochimica et Cosmochimica Acta* 43, 739–745.
- Huang, Y., Street-Perrott, F. A., Perrott, R. A., Metzger, P., Eglinton, G., 1999. Glacial-interglacial environmental changes inferred from molecular and compound specific $\delta^{13}\text{C}$ analyses of sediments from Sacred Lake, Mt. Kenya. *Geochimica et Cosmochimica Acta* 63, 1383–1404.

- Hughes, W. B., Holba, A. G., Dzou, L. I. P., 1995. The ratios of dibenzothiophene to phenanthrene and pristane to phytane as indicators of depositional environment and lithology of petroleum source rocks. *Geochimica et Cosmochimica Acta* 59, 3581–3598.
- Hutchinson, D. R., Golmshtok, A. J., Zonenshain, L. P., Moore, T. C., Scholz, C. A., Klitgord, K. D., 1992. Depositional and tectonic framework of the rift basins of Lake Baikal from multichannel seismic data. *Geology* 20, 589–592.
- Ikan, R., Baedeker, M. J., Kaplan, I. R., 1975. Thermal alteration of organic matter in recent sediments: I. Pigments, II. Isoprenoids and III. Aliphatic and steroidal alcohols. *Geochimica et Cosmochimica Acta* 39, 173–203.
- Ishiwatari, R., Uzaki, M., Yamada, K., Ogura, K., 1992. Organic matter records of environmental changes in Lake Baikal sediments. 1: carbon isotopes, organic carbon and nitrogen. In: Horie, S., Toyoda, K. (eds.), *International Project on Paleolimnology and Late Cenozoic Climate Newsletter*, volume 6. 80–88.
- Johnsen, S. J., Clausen, H. B., Dansgaard, W., Gundestrup, N. S., Hammer, C. U., Andersen, U., Andersen, K. K., Hvidberg, C. S., Dahl-Jensen, D., Steffensen, J. P., Shoji, H., Sveinbjörnsdóttir, A. E., White, J. W. C., Jouzel, J., Fisher, D., 1997. The $\delta^{18}\text{O}$ record along the Greenland Ice Core project deep ice core and the problem of possible Eemian climatic instability. *Journal of Geophysical Research* 102, 26397–26410.
- Kalis, A. J., Merkt, J., Wunderlich, J., 2003. Environmental changes during the Holocene climatic optimum in central Europe – human impact and natural causes. *Quaternary Science Reviews* 22, 33–79.
- Katz, B. J., 1983. Limitations of Rock-Eval pyrolysis for typing organic matter. *Organic Geochemistry* 4, 195–199.
- Kawamura, K., Ishiwatari, R., 1985. Distribution of lipid-class compounds in bottom sediments of freshwater lakes with different trophic status, in Japan. *Chemical Geology* 51, 123–133.
- Kawamura, K., Ishiwatari, R., Ogura, K., 1987. Early diagenesis of organic matter in the water column and sediments: Microbial degradation and resynthesis of lipids in Lake Haruna. *Organic Geochemistry* 11, 251–264.

- Kawamura, K., Ishiwatari, R., Yamazaki, M., 1980. Identification of polyunsaturated fatty acids in surface lacustrine sediments. *Chem. Geol.* 28, 31–39.
- Keeley, J. E., Sandquist, D. R., 1992. Carbon: freshwater plants. *Plant, Cell and Environment* 15, 1021–1035.
- Kerr, R. A., 1997. Greenhouseforecasting still cloudy. *Science* 276, 1040–1042.
- Killops, S. D., Killops, V. J., 1993. *An Introduction to Organic Geochemistry*. Longmann Scientific & Technical, Essex, England.
- Kolattukudy, P., 1980. Cutin, suberin and waxes. In: Stumpf, P. (ed.), *The Biochemistry of Plants, volume Lipids: Structure and Function*. Academic Press, New York, 571–645.
- Kolattukudy, P. E., Croteau, R., Buckner, J. S., 1976. Biochemistry of plant waxes. In: Kolattukudy, P. E. (ed.), *Chemistry and Biochemistry of Natural Waxes*. Elsevier, Amsterdam, The Netherlands, 289–347.
- Kutzbach, J. F., Bartlein, P. J., Foley, J. A., Harrison, S. P., Hostetler, S. W., Liu, Z., Prentice, I. C., Webb, T., 1996. Potential role of vegetation feedback in the climate sensitivity of high-latitude regions: A case study at 6000 years B.P. *Global Biogeochemical Cycles* 10, 727–736.
- Leavitt, S. W., Long, A., 1983. On a 50-year „climate-free“ $\delta^{13}\text{C}$ record from juniper tree rings. *Radiocarbon* 25(2), 267–268.
- Litt, T., 2000. Vegetation history and palaeoclimatology of the Eifel region as inferred from palaeobotanical studies of annually laminated sediments. *Terra Nostra* 6, 259–263.
- Litt, T., Brauer, A., Goslar, T., Merkt, J., Balaga, K., Müller, H., Ralska-Jasiewiczowa, M., Stebich, M., Negendank, J. F. W., 2001. Correlation and synchronisation of Lateglacial continental sequences in northern central Europe based on annually laminated lacustrine sediments. *Quaternary Science Reviews* 20, 1233–1249.
- Litt, T., Stebich, M., 1999. Bio- and chronostratigraphy of the lateglacial in the Eifel region, Germany. *Quaternary International* 61, 5–16.

- Lorenz, V., 1984. Zur Geologie des Meerfelder Maares. In: Irion, G., Negendank, J. F. W. (eds.), Cour. Forsch. Inst. Senckenberg, volume 65. Das Meerfelder Maar, 5–12.
- Lowell, T. V., Heusser, G. J., Andersen, B. G., Moreno, P. I., Hauser, A., Heusser, L. E., Schlüchter, C., Marchant, D. R., Denton, G. H., 1995. Interhemispheric correlation of late Pleistocene glacial events. *Science* 269, 1541–1549.
- Mackenzie, A. S., Brassell, S. C., Eglinton, G., Maxwell, J., 1982. Chemical fossils: The geological fate of steroids. *Science* 217, 491–504.
- Matsuda, H., Koyama, T., 1977a. Early diagenesis of fatty acids in lacustrine sediments—I Identification and distribution of fatty acids in recent sediment from a freshwater lake. *Geochimica et Cosmochimica Acta* 41, 777–783.
- Matsuda, H., Koyama, T., 1977b. Early diagenesis of fatty acids in lacustrine sediments—II A statistical approach to changes in fatty acid composition from recent sediments and source materials. *Geochimica et Cosmochimica Acta* 41, 1825–1834.
- Matsumoto, G., Torii, T., Hanya, T., 1982. High abundance of algal 24-ethylcholesterol in Antarctic lake sediment. *Nature* 299, 52–54.
- Matsumoto, K., Yamada, K., Ishiwatari, R., 2001. Sources of 24-ethylcholest-5-en-3 β -ol in Japan Sea sediments over the past 30,000 years inferred from its carbon isotopic composition. *Organic Geochemistry* 32, 259–269.
- Meinschein, W. G., Kenny, G. S., 1957. Analyses of a chromatographic fraction of organic extracts of soils. *Analytical Chemistry* 29, 1153–1161.
- Menendez, C., Bauer, Z., Huber, H., Gadon, N., Stetter, K. O., Fuchs, G., 1999. Presence of Acetyl Coenzyme A (CoA) Carboxylase and Propionyl CoA Carboxylase in Autotrophic *Crenarchaeota* and Indication for Operation of a 3-Hydroxypropionate Cycle in Autotrophic Carbon Fixation. *Journal of Bacteriology* 181(4), 1088–1098.
- Metzger, P., Casadevall, E., Couté, A., 1988. Botryococcene distribution in strains of the green alga *Botryococcus braunii*. *Phytochemistry* 27, 1383–1388.

- Metzger, P., Casadevall, E., Pouet, M. J., Pouet, J., 1985. Structures of some botryococcenes: Branched hydrocarbons from the B-race of the green alga *Botryococcus braunii*. *Phytochemistry* 24, 2995–3002.
- Meyers, P. A., 1990. Impacts of regional Late Quaternary climate changes on the deposition of sedimentary organic matter in Walker Lake, Nevada. *Palaeogeography, Palaeoclimatology, Palaeoecology* 78, 229–240.
- Meyers, P. A., 1994. Preservation of elemental and isotopic source identification of sedimentary organic matter. *Chemical Geology* 114, 289–302.
- Meyers, P. A., 1997. Organic geochemical proxies of paleoceanographic, paleolimnologic, and paleoclimatic processes. *Organic Geochemistry* 27, 213–250.
- Meyers, P. A., 2003. Applications of organic geochemistry to paleolimnological reconstructions: a summary of examples from the Laurentian Great Lakes. *Organic Geochemistry* 34, 261–289.
- Meyers, P. A., Eadie, B. J., 1993. Sources, degradation and recycling of organic matter associated with sinking particles in Lake Michigan. *Organic Geochemistry* 20, 47–56.
- Meyers, P. A., Edwards, S. J., Eady, B. J., 1980. Fatty acid and hydrocarbon content of settling sediments in Lake Michigan. *J. Great Lakes Res.* 6, 331–337.
- Meyers, P. A., Ishiwatari, R., 1993a. Lacustrine organic geochemistry-an overview of indicators of organic matter sources and diagenesis in lake sediments. *Organic Geochemistry* 20, 867–900.
- Meyers, P. A., Ishiwatari, R., 1993b. *Organic Geochemistry*, chapter 8: The Early Diagenesis of Organic Matter in Lacustrine Sediments. Plenum Press, New York, 185–209.
- Meyers, P. A., Lallier-Vergès, E., 1998. Lacustrine sedimentary organic matter records of Late Quaternary paleoclimates. *Journal of Paleolimnology* 21, 345–372.
- Meyers, P. A., Lallier-Vergès, E., 1999. Lacustrine Sedimentary Organic Matter Records of Late Quaternary Paleoclimates. *Journal of Paleolimnology* 21, 345–372.

- Meyers, P. A., Leenheer, M. J., Eadie, B. J., Maule, S. J., 1984. Organic geochemistry of suspended and settling particulate matter in Lake Michigan. *Geochimica et Cosmochimica Acta* 48, 443–452.
- Mook, W. G., Bommerson, J. C., Staberman, W. H., 1974. Carbon isotope fractionation between dissolved bicarbonate and gaseous carbon dioxide. *Earth and Planetary Science Letters* 22.
- Negendank, J. F. W., Brauer, A., Zolitschka, B., 1990. Die Eifelmaare als erdgeschichtliche Fallen und Quellen zur Rekonstruktion des Paläoenvironments. *Mainzer geowiss. Mitt.* 19, 235–262.
- Negendank, J. F. W., Zolitschka, B., 1993a. Maars and maar lakes of the West-eifel Volcanic Field, chapter Paleolimnology of European Maar Lakes. Springer, Berlin, 61–80.
- Negendank, J. F. W., Zolitschka, B., 1993b. Paleolimnology of European Maar Lakes. *Lecture Notes in Earth Sciences* 49.
- Nichols, P. D., Volkman, J. K., Palmisano, A. C., Smith, G. A., White, D. C., 1988. Occurrence of an isoprenoid C₂₅ diunsaturated alkene and high neutral lipid content in antarctic sea-ice diatom communities. *J. Phycol* 24, 90–96.
- Nishimoto, S., 1974. A Chemotaxonomic Study of *n*-Alkanes in Aquatic Plants. *J. Scr. Hiroshima Univ., Ser. A* 38, 159–163.
- Nishimura, M., Koyama, T., 1976. Stenols and stannols in lake sediments and diatoms. *Chemical Geology* 17, 229–239.
- Nishimura, M., Koyama, T., 1977. The occurrence of stanols in various living organisms and the behavior of sterols in contemporary sediments. *Geochimica et Cosmochimica Acta* 41, 379–385.
- Nott, C. J., Xie, S., Avsejs, L. A., Maddy, D., Chambers, F. M., Evershed, R. P., 2000. *n*-Alkane distributions in ombrotrophic mires as indicators of vegetation change related to climatic variation. *Organic Geochemistry* 31, 231–235.
- O'Brien, S. R., Mayewski, P. A., Meeker, L. D., Meese, D. A., Twickler, M. S., Whitlow, S. I., 1995. Complexity of Holocene climate as reconstructed from a Greenland ice core. *Science* 270, 1962–1964.

- Ogura, K., Machihara, T., Takada, H., 1990. Diagenesis of biomarkers in Biwa lake sediments over 1 million years. *Organic Geochemistry* 16, 805–813.
- O’Leary, M. H., 1981. Carbon isotope fractionation in plants. *Phytochemistry* 20, 553–567.
- Patience, A. J., Lallier-Vergès, E., Alberic, P., Desprairies, A., Tribovillard, N., 1996. Relationships between organo-mineral supply and early diagenesis in the lacustrine environment: A study of surficial sediments from the Lac du Bouchet (Haute Loire, France). *Quaternary Science Reviews* 15, 213–221.
- Peters, K. E., Moldowan, J. M., 1993. The biomarker guide, volume 1. Prentice-Hall, Englewood Cliffs, New Jersey.
- Petoukhov, V., Ganopolski, A., Brovkin, V., Claussen, M., Eliseev, A., Kubatzki, C., Rahmstorf, S., 2000. CLIMBER-2: A climate system model of intermediate complexity. Part I: Model description and performance for present climate. *Climate Dynamics* 16, 1–17.
- Phillips, K. M., Ruggio, D. M., Bailey, J. A., 1999. Precise quantitative determination of phytosterols, stanols, and cholesterol metabolites in human serum by capillary gas-liquid chromatography. *Journal of Chromatography B* 732, 17–29.
- Powell, T. G., McKirdy, D. M., 1973. Relationship between ratio of pristane to phytane, crude oil composition and geological environment in Australia. *Nature* 243, 37–39.
- Prahl, F. G., Muelhausen, L. A., Zahnle, D. A., 1988. Further evaluation of long-chain alkenones as indicators of paleoceanographic conditions. *Geochimica et Cosmochimica Acta* 52, 2303–2310.
- Prahl, F. G., Wakeham, S. G., 1987. Calibration of unsaturation patterns in long-chain ketone compositions for palaeotemperature assessment. *Nature* 330, 367–369.
- Prentice, I. C., Guiot, J., Huntley, B., Jolly, D., Chedadi, R., 1996. Reconstructing biomes from palaeoecological data: a general method and its application to European pollen data at 0 and 6 ka. *Climate Dynamics* 12, 185–194.

- Pryce, R. J., 1971. The occurrence of bound, water-soluble squalene, 4,4-dimethyl sterols and sterols in leaves of *Kalanchoe blossfeldiana*. *Phytochemistry* 10, 1303–1307.
- Radke, M., Sittard, H. G., Welte, D. H., 1978. Removal of soluble organic matter from rock samples with a flow-trough extraction cell. *Anal. Chem.* 50, 663–665.
- Radke, M., Welte, D. H., 1981. The methylphenanthrene index (MPI): A maturity parameter based on aromatic hydrocarbons. *Advances in Organic Geochemistry* 1981, 504–512.
- Radke, M., Welte, D. H., Willsch, H., 1982. Geochemical study on a well in the Western Canada Basin: relation of the aromatic distribution pattern to maturity of organic matter. *Geochimica et Cosmochimica Acta* 46, 1–10.
- Radke, M., Willsch, H., Welte, D. H., 1980. Preparative hydrocarbon group determination by automated medium pressure liquid chromatography. *Anal. Chem.* 52, 406–411.
- Ramrath, A., Zolitschka, B., Wulf, S., Negendank, J. F. W., 1999. Late Pleistocene climatic variations as recorded in two Italian maar lakes (Lago di Mezzano, Lago Grande de Monticchio). *Quaternary Science Reviews* 18, 977–992.
- Rein, B., 1996. Die Warvenchronologie des Holzmaares -Vergleichende Untersuchungen an drei Sedimentprofilen. Ph.D. thesis, Universität Potsdam.
- Renssen, H., van Geel, B., van der Plicht, J., Magny, M., 2000. Reduced solar activity as a trigger for the start of the Younger Dryas? *Quaternary International* 68-71, 373–383.
- Rieley, G., Collier, R. J., Jones, D. M., Eglinton, G., 1991. The biogeochemistry of Ellesmere Lake, U.K. - I: source correlation of leaf wax inputs into the sedimentary lipid record. *Organic Geochemistry* 17, 901–912.
- Ries-Kautt, M., Albrecht, P., 1989. Hopane-derived triterpenoids in soils. *Chemical Geology* 76, 143–151.
- Risatti, J. B., Rowland, S. J., Yan, D. A., Maxwell, J. R., 1984. Stereochemical studies isoprenoids-XII: Lipids of methanogenic bacteria and possible contributors to sediments. *Organic Geochemistry* 6, 93–104.

- Robinson, N., Cranwell, P. A., Finlay, B. J., Eglinton, G., 1984a. Lipids of aquatic organisms as potential contributors to lacustrine sediments. *Organic Geochemistry* 6, 143–152.
- Robinson, N., Eglinton, G., Brassell, S. C., 1984b. Dinoflagellate origin for sedimentary 4 α -methylsteroids and 5 α (H)-stanols. *Nature* 308, 439–441.
- Rozema, J., van Geel, B., Björn, L. A., Lean, J., Madronich, S., 2002. Towards Solving the UV Puzzle. *Science* 296, 1621–1622.
- Rudd, J. W. M., Kelly, C. A., Furutani, A., 1986. The role of sulfat reduction in long term accumulation of organic and inorganic sulfur in lake sediments. *Limnol. Oceanogr.* 31, 1281–1291.
- Scharf, B. W., Menn, U., 1992. Hydrology and morphometry. *Arch. Hydrobiol. Beih. Ergebn. Limnol.* 38, 43–62.
- Scharf, B. W., Oehms, M., 1992. Physical and chemical characteristics. *Arch. Hydrobiol. Beih. Ergebn. Limnol.* 38, 63–83.
- Schneider, H., Gelpi, E., Bennett, E. O., Oro, J., 1970. Fatty acids of geochemical significance in microscopic algae. *Phytochemistry* 9, 613–617.
- Schomburg, G., 1987. *Gaschromatographie, Grundlagen, Praxis, Kapillartechnik*. VCH, Weinheim.
- Schönfelder, I., Steinberg, C. E. W., 1999. Quantitative Rekonstruktion klimatisch bedingter Umweltveränderungen im Spätglazial und Holozän in Sedimenten von Schlaube und Spree durch Diatomeenanalyse. In: DFG-Schwerpunktprogramm: Wandel der Geo- Biosphäre während der letzten 15000 Jahre. Kontinentale Sedimente als Ausdruck sich verändernder Umweltbedingungen. DFG, Bonn, 13–14.
- Schouten, S., Rijpstra, W. I. K., Kok, M., Hopmans, E. C., Summons, R. E., Volkman, J. K., Sinninghe Damste, J. S., 2001. Molecular organic tracers of biogeochemical processes in a saline meromictic lake (Ace Lake). *Geochimica et Cosmochimica Acta* 65(10), 1629–1640.
- Schrenk-Bergt, C., Zwick, B. W., Jüttner, J., Schoenfelder, J., Facher, E., Casper, P., Wilkes, H., Steinberg, C., 1998. Paläolimnologie: Vorteile und Grenzen bei der angewandten Limnologie. *ecomed, Landsberg am Lech*, 1–49.

- Schulte, S., 1997. Erhaltung und frühe Diagenese von organischem Material in Sedimenten vom pakistanischen Kontinentalrand. Ph.D. thesis, Carl von Ossietzky Universität Oldenburg.
- Schwark, L., Zink, K., Lechterbeck, J., 2002. Reconstruction of postglacial to early Holocene vegetation history in terrestrial Central Europe via cuticular lipid biomarkers and pollen records from lake sediments. *Geology* 30, 463–466.
- Schweingruber, F. H., 1996. Tree Rings and Environment – Dendroecology. Haupt, Bern.
- Sever, J., Parker, P. L., 1969. Fatty alcohols (normal and isoprenoid) in sediments. *Science* 164, 1052–1054.
- Stein, R., 1990. Organic carbon content/sedimentation rate relation ship and its paleoenvironmental significance for marine sediments. *Geo-Marine Letters* 10, 41–56.
- Stein, R., ten Haven, H. L., Littke, R., Rullkötter, J., Welte, D. H., 1989. Accumulation of marine and terrigenous organic carbon at upwelling Site 657 and nonupwelling Sites 657 and 659: Implications for the reconstruction of paleoenvironments in the eastern subtropical Atlantic trough Late Cenozoic times. In: Ruddiman, W. (ed.), *Proceedings of the ODP, Scientific Results*, volume 108. 361–385.
- Steininger, J., 1821. *Neu Beiträge zur Geschichte der Rheinischen Vulkane*. Kupferberg.
- Stockhausen, H., Zolitschka, B., 1999. Environmental changes since 13.000 cal. BP reflected in magnetic and sedimentological properties of sediments from Lake Holzmaar (Germany). *Quaternary Science Reviews* 18, 913–925.
- Takemura, K., Marui, A., Horie, S., 1992. Comments on the core sample 323-PC1 of Lake Baikal from the sedimentological viewpoint. In: Horie, S., Toyoda, K. (eds.), *International Project on Paleolimnology and Late Cenozoic Climate Newsletter*, volume 6. 72–79.
- Talbot, M. R., Laerdal, T., 2000. The late Pleistocene-Holocene palaeolimnology of Lake Victoria, East Africa, based upon elemental and isotopic analyses of sedimentary organic matter. *Journal of Paleolimnology* 23, 141–164.

- Talbot, M. R., Livingstone, D. A., 1989. Hydrogen index and carbon isotopes of lacustrine organic matter as lake level indicators. *Paleogeography, Paleoclimatology, Paleoecology* 70, 121–137.
- ten Haven, H. L., de Leeuw, J. W., Rullkötter, J., Sinningeh Damsté, J. S., 1987. Restricted utility of the pristane/ phytane ratio as a paleoenvironmental indicator. *Nature* 330, 641–643.
- Tenzer, G. E., Meyers, P. A., Knoop, P. A., 1997. Sources and distribution of organic and carbonate carbon in surface sediments of Pyramid Lake, Nevada. *Journal of Sedimentary Research* 67, 887–893.
- Thiel, V., Peckmann, J., Seifert, R., Wehrung, P., Reitner, J., Michaelis, W., 1999. Highly isotopically depleted isoprenoids: Molecular markers for ancient methane venting. *Geochimica et Cosmochimica Acta* 63, 3959–3966.
- Thienemann, A., 1913. Physikalische und chemische Untersuchungen in den Maaren der Eifel, Teil 1. *Verhandlungen des naturhistorischen Vereins der preußischen Rheinlande und Westfalens* 70, 249–302.
- Thienemann, A., 1914. Physikalische und chemische Untersuchungen in den Maaren der Eifel, Teil 2. *Verhandlungen des naturhistorischen Vereins der preußischen Rheinlande und Westfalens* 71, 273–389.
- Thienemann, A., 1917. Über die vertikale Schichtung des Planktons im Ulmener Maar und die Planktonproduktion der anderen Eifelmaare. *Verhandlungen des naturhistorischen Vereins der preußischen Rheinlande und Westfalens* 74, 103–134.
- Thompson, L. G., Mosley-Thompson, E., Davis, M. E., Lin, P.-N., Henderson, K. A., Cole-Dai, J., Bolzan, J. F., Liu, K.-B., 1995. Late Glacial stage and Holocene tropical ice core records from Huascaran, Peru. *Science* 269, 46–50.
- Tissot, B. P., Welte, D. H., 1984. *Petroleum Formation and Occurrence*. Springer-Verlag, Heidelberg, Germany.
- van der Meer, M. T. J., Schouten, S., Rijpstra, W. I. C., Fuchs, G., Sinninghe Damsté, J. S., 2001a. Stable carbon isotope fractionations of the hyperthermophilic crenarchaeon *Metallosphaera sedula*. *FEMS Microbiology Letters* 196, 67–70.

- van der Meer, M. T. J., Schouten, S., Sinninghe Damsté, J. S., 1998. The effect of the reversed tricarboxylic acid cycle on the ^{13}C contents of bacterial lipids. *Organic Geochemistry* 28, 527–533.
- van der Meer, M. T. J., Schouten, S., van Dongen, B. E., Rijpstra, W. I. C., Fuchs, G., Sinninghe Damsté, J. S., de Leeuw, J. W., Ward, D. M., 2001b. Biosynthetic Controls on the ^{13}C Contents of Organic Components in the Photoautotrophic Bacterium *Chloroflexus aurantiacus*. *The Journal of Biological Chemistry* 276(14), 10971–10976.
- van Geel, B., Raspopov, O. M., Renssen, H., van der Plicht, J., Dergachev, V. A., Meijer, H. A. J., 1999. The role of solar forcing upon climate change. *Quaternary Science Reviews* 18, 331–338.
- Viso, A.-C., Pesando, D., Bernard, P., Marty, J.-C., 1993. Lipid components of the Mediterranean seagrass *Posidonia Oceanica*. *Phytochemistry* 34, 381–387.
- Volkman, J. K., 1986. A review of sterol markers for marine and terrigenous organic matter. *Organic Geochemistry* 9, 455–465.
- Volkman, J. K., Barrett, S. M., Blackburn, S. I., 1999. Eustigmatophyte microalgae are potential sources of C_{29} sterols, C_{22} – C_{28} *n*-alcohols and C_{28} – C_{32} *n*-alkyl diols in freshwater environments. *Organic Geochemistry* 30, 307–318.
- Volkman, J. K., Barrett, S. M., Dunstan, G. A., Jeffrey, S. W., 1993. Geochemical significance of the occurrence of dinosterol and other 4-methyl sterols in a marine diatom. *Organic Geochemistry* 20, 7–15.
- Volkman, J. K., Barrett, S. M., I., B. S., Sikes, E. L., 1995. Alkenones in *Gephyrocapsa oceanica*: Implications for studies of paleoclimate. *Geochimica et Cosmochimica Acta* 59, 513–520.
- Volkman, J. K., Eglinton, G., Corner, E. D. S., Forsberg, T. E. V., 1980a. Long-chain alkenes and alkenones in the marine coccolithophorid *Emiliana huxleyi*. *Phytochemistry* 19, 2619–2622.
- Volkman, J. K., Eglinton, G., Corner, E. D. S., Sargent, J. R., 1980b. Novel unsaturated straight-chain C_{37} – C_{39} methyl and ethyl ketones in marine sediments and a coccolithophore *Emiliana huxleyi*. In: Douglas, A. G., Maxwell, J. R. (eds.), *Advances in Organic Geochemistry 1979*. Pergamon Press.

- Volkman, J. K., Kearney, P., Jeffrey, S. W., 1990. A new source of 4-methyl sterols and 5 α -(H)stanols in sediments: prymnesiophyte microalgae of the genus *Pavlova*. *Organic Geochemistry* 15, 489–497.
- Volkman, J. K., Maxwell, J. R., 1986. Acyclic isoprenoids as biological markers. In: Johns, R. B. (ed.), *Biological Markers in the sedimentary record*. Elsevier, New York, 1–42.
- von Grafenstein, U., Erlenkeuser, H., Brauer, A., Jouzel, J., Johnsen, S. J., 1999. A Mid-European Decadal Isotope-Climate Record from 15,500 to 5000 Years B.P. *Science* 284, 1654–.
- Wardroper, A. M. K., Maxwell, J. R., Morris, R. J., 1978. Sterols of a diatomaceous ooze from Walvis Bay. *Steroids* 32, 203–221.
- Weete, J. D., 1976. Algal and fungal waxes. In: Kolattukudy, P. E. (ed.), *Chemistry and Biochemistry of Natural Waxes*. Elsevier, Amsterdam, 349–418.
- Whiticar, M. J., 1999. Carbon and hydrogen isotope systematics of bacterial formation and oxidation of methane. *Chemical Geology* 161, 291–314.
- Whiticar, M. J., Faber, E., 1986. Methane oxidation in sediment and water column environments – Isotope evidence. *Organic Geochemistry* 10, 759–768.
- Wilkes, H., Ramrath, A., Negendank, J. F. W., 1999. Organic geochemical evidence for environmental changes since 34,000 yrs BP from Lago di Mezzano, central Italy. *Journal of Paleolimnology* 22, 349–365.
- Willén, E., 1991. Planktonic diatoms – an ecological review. *Algol. Studies* 62, 69–106.
- Willsch, H., Clegg, H., Horsfield, B., Radke, M., Wilkes, H., 1997. Liquid chromatographic separation of sediment, rock and coal extracts and crude oils into compound classes. *Analytical Chemistry* 69(20), 4203–4209.
- Youngblood, W. W., Blumer, M., 1973. Alkanes and alkenes in marine benthic algae. *Marine Biology* 21, 163–172.
- Zink, K.-G., 2000. Rekonstruktion von Paläoklimabedingungen lakustriner Systeme anhand der Verteilungsmuster langkettiger Alkenone und weiterer geochemischer Proxies. Ph.D. thesis, Universität zu Köln.

- Zink, K.-G., Leythaeuser, D., Melkonian, M., Schwark, L., 2001. Temperature dependency of long-chain alkenone distributions in recent to fossil limnic sediments and in lake waters. *Geochimica et Cosmochimica Acta* 65, 253–265.
- Zolitschka, B., 1989. Jahreszeitlich geschichtete Seesedimente aus dem Holzmaar und dem Meerfelder Maar. *Z. dt. geol. Ges.* 140, 25–33.
- Zolitschka, B., 1998. Paläoklimatische Bedeutung Laminiertes Sedimente: Holzmaar (Eifel, Deutschland), Lake C2 (Nordwest-Territorien, Kanada) und Lago Grande di Monticchio (Basilicata, Italien). In: Bremer, H., Brunnacker, K., Heine, K., Lauer, W. (eds.), *Relief Boden Paläoklima*, volume 13. Gebrüder Bornträger, Berlin-Stuttgart, 176pp.
- Zolitschka, B., Behre, K.-E., Schneider, J., 2003. Human and climatic impact on the environment as derived from colluvial,uvial and lacustrine archives—examples from the Bronze Age to the Migration period,Germany. *Quaternary Science Reviews* 22, 81–100.
- Zolitschka, B., Brauer, A., Negendank, J. F. W., Stockhausen, H., Lang, A., 2000. Annually dated late Weichselian continental paleoclimate record from the Eifel, Germany. *Geology* 28, 783–786.
- Zolitschka, B., Negendank, J. F. W., 1998. A high resolution record of Holocene palaeohydrological changes from Lake Holzmaar, Germany. *Paläoklimaforschung* 25, 33–48.

Anhang

A List of Equations

A.1 Carbon Preference Indexes

$$CPI_{HC} = \frac{1}{2} * \left(\frac{C_{25} + C_{27} + C_{29} + C_{31}}{C_{26} + C_{28} + C_{30} + C_{32}} + \frac{C_{25} + C_{27} + C_{29} + C_{31}}{C_{24} + C_{26} + C_{28} + C_{30}} \right)$$

$$CPI_{HC}^{SC} = \frac{1}{2} * \left(\frac{C_{15} + C_{17} + C_{19}}{C_{16} + C_{18} + C_{20}} + \frac{C_{15} + C_{17} + C_{19}}{C_{14} + C_{16} + C_{18}} \right)$$

$$CPI_{HC}^{MC} = \frac{1}{2} * \left(\frac{C_{21} + C_{23} + C_{25}}{C_{22} + C_{24} + C_{26}} + \frac{C_{21} + C_{23} + C_{25}}{C_{20} + C_{22} + C_{24}} \right)$$

$$CPI_{HC}^{LC} = \frac{1}{2} * \left(\frac{C_{27} + C_{29} + C_{31}}{C_{28} + C_{30} + C_{32}} + \frac{C_{27} + C_{29} + C_{31}}{C_{26} + C_{28} + C_{30}} \right)$$

$$CPI_{FA} = \frac{1}{2} * \left(\frac{C_{24} + C_{26} + C_{28} + C_{30}}{C_{23} + C_{25} + C_{27} + C_{29}} + \frac{C_{24} + C_{26} + C_{28} + C_{30}}{C_{25} + C_{27} + C_{29} + C_{31}} \right)$$

B Structures of Identified Compounds

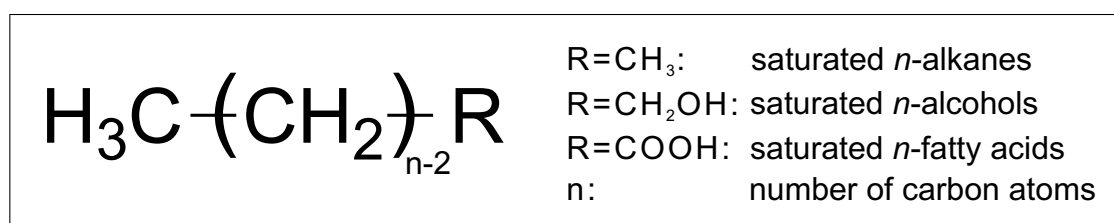


Figure B.1: Structures of normal chain lipids mentioned in text

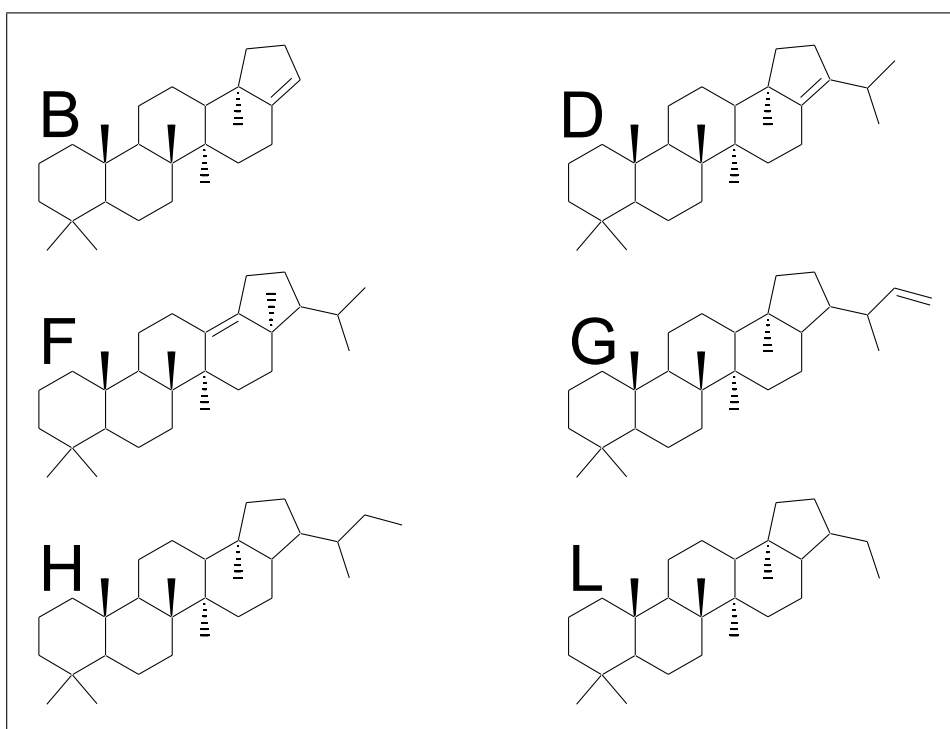


Figure B.2: Structures of hydrocarbons mentioned in text; letters refer to compound names as listed in [Table 5.2, Page 95](#)

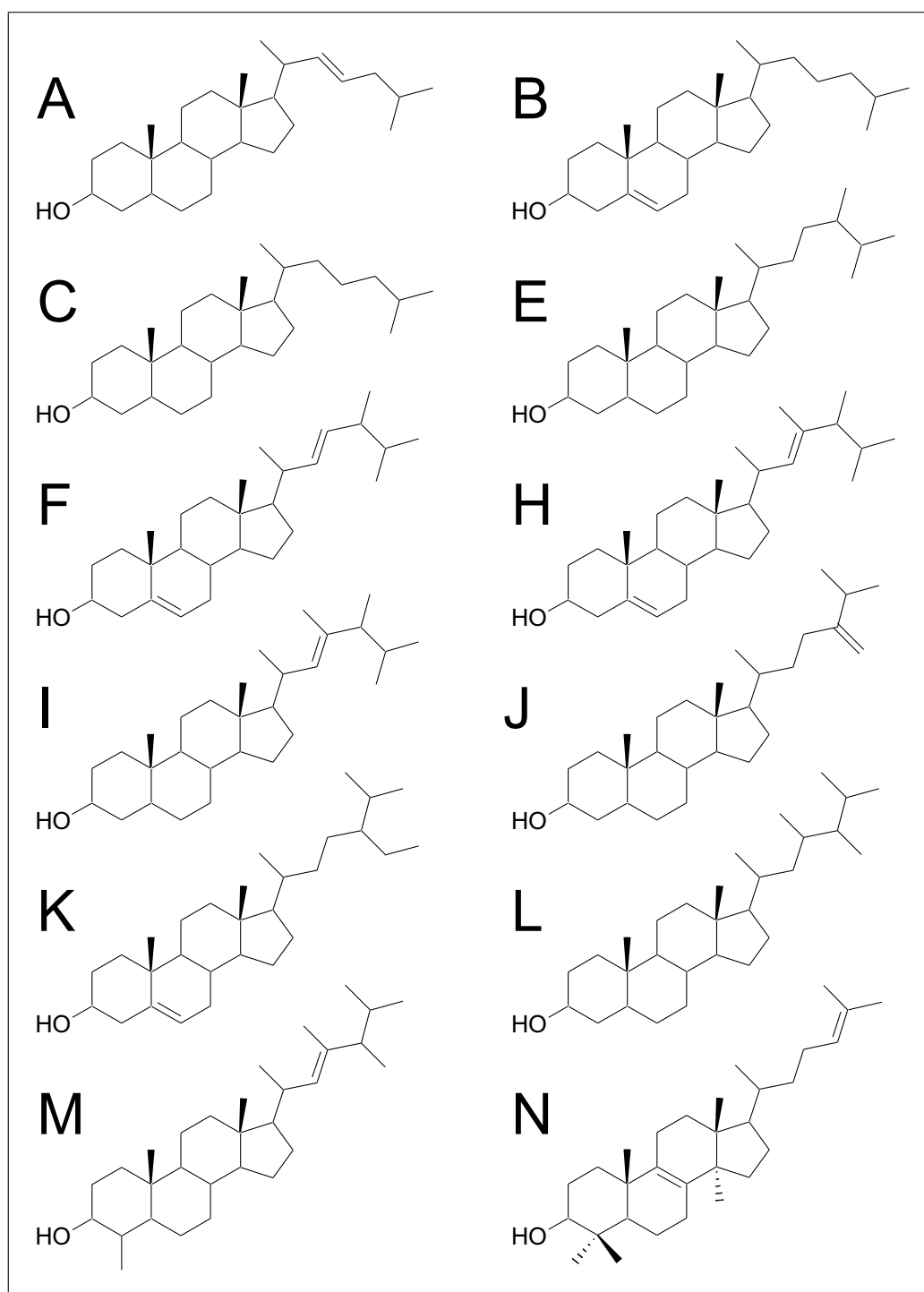


Figure B.3: Structures of sterols mentioned in text; letters refer to compound names as listed in *Table 5.4, Page 122*

C Sample Inventory

Lake Holzmaar

Table C.1: Sample Inventory: Lake Holzmaar

FZJ-Code	Core	from Depth	to Depth	Age
		cm	cm	10 ³ vyears BP
48174	HZM 4a	66	67	0.143
48175	HZM 4a	77	85	0.184
48176	HZM 4a	116	122	0.324
48177	HZM 4a	166	167	0.518
48178	HZM 4a	230	236	0.870
48179	HZM 4a	271	272	1.170
48180	HZM 4a	282	287	1.311
48181	HZM 4a	288	296	1.374
48182	HZM 4a	297	301	1.440
48183	HZM 4a	364	370	1.952
48184	HZM 4a	380	384	2.083
48185	HZM 4a	406	412	2.334
48186	HZM 4a	416	417	2.418
48187	HZM 4a	429	436	2.536
48188	HZM 4a	445	455	2.608
48189	HZM 4a	458	463	2.686
48190	HZM 4a	477	484	3.330
48191	HZM 4a	486	495	3.530
48192	HZM 4a	505	511	4.170
48193	HZM 4a	526	527	4.858
48194	HZM 4a	527	535	4.960
48195	HZM 4a	566	574	5.690

Table C.1: (continued)

FZJ-Code	Core	from Depth	to Depth	Age
		cm	cm	10 ³ vyears BP
48196	HZM 4a	596	601	6.098
48197	HZM 4a	616	621	6.340
48198	HZM 4a	646	651	6.888
48199	HZM 4a	662	668	7.220
48200	HZM 4a	670	678	7.390
48201	HZM 4a	744	745	8.775
48202	HZM 4a	772	778	9.480
48203	HZM 4a	784	785	9.610
48204	HZM 4a	804	809	10.150
48205	HZM 4a	819	824	10.325
48206	HZM 4a	843	844	10.600
48207	HZM 4a	858	864	10.910
48208	HZM 4a	880	887	11.220
48209	HZM 4a	906	915	11.540
48210	HZM 4a	927	934	11.970
48211	HZM 4a	963	964	12.895
48212	HZM 4a	977	983	12.900

Lake Meerfelder Maar

Table C.2: Sample Inventory: Lake Meerfelder Maar

FZJ-Code	Core	from Depth	to Depth	Age
		cm	cm	10 ³ vyears BP
48338	X1o	20	28	0.160
48339	X1o	38	46	0.280
48340	X1o	54	60	0.380
48341	Z1o	99	105	0.680
48342	Z1o	124	131	0.850
48343	V1o	176	182	1.240
48344	V1o	198	204	1.740
48345	V1o	208	210	1.910
48346	V1o	216	218	1.970

Table C.2: (continued)

FZJ-Code	Core	from Depth	to Depth	Age
		cm	cm	10 ³ vyyears BP
48347	Y1u	232	240	2.115
48348	Z2o	329	337	3.765
48349	W2o	343	352	4.000
48350	V2o	342	351	3.990
48350a	V2o	351	357	4.205
48351	V2o	408	413	5.455
48352	V2o	418	423	5.665
48353	Z3o	462	470	6.290
48354	Z3o	493	499	6.735
48355	V3o	545	554	7.640
48356	V3o	554	563	8.670
48357	V3o	593	604	8.850
48358	V3o	624	631	9.325
48359	V3o	634	642	9.460
48360	Y3u	644	650	10.035
48361	Y3u	653	659	10.310
48362	Z4o	672	680	10.755
48363	Z4o	696	697	11.080
48364	Z4o	727	735	11.500
48365	Z4o	745	753	11.800
48366	X4u	763	770	12.100
48367	X4u	775	783	12.250
48368	Z4u	790	798	12.355
48369	Z4u	807	808	12.480
48370	Y4u	842	851	12.900
48371	Y4u	851	860	13.000
48372	Y4u	861	868	13.240
48373	Y4u	872	880	13.390
48374	V4u	881	889	13.480
48375	V4u	890	898	13.600
48376	V4u	920	927	13.865
48377	V4u	980	986	14.245
48378	W5o	1,007	1,013	14.385
48379	Y5o	1,041	1,048	14.545
48380	Y5u	1,073	1,078	14.635
48381	Y5u	1,089	1,094	14.685

Lake Meerfelder Maar; High Resolution Sequence

Table C.3: Sample Inventory: Lake Meerfelder Maar, High Resolution Sequence; sample thickness is 1 cm for all samples, listed values for depth are upper depths for each sample

FZJ-Code	Core	Depth cm	Age 10 ³ vyyears BP
50116	y3u	645	9.970
50117	y3u	648	10.070
50118	y3u	651	10.170
50119	y3u	654	10.270
50120	y3u	657	10.380
50121	y3u	660	10.490
50122	y3u	663	10.560
50123	y3u	665	10.600
50124	z4o	666	10.620
50125	z4o	667	10.630
50126	z4o	668	10.640
50127	z4o	669	10.650
50128	z4o	670	10.670
50129	z4o	698	11.110
50130	z4o	699	11.130
50131	z4o	703	11.195
50132	z4o	704	11.210
50133	z4o	711	11.350
50134	z4o	712	11.375
50135	z4o	713	11.395
50136	z4o	714	11.410
50137	x4u	743	11.770
50138	x4u	744	11.780
50139	x4u	748	11.840
50140	x4u	749	11.855
50141	x4u	753	11.910
50142	x4u	754	11.920
50143	x4u	758	11.980
50144	x4u	759	11.990
50145	x4u	763	12.045
50146	x4u	764	12.060
50147	x4u	767	12.090

Table C.3: (continued)

FZJ-Code	Core	Depth	Age
		cm	10 ³ vyears BP
50148	x4u	768	12.100
50149	x4u	773	12.160
50150	x4u	774	12.170
50151	x4u	778	12.210
50152	x4u	779	12.220
50153	z4u	782.5	12.250
50154	z4u	783.5	12.260
50155	z4u	785.5	12.280
50156	z4u	786.5	12.290
50157	z4u	787.5	12.300
50158	z4u	788.5	12.310
50159	z4u	791.5	12.340
50160	z4u	795.5	12.380
50161	z4u	796.5	12.390
50162	z4u	797.5	12.400
50163	z4u	806.5	12.480
50164	z4u	807.5	12.490
50165	z4u	810.5	12.520

Lake Großer Treppensee

Table C.4: Sample Inventory: Lake Großer Treppensee

FZJ-Code	from Depth	to Depth	Zonation
	cm	cm	
48082	75	76	Subatlantikum II
48083	175	176	Subatlantikum II
48084	260	261	Subatlantikum II
47749	360	365	Subatlantikum II
47750	475	480	Subatlantikum I
47751	560	565	Subatlantikum I
47752	680	685	Subatlantikum I
47753	780	785	Subatlantikum I

Table C.4: (continued)

FZJ-Code	from Depth	to Depth	Zonation
	cm	cm	
47754	865	870	Subatlantikum I
47755	975	980	Subatlantikum I
47756	1,065	1,070	Subatlantikum I
47757	1,160	1,165	Subatlantikum I
47758	1,260	1,265	Subboreal
47759	1,360	1,365	Subboreal
47760	1,465	1,470	Subboreal
47761	1,585	1,590	Subboreal
47762	1,690	1,695	Subboreal
47763	1,765	1,770	Subboreal
47764	1,875	1,880	Subboreal
47765	1,975	1,980	Atlantikum II
47766	2,075	2,080	Atlantikum II
47767	2,175	2,180	Atlantikum I
47768	2,272	2,276	Atlantikum I
47769	2,385	2,390	Präboreal
48085	2,441	2,450	Younger Dryas
48086	2,451	2,460	Younger Dryas
47770	2,471	2,477	Younger Dryas

D Data Compilation

Bulk Parameters

Table D.1: Bulk Parameters for Lake Holzmaar Samples

Age	FZJ-Code	TC	TOC	TIC	TS	TN	HI	OI	T _{max}
10 ³ years BP				%			$\frac{mg\text{ HC}}{g\text{ TOC}}$	$\frac{mg\text{ CO}_2}{g\text{ TOC}}$	°C
0.084	48174	2.39	2.07	0.32	0.11	n.a.	149	223	409
0.184	48175	2.44	2.18	0.27	0.09	0.16	160	206	413
0.324	48176	3.70	3.02	0.68	0.13	0.30	202	200	410
0.870	48178	9.03	7.62	1.41	0.78	0.72	263	161	415
1.170	48179	9.69	7.86	1.83	0.71	0.68	242	176	410
1.311	48180	9.16	6.38	2.79	0.77	0.73	293	222	408
1.374	48181	9.70	7.45	2.25	1.00	0.84	287	169	410
1.440	48182	8.98	6.68	2.30	0.82	0.78	294	188	414
1.952	48183	8.29	6.22	2.07	0.53	0.65	268	172	402
2.083	48184	12.10	9.32	2.79	0.73	0.94	284	162	402
2.334	48185	12.10	9.27	2.84	0.52	0.88	261	158	405
2.536	48187	9.04	7.04	2.00	1.07	0.85	181	129	403
2.608	48188	14.60	10.85	3.75	2.37	1.30	376	147	411
2.686	48189	12.90	11.30	1.60	1.16	0.96	254	147	410
3.330	48190	8.68	7.80	0.88	1.17	0.78	280	157	412
3.530	48191	9.63	8.29	1.34	1.34	0.73	276	140	411
4.858	48193	4.99	4.45	0.54	0.86	0.43	197	159	409
4.960	48194	5.52	5.07	0.45	0.52	0.42	230	134	419
5.690	48195	8.85	7.78	1.07	1.15	0.66	244	131	404
6.098	48196	7.83	7.08	0.75	1.14	0.60	246	130	409
6.340	48197	8.82	7.97	0.86	2.33	0.69	248	124	405
6.888	48198	7.98	7.23	0.75	1.85	0.62	281	116	411
7.220	48199	9.71	8.67	1.04	2.27	0.71	406	92	413
7.390	48200	11.20	10.02	1.18	2.23	0.80	375	96	425
8.775	48201	7.09	6.65	0.44	1.83	0.49	279	96	425

Table D.1: (continued)

Age	FZJ-Code	TC	TOC	TIC	TS	TN	HI	OI	T _{max}
10 ³ years BP				%			$\frac{mg\text{HC}}{g\text{TOC}}$	$\frac{mg\text{CO}_2}{g\text{TOC}}$	°C
9.480	48202	4.21	3.96	0.26	0.96	0.57	157	151	417
9.610	48203	4.27	3.97	0.30	0.68	0.55	149	142	411
10.150	48204	3.36	3.14	0.22	0.38	0.50	139	150	415
10.325	48205	5.30	5.08	0.22	1.81	0.61	166	125	408
10.910	48207	3.35	3.08	0.27	0.31	0.50	131	155	416
11.220	48208	3.02	2.84	0.18	1.00	0.54	111	147	408
11.540	48209	2.67	2.61	0.06	0.57	0.48	160	128	418
11.970	48210	4.31	3.62	0.69	1.69	0.60	175	135	419
12.480	48212	5.15	2.84	2.31	1.34	n.a.	225	158	419

Table D.2: Bulk Parameters for Lake Meerfelder Maar Samples

Age	FZJ-Code	TC	TOC	TIC	TS	TN	HI	OI	T _{max}
10 ³ years BP				%			$\frac{mg\text{HC}}{g\text{TOC}}$	$\frac{mg\text{CO}_2}{g\text{TOC}}$	°C
0.180	48338	3.03	2.15	0.89	0.20	0.47	169	285	407
0.280	48339	6.29	4.69	1.60	0.59	0.77	237	240	380
0.380	48340	1.90	1.64	0.27	0.11	n.a.	134	249	401
0.680	48341	3.24	2.34	0.90	0.21	0.18	210	235	394
0.850	48342	5.87	4.24	1.63	0.57	0.50	292	265	373
1.240	48343	18.65	12.60	6.05	2.02	1.70	453	188	342
1.740	48344	19.95	13.15	6.80	1.74	1.90	479	191	343
1.910	48345	8.01	5.78	2.24	0.41	0.62	283	210	421
2.115	48347	13.20	9.91	3.30	0.79	1.10	356	180	382
3.765	48348	29.10	21.40	7.70	1.57	2.40	501	166	422
4.000	48349	13.90	11.20	2.70	0.87	1.10	416	163	424
3.990	48350	14.95	11.25	3.70	0.87	1.20	431	184	423
4.205	48350a	18.50	14.80	3.70	1.08	1.50	363	170	419
5.455	48351	15.15	12.80	2.35	1.47	1.30	341	160	420
5.665	48352	15.55	11.65	3.90	1.33	1.30	443	172	422
6.290	48353	9.76	7.46	2.31	0.79	0.76	299	195	420
6.735	48354	9.08	7.01	2.07	0.81	0.82	337	191	420
7.640	48355	10.80	8.55	2.25	0.77	1.00	297	210	420
8.670	48356	8.99	7.77	1.22	0.76	1.00	249	208	420
8.850	48357	12.75	9.25	3.50	1.62	1.00	424	184	422
9.325	48358	7.26	6.42	0.85	0.46	0.58	323	183	424
9.460	48359	7.40	5.91	1.49	0.54	0.54	317	208	425
10.035	48360	11.30	7.53	3.77	0.86	0.65	364	205	419
10.310	48361	10.80	7.50	3.31	0.74	0.70	356	244	420

Table D.2: (continued)

Age	FZJ-Code	TC	TOC	TIC	TS	TN	HI	OI	T _{max}
10 ³ vyears BP			%				$\frac{mg\text{HC}}{g\text{TOC}}$	$\frac{mg\text{CO}_2}{g\text{TOC}}$	°C
10.755	48362	5.39	4.20	1.19	0.72	0.42	234	250	409
11.500	48364	4.92	3.66	1.26	0.63	0.39	244	205	413
11.800	48365	2.12	1.61	0.51	0.22	0.13	189	239	415
12.100	48366	2.03	1.61	0.43	0.17	0.15	186	248	416
12.250	48367	3.96	3.08	0.88	0.46	0.30	263	208	416
12.355	48368	5.78	4.48	1.30	0.66	0.55	339	170	414
12.900	48370	7.24	4.92	2.32	0.83	0.57	284	286	404
13.000	48371	4.31	3.33	0.99	0.83	0.36	217	233	404
13.240	48372	4.31	3.25	1.06	0.80	0.38	186	259	405
13.390	48373	3.15	2.41	0.75	0.36	0.28	183	251	408
13.480	48374	2.92	2.24	0.68	0.56	0.23	178	229	409
13.600	48375	2.10	1.82	0.28	0.28	0.11	154	204	410
13.865	48376	1.33	1.10	0.23	0.13	n.a.	118	218	414
14.245	48377	1.60	1.21	0.39	0.15	n.a.	147	197	412
14.385	48378	1.58	1.14	0.44	0.20	0.05	141	214	412
14.545	48379	0.41	0.33	0.09	0.03	n.a.	113	184	427
14.635	48380	0.58	0.46	0.12	0.04	n.a.	80	267	425
14.685	48381	0.69	0.53	0.17	0.04	n.a.	104	261	428

Table D.3: Bulk Parameters for Lake Meerfelder Maar Samples (High Resolution Sequence)

Age	FZJ-Code	TC	TOC	TIC	TS	HI	OI	T _{max}
10 ³ vyears BP			%			$\frac{mg\text{HC}}{g\text{TOC}}$	$\frac{mg\text{CO}_2}{g\text{TOC}}$	°C
9.970	50116	12.80	5.82	6.99	0.92	470	239	413
10.070	50117	9.46	5.75	3.71	0.58	445	232	414
10.170	50118	9.63	7.07	2.56	1.68	377	238	420
10.270	50119	10.60	6.84	3.76	1.30	464	218	415
10.380	50120	9.77	6.85	2.93	1.22	370	242	411
10.490	50121	7.80	4.60	3.21	1.18	319	352	398
10.560	50122	6.44	4.82	1.62	0.46	318	209	407
10.600	50123	5.24	3.88	1.36	0.47	249	242	411
10.620	50124	4.82	3.82	0.99	0.37	229	216	409
10.630	50125	3.37	2.58	0.79	0.24	169	228	399
10.640	50126	4.32	3.14	1.19	0.35	193	247	402
10.650	50127	5.17	3.93	1.24	0.37	242	221	407
10.670	50128	5.01	3.96	1.05	0.42	231	219	407
11.110	50129	4.87	3.71	1.17	1.28	219	220	399
11.130	50130	4.56	3.21	1.36	0.69	223	249	403

Table D.3: (continued)

Age	FZJ-Code	TC	TOC	TIC	TS	HI	OI	T _{max}
10 ³ years BP			%			$\frac{mg\text{HC}}{g\text{TOC}}$	$\frac{mg\text{CO}_2}{g\text{TOC}}$	°C
11.195	50131	4.81	3.63	1.18	0.80	257	220	404
11.210	50132	4.51	3.25	1.26	0.84	234	242	399
11.350	50133	5.23	3.73	1.51	0.76	266	245	398
11.375	50134	5.31	4.12	1.19	0.83	228	211	396
11.395	50135	5.42	4.07	1.35	0.98	207	242	398
11.410	50136	3.82	2.68	1.15	0.67	205	267	393
11.770	50137	2.26	1.69	0.58	0.37	179	199	406
11.780	50138	1.78	1.28	0.50	0.31	181	234	410
11.840	50139	2.51	1.79	0.72	0.24	234	209	408
11.855	50140	2.29	1.70	0.60	0.24	223	199	408
11.910	50141	2.61	1.80	0.81	0.36	251	242	405
11.920	50142	2.35	1.62	0.73	0.19	225	272	401
11.980	50143	1.89	1.46	0.43	0.50	233	218	417
11.990	50144	2.36	1.73	0.63	0.40	194	204	406
12.045	50145	1.85	1.36	0.49	0.36	190	199	407
12.060	50146	1.57	1.16	0.41	0.19	180	237	407
12.090	50147	1.73	1.28	0.45	0.20	214	204	411
12.100	50148	1.84	1.34	0.50	0.15	204	229	407
12.160	50149	2.28	1.76	0.52	0.21	242	181	411
12.170	50150	2.04	1.55	0.49	0.15	218	203	408
12.210	50151	1.56	1.21	0.35	0.12	190	222	413
12.220	50152	1.60	1.20	0.40	0.17	177	222	409
12.250	50153	4.40	3.29	1.11	0.73	366	192	422
12.260	50154	4.73	3.61	1.12	0.49	349	201	408
12.280	50155	4.31	3.31	1.00	0.58	310	200	407
12.290	50156	4.23	3.14	1.09	0.57	312	196	408
12.300	50157	5.15	3.83	1.32	0.68	344	182	409
12.310	50158	4.97	3.57	1.40	0.76	374	208	408
12.340	50159	5.21	3.85	1.36	0.54	363	199	406
12.380	50160	5.48	4.10	1.39	0.84	367	187	405
12.390	50161	5.23	3.75	1.49	0.71	262	111	431
12.400	50162	4.96	3.65	1.31	0.63	356	199	405
12.480	50163	5.08	3.61	1.47	0.84	369	212	406
12.490	50164	5.12	3.80	1.33	0.80	330	197	409
12.520	50165	4.53	3.14	1.39	0.67	370	230	401

Table D.4: Bulk Parameters for Lake Großer Treppensee Samples

Depth	FZJ-Code	TC	TOC	TIC	TS	TN	HI	OI	T _{max}
m				%			$\frac{mg\text{HC}}{g\text{TOC}}$	$\frac{mg\text{CO}_2}{g\text{TOC}}$	°C
0.755	48082	13.05	8.47	4.59	0.68	n.a.	221	171	n.a.
1.755	48083	12.80	8.71	4.09	0.35	n.a.	214	177	n.a.
2.605	48084	14.75	8.30	6.45	0.43	n.a.	190	186	n.a.
3.625	47749	13.60	8.03	5.57	0.28	0.98	214	201	402
4.775	47750	13.85	7.22	6.63	0.19	0.82	202	195	400
5.625	47751	13.70	5.71	8.00	0.26	0.72	211	209	396
6.825	47752	12.65	4.91	7.74	0.34	0.64	202	203	399
7.825	47753	14.30	4.58	9.73	0.38	0.69	265	233	394
8.675	47754	14.10	6.94	7.16	0.45	0.86	206	189	393
9.775	47755	13.90	5.54	8.36	0.40	0.83	254	211	365
10.675	47756	13.45	6.41	7.05	0.45	0.83	211	191	368
11.625	47757	12.45	5.99	6.47	0.41	0.77	201	224	349
12.625	47758	12.85	5.55	7.30	0.74	0.76	175	317	389
13.625	47759	13.30	3.49	9.82	1.14	0.77	256	506	386
14.675	47760	14.40	5.43	8.97	1.26	0.78	184	282	372
15.875	47761	13.75	4.61	9.15	1.09	0.72	193	323	395
16.925	47762	13.80	4.26	9.54	0.99	0.85	272	351	379
17.675	47763	14.10	3.92	10.18	0.76	0.91	293	799	390
18.775	47764	14.05	3.83	10.22	0.87	0.82	282	640	390
19.775	47765	13.95	4.00	9.96	0.84	0.75	255	766	388
20.775	47766	13.95	4.28	9.67	0.99	0.68	226	568	388
21.775	47767	12.80	3.27	9.54	1.15	0.44	174	517	386
22.740	47768	12.50	2.96	9.54	1.09	0.37	156	591	388
23.875	47769	12.70	1.80	10.90	1.13	0.28	154	n.a.	375
24.455	48085	11.50	2.15	9.36	1.04	n.a.	135	462	n.a.
24.555	48086	10.45	2.12	8.34	1.78	n.a.	132	367	n.a.
24.740	47770	10.25	2.22	8.04	1.31	0.35	130	748	395

n-Alkanes

Table D.5: *n*-alkane concentrations for Lake Holzmaar Samples; Part 1: *n*-C₁₅-*n*-C₂₁

Age	FZJ-Code	<i>n</i> -C ₁₅	<i>n</i> -C ₁₆	<i>n</i> -C ₁₇	<i>n</i> -C ₁₈	<i>n</i> -C ₁₉	<i>n</i> -C ₂₀	<i>n</i> -C ₂₁
10 ³ years BP		$\frac{\mu g}{g\ TOC}$						
0.184	48175	0.38	0.63	6.72	2.86	7.12	5.50	21.44
1.311	48180	0.69	1.21	2.93	1.85	6.87	3.65	15.02
2.083	48184	4.92	3.04	2.68	2.08	4.51	3.81	10.79
2.536	48187	0.61	0.92	2.13	2.45	5.62	4.68	9.73
5.690	48195	0.46	0.56	0.92	0.66	1.24	0.96	2.44
6.888	48198	0.69	0.86	1.87	1.15	2.06	1.67	4.52
7.390	48200	0.44	0.56	1.77	1.55	3.50	2.54	6.61
10.150	48204	0.58	0.69	1.52	1.02	1.76	1.68	5.87
10.325	48205	0.96	1.13	2.20	1.49	2.73	2.24	6.17
10.910	48207	0.55	0.70	1.20	1.08	2.15	2.17	5.14
11.970	48210	0.89	0.71	1.08	0.75	1.37	1.28	3.42

Table D.6: *n*-alkane concentrations for Lake Holzmaar Samples; Part 2: *n*-C₂₂-*n*-C₂₈

Age	FZJ-Code	<i>n</i> -C ₂₂	<i>n</i> -C ₂₃	<i>n</i> -C ₂₄	<i>n</i> -C ₂₅	<i>n</i> -C ₂₆	<i>n</i> -C ₂₇	<i>n</i> -C ₂₈
10 ³ years BP		$\frac{\mu g}{g\ TOC}$						
0.184	48175	12.18	38.68	13.37	42.25	15.31	96.13	16.19
1.311	48180	6.12	25.82	11.87	43.05	12.92	79.59	9.79
2.083	48184	5.56	21.34	6.37	30.27	7.90	99.12	12.86
2.536	48187	6.02	17.21	6.96	27.92	7.85	79.16	10.84
5.690	48195	1.55	9.95	0.04	19.21	4.12	32.33	5.98
6.888	48198	2.57	13.24	4.78	28.90	6.57	46.97	9.50
7.390	48200	4.11	18.92	6.17	36.63	7.42	54.14	10.64
10.150	48204	5.33	22.92	12.19	65.91	17.78	157.79	21.26
10.325	48205	4.89	34.93	11.68	88.45	20.09	210.56	22.77
10.910	48207	5.77	29.84	13.73	102.51	17.80	179.59	15.51
11.970	48210	3.26	28.31	8.89	90.12	11.99	154.34	12.94

Table D.7: *n*-alkane concentrations for Lake Holzmaar Samples; Part 3: *n*-C₂₉-*n*-C₃₃

Age	FZJ-Code	<i>n</i> -C ₂₉	<i>n</i> -C ₃₀	<i>n</i> -C ₃₁	<i>n</i> -C ₃₂	<i>n</i> -C ₃₃
10 ³ vyears BP		$\frac{\mu g}{g\text{TOC}}$				
0.184	48175	88.41	12.53	92.97	9.88	43.57
1.311	48180	71.16	7.57	63.36	37.40	0.00
2.083	48184	178.42	9.40	106.02	11.25	38.79
2.536	48187	131.18	7.42	86.09	10.18	30.68
5.690	48195	67.93	4.55	47.23	2.40	12.54
6.888	48198	96.20	9.58	58.91	10.29	19.90
7.390	48200	128.25	15.47	87.50	4.85	22.82
10.150	48204	163.50	11.72	73.90	3.87	22.55
10.325	48205	191.56	11.26	91.61	4.20	30.48
10.910	48207	109.40	8.09	76.03	6.84	29.72
11.970	48210	94.13	6.02	85.22	3.05	31.90

Table D.8: *n*-alkane concentrations for Lake Meerfelder Maar Samples; Part 1: *n*-C₁₅-*n*-C₂₁

Age	FZJ-Code	<i>n</i> -C ₁₅	<i>n</i> -C ₁₆	<i>n</i> -C ₁₇	<i>n</i> -C ₁₈	<i>n</i> -C ₁₉	<i>n</i> -C ₂₀	<i>n</i> -C ₂₁
10 ³ vyears BP		$\frac{\mu g}{g\text{TOC}}$						
0.280	48339	15.57	19.79	26.15	20.73	21.21	18.29	28.04
1.740	48344	2.86	0.00	8.37	5.20	7.32	5.62	12.49
1.910	48345	3.58	4.26	6.28	5.61	7.72	5.00	17.98
3.765	48348	1.27	1.27	7.48	3.62	7.53	3.75	31.31
4.000	48349	0.52	0.58	4.08	2.52	3.90	2.62	34.07
4.205	48350a	1.11	1.68	5.39	1.82	5.20	3.68	38.12
6.290	48353	1.46	2.11	6.72	2.92	7.20	4.30	51.02
8.850	48357	0.71	0.86	2.31	1.57	4.80	3.20	29.02
10.035	48360	0.49	0.69	1.74	1.75	3.38	3.18	8.69
11.800	48365	1.38	2.07	3.23	3.61	6.93	7.65	20.99
12.250	48367	0.74	1.76	4.48	8.05	14.47	16.24	25.73
12.900	48370	0.48	0.72	1.27	1.46	3.33	5.34	10.98
13.865	4837	3.28	3.75	4.78	7.99	13.61	15.70	22.01
14.385	48378	2.33	4.70	5.53	5.46	8.18	7.89	10.14
14.635	48380	1.74	3.89	4.83	4.24	7.56	8.06	20.85

D Data Compilation

Table D.9: *n*-alkane concentrations for Lake Meerfelder Maar Samples; Part 2: *n*-C₂₂-*n*-C₂₈

Age	FZJ-Code	<i>n</i> -C ₂₂	<i>n</i> -C ₂₃	<i>n</i> -C ₂₄	<i>n</i> -C ₂₅	<i>n</i> -C ₂₆	<i>n</i> -C ₂₇	<i>n</i> -C ₂₈
10 ³ years BP		$\frac{\mu g}{g\text{TOC}}$						
0.280	48339	27.02	50.60	35.21	71.33	34.81	122.97	36.97
1.740	48344	5.51	16.73	5.99	25.47	6.35	82.58	8.56
1.910	48345	6.52	16.07	5.88	21.46	6.52	72.28	8.84
3.765	48348	6.05	26.98	7.73	33.84	6.44	56.78	7.02
4.000	48349	5.03	32.45	5.83	30.14	5.31	43.93	5.48
4.205	48350a	5.61	33.00	8.00	35.51	6.58	57.53	6.70
6.290	48353	5.96	30.43	8.45	41.68	7.91	48.15	8.27
8.850	48357	4.90	29.10	8.29	37.42	8.22	43.82	6.85
10.035	48360	4.32	23.26	4.46	14.43	4.09	17.89	3.83
11.800	48365	17.85	58.44	23.52	83.60	23.92	116.75	22.63
12.250	48367	20.99	58.54	23.57	74.47	21.90	79.71	0.00
12.900	48370	7.88	34.57	13.21	78.73	14.17	104.65	12.15
13.865	4837	21.94	50.65	28.75	108.18	31.04	269.78	36.28
14.385	48378	9.28	18.06	11.06	38.74	12.37	87.74	15.77
14.635	48380	16.88	40.13	13.69	42.69	15.39	82.50	21.70

Table D.10: *n*-alkane concentrations for Lake Meerfelder Maar Samples; Part 3: *n*-C₂₉-*n*-C₃₃

Age	FZJ-Code	<i>n</i> -C ₂₉	<i>n</i> -C ₃₀	<i>n</i> -C ₃₁	<i>n</i> -C ₃₂	<i>n</i> -C ₃₃
10 ³ years BP		$\frac{\mu g}{g\text{TOC}}$				
0.280	48339	158.24	21.03	107.85	24.08	45.20
1.740	48344	112.78	6.90	47.02	6.34	15.28
1.910	48345	98.22	6.08	40.28	5.65	14.80
3.765	48348	91.36	6.81	35.46	11.56	10.81
4.000	48349	77.10	5.03	34.54	4.63	11.03
4.205	48350a	92.59	4.93	30.85	5.03	12.59
6.290	48353	106.36	8.64	68.30	4.44	17.30
8.850	48357	56.52	6.06	30.03	2.55	14.27
10.035	48360	22.70	2.93	13.01	2.36	6.53
11.800	48365	110.74	11.77	106.27	12.40	51.47
12.250	48367	81.93	10.63	70.10	29.54	32.09
12.900	48370	108.29	8.05	79.14	6.65	42.07
13.865	4837	273.04	20.07	253.99	14.06	76.75
14.385	48378	129.33	8.48	137.93	58.67	49.31
14.635	48380	255.86	18.58	334.97	103.37	114.45

Table D.11: *n*-alkane concentrations for Lake Meerfelder Maar Samples (High Resolution Sequence); Part 1: *n*-C₁₅-*n*-C₂₁

Age	FZJ-Code	<i>n</i> -C ₁₅	<i>n</i> -C ₁₆	<i>n</i> -C ₁₇	<i>n</i> -C ₁₈	<i>n</i> -C ₁₉	<i>n</i> -C ₂₀	<i>n</i> -C ₂₁
10 ³ years BP		$\frac{\mu\text{g}}{\text{g TOC}}$						
9.970	50116	0.35	0.86	2.29	1.98	4.49	3.76	17.08
10.070	50117	0.19	0.43	0.29	0.77	1.44	0.44	0.87
10.170	50118	0.50	2.07	2.52	2.67	3.44	3.24	13.09
10.270	50119	0.26	0.89	2.93	1.29	4.79	2.40	45.41
10.380	50120	0.31	0.60	1.55	0.68	1.87	1.23	8.75
10.490	50121	0.42	1.51	3.02	3.21	3.48	2.81	7.92
10.560	50122	0.45	1.25	2.49	1.49	4.44	2.64	11.88
10.600	50123	0.50	0.98	2.80	1.55	3.66	2.48	11.09
10.620	50124	0.74	3.67	5.73	5.59	4.66	4.84	10.65
10.630	50125	0.35	0.63	1.64	0.96	3.53	2.19	7.85
10.640	50126	0.34	1.17	1.88	1.62	3.08	2.51	7.46
10.650	50127	0.28	0.51	1.51	1.14	2.75	1.87	6.48
10.670	50128	0.39	1.37	1.49	1.42	2.41	2.11	6.77
11.110	50129	0.40	1.13	1.56	2.11	2.03	1.94	5.39
11.130	50130	0.60	1.55	1.75	1.69	2.44	2.67	14.36
11.195	50131	0.37	1.26	1.07	1.60	2.32	2.81	13.43
11.210	50132	0.44	1.41	1.91	2.99	3.95	3.28	9.10
11.350	50133	0.41	0.87	1.38	0.96	1.62	1.83	12.29
11.375	50134	0.47	1.40	1.16	1.43	1.39	2.04	7.39
11.395	50135	0.41	0.87	1.08	0.95	1.28	1.57	7.52
11.410	50136	0.49	1.30	1.33	1.40	1.60	1.89	8.06
11.770	50137	0.33	1.28	1.56	1.73	2.13	2.79	12.56
11.780	50138	0.36	1.06	1.01	1.32	2.28	3.39	13.43
11.840	50139	0.30	0.88	1.17	1.34	3.44	4.16	18.22
11.910	50141	0.43	1.83	1.88	2.64	3.19	4.34	15.81
11.980	50143	0.31	0.56	0.69	0.85	2.21	2.74	14.10
11.990	50144	0.48	1.56	1.10	1.97	3.51	4.59	21.01
12.045	50145	0.34	1.29	1.35	1.92	3.50	4.47	19.04
12.060	50146	0.49	1.38	1.66	2.43	3.74	4.48	19.08
12.100	50148	0.31	1.35	1.48	2.18	4.29	5.10	19.92
12.160	50149	0.23	0.74	0.93	1.27	2.75	3.14	13.37
12.170	50150	0.50	1.65	1.47	2.38	4.17	5.07	20.60
12.210	50151	0.30	0.42	1.60	1.05	4.65	4.38	18.98
12.220	50152	0.40	1.23	3.95	6.77	9.94	8.07	20.95
12.250	50153	0.26	0.93	0.92	1.07	1.72	2.38	13.50
12.260	50154	0.27	0.67	0.96	1.02	2.39	2.21	15.01
12.280	50155	0.17	0.97	1.03	1.43	2.13	2.25	9.82
12.290	50156	0.20	1.03	1.07	1.39	3.22	2.86	14.31
12.300	50157	0.17	0.79	0.82	1.07	2.01	2.30	12.17
12.310	50158	0.19	0.96	1.13	1.05	1.60	1.88	8.83
12.340	50159	0.22	1.23	0.89	1.43	2.22	2.45	11.32
12.380	50160	0.17	0.89	1.73	1.62	2.40	2.46	10.70

Table D.11: (continued)

Age	FZJ-Code	$n\text{-C}_{15}$	$n\text{-C}_{16}$	$n\text{-C}_{17}$	$n\text{-C}_{18}$	$n\text{-C}_{19}$	$n\text{-C}_{20}$	$n\text{-C}_{21}$
10 ³ years BP					$\frac{\mu\text{g}}{\text{g TOC}}$			
12.400	50162	0.22	0.60	1.93	0.92	2.40	2.00	9.07
12.480	50163	0.24	0.93	1.80	1.17	2.18	2.37	11.25
12.490	50164	0.29	0.85	1.45	1.48	2.34	2.45	10.24

Table D.12: n -alkane concentrations for Lake Meerfelder Maar Samples (High Resolution Sequence); Part 2: $n\text{-C}_{22}\text{-}n\text{-C}_{28}$

Age	FZJ-Code	$n\text{-C}_{22}$	$n\text{-C}_{23}$	$n\text{-C}_{24}$	$n\text{-C}_{25}$	$n\text{-C}_{26}$	$n\text{-C}_{27}$	$n\text{-C}_{28}$
10 ³ years BP					$\frac{\mu\text{g}}{\text{g TOC}}$			
9.970	50116	7.70	57.46	10.16	45.23	9.81	61.76	10.26
10.070	50117	1.06	5.49	2.48	20.36	3.99	48.46	1.90
10.170	50118	6.74	52.20	8.32	44.13	8.55	68.16	10.23
10.270	50119	9.34	198.27	11.53	63.15	12.13	92.71	13.06
10.380	50120	3.98	44.95	8.14	47.42	9.31	69.09	11.93
10.490	50121	4.43	39.63	7.41	44.17	8.68	69.15	11.21
10.560	50122	6.68	33.06	10.91	61.70	12.07	84.57	14.07
10.600	50123	6.76	31.24	0.10	69.09	13.56	95.18	17.03
10.620	50124	8.33	28.46	11.97	65.44	12.75	89.96	16.49
10.630	50125	5.67	24.23	9.78	56.76	11.99	95.95	13.44
10.640	50126	5.45	21.65	10.11	56.39	12.40	99.33	13.79
10.650	50127	4.38	19.61	9.09	56.00	10.98	88.23	11.98
10.670	50128	4.96	21.66	10.79	64.62	12.76	92.74	12.37
11.110	50129	4.55	23.54	10.28	80.81	13.71	124.77	13.17
11.130	50130	6.16	33.36	13.88	119.62	17.55	168.47	14.31
11.195	50131	6.08	33.86	12.32	101.06	16.61	187.38	16.50
11.210	50132	5.96	30.70	12.69	95.15	16.46	162.38	18.22
11.350	50133	5.65	32.18	13.96	92.17	16.66	130.70	12.77
11.375	50134	5.28	26.49	10.77	72.80	13.24	113.49	11.58
11.395	50135	4.96	26.37	10.63	70.84	13.35	116.78	12.20
11.410	50136	4.54	25.95	9.24	68.29	12.46	139.73	12.16
11.770	50137	11.36	50.28	20.38	103.83	24.55	162.61	24.46
11.780	50138	11.08	47.39	17.92	90.30	21.77	158.41	24.44
11.840	50139	13.77	66.07	23.90	117.24	28.25	168.16	28.90
11.910	50141	12.83	60.74	24.01	116.83	27.61	144.13	24.51
11.980	50143	9.73	56.00	16.63	79.12	18.33	97.68	16.58
11.990	50144	13.95	88.32	24.48	121.32	26.84	144.18	24.01
12.045	50145	15.00	74.10	26.35	133.74	28.74	160.00	25.29
12.060	50146	14.18	71.79	25.71	130.02	28.20	154.93	24.68

Table D.12: (continued)

Age	FZJ-Code	<i>n</i> -C ₂₂	<i>n</i> -C ₂₃	<i>n</i> -C ₂₄	<i>n</i> -C ₂₅	<i>n</i> -C ₂₆	<i>n</i> -C ₂₇	<i>n</i> -C ₂₈
10 ³ vyears BP		$\frac{\mu g}{g \text{ TOC}}$						
12.100	50148	16.34	83.62	25.45	121.95	27.21	147.14	29.85
12.160	50149	11.01	59.58	14.44	73.72	15.15	90.76	17.73
12.170	50150	16.05	98.67	23.17	121.55	23.93	149.36	29.17
12.210	50151	15.28	75.50	19.43	91.90	20.89	129.37	24.43
12.220	50152	16.86	75.24	23.55	104.87	25.59	146.88	27.99
12.250	50153	8.41	63.28	16.05	92.86	17.44	104.34	22.14
12.260	50154	7.62	63.28	15.76	94.96	16.71	94.80	20.29
12.280	50155	6.23	41.18	10.54	62.74	11.44	74.12	14.20
12.290	50156	7.87	57.50	12.72	76.78	13.44	84.65	18.83
12.300	50157	7.23	55.13	13.24	84.62	14.69	95.69	17.63
12.310	50158	5.53	42.17	10.93	68.36	12.94	86.16	15.35
12.340	50159	6.57	52.32	13.54	87.40	14.87	87.82	13.92
12.380	50160	6.80	48.93	12.71	79.47	13.97	93.65	18.10
12.400	50162	5.92	41.63	10.92	68.38	12.91	91.68	16.98
12.480	50163	7.42	50.71	13.89	82.09	15.30	102.04	22.48
12.490	50164	6.95	44.51	13.01	77.44	15.06	103.61	21.91

Table D.13: *n*-alkane concentrations for Lake Meerfelder Maar Samples (High Resolution Sequence); Part 3: *n*-C₂₉-*n*-C₃₃

Age	FZJ-Code	<i>n</i> -C ₂₉	<i>n</i> -C ₃₀	<i>n</i> -C ₃₁	<i>n</i> -C ₃₂	<i>n</i> -C ₃₃
10 ³ vyears BP		$\frac{\mu g}{g \text{ TOC}}$				
9.970	50116	88.56	7.84	54.97	4.29	23.60
10.070	50117	3.74	5.67	5.47	40.00	1.81
10.170	50118	97.62	8.31	56.70	4.05	24.46
10.270	50119	125.19	10.04	76.16	5.17	31.35
10.380	50120	104.78	8.64	64.44	5.90	30.27
10.490	50121	88.43	7.51	60.34	6.55	35.18
10.560	50122	97.46	9.81	67.70	3.20	29.46
10.600	50123	102.78	9.00	74.00	3.81	31.43
10.620	50124	99.30	8.26	68.59	8.39	34.67
10.630	50125	107.74	9.03	79.15	4.27	33.25
10.640	50126	109.69	8.64	78.99	5.05	31.50
10.650	50127	94.22	7.16	67.81	3.13	26.38
10.670	50128	88.59	6.95	67.93	3.64	28.36
11.110	50129	88.15	7.60	74.41	4.75	33.06
11.130	50130	96.39	8.13	86.60	4.71	37.68
11.195	50131	128.90	8.42	90.98	4.89	37.53

Table D.13: (continued)

Age	FZJ-Code	$n\text{-C}_{29}$	$n\text{-C}_{30}$	$n\text{-C}_{31}$	$n\text{-C}_{32}$	$n\text{-C}_{33}$
10^3years BP		$\frac{\mu\text{g}}{\text{g TOC}}$				
11.210	50132	121.22	8.26	92.98	5.94	36.95
11.350	50133	92.07	7.78	90.22	4.75	42.87
11.375	50134	90.58	6.82	86.08	4.19	38.00
11.395	50135	94.88	7.48	87.76	4.75	42.69
11.410	50136	100.19	0.00	95.40	4.73	43.51
11.770	50137	145.59	11.64	140.07	8.01	70.97
11.780	50138	155.19	12.12	159.80	7.95	80.75
11.840	50139	165.11	13.68	155.74	8.64	85.07
11.910	50141	134.10	11.59	118.81	6.93	59.50
11.980	50143	106.54	9.43	103.73	6.32	47.29
11.990	50144	147.83	12.70	133.38	7.87	63.54
12.045	50145	153.51	12.87	144.95	7.61	69.50
12.060	50146	153.36	13.23	149.71	8.04	67.99
12.100	50148	166.69	14.67	158.34	8.60	73.20
12.160	50149	96.04	8.51	88.10	5.45	42.37
12.170	50150	170.01	13.87	156.18	9.53	77.27
12.210	50151	150.25	12.75	148.68	8.18	64.29
12.220	50152	172.12	14.24	169.44	9.25	72.70
12.250	50153	124.57	10.11	115.09	5.91	52.15
12.260	50154	98.38	8.44	85.85	6.92	42.10
12.280	50155	84.14	7.01	77.72	6.48	38.04
12.290	50156	100.80	8.72	93.81	7.37	46.03
12.300	50157	100.94	8.79	82.18	5.50	38.45
12.310	50158	85.25	6.42	68.27	6.17	36.50
12.340	50159	77.66	5.51	57.35	4.58	30.57
12.380	50160	89.66	6.94	75.17	6.80	38.87
12.400	50162	93.24	6.77	75.66	6.72	37.33
12.480	50163	111.96	8.19	85.45	7.35	43.23
12.490	50164	114.07	8.32	86.87	6.26	43.87

Table D.14: n -alkane concentrations for Lake Großer Treppensee Samples; Part 1: $n\text{-C}_{15}\text{-}n\text{-C}_{21}$

Depth	FZJ-Code	$n\text{-C}_{15}$	$n\text{-C}_{16}$	$n\text{-C}_{17}$	$n\text{-C}_{18}$	$n\text{-C}_{19}$	$n\text{-C}_{20}$	$n\text{-C}_{21}$
m		$\frac{\mu\text{g}}{\text{g TOC}}$						
0.755	48082	0.99	3.16	10.91	9.07	10.08	7.14	8.42
1.755	48083	1.48	3.64	10.21	6.32	8.06	5.80	8.27
2.605	48084	0.40	1.76	6.54	2.17	4.04	2.39	4.97
4.775	47750	0.28	0.46	1.52	0.63	1.38	1.18	3.57

Table D.14: (continued)

Depth	FZJ-Code	<i>n</i> -C ₁₅	<i>n</i> -C ₁₆	<i>n</i> -C ₁₇	<i>n</i> -C ₁₈	<i>n</i> -C ₁₉	<i>n</i> -C ₂₀	<i>n</i> -C ₂₁
m		$\frac{\mu g}{g \text{ TOC}}$						
7.825	47753	0.26	0.70	4.66	1.86	2.62	3.32	4.06
8.675	47754	1.36	1.21	6.76	1.40	4.13	1.73	6.35
9.775	47755	0.28	0.50	11.06	2.68	6.59	2.72	7.92
10.675	47756	0.44	0.77	7.31	2.19	4.66	2.20	5.10
11.625	47757	0.47	1.01	60.35	1.97	5.28	1.89	4.70
12.625	47758	0.34	0.41	6.05	1.77	6.05	2.73	4.81
13.625	47759	0.24	0.55	10.50	3.09	7.96	2.89	7.17
15.875	47761	0.78	1.13	5.27	1.58	3.49	1.72	4.06
16.925	47762	0.16	0.43	2.70	1.57	5.84	2.15	8.44
17.675	47763	0.50	1.35	7.48	2.42	8.99	2.30	8.32
18.775	47764	0.22	1.28	9.03	3.29	13.99	2.95	7.58
19.775	47765	0.48	1.18	9.54	2.30	10.99	2.08	6.89
20.775	47766	0.20	3.50	6.73	3.73	12.24	2.49	6.27
21.775	47767	0.12	0.89	2.32	1.37	2.01	1.26	3.05
23.875	47769	0.49	0.68		1.19	0.81	0.75	1.37
24.455	48085	0.71	2.36	3.28	2.70	1.85	2.16	3.16
24.555	48086	0.41	2.34	2.66	2.12	2.04	2.40	4.10
24.740	47770	1.80	0.95	0.72	1.15	1.16	1.00	2.03

Table D.15: *n*-alkane concentrations for Lake Großer Treppensee Samples; Part 2: *n*-C₂₂-*n*-C₂₈

Depth	FZJ-Code	<i>n</i> -C ₂₂	<i>n</i> -C ₂₃	<i>n</i> -C ₂₄	<i>n</i> -C ₂₅	<i>n</i> -C ₂₆	<i>n</i> -C ₂₇	<i>n</i> -C ₂₈
m		$\frac{\mu g}{g \text{ TOC}}$						
0.755	48082	5.82	14.41	7.65	19.54	6.31	57.01	28.79
1.755	48083	4.51	14.61	5.20	18.46	4.32	37.17	10.79
2.605	48084	3.21	10.87	5.73	14.86	3.73	34.08	15.12
4.775	47750	1.66	5.79	3.77	9.79	2.08	28.00	7.02
7.825	47753	2.81	6.73	4.51	12.44	4.02	32.38	13.14
8.675	47754	2.02	11.12	6.00	12.72	2.87	33.81	11.72
9.775	47755	2.94	20.84	7.01	25.32	4.20	51.00	19.59
10.675	47756	2.27	11.96	6.39	17.08	3.39	38.19	15.50
11.625	47757	2.10	11.17	7.77	17.47	3.08	40.96	15.73
12.625	47758	2.18	9.06	6.16	15.29	2.57	32.22	13.86
13.625	47759	2.62	15.64	8.73	20.72	3.42	47.14	20.45
15.875	47761	2.25	7.18	8.86	13.69	2.89	29.02	12.83
16.925	47762	2.52	17.28	7.88	22.38	3.62	45.53	17.10
17.675	47763	2.72	17.18	5.40	28.04	4.04	54.29	15.76
18.775	47764	2.78	14.65	6.56	25.70	3.79	48.58	17.11

Table D.15: (continued)

Depth	FZJ-Code	<i>n</i> -C ₂₂	<i>n</i> -C ₂₃	<i>n</i> -C ₂₄	<i>n</i> -C ₂₅	<i>n</i> -C ₂₆	<i>n</i> -C ₂₇	<i>n</i> -C ₂₈
m		$\frac{\mu\text{g}}{\text{g TOC}}$						
19.775	47765	2.12	13.15	4.62	25.29	3.65	42.94	11.79
20.775	47766	2.30	12.20	7.25	29.04	3.86	50.29	18.05
21.775	47767	1.92	7.13	4.58	17.14	2.33	28.23	9.95
23.875	47769	0.90	4.05	1.30	11.56	1.83	17.63	3.80
24.455	48085	2.28	14.11	3.37	29.80	3.81	42.68	6.61
24.555	48086	2.89	18.87	4.18	24.21	4.32	44.82	7.47
24.740	47770	1.75	7.12	2.80	13.30	3.02	25.01	5.66

Table D.16: *n*-alkane concentrations for Lake Großer Treppensee Samples; Part 3: *n*-C₂₉-*n*-C₃₃

Depth	FZJ-Code	<i>n</i> -C ₂₉	<i>n</i> -C ₃₀	<i>n</i> -C ₃₁	<i>n</i> -C ₃₂	<i>n</i> -C ₃₃
m		$\frac{\mu\text{g}}{\text{g TOC}}$				
0.755	48082	0.99	3.16	10.91	9.07	10.08
1.755	48083	1.48	3.64	10.21	6.32	8.06
2.605	48084	0.40	1.76	6.54	2.17	4.04
4.775	47750	0.28	0.46	1.52	0.63	1.38
7.825	47753	0.26	0.70	4.66	1.86	2.62
8.675	47754	1.36	1.21	6.76	1.40	4.13
9.775	47755	0.28	0.50	11.06	2.68	6.59
10.675	47756	0.44	0.77	7.31	2.19	4.66
11.625	47757	0.47	1.01	60.35	1.97	5.28
12.625	47758	0.34	0.41	6.05	1.77	6.05
13.625	47759	0.24	0.55	10.50	3.09	7.96
15.875	47761	0.78	1.13	5.27	1.58	3.49
16.925	47762	0.16	0.43	2.70	1.57	5.84
17.675	47763	0.50	1.35	7.48	2.42	8.99
18.775	47764	0.22	1.28	9.03	3.29	13.99
19.775	47765	0.48	1.18	9.54	2.30	10.99
20.775	47766	0.20	3.50	6.73	3.73	12.24
21.775	47767	0.12	0.89	2.32	1.37	2.01
23.875	47769	0.49	0.68		1.19	0.81
24.455	48085	0.71	2.36	3.28	2.70	1.85
24.555	48086	0.41	2.34	2.66	2.12	2.04
24.740	47770	1.80	0.95	0.72	1.15	1.16

$\delta^{13}\text{C}$ of *n*-Alkanes

Table D.17: $\delta^{13}\text{C}$ of *n*-alkanes for Lake Meerfelder Maar Samples; Part 1: *n*-C₂₁-*n*-C₂₆

Age	FZJ-Code	<i>n</i> -C ₂₁	<i>n</i> -C ₂₂	<i>n</i> -C ₂₃	<i>n</i> -C ₂₄	<i>n</i> -C ₂₅	<i>n</i> -C ₂₆
10 ³ years BP		‰					
0.280	48339	-28.848	-28.533	-31.250	-28.362	-32.101	-37.902
1.910	48345	n.a.	-29.276	-30.224	-29.973	-30.285	n.a.
4.000	48349	-45.672	-38.562	-36.368	-33.667	-38.348	-36.559
6.290	48353	-45.040	-32.325	-29.911	-33.292	-32.946	-34.153
8.850	48357	-43.085	-31.966	-31.802	-36.085	-37.306	-36.039
12.900	48370	n.a.	n.a.	-30.942	n.a.	-32.287	n.a.
13.865	48376	-29.337	-28.255	-30.290	-29.773	-30.572	-30.145
14.385	48378	-28.785	-28.678	-32.774	-28.673	-29.824	-28.715
14.635	48380	-33.759	-33.576	-35.575	n.a.	-31.902	n.a.

Table D.18: $\delta^{13}\text{C}$ of *n*-alkanes for Lake Meerfelder Maar Samples; Part 2: *n*-C₂₇-*n*-C₃₃

Age	FZJ-Code	<i>n</i> -C ₂₇	<i>n</i> -C ₂₈	<i>n</i> -C ₂₉	<i>n</i> -C ₃₀	<i>n</i> -C ₃₁	<i>n</i> -C ₃₃
10 ³ years BP		‰					
0.280	48339	-31.938	-35.828	-31.898	-33.715	-33.819	-33.359
1.910	48345	-36.733	n.a.	-31.241	n.a.	-34.026	n.a.
4.000	48349	-32.827	-32.982	-31.515	-34.486	-32.303	-33.313
6.290	48353	-31.806	-28.885	-30.353	n.a.	-31.744	-33.371
8.850	48357	-32.642	-32.777	-29.836	-33.706	-32.066	-30.800
12.900	48370	-34.529	n.a.	-32.150	n.a.	-35.255	-33.539
13.865	48376	-31.599	-35.555	-32.048	-32.447	-33.491	-33.666
14.385	48378	-31.085	-41.149	32.037	-41.482	-33.982	-33.399
14.635	48380	-33.763	n.a.	-32.913	n.a.	-33.263	-34.143

D Data Compilation

Table D.19: $\delta^{13}\text{C}$ of n -alkanes for Lake Meerfelder Maar Samples (High Resolution Sequence);
Part 1: $n\text{-C}_{21}\text{-}n\text{-C}_{26}$

Age 10 ³ vyears BP	FZJ-Code	$n\text{-C}_{21}$	$n\text{-C}_{22}$	$n\text{-C}_{23}$	$n\text{-C}_{24}$	$n\text{-C}_{25}$	$n\text{-C}_{26}$
		‰					
10.640	50126	-33.212	-30.286	-32.341	-32.495	-33.073	-34.900
11.195	50131	-38.981	-31.385	-32.192	-31.934	-32.224	-32.976
11.375	50134	-32.063	-29.981	-31.661	-31.910	-33.644	-33.261
11.840	50139	-34.818	-34.032	-31.048	-34.333	-32.609	-31.597
11.980	50143	-33.959	-33.779	-31.256	-34.619	-33.407	-33.800
12.045	50145	-34.771	-33.566	-31.447	-35.071	-34.959	-34.922
12.160	50149	-30.793	-31.189	-30.297	-30.571	-30.289	-31.093
12.220	50152	-32.013	-29.780	-29.236	-30.911	-30.122	-31.722
12.250	50153	-32.477	-30.974	-29.531	-32.669	-31.254	-32.385
12.280	50155	-31.151	-30.497	-28.981	-31.434	-28.376	-30.393
12.400	50162	-32.135	-32.181	-29.432	-30.521	-29.255	-30.556

Table D.20: $\delta^{13}\text{C}$ of n -alkanes for Lake Meerfelder Maar Samples (High Resolution Sequence);
Part 2: $n\text{-C}_{27}\text{-}n\text{-C}_{33}$

Age 10 ³ vyears BP	FZJ-Code	$n\text{-C}_{27}$	$n\text{-C}_{28}$	$n\text{-C}_{29}$	$n\text{-C}_{30}$	$n\text{-C}_{31}$	$n\text{-C}_{33}$
		‰					
10.640	50126	-31.600	n.a.	-33.678	n.a.	-41.746	-43.233
11.195	50131	-30.481	-32.172	-30.830	-32.719	-33.888	-33.706
11.375	50134	-32.718	-38.983	-32.072	n.a.	-32.133	-33.266
11.840	50139	-31.425	-40.332	-32.133	-31.792	-33.389	-33.312
11.980	50143	-31.669	-31.831	-31.845	n.a.	-34.457	-70.792
12.045	50145	-31.521	-31.947	-31.911	-32.812	-33.328	-33.340
12.160	50149	-30.135	-54.856	-32.620	n.a.	-37.862	-35.926
12.220	50152	-30.780	n.a.	-31.849	-31.633	-33.312	-33.562
12.250	50153	-29.778	-33.049	-31.333	n.a.	-33.994	-33.199
12.280	50155	-29.005	-32.700	-31.747	n.a.	-33.593	-33.415
12.400	50162	-30.905	n.a.	-32.494	n.a.	-31.519	-30.130

n-Fatty Acids

Table D.21: *n*-Fatty Acid concentrations for Lake Holzmaar Samples; Part 1: *n*-C₁₅-*n*-C₂₁

Age 10 ³ years BP	FZJ-Code	<i>n</i> -C ₁₅	<i>n</i> -C ₁₆	<i>n</i> -C ₁₇	<i>n</i> -C ₁₈	<i>n</i> -C ₁₉	<i>n</i> -C ₂₀	<i>n</i> -C ₂₁
$\frac{\mu g}{g\ TOC}$								
0.184	48175	0.73	8.48	2.13	3.99	0.02	20.31	12.78
1.311	48180	1.39	12.70	3.84	7.84	1.33	19.48	7.83
2.083	48184	2.04	37.08	4.65	26.66	5.57	44.27	18.80
2.536	48187	0.59	34.88	5.79	20.58	0.95	37.01	17.53
4.960	48194	1.18	11.07	2.48	5.45	1.78	14.43	5.09
5.690	48195	1.89	5.36	1.75	3.25	0.56	2.53	1.32
6.888	48198	6.03	43.86	7.98	26.37	1.44	55.83	25.57
7.390	48200	6.26	4.61	1.68	2.79	0.57	11.13	0.86
10.150	48204	2.72	21.88	2.58	10.26	1.85	9.81	4.33
10.325	48205	1.61	3.32	1.86	2.60	0.58	10.86	3.56
10.910	48207	1.48	5.86	0.94	2.95	0.35	2.65	0.69
11.970	48210	2.88	5.32	1.02	3.32	0.48	1.51	0.64

Table D.22: *n*-Fatty Acid concentrations for Lake Holzmaar Samples; Part 2: *n*-C₂₂-*n*-C₂₈

Age 10 ³ years BP	FZJ-Code	<i>n</i> -C ₂₂	<i>n</i> -C ₂₃	<i>n</i> -C ₂₄	<i>n</i> -C ₂₅	<i>n</i> -C ₂₆	<i>n</i> -C ₂₇	<i>n</i> -C ₂₈
$\frac{\mu g}{g\ TOC}$								
0.184	48175	82.07	0.20	67.59	14.69	69.81	16.29	77.58
1.311	48180	54.82	8.00	91.64	23.79	340.05	37.21	265.69
2.083	48184	151.01	31.21	273.79	56.16	455.89	60.43	495.57
2.536	48187	116.94	22.00	189.57	40.59	296.69	44.72	290.84
4.960	48194	36.45	5.36	48.34	13.45	152.19	22.82	144.71
5.690	48195	8.94	3.07	42.14	8.57	105.37	15.43	151.39
6.888	48198	157.17	21.69	228.30	44.82	544.17	61.50	573.48
7.390	48200	29.54	4.10	74.16	11.90	148.47	15.54	152.36
10.150	48204	28.03	9.94	116.28	39.29	294.22	55.42	280.74
10.325	48205	25.65	2.94	34.46	6.87	78.92	11.98	88.85
10.910	48207	10.11	4.86	66.47	21.88	201.89	30.04	169.32
11.970	48210	4.92	1.86	15.12	4.43	59.82	8.44	54.21

D Data Compilation

Table D.23: *n*-Fatty Acid concentrations for Lake Holzmaar Samples; Part 3: *n*-C₂₉-*n*-C₃₂

Age	FZJ-Code	<i>n</i> -C ₂₉	<i>n</i> -C ₃₀	<i>n</i> -C ₃₁	<i>n</i> -C ₃₂
10 ³ years BP		$\frac{\mu g}{g\text{TOC}}$			
0.184	48175	12.96	47.59	9.42	30.39
1.311	48180	15.96	62.45	6.91	31.70
2.083	48184	72.85	378.98	32.64	147.61
2.536	48187	53.31	216.54	18.38	69.69
4.960	48194	22.21	79.97	10.85	31.98
5.690	48195	18.74	99.90	10.42	38.55
6.888	48198	68.58	372.20	35.48	139.38
7.390	48200	21.03	107.06	14.67	52.25
10.150	48204	48.76	168.52	19.10	50.82
10.325	48205	10.61	39.95	5.92	14.90
10.910	48207	21.64	63.51	9.27	22.52
11.970	48210	6.57	26.71	3.70	12.44

Table D.24: *n*-Fatty Acid concentrations for Lake Meerfelder Maar Samples; Part 1: *n*-C₁₅-*n*-C₂₁

Age	FZJ-Code	<i>n</i> -C ₁₅	<i>n</i> -C ₁₆	<i>n</i> -C ₁₇	<i>n</i> -C ₁₈	<i>n</i> -C ₁₉	<i>n</i> -C ₂₀	<i>n</i> -C ₂₁
10 ³ years BP		$\frac{\mu g}{g\text{TOC}}$						
0.280	48339	2.95	35.98	3.81	22.26	0.81	15.69	7.23
0.380	48340	0.09	0.35	0.06	0.18	0.02	0.17	0.06
1.240	48343	0.71	8.39	1.20	3.25	0.84	8.48	3.74
1.740	48344	4.05	66.73	7.85	27.99	6.05	80.00	47.38
1.910	48345	3.01	60.99	7.10	28.04	4.90	44.66	24.72
2.115	48347	0.00	2.10	0.73	1.48	0.37	2.84	1.00
3.765	48348	6.05	40.07	5.36	20.25	6.23	50.70	24.80
4.000	48349	3.67	69.87	4.32	19.34	8.35	81.44	41.96
4.205	48350a	3.57	46.37	6.55	24.31	12.37	95.38	47.91
6.290	48353	3.32	44.53	4.45	20.55	6.86	68.19	39.63
8.850	48357	1.99	14.18	3.14	7.44	2.56	31.45	14.48
10.035	48360	1.29	6.35	1.99	4.19	1.00	9.02	3.88
11.800	48365	2.79	26.06	2.88	11.63	1.68	8.94	4.71
12.250	48367	3.96	9.25	1.66	7.24	0.32	2.26	0.75
12.900	48370	3.00	6.18	1.60	2.96	0.51	14.47	0.19
13.865	48376	1.06	22.69	2.21	9.62	0.05	3.91	0.11
14.385	48378	4.24	16.46	3.59	8.03	0.25	7.39	6.91
14.635	48380	2.37	21.58	2.29	8.83	0.62	24.39	15.64

Table D.25: *n*-Fatty Acid concentrations for Lake Meerfelder Maar Samples; Part 2: *n*-C₂₂-*n*-C₂₈

Age	FZJ-Code	<i>n</i> -C ₂₂	<i>n</i> -C ₂₃	<i>n</i> -C ₂₄	<i>n</i> -C ₂₅	<i>n</i> -C ₂₆	<i>n</i> -C ₂₇	<i>n</i> -C ₂₈
10 ³ years BP		$\frac{\mu\text{g}}{\text{g TOC}}$						
0.280	48339	60.98	24.28	171.54	34.34	258.77	32.58	178.97
0.380	48340	0.71	0.22	1.65	0.34	2.20	0.43	2.19
1.240	48343	26.14	3.97	46.41	5.79	56.19	6.49	34.44
1.740	48344	245.38	40.24	472.06	56.02	531.05	151.96	329.67
1.910	48345	163.69	35.22	367.42	59.66	468.31	61.90	373.59
2.115	48347	9.43	2.24	42.30	5.13	60.87	5.77	43.24
3.765	48348	185.38	32.35	547.81	60.09	1196.22	78.33	680.49
4.000	48349	249.26	41.65	520.49	68.80	1346.79	117.78	1022.36
4.205	48350a	253.08	37.10	347.91	70.97	1061.76	93.72	687.42
6.290	48353	215.86	31.54	343.09	72.10	1292.82	114.14	869.95
8.850	48357	86.10	0.81	103.59	27.05	454.24	47.09	331.33
10.035	48360	23.56	4.19	48.25	8.56	100.05	10.80	135.16
11.800	48365	30.02	10.73	105.50	32.83	330.18	52.87	286.97
12.250	48367	10.56	1.62	15.49	3.95	44.35	6.74	32.55
12.900	48370	29.35	0.32	59.61	16.78	282.96	34.34	212.17
13.865	48376	13.63	0.48	63.89	19.08	148.79	23.41	123.41
14.385	48378	24.89	0.93	20.44	14.12	40.03	7.88	41.18
14.635	48380	89.13	11.20	54.04	17.49	50.46	11.39	54.45

Table D.26: *n*-Fatty Acid concentrations for Lake Meerfelder Maar Samples; Part 3: *n*-C₂₉-*n*-C₃₂

Age	FZJ-Code	<i>n</i> -C ₂₉	<i>n</i> -C ₃₀	<i>n</i> -C ₃₁	<i>n</i> -C ₃₂
10 ³ years BP		$\frac{\mu\text{g}}{\text{g TOC}}$			
0.280	48339	28.67	121.40	17.05	55.53
0.380	48340	0.47	1.93	0.32	1.13
1.240	48343	3.66	12.81	1.41	4.76
1.740	48344	45.57	152.19	32.62	65.33
1.910	48345	47.89	181.26	32.59	79.41
2.115	48347	3.26	14.62	1.34	5.44
3.765	48348	36.26	144.21	14.66	46.79
4.000	48349	48.92	197.69	24.51	72.80
4.205	48350a	32.45	121.51	18.80	43.85
6.290	48353	57.34	274.41	39.22	113.22
8.850	48357	18.58	76.59	18.04	31.82
10.035	48360	0.91	45.14	7.80	19.87
11.800	48365	36.46	158.68	21.39	97.86
12.250	48367	3.79	15.03	3.67	6.76
12.900	48370	13.41	76.51	6.90	30.37

Table D.26: (continued)

Age	FZJ-Code	$n\text{-C}_{29}$	$n\text{-C}_{30}$	$n\text{-C}_{31}$	$n\text{-C}_{32}$
10^3vyears BP		$\frac{\mu\text{g}}{\text{g TOC}}$			
13.865	48376	18.69	78.61	10.29	38.20
14.385	48378	5.34	27.81	6.67	14.78
14.635	48380	8.63	39.76	11.59	23.29

Table D.27: n -Fatty Acid concentrations for Lake Meerfelder Maar Samples (High Resolution Sequence); Part 1: $n\text{-C}_{15}\text{-}n\text{-C}_{21}$

Age	FZJ-Code	$n\text{-C}_{15}$	$n\text{-C}_{16}$	$n\text{-C}_{17}$	$n\text{-C}_{18}$	$n\text{-C}_{19}$	$n\text{-C}_{20}$	$n\text{-C}_{21}$
10^3vyears BP		$\frac{\mu\text{g}}{\text{g TOC}}$						
9.970	E50116	3.05	26.18	3.67	17.18	2.41	13.52	5.18
10.070	E50117	1.68	16.42	3.17	10.24	2.61	14.11	6.13
10.170	E50118	3.42	31.18	4.59	17.76	2.85	26.71	9.75
10.270	E50119	1.68	22.06	3.11	9.09	3.17	43.83	18.05
10.380	E50120	2.33	31.45	3.94	18.27	4.38	45.81	15.55
10.490	E50121	2.53	39.92	5.72	27.07	4.30	47.26	13.37
10.560	E50122	2.92	30.10	3.18	16.51	2.58	22.93	8.54
10.600	E50123	1.99	26.04	3.30	24.53	2.58	19.43	5.95
10.620	E50124	2.00	18.63	2.66	12.51	1.95	10.59	4.00
10.630	E50125	1.17	12.67	1.56	8.23	1.06	4.61	1.61
10.640	E50126	1.75	19.95	2.35	12.29	1.46	9.70	2.97
10.650	E50127	1.85	27.92	3.37	18.60	3.46	23.13	8.13
10.670	E50128	2.20	27.48	3.78	21.54	2.95	21.80	6.49
11.110	E50129	2.59	30.75	3.77	15.73	2.81	14.52	5.25
11.130	E50130	3.31	45.16	5.46	26.31	4.62	22.47	9.50
11.195	E50131	3.36	61.08	6.13	26.39	5.76	34.91	15.44
11.210	E50132	3.55	64.09	7.68	33.05	8.49	50.13	18.87
11.350	E50133	1.47	22.49	2.84	15.18	3.07	18.36	6.25
11.375	E50134	3.88	32.65	5.18	21.66	4.21	28.85	10.05
11.395	E50135	7.89	35.41	5.61	23.40	5.30	28.71	9.55
11.410	E50136	1.66	18.09	3.18	11.27	2.75	11.95	5.42
11.770	E50137	1.38	12.91	1.53	8.59	1.12	3.73	1.74
11.780	E50138	2.07	19.37	1.84	10.82	1.81	2.15	1.34
11.840	E50139	1.84	20.71	2.83	12.76	2.56	10.80	6.69
11.855	E50140	1.35	12.10	1.82	8.22	1.33	4.29	2.46
11.910	E50141	2.65	25.45	2.89	14.76	1.93	8.61	3.79
11.920	E50142	2.67	26.55	3.05	15.48	1.96	4.84	2.59
11.980	E50143	2.94	24.45	2.31	12.29	1.41	3.95	2.09
11.990	E50144	1.95	20.18	1.86	11.75	1.10	3.34	1.63

Table D.27: (continued)

Age	FZJ-Code	<i>n</i> -C ₁₅	<i>n</i> -C ₁₆	<i>n</i> -C ₁₇	<i>n</i> -C ₁₈	<i>n</i> -C ₁₉	<i>n</i> -C ₂₀	<i>n</i> -C ₂₁
10 ³ vyears BP		$\frac{\mu\text{g}}{\text{g TOC}}$						
12.045	E50145	2.77	27.25	2.83	16.54	1.47	8.59	3.93
12.060	E50146	2.28	23.62	2.65	14.10	1.70	8.53	3.20
12.090	E50147	1.84	20.01	1.71	12.46	1.24	3.38	1.70
12.100	E50148	1.49	15.59	2.01	9.71	1.31	3.82	2.18
12.160	E50149	1.31	11.34	1.73	7.33	1.50	3.93	2.41
12.170	E50150	2.24	21.88	2.62	13.66	2.21	7.73	3.79
12.210	E50151	1.92	17.51	1.62	10.12	1.04	2.99	1.46
12.220	E50152	2.17	25.18	2.03	15.20	1.27	3.42	1.59
12.250	E50153	3.50	39.26	5.13	20.89	6.05	51.55	23.51
12.260	E50154	2.33	34.19	3.30	16.89	3.75	24.15	9.44
12.280	E50155	3.80	35.61	4.79	22.37	5.00	28.89	13.89
12.290	E50156	2.32	30.66	2.92	17.02	3.28	14.38	6.17
12.300	E50157	3.06	36.32	4.32	20.81	4.28	32.69	14.84
12.310	E50158	1.96	27.54	3.56	16.25	3.25	16.08	7.74
12.340	E50159	0.59	7.89	0.77	3.88	0.66	3.74	1.62
12.380	E50160	2.53	38.52	5.22	24.91	6.12	43.19	19.19
12.400	E50162	2.31	40.66	3.90	22.01	3.78	22.81	10.49
12.480	E50163	0.00	14.75	3.47	7.41	2.45	10.47	4.31
12.490	E50164	3.56	50.07	4.99	27.10	4.33	27.12	11.61
12.520	E50165	4.80	37.51	5.49	21.99	4.51	32.52	12.25

Table D.28: *n*-Fatty Acid concentrations for Lake Meerfelder Maar Samples (High Resolution Sequence); Part 2: *n*-C₂₂-*n*-C₂₈

Age	FZJ-Code	<i>n</i> -C ₂₂	<i>n</i> -C ₂₃	<i>n</i> -C ₂₄	<i>n</i> -C ₂₅	<i>n</i> -C ₂₆	<i>n</i> -C ₂₇	<i>n</i> -C ₂₈
10 ³ vyears BP		$\frac{\mu\text{g}}{\text{g TOC}}$						
9.970	E50116	34.14	7.57	83.88	17.97	202.47	39.65	254.48
10.070	E50117	33.01	7.61	77.72	14.54	163.10	34.21	265.83
10.170	E50118	67.13	15.05	199.48	32.09	387.32	47.39	450.01
10.270	E50119	121.41	16.70	200.18	37.04	418.80	52.64	910.93
10.380	E50120	112.51	14.78	188.37	38.26	485.21	59.37	445.71
10.490	E50121	109.44	13.31	169.35	34.31	503.82	58.88	463.18
10.560	E50122	68.82	12.67	254.52	41.61	774.69	76.68	525.04
10.600	E50123	49.52	11.16	149.55	39.05	635.13	67.38	433.46
10.620	E50124	27.68	6.88	78.16	21.05	310.63	39.93	231.59
10.630	E50125	13.68	5.25	57.24	17.47	164.43	26.60	144.18
10.640	E50126	25.33	7.64	83.85	29.43	361.26	50.50	275.94
10.650	E50127	66.50	14.64	178.55	58.63	891.73	105.64	656.69

Table D.28: (continued)

Age 10 ³ years BP	FZJ-Code	<i>n</i> -C ₂₂	<i>n</i> -C ₂₃	<i>n</i> -C ₂₄	<i>n</i> -C ₂₅	<i>n</i> -C ₂₆	<i>n</i> -C ₂₇	<i>n</i> -C ₂₈
					$\frac{\mu g}{g \text{ TOC}}$			
10.670	E50128	51.65	10.61	123.59	42.42	685.03	76.33	462.71
11.110	E50129	35.92	9.45	107.39	31.80	434.84	58.74	333.67
11.130	E50130	51.63	12.66	126.69	41.93	675.42	80.23	474.85
11.195	E50131	83.92	21.09	188.26	47.60	758.04	86.71	488.83
11.210	E50132	119.86	25.56	288.27	93.80	1519.60	178.24	978.96
11.350	E50133	38.90	9.11	89.40	37.40	696.89	83.50	547.07
11.375	E50134	63.94	13.98	135.00	47.91	798.45	105.80	549.73
11.395	E50135	51.11	10.07	70.54	22.49	297.56	37.83	179.88
11.410	E50136	28.12	8.33	66.55	24.59	378.31	53.08	273.70
11.770	E50137	9.21	3.48	28.85	10.07	133.63	23.72	98.91
11.780	E50138	4.64	2.13	13.77	3.81	34.67	9.40	28.20
11.840	E50139	37.12	16.88	171.09	54.55	565.02	89.14	388.46
11.855	E50140	11.62	5.04	45.89	15.60	192.90	29.99	118.77
11.910	E50141	20.68	6.97	65.11	24.83	335.15	50.55	185.73
11.920	E50142	12.77	4.55	35.58	13.66	153.37	26.11	84.95
11.980	E50143	10.53	4.46	48.04	16.13	192.45	29.91	116.85
11.990	E50144	8.51	3.39	32.33	10.65	128.40	20.38	80.50
12.045	E50145	24.67	10.51	135.34	42.77	565.08	75.14	331.06
12.060	E50146	20.04	7.29	77.84	27.53	364.62	54.51	215.94
12.090	E50147	8.42	4.11	44.78	10.52	107.36	15.31	69.31
12.100	E50148	10.33	5.18	62.95	14.57	149.72	21.94	87.65
12.160	E50149	10.28	5.57	68.71	12.45	137.99	19.12	83.35
12.170	E50150	17.65	9.48	119.61	22.17	222.78	29.21	139.57
12.210	E50151	6.92	4.25	47.07	10.40	95.54	14.04	63.50
12.220	E50152	7.38	3.45	34.11	9.04	83.61	14.53	57.85
12.250	E50153	116.77	29.44	369.53	81.86	1,022.08	125.39	631.82
12.260	E50154	59.36	19.26	298.42	79.11	1,191.93	135.56	639.37
12.280	E50155	72.04	22.65	321.60	63.03	788.96	88.90	496.22
12.290	E50156	34.61	13.00	190.32	41.35	559.58	66.07	367.81
12.300	E50157	85.30	27.81	505.84	90.19	1,114.86	107.79	668.28
12.310	E50158	41.96	15.70	257.65	48.27	553.78	61.46	344.90
12.340	E50159	11.08	3.24	57.15	12.29	180.48	19.34	97.98
12.380	E50160	105.35	27.50	452.59	83.06	1,109.02	114.26	644.95
12.400	E50162	58.47	18.56	308.49	53.45	660.74	67.58	423.08
12.480	E50163	25.12	8.67	140.06	27.31	331.21	39.49	216.44
12.490	E50164	67.68	25.55	404.26	82.81	927.78	103.15	613.24
12.520	E50165	63.70	17.72	246.70	55.40	759.41	90.11	421.51

Table D.29: *n*-Fatty Acid concentrations for Lake Meerfelder Maar Samples (High Resolution Sequence); Part 3: *n*-C₂₉-*n*-C₃₂

Age	FZJ-Code	<i>n</i> -C ₂₉	<i>n</i> -C ₃₀	<i>n</i> -C ₃₁	<i>n</i> -C ₃₂
10 ³ years BP		$\frac{\mu\text{g}}{\text{g TOC}}$			
9.970	E50116	14.88	72.81	7.00	29.65
10.070	E50117	14.14	75.34	7.80	31.48
10.170	E50118	30.70	163.11	14.60	68.91
10.270	e50119	33.13	179.47	17.25	77.06
10.380	E50120	37.41	174.40	17.15	81.16
10.490	E50121	28.81	152.44	14.92	75.06
10.560	E50122	37.70	173.27	17.32	74.95
10.600	E50123	32.49	132.82	14.60	56.82
10.620	E50124	22.28	94.34	10.23	37.71
10.630	E50125	20.28	76.77	9.33	29.53
10.640	E50126	33.00	121.45	14.71	47.67
10.650	E50127	61.54	244.31	26.73	96.28
10.670	E50128	36.80	147.65	15.23	60.24
11.110	E50129	41.39	122.32	12.55	54.82
11.130	E50130	41.61	131.97	15.39	60.56
11.195	E50131	37.99	135.22	15.80	63.70
11.210	E50132	71.70	274.24	26.63	120.14
11.350	E50133	24.36	85.86	9.32	38.83
11.375	E50134	36.99	150.42	14.97	64.08
11.395	E50135	12.25	47.12	6.83	23.35
11.410	E50136	19.37	76.59	8.05	34.89
11.770	E50137	11.11	39.36	4.70	27.12
11.780	E50138	5.00	14.83	2.54	7.85
11.840	E50139	54.92	187.63	24.10	96.80
11.855	E50140	12.79	42.47	6.37	16.84
11.910	E50141	19.22	55.45	6.39	20.24
11.920	E50142	10.43	27.63	3.95	10.74
11.980	E50143	16.40	52.58	7.76	21.35
11.990	E50144	10.65	36.17	4.67	13.65
12.045	E50145	37.46	123.14	14.61	47.82
12.060	E50146	21.41	66.78	8.26	28.11
12.090	E50147	11.88	44.74	5.45	16.44
12.100	E50148	12.67	41.17	5.84	17.03
12.160	E50149	11.73	37.93	5.35	17.39
12.170	E50150	20.74	77.97	10.21	32.53
12.210	E50151	10.04	34.51	4.83	14.78
12.220	E50152	8.98	29.67	4.32	12.30
12.250	E50153	71.09	287.21	30.01	115.37
12.260	E50154	53.29	207.35	20.78	81.62
12.280	E50155	52.96	233.10	25.39	94.69
12.290	E50156	38.96	159.54	16.60	65.73
12.300	E50157	68.06	300.75	29.59	107.74

Table D.29: (continued)

Age	FZJ-Code	$n\text{-C}_{29}$	$n\text{-C}_{30}$	$n\text{-C}_{31}$	$n\text{-C}_{32}$
10^3years BP		$\frac{\mu\text{g}}{\text{g TOC}}$			
12.310	E50158	37.02	157.96	15.04	58.27
12.340	E50159	7.32	29.46	2.42	9.84
12.380	E50160	56.51	250.96	21.47	83.11
12.400	E50162	44.24	206.54	17.76	67.50
12.480	E50163	24.96	119.82	9.77	38.83
12.490	E50164	70.72	330.76	28.84	113.93
12.520	E50165	45.56	197.95	15.55	60.12

n-Alcohols

Table D.30: *n*-Alcohol concentrations for Lake Holzmaar Samples; Part 1: *n*-C₁₅-*n*-C₂₁

Age	FZJ-Code	<i>n</i> -C ₁₅	<i>n</i> -C ₁₆	<i>n</i> -C ₁₇	<i>n</i> -C ₁₈	<i>n</i> -C ₁₉	<i>n</i> -C ₂₀	<i>n</i> -C ₂₁
10 ³ vyears BP		$\frac{\mu\text{g}}{\text{g TOC}}$						
0.184	48175	13.93	2.69	13.62	3.98	1.83	26.36	18.38
1.311	48180	26.00	2.05	25.14	4.59	1.22	21.71	7.83
2.083	48184	11.11	2.32	14.70	7.88	1.40	22.90	9.22
2.536	48187	25.15	3.51	19.55	12.22	1.76	30.02	8.85
4.960	48194	14.37	2.29	15.57	10.00	1.63	28.57	12.50
5.690	48195	17.01	2.80	17.36	13.95	2.25	32.94	11.79
6.888	48198	28.33	5.41	25.05	12.80	2.43	32.29	28.73
7.390	48200	15.47	2.07	14.17	5.76	0.93	1.02	1.10
10.150	48204	18.47	2.69	16.52	3.10	1.01	0.00	25.46
10.325	48205	18.85	4.75	21.80	15.20	3.48	0.00	7.28
10.910	48207	11.14	2.77	14.64	3.30	0.80	11.46	8.75
11.970	48210	9.53	2.14	11.39	5.73	0.95	14.94	5.00

Table D.31: *n*-Alcohol concentrations for Lake Holzmaar Samples; Part 2: *n*-C₂₂-*n*-C₂₈

Age	FZJ-Code	<i>n</i> -C ₂₂	<i>n</i> -C ₂₃	<i>n</i> -C ₂₄	<i>n</i> -C ₂₅	<i>n</i> -C ₂₆	<i>n</i> -C ₂₇	<i>n</i> -C ₂₈
10 ³ vyears BP		$\frac{\mu\text{g}}{\text{g TOC}}$						
0.184	48175	227.12	42.30	212.14	39.49	577.50	49.58	446.85
1.311	48180	56.89	14.40	107.62	28.26	127.45	41.64	314.45
2.083	48184	111.46	20.53	182.50	27.31	460.52	35.02	423.65
2.536	48187	106.24	27.92	204.65	28.26	502.97	37.28	433.27
4.960	48194	46.76	15.10	176.75	29.92	240.78	38.89	280.79
5.690	48195	29.60	10.04	160.00	27.73	279.26	35.15	291.93
6.888	48198	21.39	10.01	126.91	30.15	239.16	41.14	227.30
7.390	48200	36.47	10.09	270.25	33.38	338.80	35.39	268.56
10.150	48204	50.18	15.04	133.54	38.64	278.17	55.33	313.41
10.325	48205	44.61	12.36	111.54	39.32	277.14	58.25	338.86
10.910	48207	82.82	18.83	155.09	55.60	359.60	73.63	443.74
11.970	48210	27.10	10.50	96.68	24.02	254.62	31.57	226.64

D Data Compilation

Table D.32: *n*-Alcohol concentrations for Lake Holzmaar Samples; Part 3: *n*-C₂₉-*n*-C₃₂

Age 10 ³ years BP	FZJ-Code	<i>n</i> -C ₂₉	<i>n</i> -C ₃₀	<i>n</i> -C ₃₁	<i>n</i> -C ₃₂
		$\frac{\mu g}{g\text{TOC}}$			
0.184	48175	10.22	161.48	5.82	75.28
1.311	48180	11.46	106.58	4.61	53.45
2.083	48184	7.46	252.81	10.07	66.79
2.536	48187	9.92	245.24	12.26	50.15
4.960	48194	6.56	162.46	12.29	74.49
5.690	48195	0.00	196.53	6.82	92.63
6.888	48198	7.10	218.09	8.75	106.08
7.390	48200	4.47	244.22	4.67	130.95
10.150	48204	7.44	221.78	16.60	0.00
10.325	48205	8.82	195.16	11.31	74.11
10.910	48207	10.87	169.64	15.50	0.00
11.970	48210	6.09	121.74	9.06	54.11

Table D.33: *n*-Alcohol concentrations for Lake Meerfelder Maar Samples; Part 1: *n*-C₁₅-*n*-C₂₁

Age 10 ³ years BP	FZJ-Code	<i>n</i> -C ₁₅	<i>n</i> -C ₁₆	<i>n</i> -C ₁₇	<i>n</i> -C ₁₈	<i>n</i> -C ₁₉	<i>n</i> -C ₂₀	<i>n</i> -C ₂₁
		$\frac{\mu g}{g\text{TOC}}$						
0.380	48340	33.23	9.32	18.10	8.75	0.60	14.93	6.79
1.240	48343	2.82	0.41	3.86	0.32	0.18	0.00	1.91
1.740	48344	55.98	18.50	39.16	31.19	2.25	20.50	16.02
1.910	48345	121.76	12.15	70.42	17.85	1.13	13.99	11.39
2.115	48347	2.90	0.55	3.64	0.39	0.23	0.00	3.77
3.765	48348	20.09	18.52	19.81	3.59	1.92	19.82	14.82
4.000	48349	18.60	2.19	19.77	3.64	2.08	26.87	20.82
4.205	48350a	42.02	3.69	26.81	5.37	3.16	40.32	28.00
6.290	48353	31.71	2.51	22.12	4.30	1.84	24.53	20.03
8.850	48357	21.55	3.15	22.62	4.69	2.86	34.09	19.53
10.035	48360	41.90	5.94	28.10	9.34	3.49	46.61	13.80
11.833	48365	107.77	8.46	60.12	16.24	2.85	30.54	12.83
12.250	48367	49.63	9.38	28.26	19.56	2.91	0.00	22.02
12.900	48370	39.43	6.44	27.16	18.51	2.39	49.79	28.04
13.865	48376	61.37	6.96	28.86	11.97	1.53	0.00	8.14
14.385	48378	76.68	6.10	44.82	16.99	2.47	42.18	6.47
14.635	48380	93.63	7.49	66.76	6.25	1.42	12.23	26.29

Table D.34: *n*-Alcohol concentrations for Lake Meerfelder Maar Samples; Part 2: *n*-C₂₂-*n*-C₂₈

Age	FZJ-Code	<i>n</i> -C ₂₂	<i>n</i> -C ₂₃	<i>n</i> -C ₂₄	<i>n</i> -C ₂₅	<i>n</i> -C ₂₆	<i>n</i> -C ₂₇	<i>n</i> -C ₂₈
10 ³ years BP		$\frac{\mu\text{g}}{\text{g TOC}}$						
0.380	48340	85.30	14.47	128.30	13.71	211.55	17.42	152.88
1.240	48343	19.41	2.63	36.01	4.06	31.93	4.04	35.29
1.740	48344	199.17	28.26	335.79	38.51	263.02	40.63	304.63
1.910	48345	166.57	19.83	248.81	22.77	226.20	43.79	266.98
2.115	48347	25.26	3.63	33.18	4.93	36.39	4.78	43.85
3.765	48348	135.42	18.42	231.98	41.89	251.21	45.12	320.48
4.000	48349	113.55	18.88	225.76	37.10	241.52	50.76	398.60
4.205	48350a	149.26	24.63	233.23	44.96	260.46	54.86	403.98
6.290	48353	104.36	21.08	313.26	50.63	412.81	53.51	433.59
8.850	48357	59.45	19.60	142.15	41.90	242.96	46.58	289.47
10.035	48360	46.32	25.73	216.45	36.96	314.53	31.65	264.53
11.833	48365	75.77	35.35	210.96	73.03	541.12	94.04	511.15
12.250	48367	50.79	39.53	166.62	49.21	361.78	80.73	355.07
12.900	48370	62.19	31.53	194.75	50.11	407.63	66.21	572.22
13.865	48376	78.47	37.94	203.88	48.55	570.46	59.48	443.69
14.385	48378	59.03	35.08	157.01	41.89	503.85	47.04	293.59
14.635	48380	147.95	79.38	235.46	62.92	683.48	68.69	406.53

Table D.35: *n*-Alcohol concentrations for Lake Meerfelder Maar Samples; Part 3: *n*-C₂₉-*n*-C₃₂

Age	FZJ-Code	<i>n</i> -C ₂₉	<i>n</i> -C ₃₀	<i>n</i> -C ₃₁	<i>n</i> -C ₃₂
10 ³ years BP		$\frac{\mu\text{g}}{\text{g TOC}}$			
0.380	48340	5.30	111.29	18.88	36.57
1.240	48343	2.78	23.04	n.a.	6.19
1.740	48344	21.71	215.38	27.17	34.63
1.910	48345	15.38	164.23	17.00	34.22
2.115	48347	2.64	30.06	n.a.	5.77
3.765	48348	15.39	173.19	20.36	38.30
4.000	48349	20.17	168.69	14.02	52.20
4.205	48350a	19.29	184.81	15.94	38.60
6.290	48353	24.28	282.18	12.96	127.37
8.850	48357	25.28	231.74	22.54	49.64
10.035	48360	36.03	304.04	16.86	75.48
11.833	48365	19.75	228.43	12.11	98.49
12.250	48367	71.55	154.79	13.83	51.03
12.900	48370	19.67	287.10	3.07	72.54
13.865	48376	9.47	221.38	9.61	75.45
14.385	48378	17.28	147.45	15.47	54.80

Table D.35: (continued)

Age	FZJ-Code	$n\text{-C}_{29}$	$n\text{-C}_{30}$	$n\text{-C}_{31}$	$n\text{-C}_{32}$
10^3vyears BP		$\frac{\mu\text{g}}{\text{g TOC}}$			
14.635	48380	17.15	180.39	6.95	87.31

Table D.36: n -Alcohol concentrations for Lake Meerfelder Maar Samples (High Resolution Sequence); Part 1: $n\text{-C}_{15}\text{-}n\text{-C}_{21}$

Age	FZJ-Code	$n\text{-C}_{15}$	$n\text{-C}_{16}$	$n\text{-C}_{17}$	$n\text{-C}_{18}$	$n\text{-C}_{19}$	$n\text{-C}_{20}$	$n\text{-C}_{21}$
10^3vyears BP		$\frac{\mu\text{g}}{\text{g TOC}}$						
9.970	50116	11.91	6.52	18.46	16.95	4.06	3.12	14.51
10.070	50117	11.74	3.56	15.51	10.82	3.92	2.56	12.27
10.170	50118	0.00	1.10	0.69	5.13	2.15	1.48	9.38
10.270	50119	10.94	1.72	8.07	3.17	1.72	0.99	6.60
10.380	50120	8.41	3.63	8.39	6.93	2.79	41.41	6.59
10.490	50121	15.99	6.50	16.10	11.61	3.27	56.68	6.57
10.560	50122	9.29	3.27	11.61	6.40	1.62	27.70	3.80
10.600	50123	4.43	2.27	9.22	0.52	2.11	37.09	4.98
10.620	50124	11.49	4.32	15.04	0.52	2.35	35.49	5.11
10.630	50125	2.28	2.10	8.10	6.52	1.36	21.43	3.91
10.640	50126	1.94	2.90	9.53	5.98	1.97	26.23	4.05
10.650	50127	6.73	1.80	8.04	5.42	1.60	29.61	3.83
10.670	50128	8.37	3.76	10.02	7.42	2.37	38.17	4.53
11.110	50129	8.84	2.37	9.05	11.56	2.48	53.94	4.28
11.130	50130	9.72	2.57	11.64	13.86	3.28	72.57	6.65
11.195	50131	8.33	1.99	11.74	10.71	2.32	49.97	5.81
11.210	50132	9.40	4.72	14.29	18.73	3.66	75.26	6.29
11.350	50133	11.75	1.88	9.98	11.55	2.66	51.59	5.48
11.375	50134	9.25	2.89	11.18	13.26	2.55	51.29	5.17
11.395	50135	14.65	4.11	13.86	16.31	2.88	53.82	5.78
11.410	50136	1.85	0.00	7.93	1.37	1.54	19.72	1.84
11.770	50137	4.45	4.18	11.66	7.79	2.01	22.75	4.37
11.780	50138	1.39	2.15	6.84	6.24	1.56	20.26	3.83
11.840	50139	4.33	1.30	14.59	5.28	1.64	20.94	5.35
11.855	50140	5.05	3.55	11.41	0.86	2.20	23.67	4.81
11.910	50141	9.88	3.43	13.75	9.20	2.47	25.72	6.07
11.920	50142	4.88	2.34	16.90	7.09	2.17	20.39	5.35
11.980	50143	2.67	2.53	13.92	10.27	1.71	16.96	4.76
11.990	50144	2.78	3.27	11.33	8.32	2.08	25.31	5.45
12.045	50145	4.30	1.96	11.55	1.39	1.45	16.34	3.99
12.060	50146	5.36	3.06	10.82	5.97	1.56	18.83	5.08

Table D.36: (continued)

Age	FZJ-Code	$n\text{-C}_{15}$	$n\text{-C}_{16}$	$n\text{-C}_{17}$	$n\text{-C}_{18}$	$n\text{-C}_{19}$	$n\text{-C}_{20}$	$n\text{-C}_{21}$
10^3years BP		$\frac{\mu\text{g}}{\text{g TOC}}$						
12.090	50147	0.00	2.96	8.54	0.70	0.33	1.63	1.03
12.100	50148	3.58	3.28	12.49	7.45	2.17	24.36	6.14
12.160	50149	4.21	3.13	9.14	6.33	1.77	21.58	5.66
12.170	50150	4.00	3.68	10.35	6.79	1.99	22.89	5.89
12.210	50151	3.79	2.62	13.85	1.24	1.36	16.08	4.67
12.220	50152	1.96	6.45	12.20	11.93	1.93	19.23	5.34
12.250	50153	7.84	2.07	19.64	6.15	1.83	21.43	4.16
12.260	50154	9.47	3.37	17.08	9.51	2.22	22.45	4.65
12.280	50155	4.97	2.64	12.38	6.89	2.12	24.56	4.43
12.290	50156	4.94	6.21	12.33	10.66	2.19	26.36	4.07
12.300	50157	3.50	2.71	9.41	6.53	0.20	20.99	4.53
12.310	50158	5.75	2.52	10.28	6.59	1.83	26.24	4.06
12.340	50159	10.08	6.21	16.25	11.28	2.46	33.79	5.40
12.380	50160	9.42	7.21	11.98	8.80	3.32	29.09	5.23
12.400	50162	9.42	4.49	24.80	13.68	2.79	40.36	4.99
12.480	50163	8.40	2.19	17.49	9.29	2.13	23.31	4.12
12.490	50164	9.88	2.11	16.57	10.36	3.06	32.55	6.15
12.520	50165	14.88	9.53	9.98	19.81	2.31	21.49	7.82

Table D.37: n -Alcohol concentrations for Lake Meerfelder Maar Samples (High Resolution Sequence); Part 2: $n\text{-C}_{22}\text{-}n\text{-C}_{28}$

Age	FZJ-Code	$n\text{-C}_{22}$	$n\text{-C}_{23}$	$n\text{-C}_{24}$	$n\text{-C}_{25}$	$n\text{-C}_{26}$	$n\text{-C}_{27}$	$n\text{-C}_{28}$
10^3years BP		$\frac{\mu\text{g}}{\text{g TOC}}$						
9.970	50116	60.62	32.53	316.81	12.03	414.14	56.32	331.94
10.070	50117	52.68	31.11	245.71	10.67	400.86	44.35	329.79
10.170	50118	45.09	19.43	181.86	7.69	368.90	41.22	334.03
10.270	50119	40.52	24.92	210.80	5.70	365.26	40.45	346.54
10.380	50120	61.94	29.16	259.31	40.71	354.54	45.59	392.88
10.490	50121	50.83	24.61	174.28	40.44	361.62	49.39	364.99
10.560	50122	50.65	21.23	148.55	37.31	263.82	42.57	257.56
10.600	50123	61.16	24.98	173.65	45.16	288.72	49.57	314.41
10.620	50124	48.50	25.13	149.46	40.84	268.83	51.95	288.02
10.630	50125	69.37	20.09	165.63	36.05	288.06	41.14	295.86
10.640	50126	66.48	19.40	179.20	39.99	318.71	47.66	315.56
10.650	50127	52.40	17.08	165.64	38.69	297.73	44.25	299.43
10.670	50128	52.66	18.92	167.05	42.72	289.12	46.77	299.81
11.110	50129	59.09	17.53	141.59	54.19	326.96	49.26	302.21

Table D.37: (continued)

Age	FZJ-Code	$n\text{-C}_{22}$	$n\text{-C}_{23}$	$n\text{-C}_{24}$	$n\text{-C}_{25}$	$n\text{-C}_{26}$	$n\text{-C}_{27}$	$n\text{-C}_{28}$
10^3vyears BP					$\frac{\mu\text{g}}{\text{g TOC}}$			
11.130	50130	104.31	22.11	210.72	56.98	395.12	66.72	401.30
11.195	50131	85.97	25.48	216.01	48.68	435.21	63.25	442.16
11.210	50132	67.70	26.96	217.23	55.35	434.98	68.27	428.68
11.350	50133	58.01	21.96	168.30	54.50	406.18	64.31	387.41
11.375	50134	48.71	22.71	142.04	46.68	382.37	59.17	322.81
11.395	50135	55.53	23.86	144.64	45.25	381.68	56.02	316.33
11.410	50136	14.19	3.82	18.47	3.59	22.86	10.35	15.91
11.770	50137	56.93	20.77	185.57	55.44	501.35	63.11	430.48
11.780	50138	69.56	21.66	202.29	51.80	573.59	59.34	484.75
11.840	50139	69.20	27.62	220.36	68.74	566.07	77.51	465.13
11.855	50140	61.09	26.32	196.16	65.21	439.82	63.73	321.81
11.910	50141	51.60	28.02	182.76	69.23	434.69	69.84	355.66
11.920	50142	50.40	25.17	166.10	64.27	425.44	62.77	333.93
11.980	50143	46.09	25.90	175.08	59.37	424.87	66.05	329.13
11.990	50144	59.66	30.33	215.52	72.20	533.17	79.57	422.51
12.045	50145	61.13	31.58	209.40	72.46	506.90	75.83	400.11
12.060	50146	61.92	27.77	187.65	69.26	449.42	67.00	383.20
12.090	50147	1.98	2.38	18.24	15.09	109.46	29.16	158.95
12.100	50148	63.97	32.60	191.68	59.83	466.90	60.62	386.20
12.160	50149	64.16	32.43	181.97	49.80	394.82	52.77	325.11
12.170	50150	82.85	38.02	209.72	59.73	514.54	64.34	451.59
12.210	50151	56.46	29.55	138.35	32.78	281.33	32.74	194.44
12.220	50152	76.43	37.77	221.61	60.09	529.90	64.36	424.75
12.250	50153	41.37	28.14	171.75	45.01	410.14	58.39	363.42
12.260	50154	48.31	30.60	195.36	55.73	408.66	88.47	361.83
12.280	50155	37.10	21.95	136.09	33.81	321.17	50.94	284.07
12.290	50156	44.74	27.62	164.59	36.24	378.83	46.65	352.56
12.300	50157	51.29	30.24	179.29	39.55	374.01	53.69	366.49
12.310	50158	44.24	25.69	149.80	31.75	328.88	45.74	330.12
12.340	50159	54.96	29.66	202.08	54.74	391.29	68.61	349.71
12.380	50160	45.36	20.80	178.79	37.96	356.07	50.42	301.20
12.400	50162	51.21	41.43	172.44	33.03	379.58	49.02	331.07
12.480	50163	48.48	21.19	189.67	38.43	396.93	61.87	353.79
12.490	50164	62.67	0.32	210.02	40.61	423.18	62.09	342.26
12.520	50165	27.27	15.00	95.58	19.06	153.51	24.87	110.49

Table D.38: *n*-Alcohol concentrations for Lake Meerfelder Maar Samples (High Resolution Sequence); Part 3: *n*-C₂₉-*n*-C₃₂

Age	FZJ-Code	<i>n</i> -C ₂₉	<i>n</i> -C ₃₀	<i>n</i> -C ₃₁	<i>n</i> -C ₃₂
10 ³ years BP		$\frac{\mu g}{g \text{ TOC}}$			
9.970	50116	50.59	376.14	54.61	71.93
10.070	50117	48.53	357.13	41.51	84.98
10.170	50118	51.03	403.84	30.73	22.96
10.270	50119	49.09	364.24	29.63	76.79
10.380	50120	61.40	385.35	33.54	91.77
10.490	50121	54.36	377.51	31.83	92.61
10.560	50122	40.27	257.58	33.30	76.76
10.600	50123	39.68	323.89	41.64	91.99
10.620	50124	51.35	274.07	41.55	88.65
10.630	50125	37.27	265.41	52.86	111.24
10.640	50126	41.99	298.98	57.40	115.13
10.650	50127	33.73	260.36	40.77	102.97
10.670	50128	33.39	236.25	32.28	84.19
11.110	50129	33.42	206.15	25.43	52.34
11.130	50130	36.65	216.73	21.13	65.03
11.195	50131	39.11	235.10	33.20	73.76
11.210	50132	41.93	244.19	33.45	76.80
11.350	50133	33.56	171.56	34.39	56.00
11.375	50134	35.86	161.54	28.16	54.13
11.395	50135	35.76	157.67	34.32	50.04
11.410	50136	9.10	25.94	6.84	0.00
11.770	50137	45.15	190.65	32.22	70.43
11.780	50138	44.73	213.61	43.33	68.75
11.840	50139	68.78	224.98	39.16	64.14
11.855	50140	41.29	142.11	24.56	40.07
11.910	50141	49.73	145.90	30.05	41.77
11.920	50142	43.63	133.41	31.35	35.95
11.980	50143	47.21	140.62	26.66	42.42
11.990	50144	57.97	179.42	35.10	52.38
12.045	50145	56.61	168.42	5.97	52.78
12.060	50146	50.69	162.72	6.37	50.67
12.090	50147	61.87	105.51	1.52	37.39
12.100	50148	52.92	157.09	26.08	49.31
12.160	50149	55.04	148.48	30.85	50.58
12.170	50150	77.78	192.70	32.99	62.08
12.210	50151	25.54	74.92	20.39	25.41
12.220	50152	60.23	196.85	36.87	67.04
12.250	50153	95.31	158.64	31.72	52.36
12.260	50154	108.25	159.41	27.35	54.77
12.280	50155	70.90	141.00	47.04	47.64
12.290	50156	87.59	152.11	30.03	51.62
12.300	50157	70.34	160.07	23.83	54.70

Table D.38: (continued)

Age	FZJ-Code	$n\text{-C}_{29}$	$n\text{-C}_{30}$	$n\text{-C}_{31}$	$n\text{-C}_{32}$
10^3years BP		$\frac{\mu\text{g}}{\text{g TOC}}$			
12.310	50158	58.15	135.89	22.74	50.43
12.340	50159	33.67	155.95	27.37	49.46
12.380	50160	34.70	134.06	4.20	46.39
12.400	50162	37.89	154.17	22.03	54.62
12.480	50163	61.93	158.82	9.04	2.65
12.490	50164	45.65	159.80	2.65	4.46
12.520	50165	19.90	63.90	19.19	17.65

Sterols

Table D.39: Sterol concentrations for Lake Holzmaar Samples; Part 1: Compounds A to G
(Labels are assigned to systematic names of Sterols as listed in *Table 5.4, Page 122*)

Age	FZJ-Code	A	B	C	D	E	F	G
10^3years BP		$\frac{\mu\text{g}}{\text{g TOC}}$						
0.184	48175	11.85	39.93	33.47	7.66	13.36	11.01	10.22
1.311	48180	20.50	46.15	41.93	12.89	11.94	7.10	11.46
2.083	48184	9.05	23.29	39.11	7.28	8.15	5.60	7.46
2.536	48187	13.61	28.35	34.06	13.57	11.25	12.95	9.92
4.960	48194	5.30	28.35	29.74	9.57	7.75	7.67	6.56
5.690	48195	7.75	17.29	23.94	4.63	5.10	2.60	2.13
6.888	48198	13.22	26.37	26.28	7.78	10.13	3.41	7.10
7.390	48200	7.70	14.66	16.34	5.22	7.54	1.94	4.47
10.150	48204	10.12	19.97	16.32	12.61	12.37	4.51	7.44
10.325	48205	8.79	27.45	26.89	12.79	14.09	7.05	8.82
10.910	48207	8.74	23.53	18.99	13.71	16.79	7.11	4.39
11.970	48210	8.47	16.63	12.94	9.96	6.82	4.12	3.41

Table D.40: Sterol concentrations for Lake Holzmaar Samples; Part 2: Compounds H to N
(Labels are assigned to systematic names of Sterols as listed in [Table 5.4, Page 122](#))

Age	FZJ-Code	H	I	J	K	L	M	N
10 ³ years BP		$\frac{\mu g}{g\text{TOC}}$						
0.184	48175	16.75	43.92	22.05	64.15	71.47	32.34	1.24
1.311	48180	11.73	39.15	n.a.	60.57	22.70	30.32	n.a.
2.083	48184	5.58	19.83	n.a.	49.54	39.44	43.73	n.a.
2.536	48187	17.65	34.22	16.61	80.02	71.52	44.35	131.77
4.960	48194	4.93	30.38	n.a.	82.61	37.10	31.74	n.a.
5.690	48195	7.71	20.22	11.42	37.75	31.35	30.77	n.a.
6.888	48198	5.96	16.31	48.81	79.05	18.88	22.62	8.28
7.390	48200	7.29	44.63	111.11	158.51	28.29	24.80	12.73
10.150	48204	6.89	23.47	n.a.	34.30	n.a.	51.97	0.25
10.325	48205	17.17	23.29	12.68	30.24	12.88	45.06	47.12
10.910	48207	10.95	20.28	19.49	36.04	n.a.	77.06	0.86
11.970	48210	12.02	15.10	10.01	23.33	55.16	37.12	16.12

Table D.41: Sterol concentrations for Lake Holzmaar Samples; Part 3: Compounds O to Q
(Labels are assigned to systematic names of Sterols as listed in [Table 5.4, Page 122](#))

Age	FZJ-Code	O	P	Q
10 ³ years BP		$\frac{\mu g}{g\text{TOC}}$		
0.184	48175	23.87	4.39	19.83
1.311	48180	10.62	1.47	8.61
2.083	48184	28.07	5.87	8.84
2.536	48187	34.19	13.76	4.87
4.960	48194	66.57	4.72	3.33
5.690	48195	173.94	8.10	3.17
6.888	48198	124.30	16.52	5.31
7.390	48200	135.62	22.84	5.04
10.150	48204	37.78	2.70	6.27
10.325	48205	67.42	19.38	4.16
10.910	48207	55.65	74.25	4.89
11.970	48210	44.82	1.99	3.96

D Data Compilation

Table D.42: Sterol concentrations for Lake Meerfelder Maar Samples; Part 1: Compounds A to G (Labels are assigned to systematic names of Sterols as listed in *Table 5.4, Page 122*)

Age	FZJ-Code	A	B	C	D	E	F	G
10 ³ years BP		$\frac{\mu g}{g \text{ TOC}}$						
0.600	48340	2.83	12.12	10.42	12.53	7.90	4.89	5.30
1.240	48343	1.88	0.00	0.00	5.14	3.44	0.27	0.87
1.740	48344	8.62	48.03	40.19	15.00	39.28	9.95	21.71
1.910	48345	18.93	30.06	26.33	9.88	17.56	8.91	15.38
2.115	48347	1.54	5.98	4.52	2.85	4.45	2.87	0.82
3.765	48348	12.23	41.31	32.91	8.68	45.80	7.57	15.39
3.990	48349	0.00	42.96	35.51	11.48	71.58	9.33	20.17
4.205	48350a	8.24	50.87	38.24	22.07	61.38	6.59	19.29
6.290	48353	10.38	35.56	29.52	16.15	64.41	9.80	24.28
8.670	48357	0.00	56.35	41.76	6.51	38.81	10.83	25.28
10.035	48360	8.58	62.29	27.61	92.11	32.20	7.64	36.03
11.833	48365	27.72	55.62	33.52	30.37	35.51	18.92	19.75
12.210	48367	16.49	36.44	25.95	23.47	28.09	16.09	21.07
13.030	48370	11.53	45.39	29.17	26.51	23.09	15.38	19.67
13.865	48376	14.13	22.16	16.01	25.63	11.80	10.18	9.47
14.385	48378	28.75	38.69	30.80	23.52	15.17	16.40	17.28
14.635	48380	48.25	40.00	63.79	12.26	17.62	7.94	17.15

Table D.43: Sterol concentrations for Lake Meerfelder Maar Samples; Part 2: Compounds H to N (Labels are assigned to systematic names of Sterols as listed in *Table 5.4, Page 122*)

Age	FZJ-Code	H	I	J	K	L	M	N
10 ³ years BP		$\frac{\mu g}{g \text{ TOC}}$						
0.600	48340	16.11	16.52	2.68	32.18	52.17	16.69	57.96
1.240	48343	3.53	6.00	0.00	13.81	6.64	22.32	3.00
1.740	48344	50.07	65.94	26.40	49.23	98.94	120.88	99.52
1.910	48345	28.46	23.33	20.19	33.54	55.08	44.97	6.17
2.115	48347	4.16	6.54	5.15	12.78	8.66	8.90	1.73
3.765	48348	24.47	43.88	n.a.	95.74	129.96	n.a.	74.25
3.990	48349	24.54	79.97	n.a.	75.24	99.90	89.39	19.76
4.205	48350a	25.57	51.39	n.a.	89.90	121.60	75.77	43.51
6.290	48353	85.02	90.95	n.a.	83.08	115.33	57.48	20.60
8.670	48357	40.74	52.31	n.a.	77.96	128.36	99.99	358.55
10.035	48360	28.34	30.73	35.08	66.39	88.47	25.60	476.34
11.833	48365	29.16	70.84	20.29	75.27	146.69	98.12	106.24
12.210	48367	31.84	60.33	19.05	86.97	91.93	50.41	75.75

Table D.43: (continued)

Age	FZJ-Code	H	I	J	K	L	M	N
10 ³ vyears BP					$\frac{\mu g}{g} \text{TOC}$			
13.030	48370	29.84	62.69	65.04	84.63	83.66	50.57	83.89
13.865	48376	10.25	23.21	4.88	76.56	96.45	25.60	19.55
14.385	48378	17.61	38.05	8.91	44.84	52.70	21.45	0.09
14.635	48380	20.72	19.28	n.a.	30.74	102.69	18.44	16.86

Table D.44: Sterol concentrations for Lake Meerfelder Maar Samples; Part 3: Compounds O to Q (Labels are assigned to systematic names of Sterols as listed in *Table 5.4, Page 122*)

Age	FZJ-Code	O	P	Q
10 ³ vyears BP			$\frac{\mu g}{g} \text{TOC}$	
0.600	48340	53.28	24.54	10.90
1.240	48343	0.72	0.00	3.91
1.740	48344	149.43	43.69	12.51
1.910	48345	24.83	1.32	9.15
2.115	48347	5.91	0.58	1.77
3.765	48348	81.32	90.19	0.00
3.990	48349	79.07	56.05	0.00
4.205	48350a	84.47	61.21	7.09
6.290	48353	192.68	67.96	7.75
8.670	48357	151.99	148.57	0.00
10.035	48360	64.77	31.39	8.21
11.833	48365	77.13	26.79	15.92
12.210	48367	73.15	71.44	9.99
13.030	48370	61.01	56.39	12.90
13.865	48376	73.07	29.21	10.08
14.385	48378	64.08	6.71	16.24
14.635	48380	33.81	1.62	31.54

D Data Compilation

Table D.45: Sterol concentrations for Lake Meerfelder Maar Samples (High Resolution Sequence) (High Resolution Sequence); Part 1: Compounds A to G (Labels are assigned to systematic names of Sterols as listed in *Table 5.4, Page 122*)

Age 10 ³ years BP	FZJ-Code	A	B	C	D	E	F	G
		$\frac{\mu g}{g\text{TOC}}$						
9.970	50116	7.84	5.89	5.46	3.61	2.23	4.75	3.12
10.070	50117	9.47	10.98	6.59	8.74	0.00	6.10	4.71
10.170	50118	9.13	5.65	4.49	3.14	2.81	2.41	5.97
10.270	50119	7.13	8.82	4.61	4.03	2.98	2.20	5.49
10.380	50120	6.19	8.02	7.21	4.61	3.55	0.00	2.45
10.490	50121	7.66	40.08	15.73	8.32	1.90	3.28	5.37
10.560	50122	8.77	11.78	8.85	6.18	2.21	2.77	4.14
10.600	50123	7.02	8.85	8.69	3.08	1.84	2.59	2.03
10.620	50124	9.16	9.54	5.95	2.99	4.36	3.10	2.20
10.630	50125	7.28	4.80	3.39	2.01	2.00	2.30	0.70
10.640	50126	7.59	12.01	6.35	7.59	1.71	0.59	4.65
10.650	50127	7.25	5.79	4.89	1.74	1.96	2.89	2.27
10.670	50128	9.82	1.05	5.61	4.45	2.58	5.60	4.15
11.110	50129	9.13	0.53	2.56	1.63	0.00	3.12	1.44
11.130	50130	9.94	5.96	5.66	1.73	1.64	2.15	2.32
11.195	50131	9.38	0.82	4.85	1.67	1.25	2.34	1.51
11.210	50132	11.21	12.24	8.65	2.71	1.82	1.13	3.05
11.350	50133	10.03	0.80	0.83	1.75	2.42	4.60	1.39
11.375	50134	15.87	7.78	1.96	2.02	2.50	3.06	2.34
11.395	50135	18.68	1.87	2.76	1.88	2.98	6.14	3.33
11.410	50136	7.82	53.70	17.58	12.52	12.76	6.08	14.08
11.770	50137	12.62	0.88	2.85	3.90	4.13	1.57	3.30
11.780	50138	10.41	11.46	3.79	2.20	4.20	4.95	5.11
11.840	50139	14.54	8.02	11.54	3.72	4.29	4.99	3.70
11.855	50140	16.73	38.84	11.74	5.38	4.42	4.12	9.80
11.910	50141	18.74	1.09	9.81	3.81	3.15	5.58	6.70
11.920	50142	20.01	9.84	11.75	3.28	4.04	3.44	1.48
11.980	50143	16.43	0.68	5.05	4.23	4.89	3.67	8.63
11.990	50144	13.98	16.46	0.97	3.73	5.04	6.11	7.09
12.045	50145	11.26	9.19	1.40	2.81	4.64	3.45	5.26
12.060	50146	11.41	5.80	9.81	2.86	4.03	3.00	1.80
12.090	50147	0.85	1.28	2.58	3.02	5.71	4.32	4.28
12.100	50148	25.39	0.48	10.13	2.37	3.91	3.76	8.01
12.160	50149	14.80	23.82	11.32	3.17	1.22	8.19	9.53
12.170	50150	21.08	26.82	12.32	4.83	4.95	8.22	12.67
12.210	50151	10.88	35.92	20.43	18.63	16.50	4.02	17.56
12.220	50152	10.82	9.45	2.70	2.19	7.16	2.41	1.83
12.250	50153	12.06	4.92	8.51	3.90	7.09	7.61	4.84
12.260	50154	14.08	4.80	10.69	3.77	5.15	8.44	2.54
12.280	50155	13.23	3.56	4.17	1.28	4.01	6.31	3.02
12.290	50156	12.78	10.45	7.04	2.56	5.58	7.71	4.06

Table D.45: (continued)

Age	FZJ-Code	A	B	C	D	E	F	G
10^3 years BP		$\frac{\mu g}{g} \text{TOC}$						
12.300	50157	9.18	2.52	6.82	3.87	6.35	7.54	4.62
12.310	50158	12.51	0.39	3.29	2.00	4.36	0.54	2.36
12.340	50159	13.73	5.11	4.86	0.53	3.99	5.82	2.79
12.380	50160	10.25	1.21	4.34	2.35	3.04	3.72	3.25
12.400	50162	12.19	0.90	6.66	5.54	1.00	7.10	5.42
12.480	50163	1.16	7.23	1.44	2.37	7.20	5.80	4.71
12.490	50164	0.56	14.00	2.02	2.71	2.58	3.78	7.92
12.520	50165	19.30	3.85	5.87	3.28	5.36	5.28	3.79

Table D.46: Sterol concentrations for Lake Meerfelder Maar Samples (High Resolution Sequence); Part 2: Compounds H to N (Labels are assigned to systematic names of Sterols as listed in *Table 5.4, Page 122*)

Age	FZJ-Code	H	I	J	K	L	M	N
10^3 years BP		$\frac{\mu g}{g} \text{TOC}$						
9.970	50116	6.41	7.05	19.37	60.85	14.65	12.66	138.19
10.070	50117	10.36	13.05	16.69	65.21	16.63	17.43	126.89
10.170	50118	11.65	2.09	26.09	37.34	6.56	22.96	0.00
10.270	50119	7.60	11.89	9.58	42.04	8.09	20.25	401.25
10.380	50120	11.23	10.83	27.18	32.31	12.10	32.29	159.59
10.490	50121	6.20	19.12	17.51	86.40	22.75	19.50	129.21
10.560	50122	14.07	18.01	17.46	98.97	31.69	32.84	112.11
10.600	50123	10.70	6.64	16.81	31.45	15.02	28.70	60.46
10.620	50124	7.24	7.58	15.77	39.38	16.33	72.05	66.89
10.630	50125	8.44	7.06	6.04	39.09	16.48	30.11	34.93
10.640	50126	10.98	22.00	12.43	101.07	44.02	27.68	37.74
10.650	50127	8.84	8.08	25.98	37.44	17.65	36.08	51.89
10.670	50128	9.63	14.63	21.35	59.83	23.88	27.60	72.05
11.110	50129	12.06	12.26	6.70	32.34	13.60	18.08	54.47
11.130	50130	12.41	8.94	27.42	22.20	9.29	20.35	54.58
11.195	50131	8.57	7.92	8.76	26.98	9.54	18.22	50.39
11.210	50132	9.32	11.62	31.68	48.40	14.31	26.76	58.28
11.350	50133	n.a.	7.01	48.58	23.82	11.07	22.72	41.15
11.375	50134	n.a.	11.69	26.12	31.54	13.72	29.57	29.91
11.395	50135	n.a.	11.90	28.04	42.41	18.73	30.74	27.97
11.410	50136	11.57	41.28	3.31	93.98	117.81	n.a.	6.72
11.770	50137	9.65	4.78	13.27	39.75	21.44	35.18	41.17
11.780	50138	13.10	11.39	4.56	41.80	19.89	44.42	52.11
11.840	50139	0.00	10.86	21.30	21.27	4.91	74.47	76.34

Table D.46: (continued)

Age	FZJ-Code	H	I	J	K	L	M	N
10 ³ years BP					$\frac{\mu g}{g} \text{TOC}$			
11.855	50140	27.85	32.33	21.63	64.71	39.67	93.36	72.76
11.910	50141	16.64	7.51	9.63	34.51	12.00	55.79	77.56
11.920	50142	7.57	8.15	12.14	17.56	6.19	83.06	79.80
11.980	50143	15.50	5.47	12.50	29.46	9.31	33.87	45.82
11.990	50144	n.a.	17.40	19.29	44.27	17.57	51.78	50.23
12.045	50145	2.70	3.38	14.56	37.98	10.96	52.99	48.91
12.060	50146	1.52	10.39	19.77	20.41	6.47	20.28	44.85
12.090	50147	14.47	5.63	n.a.	8.53	3.58	10.48	7.13
12.100	50148	35.54	9.33	13.00	24.10	7.72	92.44	38.12
12.160	50149	26.84	14.67	13.38	41.99	15.80	102.58	30.25
12.170	50150	30.87	18.13	12.50	36.98	12.20	136.59	0.00
12.210	50151	26.31	64.55	12.14	90.63	130.27	22.06	25.26
12.220	50152	15.94	16.02	11.12	35.06	18.43	42.64	19.50
12.250	50153	0.00	19.62	33.29	56.42	17.81	45.25	53.05
12.260	50154	14.47	13.74	21.42	57.88	10.86	33.75	42.96
12.280	50155	18.79	15.62	2.69	57.38	18.23	45.47	44.77
12.290	50156	14.28	19.17	12.46	67.94	21.26	33.12	44.51
12.300	50157	12.28	13.52	5.41	41.12	11.81	15.42	38.30
12.310	50158	15.02	11.43	5.39	37.68	11.37	23.86	45.87
12.340	50159	16.91	2.18	21.55	21.06	11.00	32.55	34.65
12.380	50160	16.55	16.19	7.26	27.96	9.14	24.72	51.03
12.400	50162	6.22	30.19	74.07	36.69	21.03	17.08	67.75
12.480	50163	1.85	31.44	43.91	50.82	23.91	24.75	41.21
12.490	50164	n.a.	41.01	3.74	82.00	49.35	18.36	36.20
12.520	50165	13.70	25.58	7.31	21.85	14.33	17.59	52.28

Table D.47: Sterol concentrations for Lake Meerfelder Maar Samples (High Resolution Sequence); Part 3: Compounds O to Q (Labels are assigned to systematic names of Sterols as listed in *Table 5.4, Page 122*)

Age	FZJ-Code	O	P	Q
10 ³ years BP			$\frac{\mu g}{g} \text{TOC}$	
9.970	50116	14.04	32.12	2.32
10.070	50117	15.35	40.00	0.40
10.170	50118	43.37	21.75	2.05
10.270	50119	47.25	23.08	1.28
10.380	50120	32.23	35.25	1.22
10.490	50121	48.93	50.92	6.15
10.560	50122	67.30	20.71	2.15

Table D.47: (continued)

Age 10 ³ years BP	FZJ-Code	O	P	Q
		$\frac{\mu g}{g \text{ TOC}}$		
10.600	50123	62.73	16.38	1.69
10.620	50124	59.17	41.60	2.77
10.630	50125	42.04	19.17	1.57
10.640	50126	39.73	16.13	1.94
10.650	50127	71.22	25.35	1.77
10.670	50128	77.58	28.04	1.95
11.110	50129	68.92	15.83	3.12
11.130	50130	34.35	11.98	3.49
11.195	50131	22.71	n.a.	2.55
11.210	50132	38.81	2.93	3.28
11.350	50133	21.92	11.33	2.93
11.375	50134	20.77	8.93	3.21
11.395	50135	19.22	20.95	3.06
11.410	50136	0.11	2.83	2.45
11.770	50137	1.54	9.27	3.40
11.780	50138	22.72	6.99	4.80
11.840	50139	24.22	15.12	18.06
11.855	50140	20.59	n.a.	13.83
11.910	50141	24.30	8.59	4.86
11.920	50142	25.91	19.11	5.35
11.980	50143	22.04	16.90	19.22
11.990	50144	21.84	15.72	30.06
12.045	50145	27.88	19.04	4.98
12.060	50146	20.93	12.51	4.57
12.090	50147	3.35	39.10	0.80
12.100	50148	28.90	14.40	5.92
12.160	50149	25.77	14.87	5.48
12.170	50150	30.84	19.79	6.14
12.210	50151	26.55	8.91	3.09
12.220	50152	17.74	15.44	4.18
12.250	50153	30.22	27.96	9.86
12.260	50154	22.08	4.01	16.43
12.280	50155	35.56	25.56	20.20
12.290	50156	30.63	1.69	14.85
12.300	50157	22.89	8.44	12.79
12.310	50158	31.42	16.79	9.67
12.340	50159	29.28	4.98	13.50
12.380	50160	35.71	9.82	6.42
12.400	50162	43.14	23.79	3.86
12.480	50163	42.55	15.50	3.31
12.490	50164	1.46	10.25	5.89
12.520	50165	27.20	8.67	0.10